

Amidine-based Sphingosine Kinase Inhibitors:
Optimization of Selectivity, Solubility, and Metabolism

Morgan Lee Bolden
Woodstock, Virginia

B. S. Chemistry, Minor Mathematics
James Madison University, 2008
A. A. S. Lord Fairfax Community College, 2005

A Dissertation presented to the Graduate Faculty
of the University of Virginia in Candidacy for the Degree of
Doctor of Philosophy

Department of Chemistry

University of Virginia
August 2013

Abstract

Soon cancer will be the leading cause of death in the United States; unfortunately, the treatments available to patients have severe side effects. Chemotherapies target dividing cells with the goal to kill the rapidly dividing cancer cells before the patient. Researchers have been focusing on determining the cause of the disease and developing better modes of treatment. This has been difficult due to cancer developing resistance to drugs over time and the vast differences among the different types of the disease. One strategy is to develop targeted therapies that inhibit a particular pathway cancer cells rely on to survive. One such pathway is the “Sphingolipid Rheostat” and targeting either the production and/or signaling of sphingosine 1-phosphate (S1P). The research herein describes the design and synthesis of amidine-based inhibitors of the sphingosine kinases (SphKs) to limit the production of S1P since they are the sole producers of the molecule.

Signaling by S1P leads to cell migration, proliferation, and survival. There are two isoforms of the SphKs, SphK1 and SphK2. Of the two, SphK1 has been studied much more since higher concentrations of this enzyme have been found in a variety of cancer cell lines. Our lab has been very successful in selectively targeting SphK1 using amidine-based inhibitors. These molecules lower S1P levels *in vitro* as well as *in vivo*. Only recently has SphK2 been more intensely investigated and found to play a more complex role in cell fate. S1P produced by this enzyme, depending on its cellular location, will either lead to cell migration

and survival or apoptosis. These contradicting roles of the same endogenous molecule have left researchers needing further understanding of SphK2's roles in cell fate. The development of potent dual and sub-type selective inhibitors will be useful in elucidating the cellular roles of each of these kinases. Herein is described an attempt to selectively target SphK2 over SphK1 using amidine-based inhibitors. Structure-activity relationship (SAR) studies were performed on these molecules and it was found that these molecules bind to SphK2 at approximately equal strength. These studies lead us to believe that SphK2 is a promiscuous protein that will bind molecules with a variety of functionalization at similar strength.

The Macdonald laboratory has developed some of the *most potent* SphK1-*selective* inhibitors in the chemical literature. In order to use these molecules in whole animal studies, they must be long-lived. Unfortunately, these amidine-based inhibitors have a short half-life due to their quick metabolism. The amide linkage of these molecules has been replaced with more metabolically stable 5-membered heterocycles to circumvent this issue. SAR studies were performed on these heterocyclic inhibitors to determine the optimal heterocycle to increase potency, selectivity, and half-life. These heterocyclic inhibitors were found to increase the half-life of the amidine-based SphK inhibitors and are equipotent to their amide counterparts. These potent, longer-lived inhibitors will be useful to scientists to determine the role of the SphKs in cancer cells and other diseases.

To Mom and Dad, for always believing in me
and pushing me to meet my potential

and

To Ben, for his love, food, and moral compass

Contents

Abstract	i
Acknowledgements	iii
Contents	iv
Figures	vii
Schemes	iv
Tables.....	xi
Abbreviations.....	xii
VPC Number Index.....	xiv

Chapter 1: Cancer and the Role of Sphingosine 1-Phosphate 1

1.1 Cancer Today	1
1.2 The Tumorigenic State.....	3
1.3 Hallmarks of Cancer	4
1.4 Current Modes of Cancer Treatment	5
1.5 The Sphingolipid Rheostat.....	8
1.6 S1P Signaling	9
1.7 Interaction between S1P-signaling and Growth Factors	13
1.8 Conclusion	14
1.9 References	15

Chapter 2: The Sphingosine Kinases 17

2.1 The Sphingosine Kinases	17
2.2 Sphingosine Kinase 1	20
2.3 Sphingosine Kinase 2	22
2.4 The Sphingosine Kinases and Non-Cancerous Diseases.....	26
2.5 Current Inhibitors in the Literature	27
2.5.1 Sphingosine-based Inhibitors	28
2.5.2 Analogs of Fingolimod as Inhibitors.....	30
2.5.3 Non-lipid Inhibitors.....	33
2.5.4 Natural Product Inhibitors	35
2.6 Conclusion	36
2.7 References	37

Chapter 3: Discovery and Optimization of Amidine-based Sphingosine Kinase Inhibitors 40

3.1 From Substrates to Inhibitors.....	40
--	----

3.2 Biological Evaluation of Sphingosine Kinase Inhibitors.....	44
3.3 Optimization of Amidine-based Sphingosine Kinase Inhibitors	46
3.3.1 Head Group Structure-Activity Relationships.....	47
3.3.2 Tail Group Structure-Activity Relationships	49
3.3.3 Structure-Activity Relationships of the Amide Bond.....	50
3.4 Biological Evaluation of Amidine-based inhibitors at Recombinant Enzyme	51
3.4.1 Evaluation of the Head Group Analogues	52
3.4.2 Evaluation of the Tail Analogues	54
3.4.3 Biological Evaluation of Amide-bond Analogues	57
3.5 Second-Generation Amidine-based Sphingosine Kinase Inhibitors...	59
3.5.1 SAR and Biological Evaluation of 3.42	59
3.5.2 Head Group Analysis of Second-Generation Inhibitors	62
3.5.3 A Rational Approach to Drug Design	64
3.6 Conclusion	69
3.7 References	70
 Chapter 4: Design of Amidine-based SphK2-selective Inhibitors	71
4.1 Introduction	72
4.2 Stereochemical Preference for Sphingosine Kinase 2.....	73
4.2.1 Synthesis of Inhibitors Containing Bulky Groups at the Alpha Position	73
4.2.2 Biological Evaluation of Inhibitors with Varying Alpha Substituents	80
4.3 Hydrazine-based Inhibitors	82
4.4 Rationally Designed SphK2-selective Inhibitors.....	84
4.4.1 Synthesis of Rationally Designed SphK2-selective Inhibitors...	85
4.4.2 Evaluation of Rationally Designed SphK2-selective Inhibitors...	89
4.5 Conclusion	91
4.6 References	92
 Chapter 5: Optimization of the Metabolism of SphK Inhibitors.....	93
5.1 <i>In vivo</i> Evaluation of Amide-containing SphK Inhibitors	93
5.2 Investigating Possible Modes of Metabolism	95
5.2.1 Amidine Prodrugs	96
5.2.2 Amide Isosteres.....	97
5.3 Nitrogen-based 5-Membered Heterocyclic Amide Bioisostere Inhibitors	102
5.3.1 Synthesis of N-based Heterocycles.....	103
5.3.2 Biological Evaluation of N-based Heterocyclic Analogues.....	106
5.4 Pyridine Inhibitors	109
5.5 Conclusion	114

5.6 References	115
Chapter 6: Experimental Procedures	117
6.1 Biological Methods	117
6.2 Chemical Syntheses	118

Figures

Figure 1.1: Rates of incidence and death of Cancer in the United States	2
Figure 1.2: The division of normal and cancer cells.....	3
Figure 1.3: The Hallmarks of Cancer	4
Figure 1.4: The Philadelphia chromosome, Bcr-Abl protein, and Gleevec™	6
Figure 1.5: The production of S1P and its signaling	10
Figure 1.6: Signaling effects of S1P binding to S1PR ₁₋₅	13
Figure 2.1: General sequence comparison of SphK1 and SphK2	18
Figure 2.2: Signaling of S1P produced by SphK2.....	23
Figure 2.3: Structure of Fingolimod (Gilenya™, Novatis)	26
Figure 2.4: Structures of Sphingosine-based inhibitors	29
Figure 2.5: Structures of inhibitors based on the structure of Fingolimod.....	33
Figure 2.6: Structures of non-lipid SphK inhibitors.....	35
Figure 3.1: Design of SphK inhibitors	41
Figure 3.2: Radio-labeled Sph assay.....	44
Figure 3.3: Evaluation of (S)-3.8 and 3.5 as SphK inhibitors	45
Figure 3.4: Structure Activity Relationships of (S)-3.8	46
Figure 3.5: Amide configuration vs tail length	58
Figure 3.6: SphK1-selective inhibitor design from 3.42	59
Figure 3.7: SphK homology model	66
Figure 3.8: Progression of linker design using homology model	67
Figure 3.9: Generic scaffold designed in the SphK1 homology model	67
Figure 4.1: Inhibitor designed using the SphK2 homology	84

Figure 5.1: Measurement of the half-life of amide 3.57	94
Figure 5.2: Structures of amidine prodrugs	97
Figure 5.3: Design of heterocyclic isosteres based on (R)-VPC45129	98
Figure 5.4: Wild-type C57BL/6 mice dosed with oxadiazole 5.4	101
Figure 5.5: Wild-type C57BL/6 mice dosed with triazole 5.15	108
Figure 5.6: Nitrogen-based heterocyclic inhibitors in the homology model	109

Schemes

Scheme 1.1: The “Sphingolipid Rheostat”	9
Scheme 3.1: Synthesis of lead (S)-3.8	42
Scheme 3.2: Independent synthesis of (S)-3.8	43
Scheme 3.3: Synthesis of oxadiazole 3.5	44
Scheme 3.4: Synthesis of serine-based inhibitor 3.22	49
Scheme 3.5: Synthesis of ether tail analogues	50
Scheme 4.1: Synthesis of alanine (R)-4.6	74
Scheme 4.2: Synthesis of alanine (S)-4.6	74
Scheme 4.3: Synthesis of aryl deletion alanine 4.10	75
Scheme 4.4: Synthesis of L-serine derivative (S)-4.12	76
Scheme 4.5: Synthesis of D-serine analogue (R)-4.12	77
Scheme 4.6: Synthesis of valine derivatives (R)- and (S)-4.23	78
Scheme 4.7: Synthesis of cyclobutyl analogue 4.27	79
Scheme 4.8: Synthesis of cyclopentyl analogue 4.32	79
Scheme 4.9: Synthesis of hydrazine 4.36	83
Scheme 4.10: Synthesis of thiazole 4.47	86
Scheme 4.11: Synthesis of 2,6-naphthalene substituted inhibitor 4.53	87
Scheme 4.12: Synthesis of the 1,5-naphthalene based inhibitor 4.60	88
Scheme 4.13: Synthesis of the 1,4-substituted naphthalene derivative 4.68	89
Scheme 5.1: Modes of metabolism of 3.57	95
Scheme 5.2: Synthesis of 1,2,4-triazole analogue 5.15	103
Scheme 5.3: Synthesis of pyrazole analogue 5.19	104

Scheme 5.4: Proposed synthesis of pyrrole analogue 5.27	106
Scheme 5.5: Synthesis of pyridine 5.31	111
Scheme 5.6: Synthesis of pyridine 5.36	111
Scheme 5.7: Synthesis of triazole 5.42	112

Tables

Table 3.1: K_i values and SphK1 selectivity of head group analogues	53
Table 3.2: K_i values of alkyl and ether tail derivatives	56
Table 3.3: K_i values of amide derivatives	57
Table 3.4: K_i values for aryl deletion and substituted tail terminus	61
Table 3.5: K_i values for head group modifications	64
Table 3.6: K_i values for the predicted inhibitors	68
Table 4.1: K_i values for inhibitors testing stereochemical preference	81
Table 4.2: K_i values for the hydrazine-based and related inhibitors	84
Table 4.3: K_i values of rationally designed SphK2-selective inhibitors	90
Table 5.1: K_i and IC_{50} values of oxadiazole inhibitors	99
Table 5.2: K_i values of N-based heterocyclic inhibitors	107
Table 5.3: K_i values of pyridine-based inhibitors	114

Abbreviations

9-BBN	9-borabicyclo[3.3.1]nonane
AcOH	acetic acid
ADP	adenosine diphosphate
Akt	protein kinase B
ATP	adenosine triphosphate
BH3	BH3 interacting-domain death agonist
Boc	<i>tert</i> -butyl carbomate
C1B1	calcium- and integrin-binding protein 1
Cbz	carboxybenzoyl
Cer	ceramide
CML	chronic myeloid leukemia
DCM	dichloromethane
DGKB	diacylglycerol kinase β
DIEA	N,N-diisopropylethylamine
DMF	N,N-dimethylformamide
DMSO	dimethyl sulfoxide
dppf	1,1'-bis(diphenylphosphino)ferrocene
EGF	epidermal growth factor
EGFR	epidermal growth factor receptor
ER	endoplasmic reticulum
ERK	extracellular signal regulated kinase
Et	ethyl
EtOAc	ethyl acetate
EtOH	ethanol
HDAC	histone deacetylase
HER2	Human epidermal growth factor receptor 2
IR	ischemia/reperfusion
K_i	inhibitor constant
K_M	Michaelis constant
MAPK	mitogen-activated protein kinase
MCF-7	Human breast cancer adenocarcinoma cell line
Me	methyl
MeOH	methanol
MOE	Molecular Operating Environment
MPT	mitochondria permeability transition
NES	nuclear export signal
NGF	nerve growth factor
NLS	nuclear localization signal
NMR	nuclear magnetic resonance
p21	cyclin-dependent kinase inhibitor 1
PA	phosphatidic acid
PDGF	platelet-derived growth factor
PI3K	Phosphatidylinositide 3-kinases
PKC	protein kinase C

PKD	protein kinase D
PLC	phospholipase C
PS	phosphotidyl serine
PyBOP	benzotriazol-1-yl-oxytripyrrolidinophosphonium hexafluorophosphate
Rac	ras-related C3 botulinum toxin substrate 1
Rho	ras homolog gene family, member A
RTK	receptor tyrosine kinase
S1P	sphingosine 1-phosphate
S1PR	sphingosine 1-phosphate receptor
SAR	structure-activity relationship
Sph	sphingosine
SphK	sphingosine kinase
SPNS2	spinster homolog 2
<i>t</i> Bu	<i>tert</i> -butyl
TEA	triethylamine
TFA	trifluoroacetic acid
TFAA	trifluoroacetic anhydride
THF	tetrahydrofuran
TM	transmembrane
TOH	two of hearts transporter
U937	a common human leukemia cell line
VEGF	vascular endothelial growth factor

VPC Number Index

(S)-3.8	VPC94075	3.56	VPC143144
(R)-3.8	VPC95201	3.57	VPC14a1058
3.5	VPC9	3.58	VPC143237
3.28	VPC9	3.59	VPC143253
3.29	VPC9	3.60	VPC143257
3.30	VPC9	3.61	VPC143275
3.31	VPC9	3.62	VPC143278
3.32	VPC94131	3.63	VPC143283
3.33	VPC96031	(S)-4.6	VPC9b1075
3.22	VPC95139	(R)-4.6	VPC172057
3.27a	VPC171117	(S)-4.12	VPC175057
3.27b	VPC171147	(R)-4.12	VPC175027
3.27c	VPC171167	(S)-4.23	VPC171271
3.27d	VPC171137	(R)-4.23	VPC17a1029
3.34	VPC95287	4.27	VPC172087
3.35	VPC96047	4.32	VPC173213
3.38	VPC96021	4.36	VPC173031
3.39	VPC96055	4.47	VPC173013
(S)-3.40	VPC96091	4.53	VPC173143
(R)-3.40	VPC96115	4.60	VPC173175
3.42	VPC143033	4.68	VPC173181
3.43	VPC143081	5.4	VPC184091
3.44	VPC143064	5.5	VPC185083
3.45	VPC143065	5.6	VPC185081
3.46	VPC143057	5.7	VPC18a1143
3.47	VPC143046	5.8	VPC201091
3.48	VPC14a1002	5.8	VPC201075
3.49	VPC143078	5.15	VPC174065
3.50	VPC143129	5.19	VPC174171
3.51	VPC143119	5.31	VPC174261
3.52	VPC143113	5.36	VPC174037
3.53	VPC143105	5.42	VPC174173
3.54	VPC143126	5.43	VPC174169
3.55	VPC143090		

1

Cancer and the Role of Sphingosine 1-Phosphate

Sphingosine 1-phosphate is an endogenous signaling molecule that has been implicated in cancer due to its role in proliferation, migration, and angiogenesis. To control its signaling effects, researchers have been developing small molecules to inhibit the kinases responsible for its production as well as agonists and antagonists of its receptors.

1.1 Cancer Today

Over the past few decades, cancer has become a household name due to the growing number of incidences and diagnoses. Everyone has a relative, friend, or even themselves whose life has been affected by this terrible disease.¹ Research efforts to determine the cause and discover cures for cancer have grown tremendously thanks to public awareness and financial support given by many government agencies and organizational fundraising. This drive for information has allowed researchers to make tremendous advances in the understanding of this disease and unfortunately, discover how complex it is. This complexity is why there is no single cure for cancer and why progress has been slow.^{2,3}

Even though many advances have been made toward understanding the disease, still one in four deaths in the U.S. is caused by cancer. This information may lead you to believe that cancer research has made little progress, however, although the number of incidences is on the rise, the percentage of deaths overall has been declining since the early 1990s (Figure 1.1). The current leading cause of death in the United States is heart disease, but due to advances in treatment and lifestyle changes, the number of deaths has been declining. Cancer is the second leading cause of death in the U.S. and will soon surpass heart disease if more medical advances are not made.⁴

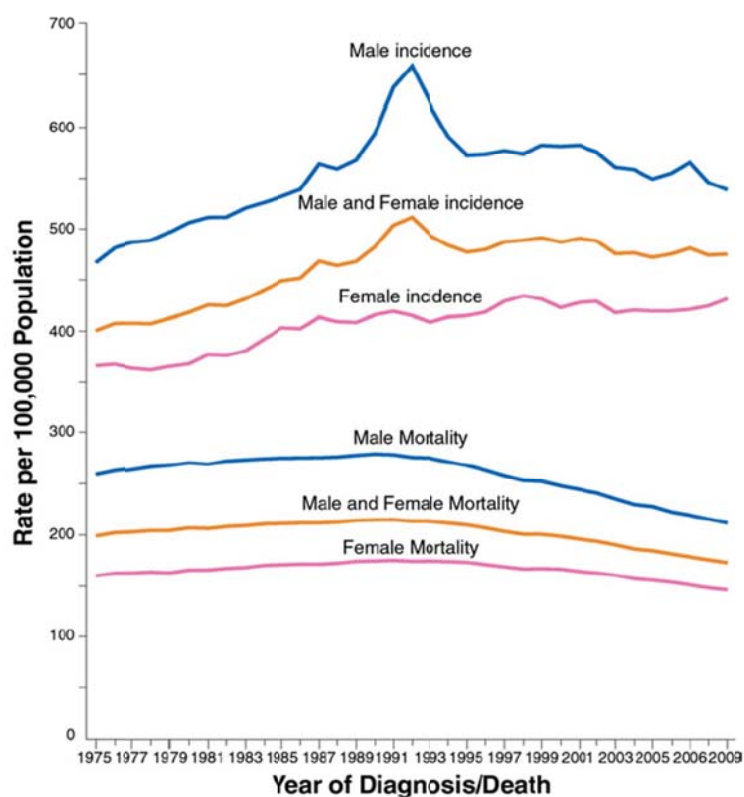


Figure 1.1: Cancer incidence and death rates by sex, U.S., 1975 to 2009.⁴

1.2 The Tumorigenic State

New and old cells are kept in constant balance within the body through new cell growth and apoptosis (cell mediated death). During normal cell division, mutations will often occur, but normally, the body recognizes these changes and signals the cell to die (Figure 1.2). If this mutation goes unnoticed, it too can replicate and produce additional mutated cells. During future replications, more mutations will occur until there is uncontrolled cell growth and a cancerous tumor develops.⁵

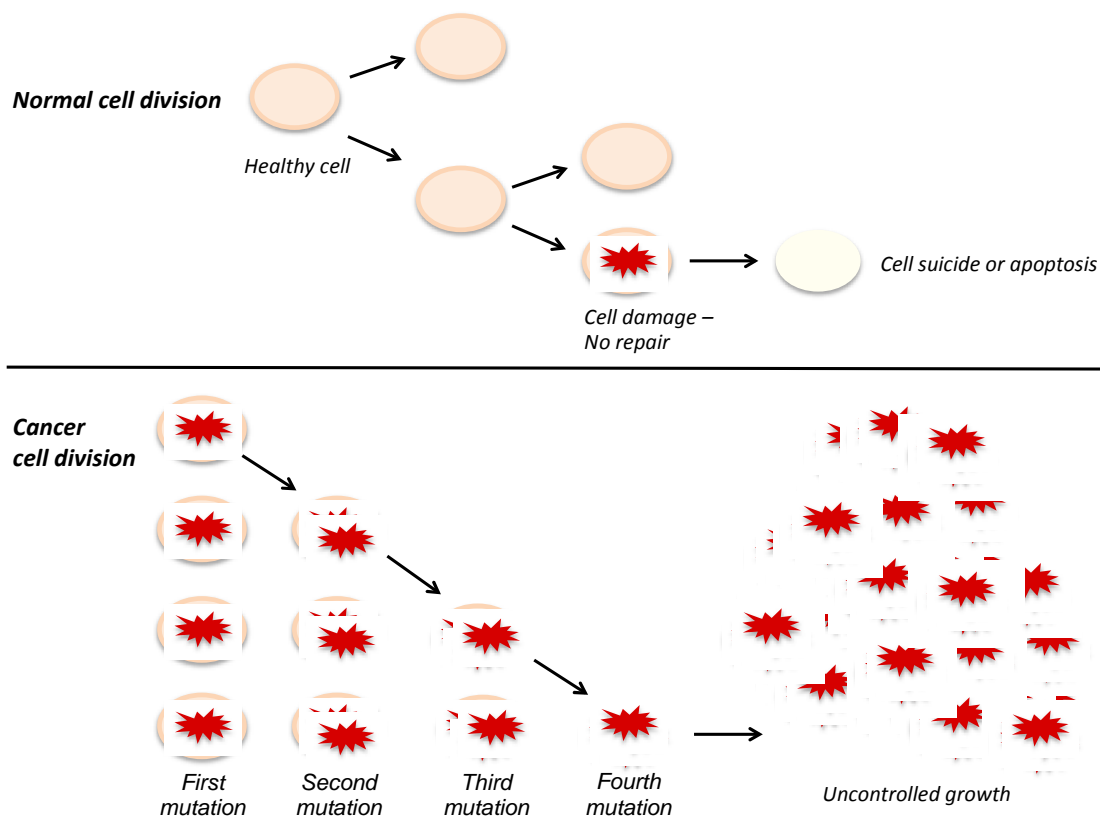


Figure 1.2: Normal cell division and cancer cell division. (top) Keeping cell division and death in check through apoptosis. (bottom) The development of a cancerous tumor through the replication of cells with mutations.⁵

1.3 Hallmarks of Cancer

In 2000, Hanahan and Weinberg analyzed the research and discoveries in cancer thus far, and determined that even though there are over 100 distinct types of cancer, most or all manifest from six essential alterations. They coined these the Hallmarks of Cancer (Figure 1.3): self-sufficiency in growth signals, insensitivity to growth-inhibitory signals, evasion of apoptosis, limitless replicative potential, sustained angiogenesis, and tissue invasion and metastasis.³ Also, identified were six stress phenotypes that support the tumorigenic state.² All of these changes stem from mutations during cell division and ultimately lead to the development of a tumor.^{3,6}

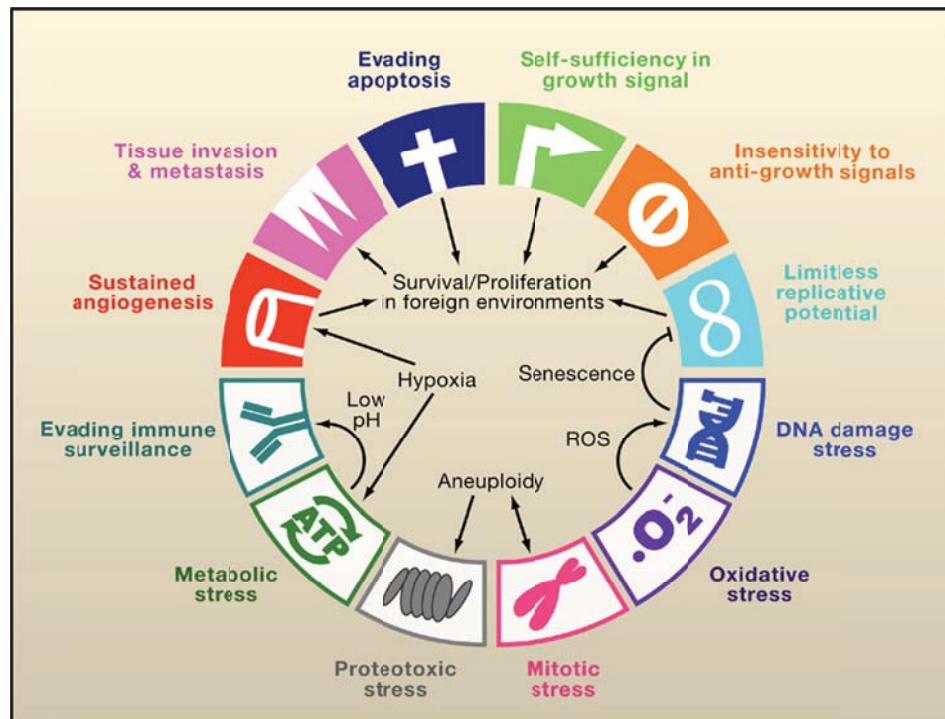


Figure 1.3: The Hallmarks of Cancer (top arc) and the six phenotypes (lower arc) that support the tumorigenic state.² Reprinted with permission.

Many of these phenotypes are caused by alterations to kinases, producing oncogenes that support the tumorigenic state. Not all cancer support pathways use oncogenes, but they can deregulate intrinsic signaling cascades necessary for normal cell survival and are considered non-oncogenes. The key to treating cancer will be to identify and target key signaling proteins that are involved in the tumorigenic state that will lead to apoptosis, necrosis, senescence, or differentiation.²

1.4 Current Modes of Cancer Treatment

Treating cancer has been very difficult due to the rapid mutations and the various survival pathways. The most successful form of treatment is to surgically remove the tumor before it metastasizes, but often, the cancer has been detected too late or surgery is not possible due to the location or size. The most common form of treatment is chemotherapy. These are chemicals that target dividing cells, but since all cells are constantly dividing, they produce severe side effects. Cancer cells divide much more rapidly than normal cells and thus the goal is to kill the tumor without killing too many healthy cells and before the tumor develops pathways of resistance.⁷

To prevent the killing of healthy cells, many researchers are looking toward targeted therapies. These are drugs that target a protein that is specific to the disease and will not effect healthy cells. There have been a few success stories with the most well known being Imatinib (Gleevec™, Novartis) for the treatment of chronic myeloid leukemia (CML) (Figure 1.4C). Unique to this

disease is the presence of the oncoprotein Bcr-Abl that results from the translocation of DNA on chromosomes 9 and 22 (Figures 1.4A and B).^{8,9} Since this protein is only found in patients with CML, it was a natural target for the development of an inhibitor. This protein is a tyrosine kinase and bypasses all regulatory control mechanisms and induces growth and survival of these cancer cells. Novartis developed Imatinib to selectively target the ATP-binding site of Bcr-Abl, which stabilizes the inactive form of the protein, thus shutting down the uncontrolled survival pathways. The use of this single treatment for CML has sent >95% of patient into remission.⁹

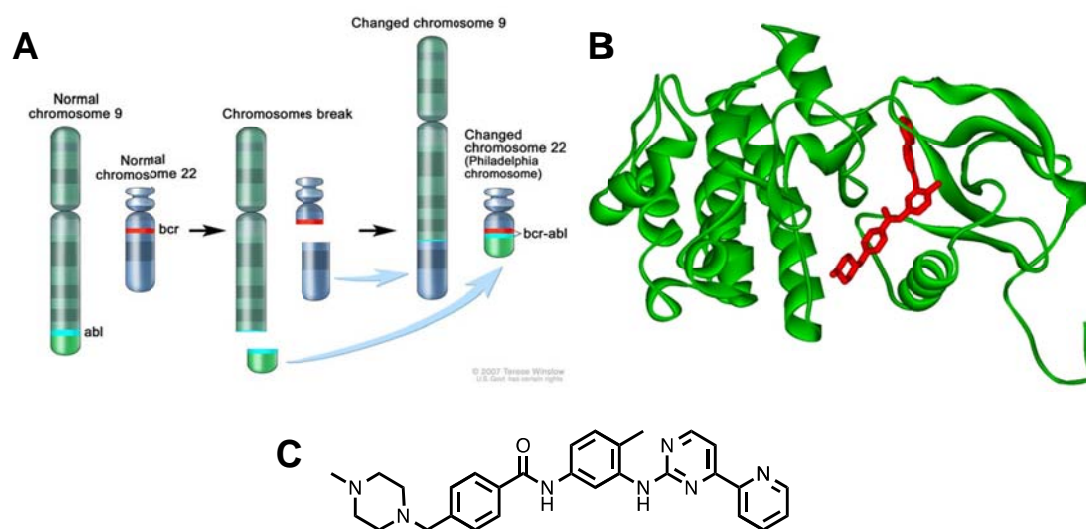


Figure 1.4: (A) The Philadelphia chromosome resulting from the translocation of the *Abl* gene from chromosome 9 and the *Bcr* gene from chromosome 22.¹⁰ (B) Bcr-Abl protein with GleevecTM bound in the active-site.¹¹ (C) Molecular structure of GleevecTM.

With the great success of GleevecTM, it may seem that targeted cancer therapies are simple to develop; however, CML is unique in that it results from a single point mutation. Many cancer types do not have a single oncoprotein to

target, but have many different oncogenes and survival pathways resulting from numerous mutations. This complexity is making the development of other targeted therapies difficult. For instance, the first receptor tyrosine kinase discovered, epidermal growth factor receptor (EGFR), has been heavily researched with limited success.¹² This protein is over-expressed and deregulated in many different cancer types making it a target of interest.^{12,13} Several different inhibitors have been developed to target EGFR, Iressa™ (AstraZeneca) and Tarceva® (Genentech/Roche/OSI Pharmaceuticals), have FDA approval for the treatment of lung and other cancers caused by the mutation of EGFR. These inhibitors have had limited success in that only 10-20% of patients show a response to treatment.¹³ Other inhibitors of EGFR have shown similar success rates demonstrating that cancer may not always be cured by targeting only one protein, but will need to be combined with other therapies, such as, chemotherapy, in order to more effectively treat the disease due to its complexity.⁷

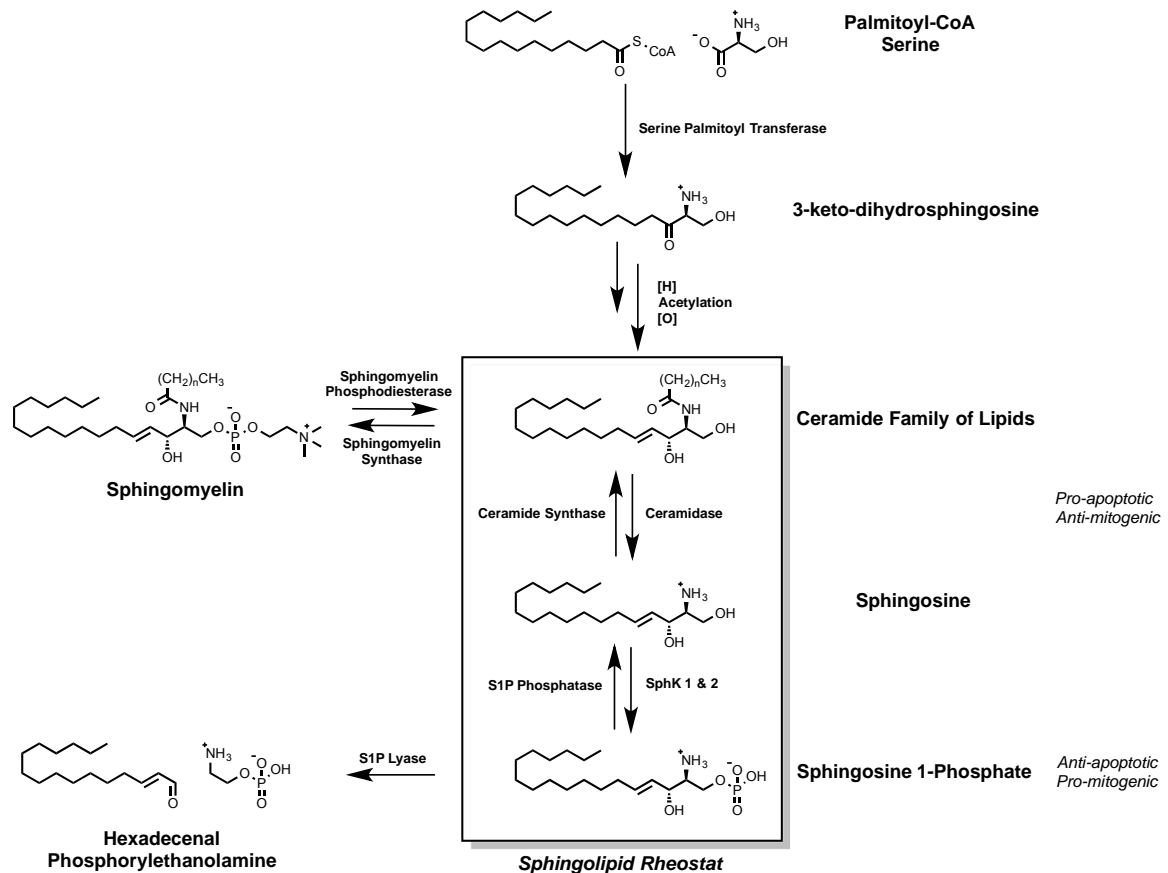
One such therapy may be inhibitors of the sphingosine kinases, which control the production of sphingosine 1-phosphate (S1P), an endogenous signaling molecule that promotes cell growth and survival. The research herein describes progress made toward inhibiting the sphingosine kinases as possible cancer therapeutics. Inhibition of the sphingosine kinases will control the amount of S1P available to the cells and thus can be used to slow the growth of cancer cells and possibly lead to apoptosis.

1.5 The Sphingolipid Rheostat

The cellular level of S1P is tightly controlled through its production by the sphingosine kinases and its degradation by S1P lyase and S1P phosphatases. These enzymes keep the concentration of S1P low relative to its precursors (Scheme 1.1).¹⁴ The production of sphingolipids begins *de novo* from serine and palmitate, which condense to form 3-ketodihydrosphingosine. Reduction and acetylation of this molecule affords the family of ceramides, which can be phosphorylated to sphingomyelins or deacetylated to produce sphingosine. Sphingosine is in turn phosphorylated by one of two isoforms of the sphingosine kinases to yield sphingosine 1-phosphate. There are two pathways for the degradation of S1P. It can be dephosphorylated by the S1P phosphatases or it can be irreversibly cleaved by S1P lyase.^{15,16}

The conversion between the sphingolipids has been termed the “sphingolipid rheostat” because the relative levels of ceramide, sphingosine, and S1P are tightly controlled due the opposing signaling effects of these molecules just as a resistor does in an electrical circuit.¹⁴ Ceramide and sphingosine have pro-apoptotic and anti-mitogenic properties, whereas, S1P is pro-mitogenic and anti-apoptotic. Since the concentration of ceramide is approximately 1 order of magnitude greater than sphingosine and there is about 100 times more sphingosine than S1P, small changes in the concentration of any of these molecules will cause large changes in the amount of the others and elicit changes in the cellular response.¹⁶ For instance, ceramide can be quickly

synthesized through the dephosphorylation of sphingomyelin, which is induced by stress, leading to apoptosis by causing the clustering of death receptors.¹⁷



1.6 S1P Signaling

Once S1P is produced intracellularly, there are many different targets it will interact with, most notably, the five S1P G-protein coupled receptors S1PR₁₋₅. S1P is an inside-out signaling molecule because it is transported out of the cell by the two of hearts (TOH) transporter (or SPNS2, spinster homolog 2) where it

binds to these receptors leading to many different cellular responses, such as cell migration, proliferation, and survival (Figure 1.5).^{14,18}

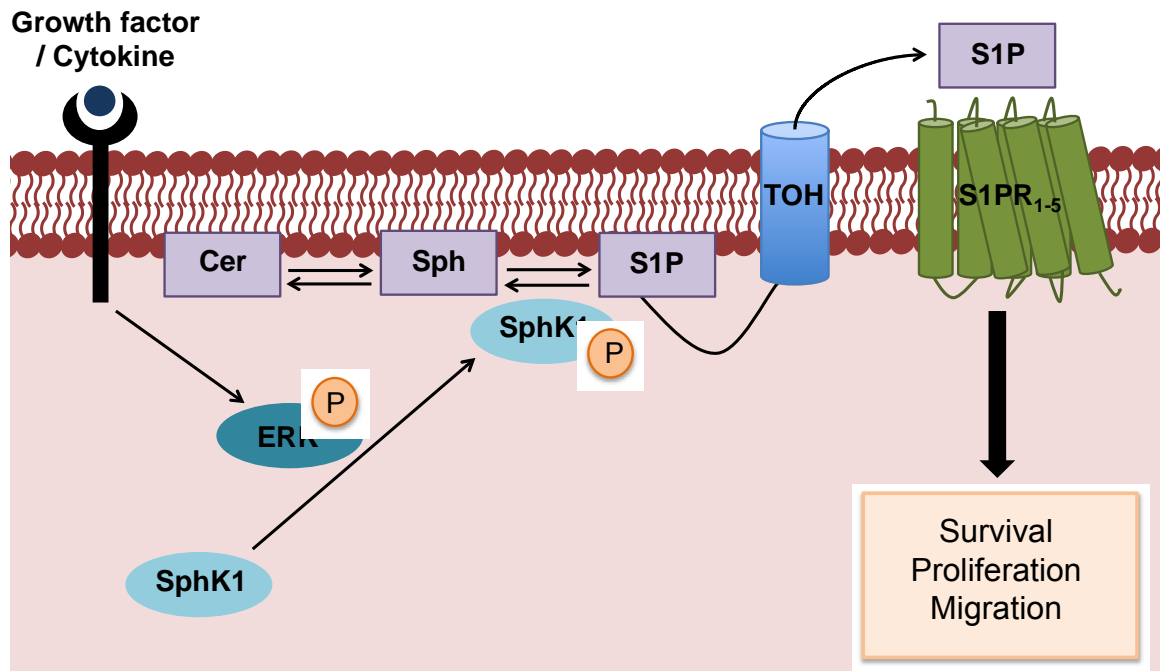


Figure 1.5: The production of S1P and its signaling. SphK1 phosphorylated sphingosine to S1P, which is then transported out of the cell by the two of hearts transporter. Once extracellular, S1P will bind to one of the five G-protein coupled receptors, S1PR₁₋₅.

The interaction of S1P with S1PR₁₋₅ plays an important role in the development of mammals (Figure 1.6). S1PR₁, found in numerous organs, has been shown to be essential for vasculature development and maturation and when knocked-out of mice, it is embryonically lethal. Also, this receptor has been linked to the activation of Rac and Rho, which allow cells to migrate to areas with high concentration of S1P as well as promoting adhesion molecules on the cell surface in order to interact with migrating cells.^{19,20} As discussed earlier, two important hallmarks of cancer cells are metastasis and angiogenesis and the

migration of cells play a large role in these processes. S1PR₁ has been implicated as a key player in the progression of tumors and their ability to metastasize and promote the growth of blood vessels.^{21,22} The cell growth signals associated with S1P binding to S1PR₁ are caused by the stimulation of the PI3K/Akt pathways which intern stimulate Rac.²⁰

An interesting function of S1P binding to S1PR₂ is its importance in lymphocyte trafficking and immune responses.^{21,23} Also, S1PR₂ has been shown to play an integral role in the development and mediation of neuronal excitability. For this reason, mice deficient in S1PR₂ develop seizures and are deaf.^{22,23} Even though S1PR₁ and S1PR₂ are of the same family, they have been found to have opposing roles in the migration of cells. S1PR₂ inhibits Rac by activating Rho, which promotes stress fiber assembly in certain types of cells where migration is not favorable such as melanoma cells.^{20,24}

Like S1PR₁, S1PR₃ is found in many different organs but when knocked-out of mice, no phenotypic deficiencies have been found. This suggests that this receptor is redundant and performs similar functions to other S1PRs. This receptor has been found to activate phospholipase C (PLC) and is known to control some cardiovascular functions in adults.^{22,24} Since it is associated to these functions, it is not surprising that agonism of this receptor leads to negative effects, like bradycardia and hypertension.²²

S1PR₄ has an affinity approximately 150 times lower for S1P as compared to the other receptors; however, little is known of the function of S1PR₄.²⁵ It has been found in lymphoid and hematopoietic tissues where it activates ERK1/2 and

PLC.²⁴ The role of S1PR₄ in the immune system has not yet been fully characterized and there is debate to whether or not it plays a role in neutrophil trafficking.^{23,25} To fully understand the role of this receptor in normal and diseased cells, further investigations need to be completed.

The final receptor, S1PR₅ plays an important role in the immune system by signaling for egress of natural killer T cells from lymph organs.²³ It is found in oligodendrocytes and in the white matter of the central nervous system where it functions in myelination. Its role in myelination is still in debate since S1PR₅-knockout mice do not show signs of defects in myelination.²²

All of these receptors play an important role in the function of many different cellular processes, the most important being the immune system. S1PR₁ has been implicated most in diseases, such as cancer, since upon the binding of S1P it elicits effects leading to cell migration and angiogenesis. Because of this, it is important to control the amount of S1P available to diseased cells through either controlling its production or antagonism at the receptors.

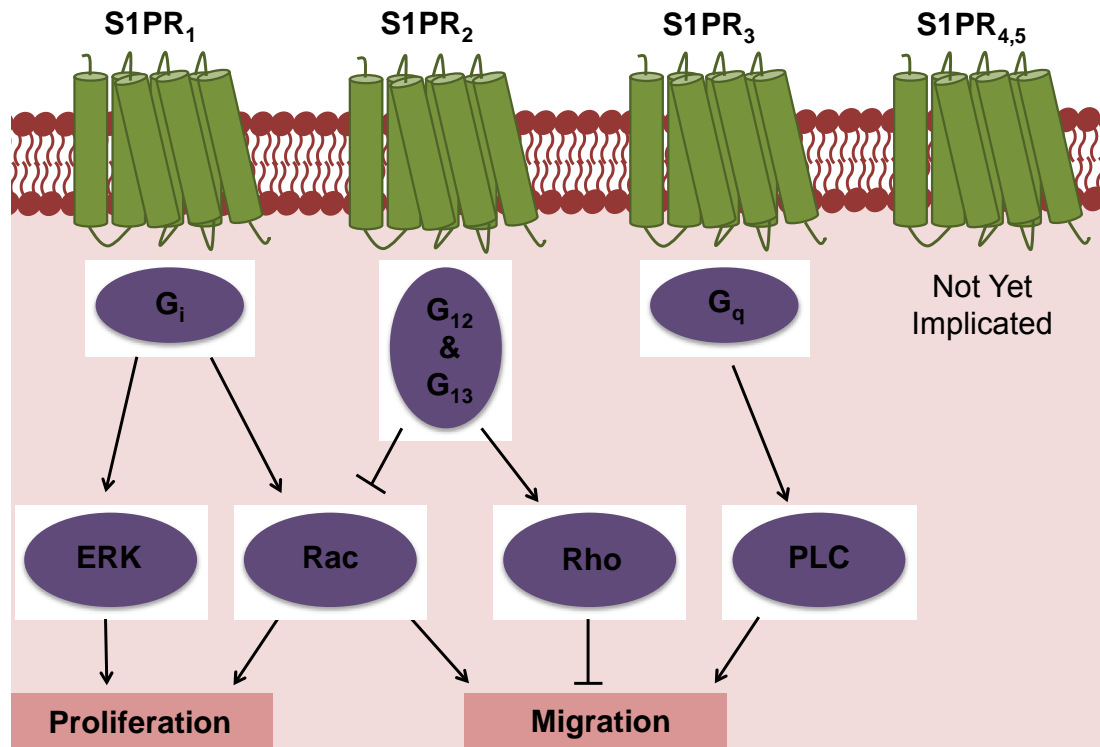


Figure 1.6: Pro-survival responses in cancer cells resulting from the activation of individual S1P receptors upon the binding of S1P. ERK, extracellular-signal-regulated kinases; Rac, Ras – related C3 botulinum toxin substrate 1; Rho, Ras homolog gene family, member A; PLC, phospholipase C. Modified from Pyne and Pyne.²⁶

1.7 Interaction between S1P-signaling and Growth Factors

It has been shown that there are interactions between growth factors and S1P-signaling pathways in cancer cells. These growth factors, epithelial growth factor (EGF), platelet-derived growth factor (PDGF), and vascular endothelial growth factor (VEGF), work in concert with S1P to promote proliferation, migration, and angiogenesis through the function of many different receptor tyrosine kinases (RTKs). Some of these growth factors stimulate or bind to S1P, whereas, others increase the expression or stimulate the activity of the kinases, most commonly SphK1.²⁶

SphK1 activity is stimulated by many different growth factors including EGF and heregulin to regulate migration in many different cell types, such as A7 melanoma cells and MCF-7 breast cancer cells. S1P will activate Human Epidermal Growth Factor Receptor 2 (HER2) in gastric cancer cells, which starts a signaling loop prolonging the release of EGF. Upon binding to S1PR₃, S1P stimulates ERK and Akt by the transactivation of the PDGF receptor (PDGF β) in ovarian cells. Activation of ERK in smooth muscle cells results from the signaling complex of S1PR₁ and PDGF β to enhance the signaling of PDGF causing migration of the cells. This is an example of 'integrative signaling', which has been termed 'GPCR jacking'.²⁶

VEGF interacts with S1P in an intracellular S1P regulatory loop in cancer. The Ras-GAP activity is controlled through activation by sphingosine and inactivation by S1P. VEGF stimulates the activity of SphK1 to produce S1P, causing inhibition of Ras-GAP, activating Ras-ERK, and inducing angiogenesis. This has been observed in bladder, breast, prostate, and neuroblastoma cancer cell lines.²⁶ All of these effects from growth factors working in concert with S1P and the SphKs may be controlled by the inhibition of the SphKs with small molecules.

1.8 Conclusion

Society is looking at researchers for a cure to cancer; even though, extensive research and much information have been obtained, there still is not a single cure for the disease. The complexity of cancer has demonstrated that a

cure will need to stem from the attack on many different pathways. One such pathway is the 'Sphingolipid Rheostat' where there are many different targets to control the signaling effects of S1P. Progress has been made in the development of agonists and antagonists of the S1P receptors; however, it has been difficult to develop a molecule that is specific to only one receptor, resulting in negative side effects. The research herein describes progress toward the development of sphingosine kinase inhibitors to prevent the production of S1P. If there is less S1P produced, the signaling effects at the receptors and with many different growth factors will reduce migration, proliferation, and angiogenesis in a number of different cancer cells.

1.9 References

- (1) Howlader N, N. A., Krapcho M, Neyman N, Aminou R, Waldron W, Altekruse SF, Kosary CL, Ruhl J, Tatalovich Z, Cho H, Mariotto A, Eisner MP, Lewis DR, Chen HS, Feuer EJ, Cronin KA (eds). http://seer.cancer.gov/csr/1975_2009_pops09/ (May 14).
- (2) Luo, J.; Solimini, N. L.; Elledge, S. J. *Cell* **2009**, *136* (5), 823-837.
- (3) Hanahan, D.; Weinberg, R. A. *Cell* **2000**, *100* (1), 57-70.
- (4) Siegel, R.; Naishadham, D.; Jemal, A. *Ca-Cancer J Clin* **2013**, *63* (1), 11-30.
- (5) National Cancer Institute. <http://www.cancer.gov/cancertopics/cancerlibrary/what-is-cancer> (May 14, 2013).
- (6) Hanahan, D.; Weinberg, R. A. *Cell* **2011**, *144* (5), 646-674.
- (7) Sawyers, C. *Nature* **2004**, *432* (7015), 294-297.
- (8) Jones, D.; Thomas, D.; Yin, C. C.; O'Brien, S.; Cortes, J. E.; Jabbour, E.; Breeden, M.; Giles, F. J.; Zhao, W.; Kantarjian, H. M. *Cancer* **2008**, *113* (5), 985-994.
- (9) Vaidya, S.; Ghosh, K.; Vundinti, B. R. *European Journal of Haematology* **2011**, *87* (5), 381-393.
- (10) NCI Dictionary. <http://www.cancer.gov/dictionary?Cdrid=44179> (May 15, 2013).
- (11) Fvasconcellos. http://en.wikipedia.org/wiki/File:Bcr_abl_STI_1IEP.png (May 15, 2013).

- (12) Gschwind, A.; Fischer, O. M.; Ullrich, A. *Nat Rev Cancer* **2004**, 4 (5), 361-370.
- (13) Paez, J. G.; Janne, P. A.; Lee, J. C.; Tracy, S.; Greulich, H.; Gabriel, S.; Herman, P.; Kaye, F. J.; Lindeman, N.; Boggon, T. J.; Naoki, K.; Sasaki, H.; Fujii, Y.; Eck, M. J.; Sellers, W. R.; Johnson, B. E.; Meyerson, M. *Science* **2004**, 304 (5676), 1497-1500.
- (14) Chan, H. S.; Pitson, S. M. *Bba-Mol Cell Biol L* **2013**, 1831 (1), 147-156.
- (15) Siow, D. L.; Anderson, C. D.; Berdyshev, E. V.; Skobeleva, A.; Natarajan, V.; Pitson, S. M.; Wattenberg, B. W. *Advances in enzyme regulation* **2011**, 51 (1), 229-244.
- (16) Hannun, Y. A.; Obeid, L. M. *Nat. Rev. Mol. Cell Biol.* **2008**, 9 (2), 139-150.
- (17) Wymann, M. P.; Schneider, R. *Nat Rev Mol Cell Bio* **2008**, 9 (2), 162-176.
- (18) Hisano, Y.; Kobayashi, N.; Kawahara, A.; Yamaguchi, A.; Nishi, T. *J Biol Chem* **2011**, 286 (3), 1758-1766.
- (19) Spiegel, S.; Milstien, S. *Nat. Rev. Mol. Cell Biol.* **2003**, 4 (5), 397-407.
- (20) Hla, T.; Lee, M. J.; Ancellin, N.; Paik, J. H.; Kluk, M. J. *Science* **2001**, 294 (5548), 1875-1878.
- (21) Spiegel, S.; Milstien, S. *FEBS Lett.* **2000**, 476 (1-2), 55-57.
- (22) Brinkmann, V. *Pharmacol. Ther.* **2007**, 115 (1), 84-105.
- (23) Maceyka, M.; Harikumar, K. B.; Milstien, S.; Spiegel, S. *Trends in cell biology* **2012**, 22 (1), 50-60.
- (24) Spiegel, S.; Milstien, S. *J. Biol. Chem.* **2002**, 277 (29), 25851-25854.
- (25) Schulze, T.; Golfier, S.; Tabeling, C.; Rabel, K.; Graler, M. H.; Witzenrath, M.; Lipp, M. *Faseb Journal* **2011**, 25 (11), 4024-4036.
- (26) Pyne, N. J.; Pyne, S. *Nat Rev Cancer* **2010**, 10 (7), 489-503.

2

The Sphingosine Kinases

The sphingosine kinases (SphKs) are responsible for the production of S1P, the molecule responsible for pro-survival signaling in normal and diseased cells. This process is deregulated in diseased cells and controlling the production of S1P may be a viable way to control cell fate. Both sphingosine kinase 1 (SphK1) and sphingosine kinase 2 (SphK2) produce S1P, however, S1P produced by SphK1 sends pro-survival signals but S1P produced by SphK2 signals for cell death. The full mechanism of action of each SphK and S1P has not been fully characterized. Selective, potent inhibitors of these enzymes will help to elucidate the functions of these molecules.

2.1 The Sphingosine Kinases

There are two isoforms of the sphingosine kinases, SphK1 and SphK2. SphK1 and SphK2 originate from two distinct genes located on chromosome 17 and 19, respectively.¹ Both of these kinases bind sphingosine and using ATP, attach a phosphate group to the terminal alcohol to produce S1P (Scheme 1.1). Even though these kinases perform the same function, the S1P produced by each has diverse roles due to their difference in cellular localization, adult tissue distribution, and developmental expression.^{2,3}

SphK1 and SphK2 are members of the diacylglycerol kinase family, but even though they have a high degree of sequence homology to other members of the family, they have a unique catalytic domain. The sphingosine kinases have five conserved domains (C1 – C5), but differ enough to indicate they did not arise from a single point mutation (Figure 2.1).³ SphK1 and SphK2 share a sequence homology of 45% overall identity and 80% similarity but SphK2 is approximately 50% larger than SphK1.^{2,4}

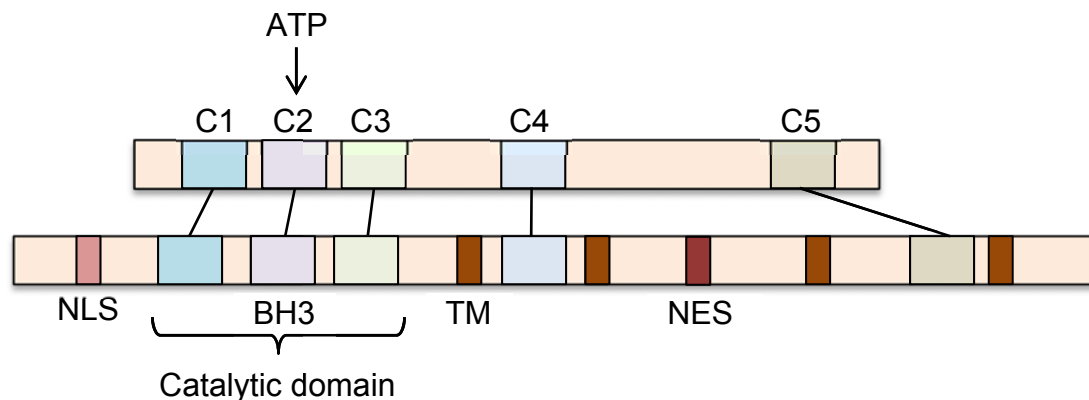


Figure 2.1: General sequence comparison of SphK1 and SphK2. SphK2 is approximately 50% larger than SphK1 and they have five conserved domains, C1 – C5. The ATP binding site is located in the C2 domain. The catalytic domain is unique to these kinases. SphK2 contains four transmembrane regions (TM), a nuclear localization signal (NLS), a nuclear export signal (NES), and a BH3 domain located in the C2 domain. Modified from Spiegel and Neubauer.^{1,3}

The ATP-binding site is conserved across the diacylglycerol family; however, SphK2 contains regions not found in SphK1. It contains four transmembrane regions (TM), a nuclear localization signal (NLS), a nuclear export signal (NES), as well as a BH3 domain.³ The BH3 domain is associated with the pro-apoptotic function of SphK2 because it interacts with Bcl-x_L, which is a member of the pro-survival Bcl-2 family.¹ Most known roles of SphK1 and SphK2 are associated with cell survival; however, these and other recent findings

have shown SphK2 to play an alternative role in promoting apoptosis. It is clear that more research must be done to fully understand the roles these kinases play on cell fate.

Early studies of these enzymes included knockout mice to determine the roles of SphK1 and SphK2 during development. The structural and localization differences between the two kinases implies they produce S1P to perform different functions; however, SphK1^{-/-} and SphK2^{-/-} single-knockout mice developed normally. The levels of S1P circulating were greatly reduced with respect to wild type mice. When both kinases were knocked out of mice, this was embryonically lethal at day 13 due to cranial hemorrhaging. It is clear that the kinases are necessary to produce S1P for proper vasculature development, which correlates well to the function of S1PR₁ and its role in angiogenesis. From these results, it can be concluded that the individual kinases will assume the role of the other and produce enough S1P to perform all necessary functions.⁵ It was discovered, however, that both kinases are expressed throughout embryonic development, but SphK1 peaks earlier and SphK2 did not peak until the later stages of development. From this, it can be concluded that SphK1 is more important for vasculature development and SphK2 may be responsible for other development roles.¹ All of the null mice exhibited reduced cell proliferation and increased cell death implying that inhibition of these kinases may be a good avenue to treat cancer, characterized by uncontrolled cell growth and/or diminished cell death.⁵

2.2 Sphingosine Kinase 1

Of the two isozymes, SphK1 has been studied more extensively since it is responsible for producing the majority of the circulating S1P.⁶ SphK1 is mainly a cytosolic enzyme and its mechanism of action is shown in Figure 1.5.³ The activity of SphK1 is increased through interaction with and phosphorylation by other proteins, in particular ERK1/2, upon extracellular signaling by cytokines and growth factors. Growth factors that participate in the activation of SphK1 are PDGF, nerve growth factor (NGF), EGF, and others.^{2,6,7} In most cases, activation of SphK1 is necessary for the production of S1P. This increases its activity by at least two-fold, which results in a significant increase in cellular and secreted S1P.^{2,7}

Phosphorylation of SphK1 by ERK1/2 at Ser225 results in a 14-fold increase in catalytic activity and does not change its affinity for ATP or sphingosine. Depending on the cellular response desired, particular proteins will interact with SphK1 to increase or decrease its activity. For instance, interaction with Fyn, phosphatidic acid (PA), or phosphatidylserine (PS) will increase its activity, but interaction with PECAM-1 or SKIP decreases its activity. These interactions are not a phosphorylation event, but may regulate the activity by keeping the enzyme in certain locations. For example, once SphK1 is phosphorylated by ERK1/2 it translocates to the inner leaflet of the plasma membrane where it interacts with PA or PS to retain it at that location where it will find sphingosine and fulfill its phosphorylation duties. The translocation of P-SphK1 to the inner leaflet of the plasma membrane is mediated by calcium- and

integrin-binding protein 1 (C1B1).^{2,8} As can be seen, there are many different types of post-translational modifications to SphK1 that mediate its location and ultimately its activity.²

Other enzymes involved in the 'Sphingolipid Rheostat' have been investigated for activation by other proteins, such as sphingomyelinase and ceramidase. It was found, however, that S1P phosphatase and S1P lyase are not regulated by external stimuli suggesting that the natural, low levels of cellular S1P are primarily regulated by its synthesis and not degradation. For this reason, enzymes involved in the production of S1P have received major attention of investigators.⁷

SphK1 is primarily expressed in leukocytes, brain, heart, lung, and spleen tissues.^{1,7} Due to the cell survival and proliferative effects of S1P, SphK1 has recently been a target of interest in cancer research especially since overexpression has been linked to neoplastic transformation.¹ Cancer has many different routes of survival (Figure 1.3) and often these pathways are induced or controlled by the release of growth factors. The growth factors that are responsible for the activation of SphK1 are tightly regulated in different cancer types. For instance, PDGF not only induced migration of cells but also induces the translocation of SphK1 to the cell membrane to increase the pro-survival signaling of S1P.³

In a number of different types of cancer, expression of SphK1 is found to be higher and correlates to poor patient prognosis.¹ The expression of SphK1 has been linked to prostate,^{9,10} breast,^{11,12} stomach,^{11,13} cervical,¹⁴ kidney,¹¹

colon,¹¹ and other cancers.¹⁵⁻¹⁷ Activation of SphK1 is shown to contribute to cancer progression, neoplastic transformation, increased tumor growth, and the reduction of apoptosis. The S1P produced by SphK1 leads to angiogenesis and migration of cells causing cancer to be addicted to SphK1. Recently S1P from SphK1 has been shown to increase resistance to chemotherapies through activation of down-signaling pathways.^{9,18} These effects of S1P make SphK1 a good target to inhibit in the treatment of cancer.

2.3 Sphingosine Kinase 2

The lesser studied of the two kinases, SphK2, has a very interesting story to tell. It was originally thought that SphK1 should be the main target for a cancer therapeutic, but SphK2 has recently emerged with fascinating characteristics. Both kinases produce S1P in a similar manner to function as a pro-survival signal, but some S1P synthesized by SphK2 causes cell cycle arrest and eventually apoptosis. This is counter to other known pro-survival functions of S1P and may possibly be due to the cellular location of its synthesis. With its charged head and non-polar tail, S1P is not normally found in the cytosol, but associates to membranes and other more non-polar molecules. For this reason, it usually acts upon a target at the location in which it is synthesized and may be the reason for the different cellular responses observed.¹

SphK2 is located in the cytosol as well as associated to membranes, whereas, SphK1 is only found in the cytosol. Unlike SphK1, SphK2 contains transmembrane regions in its sequence, causing it to associate to membranes in

the nucleus, endoplasmic reticulum (ER), and the mitochondria.¹⁹ The function of SphK2 is much like SphK1 since extracellular molecules enhance its activity. EGF and other molecules have been shown to enhance the phosphorylation of Ser351 or Thr578 by ERK1/2 on SphK2. At this point, SphK2 can operate in the same manner as SphK1, or it can translocate to the ER, nucleus, or mitochondria (Figure 2.2). It is still unclear what protein mediates this movement, but it appears as though the NLS and NES of SphK2 play parts in locating the enzyme in the nucleus.²

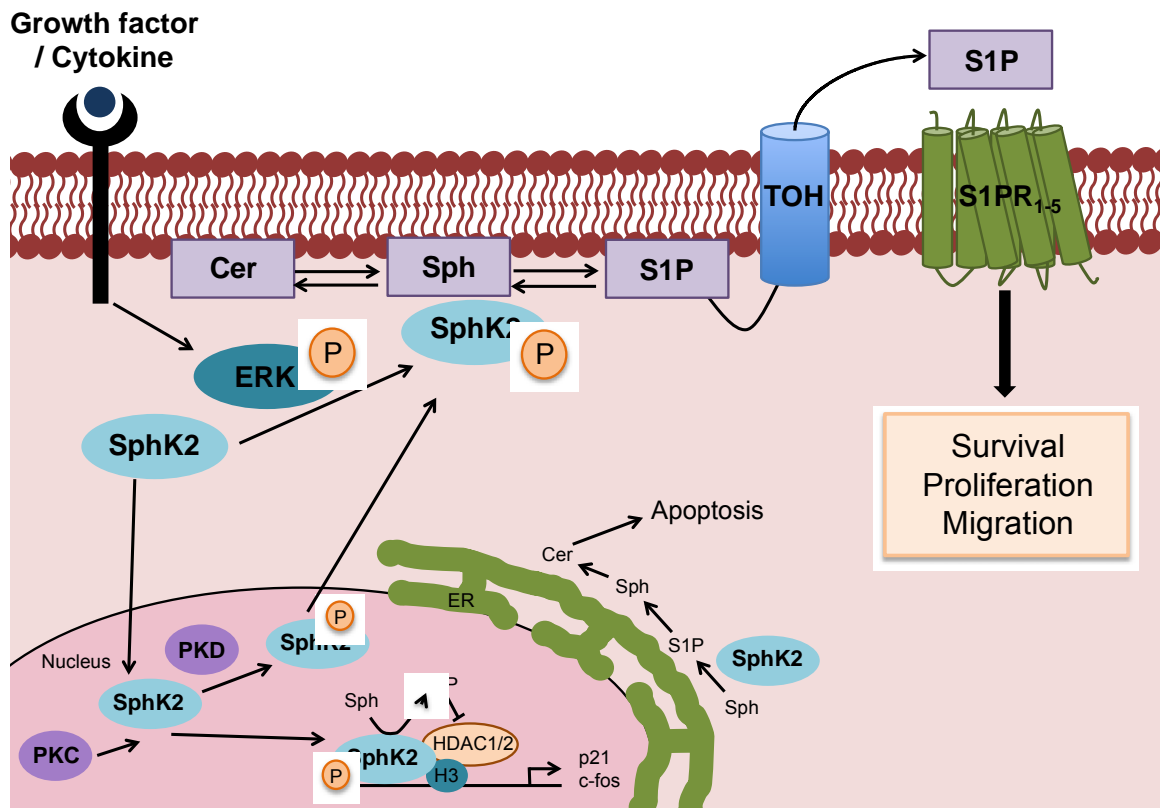


Figure 2.2: Signaling of S1P produced by SphK2. Upon extracellular signaling, SphK2 is phosphorylated by ERK1/2 increasing its activity to produce S1P or initiating its translocation to various organelles. Protein kinase C (PKC) promotes P-SphK2 to bind to histone 3 (H3) where S1P inhibits histone deacetylase 1/2 (HDAC1/2) leading to the transcription of cyclin-dependent kinase inhibitor p21 and transcriptional regulator c-fos. When localized in the ER, the S1P produced fuels a sphingosine (Sph) salvage pathway to ceramide (Cer) leading to apoptosis. Cytosolic SphK2 will move to the inner leaflet of the plasma membrane where it will produce S1P that is transported out of the cell by the 'Two of Hearts' transporter where it binds to S1PR₁₋₅. Modified from Neubauer and Pitson.

As with SphK1, SphK2 will also interact with other proteins to regulate its function. SphK2 contains a BH3 region in its C2 domain. This region of its sequence interacts with Bcl-x_L, a member of the pro-survival Bcl-2 family and leads to apoptosis.²⁰ This interaction was only observed under the forced overexpression of SphK2; thus, further investigation must be completed to determine if this is observed in cells with normal levels of SphK2.^{1,2,21}

Under stress conditions, SphK2 will localize in the ER where S1P produced will fuel a sphingosine recovery pathway to generate ceramide leading to apoptosis. When SphK2 is localized in the mitochondria, the S1P produced promotes apoptosis by interaction with BAK and increasing the permeability of the membrane releasing cytochrome c. Only SphK2 has the ability to localize in these organelles and thus it can promote apoptosis, unlike SphK1.¹ Nuclear SphK2 interacts with HDAC1/2 on histone 3 where S1P binds to HDAC1/2 preventing the deacetylation of DNA leading to transcription of cyclin-dependent kinase inhibitor p21 and the transcriptional regulator c-fos.^{1,2,22} While in the nucleus, the export of SphK2 is mediated by protein kinase D (PKD).^{1,2,23}

Another interesting function of SphK2 is the ability for it to be cleaved by caspase-1 allowing it to be released from apoptotic cells. Upon exportation, it will bind to phosphatidylserine on the outer surface of the plasma membrane. S1P produced extracellularly has been linked to immune cell infiltration.^{1,2}

The pro-apoptotic functions of S1P produced by SphK2 may imply that it would not be a target of inhibition in hyperproliferative disease. Localization of the enzyme is tissue dependent and in the future it may be possible to interrupt

the interaction with membranes increasing its expression in the cytosol. Once able to do this, a small molecule inhibitor could be used to increase apoptosis in cancerous cells as with SphK1. Preliminary studies have shown that the BH3 domain as well as the cellular location of SphK2 is involved in cellular proliferation and chemoresistant mechanisms in cancer. It may become important to take advantage of this due to the increase in therapeutic resistance when treating cancers.²¹ Other studies have shown that inhibition of SphK2 leads to apoptosis, reduction in tumor cell proliferation, and migration in cancer.¹⁹ Interestingly, Kharel *et al.* showed inhibition of SphK2 in whole animal leads to an increase in circulating S1P. This is thought to result in an increase in SphK1 activity but further studies need to be conducted to rule out other causes.²⁴

Expression of SphK2 occurs in many different tissue types but is highest in liver and kidney.¹ The enzyme has been linked to tumors found in breast,^{21,25,26} kidney,²⁷ pancreatic,²⁷ liver,²⁸ glial,²⁹ and colon cells.³⁰ Many of the studies investigating the role of SphK2 in these diseases have used knockdown studies. It is interesting that in SphK2-null mice expressing glioblastoma tumors, cell proliferation was decreased and apoptosis increased.^{16,29} In MCF-7 breast cancer tumors, inhibition of SphK2 has shown to control tumor growth.^{16,31} From these and other studies, it is evident that inhibition of SphK2 may in fact be a viable option for cancer treatment. It has been proposed that inhibition of SphK2 production of S1P, while not limiting the effect of the BH3 domain, may be the best route to target SphK2 in cancer.³²

2.4 The Sphingosine Kinases and Non-Cancerous Diseases

Cancer is not the only disease researchers are investigating uses of inhibitors of the SphKs. S1P and these enzymes have been linked to many other diseases such as, multiple sclerosis³³, arthritis³⁴, and ischemia/reperfusion injuries³⁵. Rheumatoid Arthritis (RA) has higher levels of S1P than other forms of arthritis, and S1P levels are reduced using known SphK inhibitors. Knockdown of SphK1 has resulted in lower S1P, suppression of synovial inflammation, joint erosion, and pro-inflammatory cytokine responses. In SphK2-null mice, RA is much more severe, thus linking both enzymes to the disease.³⁴ It is clear that an inhibitor of SphK1 and not SphK2 may be useful in treating RA.

The investigation of the roles of S1P and the SphKs in multiple sclerosis (MS) has been on going for many years. Fingolimod (Gilenya™, Novartis) has been extensively investigated for the treatment of MS and gained FDA approval in 2010 (Figure 2.3). This molecule is phosphorylated by SphK2 and then binds to four of the five S1PRs resulting in the ubiquitin-mediated degradation of S1PR₁ and the inability of lymphocytes to leave lymphoid tissues thus reducing the inflammatory response.¹⁹ Perhaps, reducing the production of S1P by inhibiting the SphKs would also be an avenue for treating this disease.

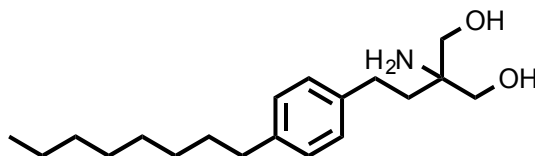


Figure 2.3: Fingolimod (Gilenya™, Novartis) also known as FTY720. FDA approved for the treatment of multiple sclerosis.

Recently it has been shown that SphK2 plays a vital role in protection during ischemia/reperfusion (IR) injury. SphK2-null mice displayed 25% larger ischemia lesions than wild-type mice.³⁶ Another study shows that after IR, the expression of S1P is higher due to an up-regulation of SphK2 and leads to mitochondrial permeability transition (MPT). This reduces the membrane potential, reduction in oxidative phosphorylation, initiates necrotic cell death, and ultimately the release of cytochrome c, triggering apoptosis.³⁷ Studies have shown that the production of S1P by SphK2 in the mitochondria helps to protect tissue by preconditioning against IR. SphK2-null mice had an increase in myocardial injury due to the lack of preconditioning.^{38,39} More research will need to be conducted on the kinases' involvement in this and other diseases to fully understand its roles.

2.5 Current Inhibitors in the Literature

Through the vast studies of S1P and the SphKs, it is clear that they are involved in many different cellular processes in normal and diseased cells. They contribute to the initiation, maintenance, and progression of disease and their roles may fully be understood with the use of dual and subtype-selective inhibitors. The discovery of potent inhibitors may be useful in the treatment of diseases such as cancer and inflammatory diseases. Early development of kinase inhibitors targeted the ATP-binding site; however, all kinases use ATP to function, and thus many off-target effects were observed with these inhibitors. The ATP-binding site is often still targeted, but many have turned to targeting the

substrate-binding pocket of the SphKs as a means to more selectively inhibit these enzymes.

2.5.1 Sphingosine-based Inhibitors

The earliest inhibitors of the SphKs were designed from the structure of sphingosine. The first inhibitor discovered was DL-*threo*-dihydrosphingosine (DHS) (Figure 2.4), which is a competitive inhibitor selective for SphK1 with a moderately potent K_i value of 3-6 μ M. It will also bind to SphK2, but acts as a substrate instead of an inhibitor and becomes integrated into the 'Sphingolipid Rheostat'. The L-*threo*-DHS is not selective for the SphKs and inhibits other kinases such as PKC. This makes DHS not an ideal inhibitor to probe the roles of these enzymes or to act as a therapeutic.¹⁹

Perhaps the most studied of all of the SphK inhibitors, N,N-dimethylsphingosine (DMS) (Figure 2.4), is a moderately potent inhibitor of both kinases. It inhibits SphK1 ($K_i = 5 \mu$ M) competitively and SphK2 ($K_i = 12 \mu$ M) non-competitively but was originally developed to be an inhibitor of PKC. Due to this, DMS has off-target effects by inhibiting other kinases including ceramide kinase, PKC, MAPK and activates kinases such as phosphatidylinositol kinase and EGFR.¹⁹ DMS and DHS both inhibit cell growth and induce apoptosis in many different cancer cells including colon⁴⁰, breast⁴¹, prostate⁴², gastric⁴⁰, and lung⁴³. Neither inhibitor is a good tool to elucidate the roles of the SphKs, but despite this, DMS is the industry standard since it has been vastly researched.^{19,44}

In an effort to synthesize an inhibitor that resembles the natural substrate, sphingosine, Wong *et al* developed inhibitors that would be more selective for the SphKs in comparison to DHS and DMS. This would allow researchers to properly probe the roles of these enzymes without having to worry about off-target effects. During the development of their molecules, the researchers tested the precursors of their target compounds for their effectiveness as inhibitors of the SphKs. It turned out that one of the intermediates inhibited the SphKs twice as well as other molecules tested. **Wong 5c** (Figure 2.4) was tested against U937 cells displaying an IC_{50} value of 3.3 μ M at SphK1.⁴⁵ This molecule is less toxic than DMS and is specific for SphK1 having K_i values of 15 μ M and 46 μ M at SphK1 and SphK2, respectively.^{45,46} This inhibitor has the potential to be a good tool to fully understand the functions of SphK1.

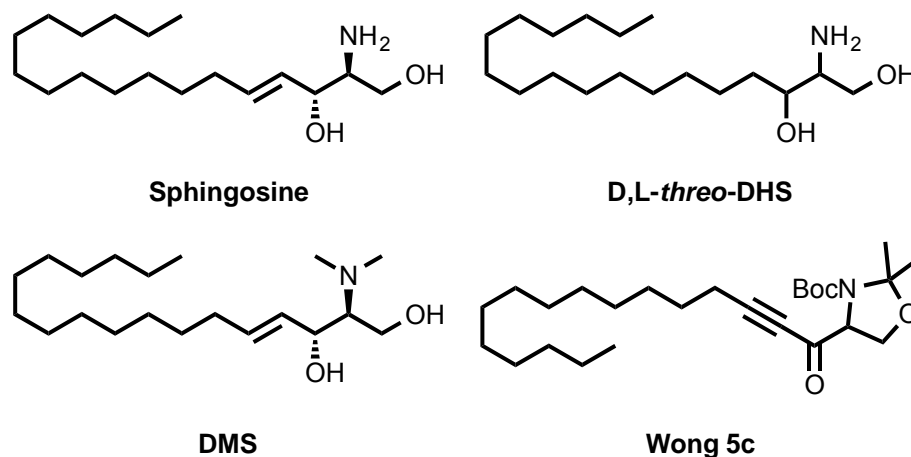


Figure 2.4: Structures of Sphingosine-based inhibitors.

2.5.2 Analogs of Fingolimod as Inhibitors

Fingolimod (FTY720) is a known substrate of SphK2 and thus a natural molecule to begin designing inhibitors. The majority of inhibitors designed from Fingolimod are more potent than DMS. The (*S*)-FTY720-vinylphosphonate (Figure 2.5) inhibits recombinant SphK1 ($K_i = 15 \mu\text{M}$) and ultimately leads to the degradation of the enzyme in cells but is also an antagonist at all five S1PRs. Once again these off-target effects may not make this molecule an ideal inhibitor.¹⁹

A moderately potent competitive inhibitor of SphK2 is (*R*)-FTY720-OMe with K_i values of $50 \mu\text{M}$ and $16.5 \mu\text{M}$ at SphK1 and SphK2, respectively (Figure 2.5). This molecule blocks the phosphorylation event with SphK2 since the hydroxyl of Fingolimod that is converted to a phosphate is replaced with a methoxy group.^{1,19} Preliminary studies have shown promise in using this inhibitor to investigate SphK2 by inducing ubiquitin-mediated SphK2 degradation in MCF-7 breast cancer cells.^{19,47} This decrease in SphK2 expression in LNCaP prostate cancer cells stimulates autophagy but not apoptosis.¹

BML-258 (**SK1-I**) (Figure 2.5) is a molecule selective for SphK1 over other kinases with a K_i value of $10 \mu\text{M}$. This molecule inhibited the growth and survival of leukemia xenograph tumors as well as inhibition of angiogenesis and lymphangiogenesis in breast cancer cells. The use of this inhibitor resulted in the down regulation of ERK and Akt, which are pro-survival signaling pathways.¹⁹ This molecule displays selectivity for SphK1 and is a good tool to investigate the

enzyme, but herein are described SphK1-selective inhibitors that are much more potent.

Researchers at Genzyme developed inhibitors similar to FTY720 using available amino acids. **9ab** (Figure 2.5) was their most potent inhibitor displaying selectivity for SphK1 over SphK2 with K_i values of 1.4 μM and 31 μM , respectively, which is much more potent and selective than DMS.^{44,46} During the development of their series, they determined that the amide bond was essential for activity at the kinases.⁴⁴ Once the structure is fully optimized, the potency may increase making it an excellent tool to investigate the role of SphK1 in the 'Sphingolipid Rheostat'.

Also, this scaffold was used to develop SphK2-selective inhibitors SLR080811 (**BD-10**), **SG-12**, and **trans-12a**. **BD-10** is a competitive inhibitor with respect to sphingosine with a K_i of 12 μM for SphK1 and 1.3 μM for SphK2. This molecule lowers S1P levels in U937 cells but does not have an effect of survival or proliferation. When dosed *in vivo*, **BD-10** raised circulating S1P levels with respect to wild type mice, which has not been observed with the use of other SphK2-selective inhibitors. This result correlates to S1P levels observed with SphK2^{-/-} mice. Further investigation is underway to fully understand these results.^{1,24}

To combine the structures of sphingosine and FTY720, **SG-12** was synthesized and displayed no activity against SphK1. Its IC_{50} value at SphK2 is 22 μM . This molecule also displays inhibition of PKC and is phosphorylated by SphK2 inducing cell death. These effects make it a non-ideal candidate to probe

the roles of SphK2.^{20,48} A molecule containing a quaternary salt at the warhead was synthesized and labeled **trans-12a** (Figure 2.5). The inhibitor is moderately potent with K_i values for SphK1 and SphK2 being 60 μ M and 8 μ M, respectively. Upon testing in U937 leukemia cells, S1P levels were not altered but when dosed alongside FTY720, there was a marked reduction in FTY720-P produced implying inhibition of SphK2.⁴⁹

Bitman and Pyne have recently developed a SphK1 selective inhibitor that displays results similar to (S)-FTY720-vinylphosphonate, **RB-005** (Figure 2.5). Of all the molecules synthesized in this series, **RB-005** was the most effective in preventing the synthesis of S1P by 95% and 60% at SphK1 and SphK2, respectively, when dosed at 50 nM. It has an IC_{50} value of 3.6 nM at SphK1 in HEK 293 cell lysates. In this series, the size of the heterocyclic ring was important for selectivity and changes to substituents on the ring drastically altered the selectivity and potency. As with (S)-FTY720-vinylphosphonate, **RB-005** promotes the degradation of SphK1 in cells and since this molecule also has an alcohol as the warhead, it could act as a substrate of the SphKs and then act as an antagonist at the receptors.⁵⁰ This molecule is one of the least potent SphK1-selective inhibitors in the literature, but once optimized, the potency will increase and the full function of this molecule can be determined.

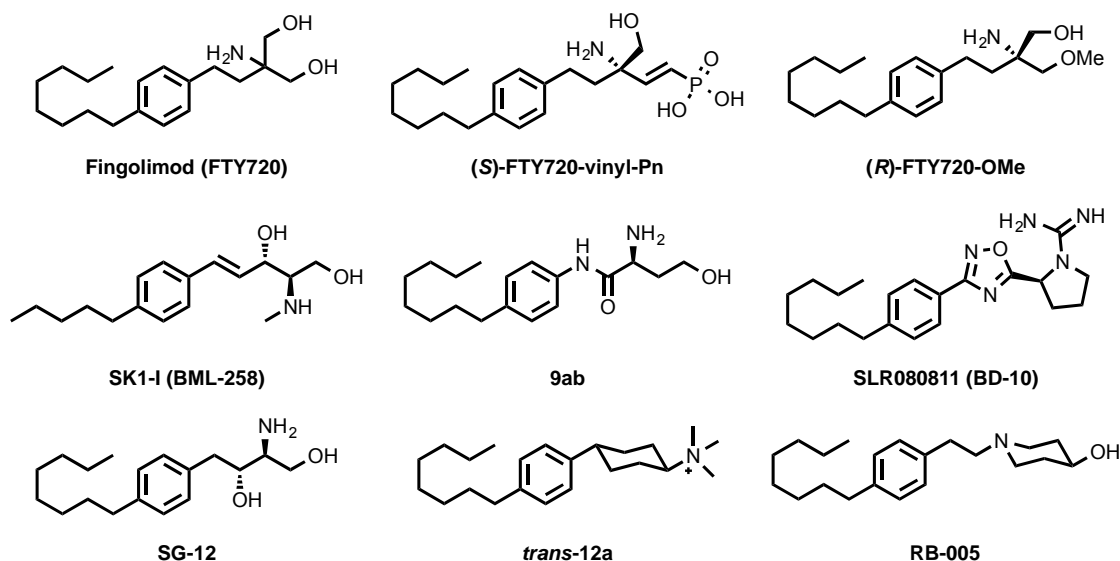


Figure 2.5: Structures of inhibitors based on the structure of Fingolimod.

2.5.3 Non-lipid Inhibitors

Most developed SphK inhibitors are lipid-like with a non-polar alkyl tail and a more polar head group. A group at Penn State has been developing non-lipid molecules as inhibitors of the SphKs. These molecules tend to be polyaromatic thus possibly targeting the ATP-binding site and causing off-target effects. One of the most studied of the SKi molecules is **SKi-II** (Figure 2.6). This molecule is a competitive inhibitor at SphK1 with a K_i value of 17 μM and a non-competitive inhibitor at SphK2 with a K_i value of 48 μM .¹⁹ Early studies showed this molecule to be highly selective for SphK1 and not effective toward other kinases.⁵¹ More recent studies have shown this molecule to be a dual SphK1 and SphK2 inhibitor.¹⁷ **SKi-II** has good oral bioavailability reducing cellular S1P, proliferation, and induces apoptosis in many different cell lines thought to be the result of the degradation of SphK1.^{17,19,51}

Another inhibitor in the SKi series is **SKi-I** (Figure 2.6). This molecule is slightly more effective than **SKi-II** but is not as orally bioavailable. In an effort to increase this, optimization of this molecule led to the synthesis of **SKi-178** (Figure 2.6). **SKi-178** contains methyl and methoxy groups, enhancing its pharmacological properties, decreasing cytotoxicity, and increasing SphK1-selectivity. This molecule is competitive with sphingosine and has a K_i value of 1.3 μ M at SphK1 and is the first SphK1-selective non-lipid-based inhibitor.¹⁹

One of the most successful inhibitor developed is **ABC294640** (Figure 2.6), which is a SphK2-selective inhibitor with a K_i value of 9.8 μ M and shows no effect on SphK1.^{1,19} Upon its discovery in 2009, it has been used to uncover many unknown functions of SphK2 as well as show potential as a therapeutic in many diseases such as cancer and inflammatory diseases.^{1,19} It promotes cell death in both apoptotic and non-apoptotic manners, reduces chemo resistance in breast cancer,²¹ and works in concert with chemotherapies to decrease pro-survival signals in hepatocellular cancer.²⁸ Estrogen and its E2 receptor have been implicated in breast cancer and **ABC294640** displays antagonism at the E2 receptor. This may cause problems when using this inhibitor to study cancer, but it has shown positive results when treating endocrine-related diseases. In diseases such as thyroid, prostate, ovarian, and breast cancers, steroid hormones and sphingolipids are deregulated and **ABC294640** may be a useful tool to inhibit the SphKs and alter E2 signaling due to an increase in resistance to current therapeutics.⁵²

A group at Pfizer developed a SphK1-selective inhibitor, **PF-543** (Figure 2.6), that is competitive with sphingosine with a K_i value of 3.6 nM and over 100-fold selective over SphK2. It, unlike other potent SphK1-selective inhibitors, is able to easily enter U937 cells and decrease proliferation and in 1483 head and neck carcinoma cells it reduces S1P levels greater than 90%. Even though this molecule is polyaromatic, studies do not show it being competitive with ATP allowing it to be highly specific for SphK1. This is the most potent and selective inhibitor of SphK1 in the literature.⁵³

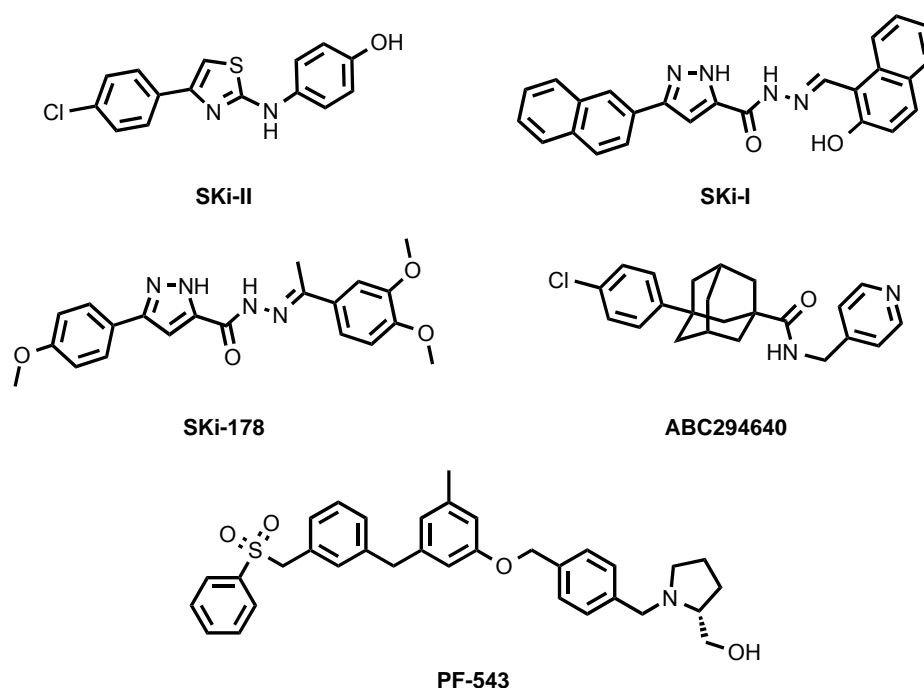


Figure 2.6: Structures of non-lipid SphK inhibitors.

2.5.4 Natural Product Inhibitors

The final class of SphK inhibitors is natural products that have been isolated from bacteria and fungi and are the least characterized. Isolated from a

marine bacterium, **B-5354** is a dual inhibitor of the SphKs with a K_i value of 3 μM and is non-competitive with respect to sphingosine. This molecule has demonstrated the ability to sensitize prostate cancer cells to chemotherapies. Another natural product is **F-12509A**, which is a competitive dual inhibitor inducing apoptosis. It was isolated from *Trichopexixella barbata*. **S-15183a/b** were isolated from fungus *Zopfiella inermis* and their specificity has not yet been determined, though, they have been found to reduce S1P formation in platelets. All of these molecules need to be further characterized to determine their effectiveness as therapeutics by inhibiting the SphKs.^{15,19}

2.6 Conclusion

The Sphingosine kinases are the switch that controls the fate of cells. This is especially true in diseases that deregulate the 'Sphingolipid Rheostat', such as cancer and autoimmune diseases. Since the SphKs control the production of the pro-survival molecule S1P, by inhibiting their activity, it may be possible to develop a targeted therapy against these diseases. Progress has been made in this direction over the past 20 years with the development of inhibitors resembling sphingosine and Fingolimod, non-lipid molecules, and natural products, but the effectiveness of many of these molecules is limited by off-target effects. The research herein describes the development of some of the most potent and selective inhibitors of the SphKs using an amidine warhead and have not yet been found to bind to other cellular proteins. The hurdle now facing researchers is correlating the effects observed *in vitro* with those found *in vivo*.

Once this has been accomplished, it will be possible to further elucidate the roles of each of the SphKs as well as S1P in normal and diseased cells.

2.7 References

- (1) Neubauer, H. A.; Pitson, S. M. *FEBS J* **2013**.
- (2) Chan, H. S.; Pitson, S. M. *Bba-Mol Cell Biol L* **2013**, 1831 (1), 147-156.
- (3) Spiegel, S.; Milstien, S. *Nat. Rev. Mol. Cell Biol.* **2003**, 4 (5), 397-407.
- (4) Gao, P.; Peterson, Y. K.; Smith, R. A.; Smith, C. D. *PLoS One* **2012**, 7 (9), e44543.
- (5) Mizugishi, K.; Yamashita, T.; Olivera, A.; Miller, G.; Spiegel, S.; Proia, R. *Mol. Cell Biol.* **2005**, 25 (24), 11113-11121.
- (6) Kharel, Y.; Mathews, T. P.; Gellett, A. M.; Tomsig, J. L.; Kennedy, P. C.; Moyer, M. L.; Macdonald, T. L.; Lynch, K. R. *Biochem J* **2011**, 440 (3), 345-353.
- (7) Maceyka, M.; Payne, S. G.; Milstien, S.; Spiegel, S. *Biochim. Biophys. Acta* **2002**, 1585 (2-3), 193-201.
- (8) Baker, D. L.; Pham, T. C.; Sparks, M. A. *Biochim Biophys Acta* **2013**, 1831 (1), 139-146.
- (9) Pchejetski, D.; Bohler, T.; Stebbing, J.; Waxman, J. *Nat Rev Urol* **2011**, 8 (10), 569-578.
- (10) Baek, D. J.; MacRitchie, N.; Pyne, N. J.; Pyne, S.; Bittman, R. *Chem Commun* **2013**, 49 (21), 2136-2138.
- (11) French, K. J.; Schrecengost, R. S.; Lee, B. D.; Zhuang, Y.; Smith, S. N.; Eberly, J. L.; Yun, J. K.; Smith, C. D. *Cancer Research* **2003**, 63 (18), 5962-5969.
- (12) Erez-Roman, R.; Pienik, R.; Futerman, A. H. *Biochem Bioph Res Co* **2010**, 391 (1), 219-223.
- (13) Li, W.; Yu, C. P.; Xia, J. T.; Zhang, L.; Weng, G. X.; Zheng, H. Q.; Kong, Q. L.; Hu, L. J.; Zeng, M. S.; Zeng, Y. X.; Li, M. F.; Li, J.; Song, L. B. *Clinical Cancer Research* **2009**, 15 (4), 1393-1399.
- (14) Wong, Y. F.; Selvanayagam, Z. E.; Wei, N.; Porter, J.; Vittal, R.; Hu, R.; Lin, Y.; Liao, J.; Shih, J. W.; Cheung, T. H.; Lo, K. W. K.; Yim, S. F.; Yip, S. K.; Ngong, D. T.; Siu, N.; Chan, L. K. Y.; Chan, C. S.; Kong, T.; Kutlina, E.; McKinnon, R. D.; Denhardt, D. T.; Chin, K. V.; Chung, T. K. H. *Clinical Cancer Research* **2003**, 9 (15), 5486-5492.
- (15) Pyne, N. J.; Pyne, S. *Nat Rev Cancer* **2010**, 10 (7), 489-503.
- (16) Shida, D.; Takabe, K.; Kapitonov, D.; Milstien, S.; Spiegel, S. *Curr. Drug Targets* **2008**, 9 (8), 662-673.
- (17) Pyne, S.; Bittman, R.; Pyne, N. J. *Cancer Res* **2011**, 71 (21), 6576-6582.

- (18) Sharma, A. K.; Sk, U. H.; Gimbor, M. A.; Hengst, J. A.; Wang, X. J.; Yun, J.; Amin, S. *Eur J Med Chem* **2010**, *45* (9), 4149-4156.
- (19) Orr Gandy, K. A.; Obeid, L. M. *Biochim Biophys Acta* **2013**, *1831* (1), 157-166.
- (20) Hara-Yokoyama, M.; Terasawa, K.; Ichinose, S.; Watanabe, A.; Podyma-Inoue, K. A.; Akiyoshi, K.; Igarashi, Y.; Yanagishita, M. *Bioorganic & Medicinal Chemistry Letters* **2013**, *23* (7), 2220-2224.
- (21) Antoon, J. W.; White, M. D.; Slaughter, E. M.; Driver, J. L.; Khalili, H. S.; Elliott, S.; Smith, C. D.; Burow, M. E.; Beckman, B. S. *Cancer Biology & Therapy* **2011**, *11* (7), 678-689.
- (22) Hait, N. C.; Allegood, J.; Maceyka, M.; Strub, G. M.; Harikumar, K. B.; Singh, S. K.; Luo, C.; Marmorstein, R.; Kordula, T.; Milstien, S.; Spiegel, S. *Science* **2009**, *325* (5945), 1254-1257.
- (23) Ding, G.; Sonoda, H.; Yu, H.; Kajimoto, T.; Goparaju, S. K.; Jahangeer, S.; Okada, T.; Nakamura, S. *J Biol Chem* **2007**, *282* (37), 27493-27502.
- (24) Kharel, Y.; Raje, M.; Gao, M.; Gellett, A. M.; Tomsig, J. L.; Lynch, K. R.; Santos, W. L. *Biochem J* **2012**, *447* (1), 149-157.
- (25) French, K. J.; Zhuang, Y.; Maines, L. W.; Gao, P.; Wang, W.; Beljanski, V.; Upson, J. J.; Green, C. L.; Keller, S. N.; Smith, C. D. *J Pharmacol Exp Ther* **2010**, *333* (1), 129-139.
- (26) Antoon, J. W.; White, M. D.; Driver, J. L.; Burow, M. E.; Beckman, B. S. *Exp Biol Med* **2012**, *237* (7), 832-844.
- (27) Beljanski, V.; Knaak, C.; Zhuang, Y.; Smith, C. D. *Invest New Drug* **2011**, *29* (6), 1132-1142.
- (28) Beljanski, V.; Lewis, C. S.; Smith, C. D. *Cancer Biology & Therapy* **2011**, *11* (5), 524-534.
- (29) Van Brocklyn, J. R.; Jackson, C. A.; Pearl, D. K.; Kotur, M. S.; Snyder, P. J.; Prior, T. W. *J Neuropathol Exp Neurol* **2005**, *64* (8), 695-705.
- (30) Chumanevich, A. A.; Poudyal, D.; Cui, X.; Davis, T.; Wood, P. A.; Smith, C. D.; Hofseth, L. J. *Carcinogenesis* **2010**, *31* (10), 1787-1793.
- (31) Weigert, A.; Schiffmann, S.; Sekar, D.; Ley, S.; Menrad, H.; Werno, C.; Grosch, S.; Geisslinger, G.; Brune, B. *Int J Cancer* **2009**, *125* (9), 2114-2121.
- (32) Gao, P.; Smith, C. D. *Mol Cancer Res* **2011**, *9* (11), 1509-1519.
- (33) Brinkmann, V. *Pharmacol. Ther.* **2007**, *115* (1), 84-105.
- (34) Lai, W. Q.; Irwan, A. W.; Goh, H. H.; Melendez, A. J.; McInnes, I. B.; Leung, B. P. *J Immunol* **2009**, *183* (3), 2097-2103.
- (35) Yung, L. M.; Wei, Y.; Qin, T.; Wang, Y.; Smith, C. D.; Waeber, C. *Stroke; a journal of cerebral circulation* **2012**, *43* (1), 199-204.
- (36) Pfeilschifter, W.; Czech-Zechmeister, B.; Sujak, M.; Mirceska, A.; Koch, A.; Rami, A.; Steinmetz, H.; Foerch, C.; Huwiler, A.; Pfeilschifter, J. *Biochem Biophys Res Commun* **2011**, *413* (2), 212-217.
- (37) Shi, Y. J.; Rehman, H.; Ramshesh, V. K.; Schwartz, J.; Liu, Q. L.; Krishnasamy, Y.; Zhang, X.; Lemasters, J. J.; Smith, C. D.; Zhong, Z. *Journal of Hepatology* **2012**, *56* (1), 137-145.

- (38) Gomez, L.; Paillard, M.; Price, M.; Chen, Q.; Teixeira, G.; Spiegel, S.; Lesnefsky, E. J. *Basic Res Cardiol* **2011**, *106* 1341-1353.
- (39) Vessey, D. A.; Li, L.; Jin, Z.; Kelley, M.; Honbo, N.; Zhang, J.; Karliner, J. S. *Oxid Med Cell Longev* **2011**, 2011 1-?
- (40) Sweeney, E. A.; Sakakura, C.; Shirahama, T.; Masamune, A.; Ohta, H.; Hakomori, S.; Igarashi, Y. *International Journal of Cancer* **1996**, *66* (3), 358-366.
- (41) Nava, V. E.; Hobson, J. P.; Murthy, S.; Milstien, S.; Spiegel, S. *Exp Cell Res* **2002**, *281* (1), 115-127.
- (42) Nava, V. E.; Cuvillier, O.; Edsall, L. C.; Kimura, K.; Milstien, S.; Gelmann, E. P.; Spiegel, S. *Cancer Research* **2000**, *60* (16), 4468-4474.
- (43) Endo, K.; Igarashi, Y.; Nisar, M.; Zhou, Q. H.; Hakomori, S. I. *Cancer Research* **1991**, *51* (6), 1613-1618.
- (44) Xiang, Y.; Asmussen, G.; Booker, M.; Hirth, B.; Kane, J. L., Jr.; Liao, J.; Noson, K. D.; Yee, C. *Bioorg Med Chem Lett* **2009**, *19* (21), 6119-6121.
- (45) Wong, L.; Tan, S. S. L.; Lam, Y.; Melendez, A. J. *J. Med. Chem.* **2009**, *52* 3618-3626.
- (46) Kharel, Y.; Mathews, T. P.; Kennedy, A. J.; Houck, J. D.; Macdonald, T. L.; Lynch, K. R. *Analytical biochemistry* **2011**, *411* (2), 230-235.
- (47) Lim, K. G.; Sun, C.; Bittman, R.; Pyne, N. J.; Pyne, S. *Cellular signalling* **2011**, *23* (10), 1590-1595.
- (48) Kim, J. W.; Kim, Y. W.; Inagaki, Y.; Hwang, Y. A.; Mitsutake, S.; Ryu, Y. W.; Lee, W. K.; Ha, H. J.; Park, C. S.; Igarashi, Y. *Bioorgan Med Chem* **2005**, *13* (10), 3475-3485.
- (49) Rajee, M. R.; Knott, K.; Kharel, Y.; Bissel, P.; Lynch, K. R.; Santos, W. L. *Bioorg Med Chem* **2012**, *20* (1), 183-194.
- (50) Baek, D. J.; MacRitchie, N.; Pyne, N. J.; Pyne, S.; Bittman, R. *Chem. Commun.* **2013**, 49 2136-2138.
- (51) Sharma, A.; Sk, U. H.; Gimbor, M. A.; Hengst, J. A.; Wang, X.; Yun, J.; Amin, S. *Eur J Med Chem* **2010**, *45* 4149-4156.
- (52) Antoon, J. W.; White, M. D.; Meacham, W. D.; Slaughter, E. M.; Muir, S. E.; Elliott, S.; Rhodes, L. V.; Ashe, H. B.; Wiese, T. E.; Smith, C. D.; Burow, M. E.; Beckman, B. S. *Endocrinology* **2010**, *151* (11), 5124-5135.
- (53) Schnute, M. E.; McReynolds, M. D.; Kasten, T.; Yates, M.; Jerome, G.; Rains, J. W.; Hall, T.; Chernick, J.; Krauss, M.; Cronin, C. N.; Saabye, M.; Highkin, M. K.; Broadus, R.; Ogawa, S.; Cukyrne, K.; Zawadzke, L. E.; Peterkin, V.; Iyanar, K.; Scholten, J. A.; Wendling, J.; Fujiwara, H.; Nemorovski, O.; Wittwer, A. J.; Nagiec, M. *Biochem J* **2012**, *444* 79-88.

#

#

3

Discovery and Optimization of Amidine-based Sphingosine Kinase Inhibitors

Often when designing inhibitors of kinases, the ATP binding site is targeted. The ATP binding site is conserved for many families of kinases, therefore, it is often difficult to selectively target the kinase of choice. Since this is the case for the sphingosine kinases, our lab has set out to design inhibitors targeting the substrate-binding domain in hopes of synthesizing three different inhibitors: dual and subtype selective inhibitors. There is still much unknown of SphK1 and SphK2; thus, potent subtype-selective inhibitors will be able to assist in elucidating their roles in normal and diseased cells. The design of inhibitors was based on substrates of the SphKs and, using classical structure-activity relationships (SARs), we were able to elucidate the pharmacophores of inhibitors and eventually achieve two of our goals: a dual and SphK1-selective inhibitors.

3.1 From Substrates to Inhibitors

One strategy for attenuating the signaling effects of S1P is to synthesize agonists and antagonists of the S1P receptors. There have been significant advances in this field, most notably the identification of **FTY720** that is a substrate for SphK2 and a potent S1P₁ agonist.^{1,2} The Macdonald and Lynch

labs designed and synthesized analogs of sphingosine 1-phosphate and **FTY720** to improve the potency and efficacy at the S1P receptors.³⁻⁷

To determine the efficacy of the molecules as possible agonists and antagonists of the S1P receptors, we first ensured their ability to act as substrates for both SphK1 and SphK2. As found in the literature, as well as through our studies, it is difficult to develop novel SphK1 substrates, as most of them are predominantly phosphorylated by SphK2.⁷⁻⁹ We did find, however, the 5-phenyl-1,2,4-oxadiazole substrate (Figure 3.1) did have activity at both kinases while similar scaffolds had no activity at SphK1.^{7,8}

Even though these heterocycle-based substrates gave great insight into the structure-activity relationships of the SphKs, they were poor receptor agonists. Using this new information, it was hypothesized that by removing the methylene hydroxyl from the scaffold, thus removing the site of phosphorylation, we could design and synthesize SphK inhibitors that would target the substrate-binding domain (Figure 3.1).⁸

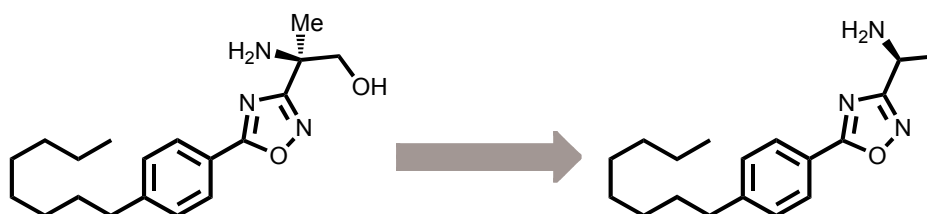
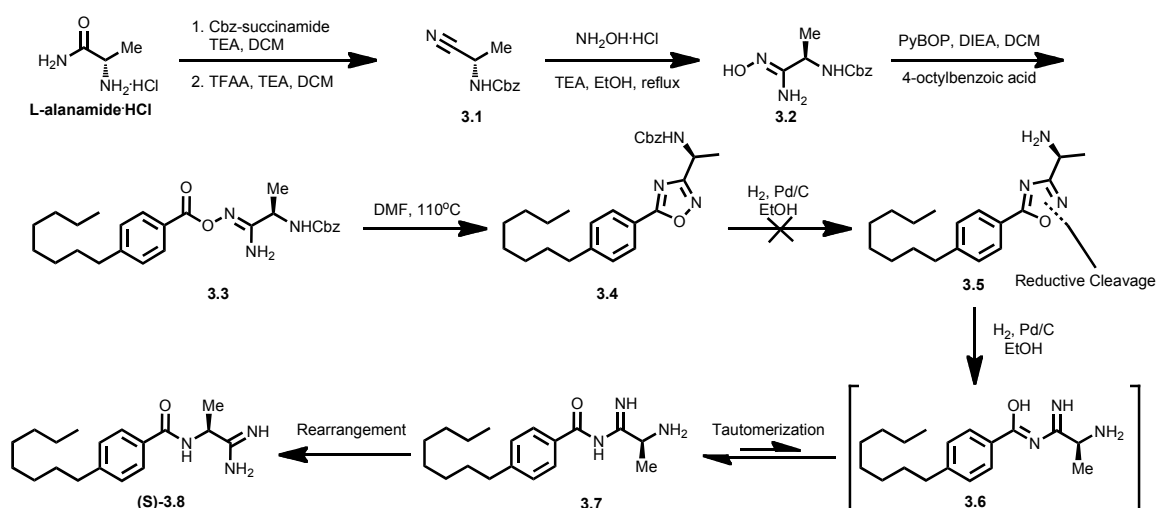


Figure 3.1: Deletion of the α -hydroxyl methyl from **FTY720** analogues as SphK inhibitors.

The synthesis of this analog was straightforward starting with the commercially available L-alaninamide•HCl (Scheme 3.1). After a Cbz-protection,

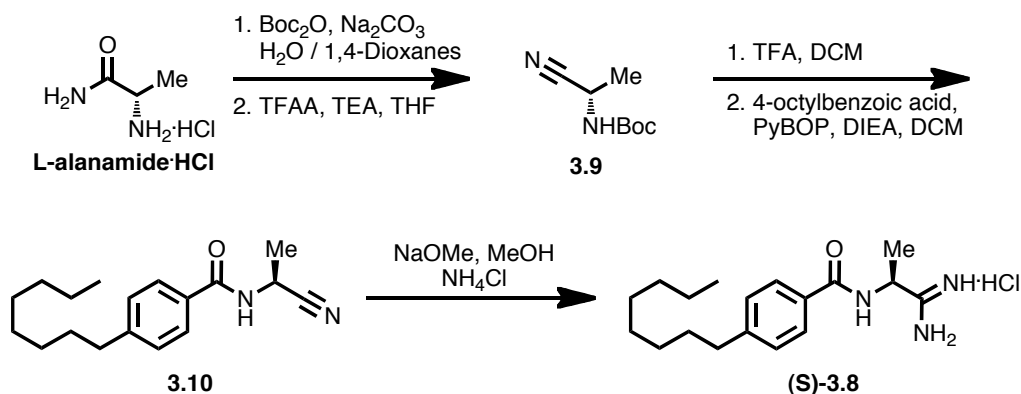
the amide was dehydrated to nitrile **3.1**. Stirring the nitrile in basic ethanol and hydroxylamine hydrochloride afforded amideoxime **3.2**. The amideoxime was coupled to *p*-octylbenzoic acid using PyBOP to yield **3.3**. Heating in DMF afforded the protected oxadiazole **3.4**. The removal of the Cbz group through normal, palladium-catalyzed hydrogenolysis yielded an unexpected product. Once the Cbz group was removed, further reduction of the N-O bond lead to the formation of **3.6**. Upon tautomerization and rearrangement to the more stable form, the final product obtained was the primary amidine (**S**)-**3.8**.⁸



Scheme 3.1: Synthesis toward the desired 5-phenyl-1,2,4-oxadiazole amine **3.5** ultimately leading to the unanticipated primary amidine molecule (**S**)-**3.8**.

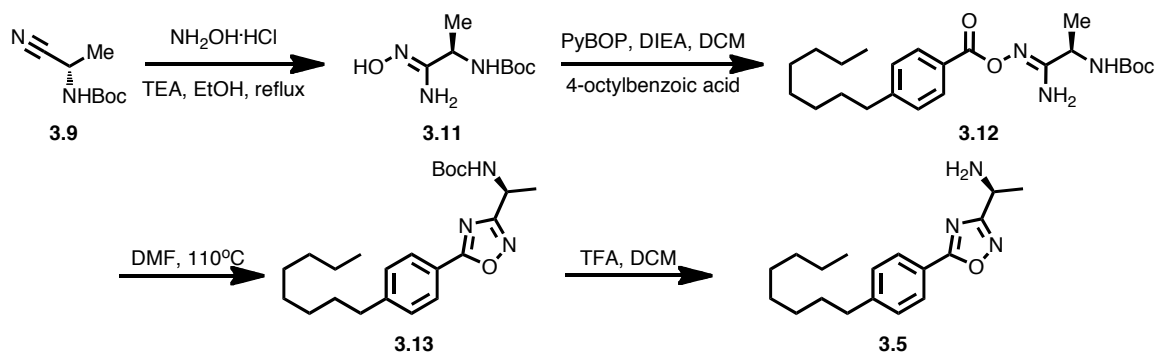
To verify the structure of (**S**)-**3.8**, the molecule was independently synthesized (Scheme 3.2). The synthesis began with *N*-Boc protection of L-alaninamide·HCl and subsequent dehydration to afford nitrile **3.9**. The amine was deprotected and then coupled to 4-octylbenzoic acid using a PyBOP coupling to yield amide **3.10**. Using modified Pinner conditions, the nitrile was

converted to the primary amidine under mild, basic conditions to afford the desired compound **(S)**-**3.8**. The structure was confirmed using ^1H NMR, ^{13}C NMR, and mass spectrometry. Also, it was determined that these conditions did not racemize the stereocenter and that this was indeed the structure obtained from the hydrogenolysis of **3.4**.⁸



Scheme 3.2: Independent synthesis of **(S)**-**3.8**. for structural verification.

To validate our original hypothesis, the proposed inhibitor was synthesized starting with a *tert*-butyloxycarbonyl (Boc) protected amine (Scheme 3.3). The synthesis began using the alanine derivative **3.9** and reacting it with hydroxylamine under refluxing conditions to provide the amideoxime **3.11**. Using a PyBOP coupling, this was then coupled to 4-octylbenzoic acid to afford **3.12**. Cyclization in DMF gave the 1,2,4-oxadiazole ring system **3.13** followed by deprotection of the amine to afford the desired compound **3.5**. The structure was verified via ^1H NMR, ^{13}C NMR, and mass spectrometry.⁸



Scheme 3.3: Successful synthesis of **3.5** using *N*-Boc protected amine to prevent N-O bond cleavage during hydrogenation.

3.2 Biological Evaluation of Sphingosine Kinase Inhibitors

The SphKs use the γ -phosphate of ATP to convert the alcohols of their substrates to phosphates and release ADP. Using γ - ^{32}P ATP, an absorbance assay can be used to evaluate a molecule's efficiency at inhibiting the SphKs. This assay will quantify the amount of S1P that is produced by the kinase by measuring the amount of absorbance of the isotope-labeled product (Figure 3.2).¹⁰

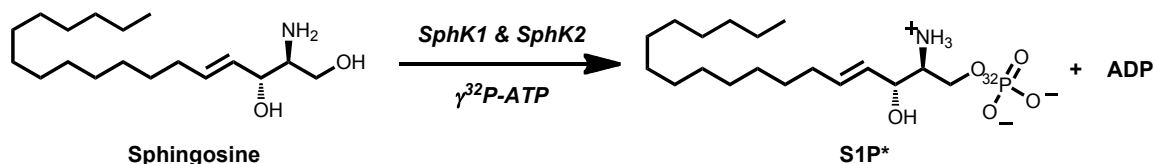


Figure 3.2: Phosphorylation of Sph by γ - ^{32}P ATP results in radio labeled S1P.

This assay was used to evaluate the efficacy of our molecules, (**S**)-**3.8** and **3.5**, at inhibiting the phosphorylation of Sph to S1P. If the molecule is successful at preventing this reaction from taking place, we should see a significant decrease in the amount of radio-labeled S1P produced. The activity of these inhibitors and *N,N*-dimethylsphingosine (DMS) were normalized to the amount of

phosphorylation of sphingosine by SphK1 and SphK2 from mice and humans. Even though DMS is a poor inhibitor of the SphKs, it is commonly used as a comparison due to its extensive study. The 5-phenyl-1,2,4-oxadiazole scaffold showed little activity as a SphK inhibitor with the exception of moderate inhibition at mouse SphK2. Surprisingly, the primary amidine **(S)**-3.8 displayed significant inhibition at both SphK1 and SphK2 which had not been seen previously in the literature (Figure 3.3).⁸

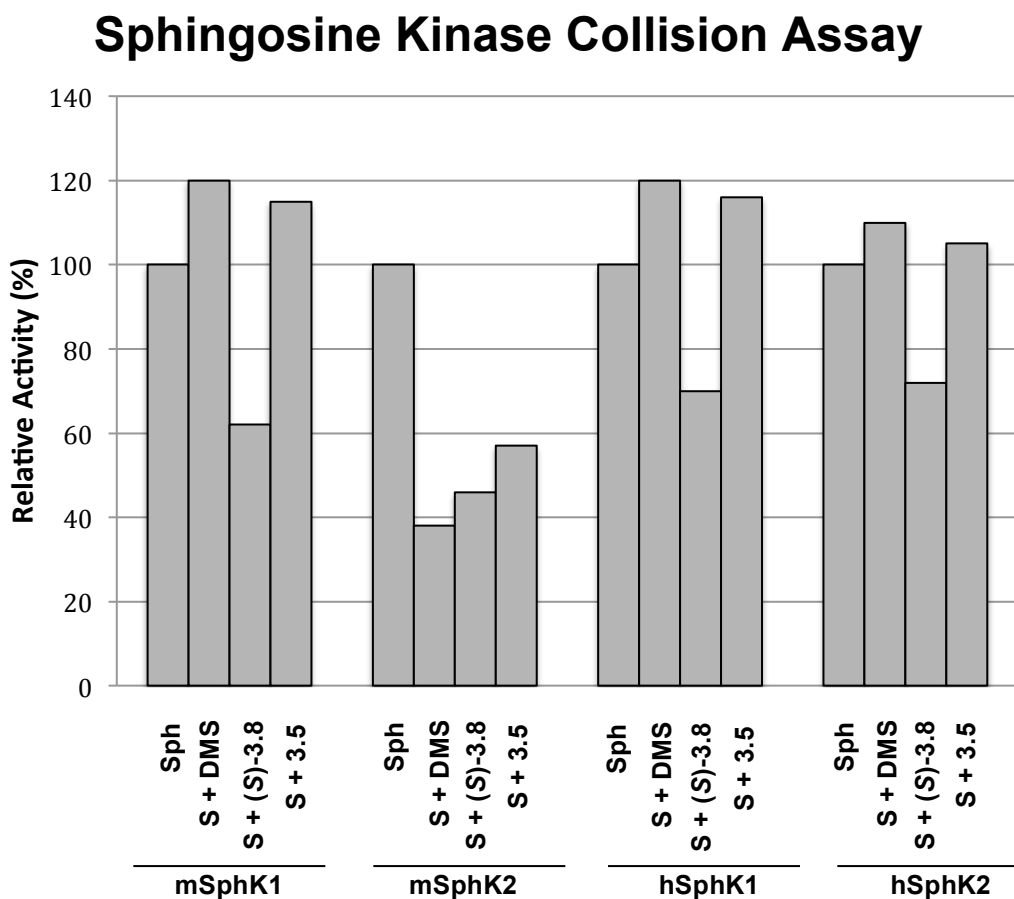


Figure 3.3: Evaluation of **(S)**-3.8 and 3.5 as SphK inhibitors. 3.5 was not an effective inhibitor, however, primary amidine **(S)**-3.8 inhibited SphK1 and SphK2 from mice and humans.

3.3 Optimization of Amidine-based Sphingosine Kinase Inhibitors

Once the primary amidine, **(S)**-3.8, was identified as a potent dual inhibitor of the SphKs, it was necessary to better understand the pharmacophore that is associated with its activity. In order to successfully accomplish this, we divided the lead molecule, **(S)**-3.8, into three regions and assessed each individually (Figure 3.4).

FTY720 and **(S)**-3.8 have structural similarities thus providing us with great insight into how to increase the potency of our inhibitor. There were many different modifications that could be made that would be facile to synthesize from commercially available starting materials. These dynamic changes would allow identify structural motifs that could lead to an increase in potency and selectivity (Figure 3.4).

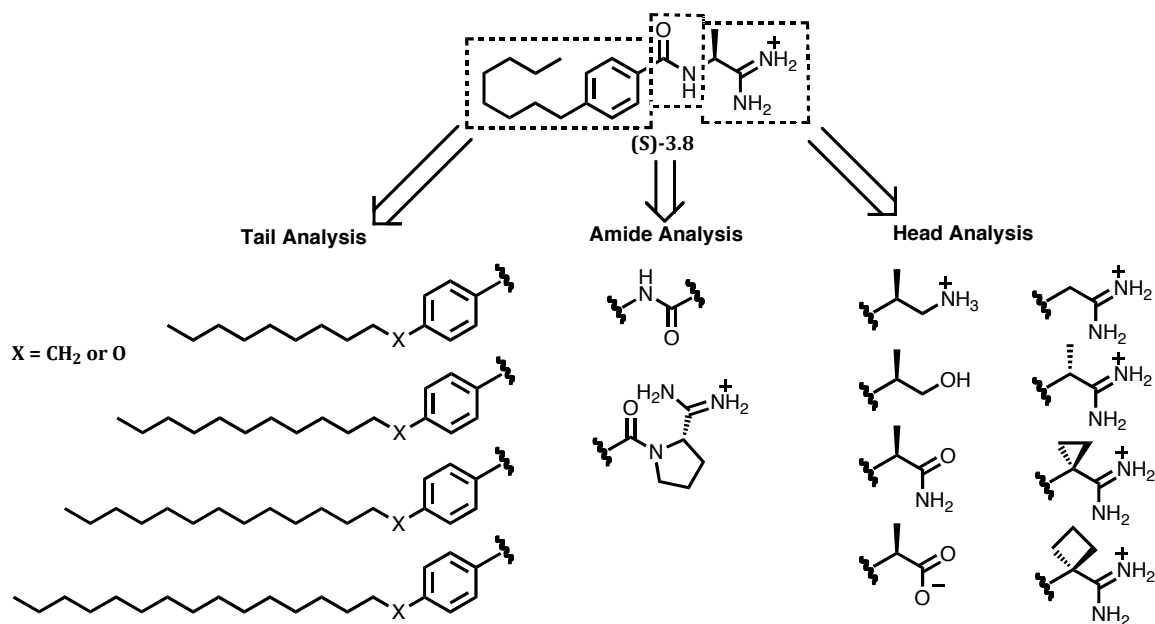


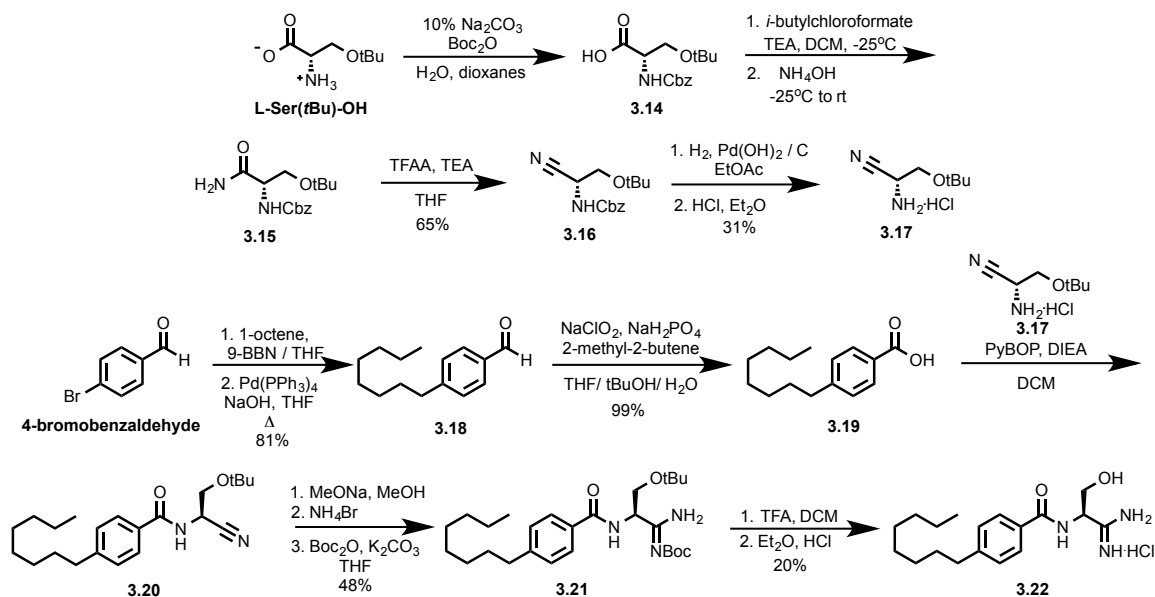
Figure 3.4: Structural modifications to lead **(S)**-3.8 in order to elucidate the pharmacophore of the amidine-based inhibitors.

3.3.1 Head Group Structure-Activity Relationships

An interesting moiety of our inhibitor is the amidine head group. Amidines are not common motifs in the chemical literature, particularly in pharmaceuticals, thus signaling us to question its importance for potency in our inhibitors. There are two properties the amidine group provides, positive charge and planarity. The positive charge may be important for recognition in the active site since sphingosine has a positively charged amine at physiological pH. Also, the planarity of the amidine may be favorable due to the angle the head group would be presented for possible chelation in the active site of the kinases. Replacing the amidine with a primary amine, amide, alcohol, and carboxylic acid tested these hypotheses. The amine would test to see if only a positive charge is needed for recognition while the amide would only test for planarity. As controls, the alcohol would be uncharged and non-planar whereas the carboxylic acid would be planar and negatively charged.⁸

The steric bulk at the α -position to the amidine was also investigated by deleting the methyl, inverting the methyl, a methylene hydroxyl, and the installation of a cyclopropyl. The enantiomer of (**S**)-**3.8** was synthesized from *N*-Boc protected D-alanine ((**R**)-**3.8**) and glycine was used to synthesize the inhibitor eliminating the steric bulk at the α -carbon (**3.32**). The cyclopropyl derivative (**3.33**) was achieved through a similar synthesis as (**S**)-**3.8** using commercially available 1-amino-1-cyclopropanecarbonitrile in place of the alanine-derived moiety.

A methylene hydroxyl was tested at the position alpha to the amidine to mimic the methylene hydroxyl in sphingosine. This was done to test for steric effects and if there was a possible positive interaction between the hydroxyl group and a nearby residue in the pocket. The synthesis began with the Cbz-protection of the amine of L-Ser(*t*Bu)-OH to afford **3.14**. The carboxylic acid was converted to the primary amide using *i*-butylchloroformate and ammonium hydroxide to yield **3.15**, which was subsequently dehydrated using trifluoroacetic anhydride to afford nitrile **3.16**. The C-8 tail was appended to 4-bromobenzaldehyde using a Suzuki coupling to yield aldehyde **3.18**. Using a Pinnick oxidation, the aldehyde was oxidized to carboxylic acid **3.19**.¹¹ Once the Cbz-group in **3.16** was removed through Pd-catalyzed hydrogenation to yield **3.17**, this was coupled to carboxylic acid **3.19** to afford amide **3.20**. The nitrile was converted to a primary amidine, which was immediately Boc-protected to yield **3.21**. The Boc and *t*-butyl groups were cleaved using TFA to afford primary amidine **3.22** as a hydrochloride salt.



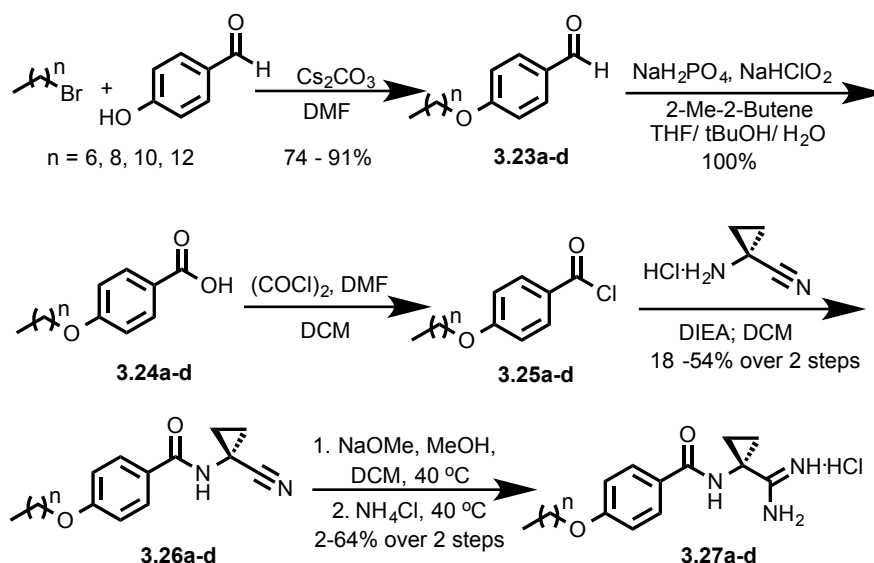
Scheme 3.4: Synthesis of serine-based inhibitor **3.22** starting with L-Ser(tBu)-OH and 4-bromobenzaldehyde.

3.3.2 Tail Group Structure-Activity Relationships

Next, we analyzed the tail region of our scaffold by adjusting the length of the alkyl chain. Longer alkyl chains would be more hydrophobic and we hypothesized this would increase activity at the kinases. This was tested by synthesizing derivatives of **3.33** with alkyl tails from C-10 to C-16, increasing in two-carbon increments. Longer alkyl chains would more closely resemble the length of sphingosine.

Preliminary whole cell testing of some of our inhibitors, it appeared as though the molecules were not getting into cells. We believed that this may have been due to our inhibitors not being very water-soluble, and so, ether tail analogues with alkyl chains ranging from C-7 to C-13, increasing in two-carbon increments, were synthesized (Scheme 3.4). The synthesis of these derivatives began with an S_N2 reaction using 4-hydroxybenzaldehyde and the corresponding

alkyl bromide to yield aldehydes **3.23a-d**. Using a Pinnick oxidation, the aldehyde was converted to carboxylic acids **3.24a-d**.¹¹ Formation of the acid chloride, followed by subsequent reaction with 1-amino-1-cyclopropanecarbonitrile hydrochloride afforded nitriles **3.26a-d**. Modified Pinner conditions yielded the desired primary amidines **3.27a-d**.



Scheme 3.5: Synthesis of ether tail analogues containing the cyclopropyl linker.

3.3.3 Structure-Activity Relationships of the Amide Bond

Finally, analysis of the amide bond of these molecules was investigated. While exploring the pharmacophore of the Macdonald Lab substrates of the SphKs, restricting bond rotation, lead to an increase in selectivity and potency.³ This information was used to test its effectiveness in our inhibitor scaffold. We chose to restrict the bond between the amide-nitrogen and the carbon alpha to the amidine. This would restrict the rotation about the nitrogen-carbonyl carbon

bond even further as well as reducing the degrees of freedom available to the amidine. This molecule could easily be synthesized from the amino acid L-proline.

Also synthesized were analogues of the cyclopropyl derivative with an inverted amide where the amide nitrogen is bound directly to the aromatic ring. This would change the electronics of the molecule and give insight into the possibility of the amide acting as a hydrogen bond donor in the binding pocket. Derivatives with alkyl tails ranging from C-10 to C-16 were synthesized to compare to the original amide configuration.

3.4 Biological Evaluation of Amidine-based inhibitors at Recombinant Enzyme

The molecules discussed were evaluated as SphK inhibitors using the previously described broken-cell assay (Figure 3.2).¹² Compounds whose K_i value exceeded 100 μM were beyond the limits of detection and are listed as $>100 \mu\text{M}$. Approximate values are listed for molecules where a K_i was not calculated. In addition to K_i values, the selectivity of the inhibitors for SphK1 was calculated as $(K_i / K_M)^{\text{SphK2}} / (K_i / K_M)^{\text{SphK1}}$. This takes into account the different K_M values of sphingosine at each kinase. Due to structural similarity of our inhibitors to sphingosine and **FTY720**, we believed our molecules would bind in the substrate-binding pocket and be competitive inhibitors of the SphKs. These molecules were determined to be competitive inhibitors because they increase the K_M , but did not lower the V_{max} for D-*erythro*-sphingosine.⁸

3.4.1 Evaluation of the Head Group Analogues

We hypothesized that the primary amidine was necessary for our molecules to act as inhibitors of the SphKs since the positively charged amidine could mimic the positively charged amine on sphingosine and thus be recognized by the kinases. Upon testing, this hypothesis held true (Table 3.1). The carboxylic acid **3.28**, primary amide **3.29**, primary amine **3.30**, and alcohol **3.31** completely lost activity at both kinases. Since the carboxylic acid and primary amide are both planar but neither are positively charged, it was concluded that the charge is important for inhibition of the SphKs by our inhibitors. Also, since the primary amine is positively charge but not planar, we conclude that the planarity of the amidine is important for inhibition. The alcohol served as a control for both electronics and planarity and thus confirms our hypothesis.

Table 3.1: K_I values and SphK1 selectivity of head group analogues at recombinant SphKs.

	Structure	K_I (μ M) ^a		SphK1 Selectivity ^b
		SphK1	SphK2	
(S)-3.8		55	20	0.7
3.28		>100	>100	N/A
3.29		>100	>100	N/A
3.30		>100	>100	N/A
3.31		>100	>100	N/A
3.32		>100	60	1.2
(R)-3.8		>100	25	0.5
3.33		25	23	1.8
3.22		>100	40	0.8

^a $K_I = [I] / (K'_M / K_M - 1)$. K'_M of sphingosine at SphK1 is 10 μ M. K_M of sphingosine at SphK2 is 5 μ M.^b Selectivity = $(K_I / K'_M)^{\text{SphK2}} / (K_I / K'_M)^{\text{SphK1}}$.

Substitution at the position alpha to the amidine gave interesting results (Table 3.1). Removal of the methyl group, **3.32**, completely lost activity at SphK1 but only slightly lost potency at SphK2. Compounds (**R**)-**3.8** and **3.22** also lost potency at SphK1 but maintained potency at SphK2. These results were not surprising since we had previously been successful at synthesizing substrates of SphK2 but minimally successful at SphK1. However, it was puzzling that (**R**)-**3.8** and **3.22** are opposite stereochemistry but they both are inhibitors of SphK2 and not SphK1. We were expecting that **3.22** would preferentially bind to SphK1 since its stereochemistry matches that of (**S**)-**3.8**. It was apparent that this needed to be investigated further. Installation of a cyclopropyl ring in **3.33** gained potency at SphK1 and remained a mid-micromolar dual inhibitor. We believe the angle strain of the cyclopropyl ring alters the angle at which the amidine is presented, thus maximizing its recognition and chelating ability within the kinase.⁸

3.4.2 Evaluation of the Tail Analogues

The cyclopropyl ring gained some potency at SphK1 giving a mid-micromolar dual inhibitor (Table 3.1). Due to this increase in potency, this head group was carried on with our tail analogues. Since sphingosine has a long hydrophobic tail, we thought that lengthening the tail of our analogues would increase the binding affinity and this would translate to a lower K_i .

To test this, a series of inhibitors with tail length increasing by two-carbons was synthesized (Table 3.2). The most potent analogue of this series was **3.36** with a 12-carbon tail. The length of this molecule more closely resembles the

length of sphingosine, giving it high nanomolar K_i values for both SphK1 and SphK2 that are well below the K_M of sphingosine for both kinases. The increase in tail length past 12-carbons did not continue to increase potency but actually lowered activity showing a parabolic relationship between tail length and potency. These larger molecules must exceed the limit of capacity of the kinases' binding pockets.⁸

With initial data leading us to believe our inhibitors may not be entering cells, we sought to solve this problem by increasing the molecule's water solubility using ether tails (Table 3.2). Once again, a parabolic relationship between tail length and potency was observed with the 12-carbon equivalent chain being the most potent; however, all molecules lost a log-order or more of potency at both kinases. When performing the assay, it was observed that these molecules were more soluble, however, they were not tested in whole cells due to their loss in potency.

Table 3.2: K_i values of alkyl and ether tail derivatives.

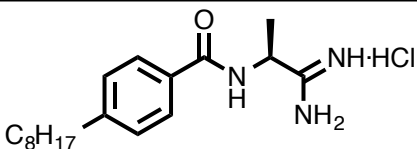
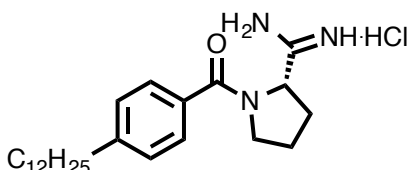
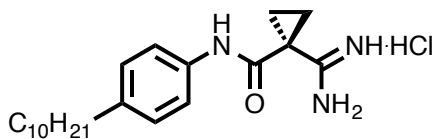
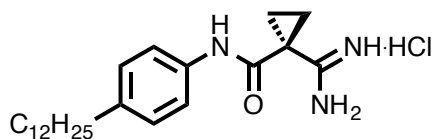
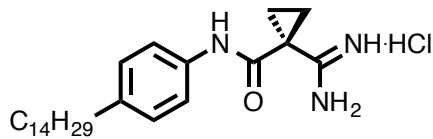
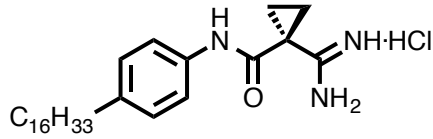
	Structure	K_i (μM) ^a		SphK1 Selectivity ^b
		SphK1	SphK2	
(S)-3.8		55	20	0.7
3.33		25	23	1.8
3.36		5	4	1.6
3.37		0.2	0.5	5
3.38		10	32	6.4
3.39		36	10	0.6
3.27a		~31	~35	N/A
3.27b		~43	~36	N/A
3.27c		~5	~19	N/A
3.27d		~40	~59	N/A

^a $K_i = [I] / (K'_M / K_M - 1)$. K_M of sphingosine at SphK1 is 10 μM . K_M of sphingosine at SphK2 is 5 μM .^b Selectivity = $(K_i / K_M)^{\text{SphK2}} / (K_i / K_M)^{\text{SphK1}}$.

3.4.3 Biological Evaluation of Amide-bond Analogues

Since increasing steric bulk and altering the presentation of the amidine increased potency, we thought that using a proline derivative, **(S)**-3.40, would give similar results (Table 3.3). The proline did increase the potency at SphK1 but lost potency at SphK2 giving a mid-nanomolar slightly SphK1 selective inhibitor.

Table 3.3: K_i values of amide derivatives.

	Structure	K_i (μ M) ^a		SphK1 Selectivity ^b
		SphK1	SphK2	
(S) -3.8		55	20	0.7
(S) -3.40		0.125	1.5	24
3.41		3	4	2.7
3.42		0.3	6	40
3.43		8.4	>100	N/A
3.44		30	>100	N/A

^a $K_i = [I] / (K'_M / K_M - 1)$. K_M of sphingosine at SphK1 is 10 μ M. K_M of sphingosine at SphK2 is 5 μ M.

^b Selectivity = $(K_i / K_M)^{\text{SphK2}} / (K_i / K_M)^{\text{SphK1}}$.

Perhaps the most interesting results stemmed from the inversion of the amide bond. The familiar parabolic trend was observed with increasing tail length and the most potent being the 12-carbon tail, however, these molecules showed a large preference for inhibition at SphK1 with **3.42** being 40-fold selective. When compared to the original amide, these molecules are dual inhibitors through the 10-carbon tail, but the inverse-amide at 12-carbons or longer shows SphK1-selectivity, whereas, the original amide is a dual inhibitor at all lengths (Figure 3.5). The rationale for this difference between the two scaffolds is that the inverse amide may display an altered binding mode because the amide may have a negative electrostatic interaction with a nearby residue that the original amide would not encounter. At longer lengths, the substrate-binding pocket of SphK2 may not be large enough to accommodate the altered binding and forces the amide near this electrostatic interaction and thus lowers the binding affinity for these molecules. This information gave us two scaffolds to use as new leads for dual and SphK1-selective inhibitors during the design of our second-generation inhibitors.⁸

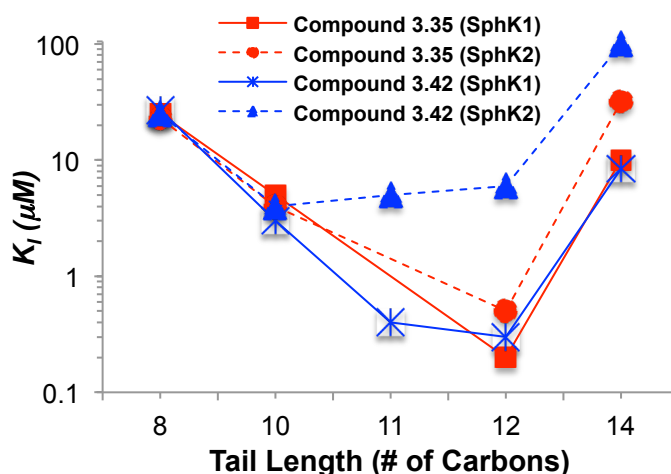


Figure 3.5: Comparison of inhibitors with the original amide (red) and the inverse amide (blue) showing the inverse amide at longer tail lengths having a preference for SphK1 inhibition.

3.5 Second-Generation Amidine-based Sphingosine Kinase Inhibitors

Upon completion of the first-generation inhibitors, we had accomplished one of our goals with the synthesis of a potent dual inhibitor. With the data collected from the first round of SAR, there was much that could be done in the tail region to improve the selectivity and potency of our inhibitors as SphK1-selective inhibitors.

3.5.1 SAR and Biological Evaluation of 3.42

Taking advantage of the tail length and amide direction dependency on SphK1-selectivity, we designed new SAR to further elucidate the pharmacophore of the SphKs (Figure 3.6).¹³

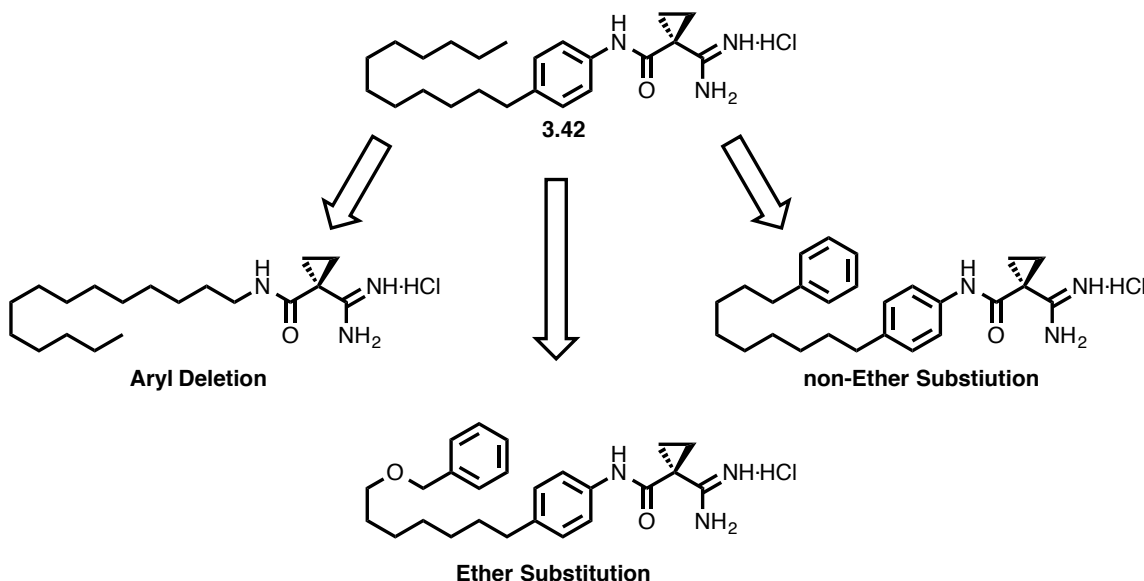


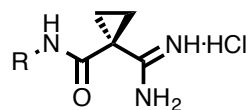
Figure 3.6: SphK1-selective inhibitor design from the 40-fold SphK1-selective 3.42.

The aryl deletion series was used to test the importance of the benzene ring on potency and selectivity. In this series, commercially available alkyl amines with 14, 16, and 18 carbons were used to synthesize these inhibitors. Because

SphK1 seems to have a large pocket in the tail-binding region, we placed benzene rings at the terminus position with 8 or 9 carbon linkers to the benzene ring. Solubility seemed to be an issue during biological testing of our inhibitors; therefore, molecules containing rings of different sizes with an ether linkage in compounds with and without the benzene ring were synthesized.¹³

The most striking results came from the aryl deletion series. These molecules resemble sphingosine more closely, however, upon testing with SphK1 and SphK2, they displayed a very flat SAR with K_i values in the low micromolar range. The molecules with longer tails (**3.46** and **3.47**) did, however, maintain selectivity for SphK1. We hypothesize, since these molecules resemble sphingosine more closely, they probably have a high affinity for the active site, but due to their hydrophobicity, they are so water insoluble that they aggregate in solution lowering their active concentration in the assay.¹³

Table 3.4: K_i values for aryl deletion and substituted tail terminus analogues of **3.42**.



	Tail Group	K_I (μM) ^a		SphK1 Selectivity ^b
		SphK1	SphK2	
3.42		0.3	6	40
3.45		6	7.5	2.5
3.46		5.4	>100	>37
3.47		9	>100	>22
3.48		5	38	15
3.49		0.50	>10	>40
3.50		1.3	>10	15
3.51		0.39	12	61
3.52		0.24	7	58
3.53		0.80	>20	>50
3.54		1.5	4.6	6.1
3.55		0.11	26	470
3.56		0.45	25	110

^a $K_I = [I] / (K'_M / K_M - 1)$. K'_M of sphingosine at SphK1 is 10 μM . K_M of sphingosine at SphK2 is 5 μM .

^b Selectivity = $(K_I / K_M)_{\text{SphK2}} / (K_I / K_M)_{\text{SphK1}}$.

The added steric bulk at the terminal position was more consistent with SAR previously observed with inhibitors in the aryl deletion series with longer alkyl chains. The inhibitor with the longer linker (**3.49**) was more potent than the shorter linker (**3.50**) but equipotent to its alkyl counterpart (**3.42**). As seen previously, the ether derivatives were more soluble and thus gave a more insightful SAR. Bulky, hydrophobic alkyl rings and arenes were used to test the capacity of this region of the pocket. With the ether adding water solubility, these molecules increased potency and selectivity overall. It was determined that the cyclohexyl ring (**3.52**) was preferred over the benzene ring (**3.48**) being more than a log-order more potent. The adamantyl ring (**3.54**) must have exceeded the capacity of the pocket thus increasing its K_i value to 1.5 μM as compared to 0.24 μM for **3.52**.¹³

Still thinking that a molecule more closely resembling sphingosine would make a better inhibitor, we synthesized two inhibitors with the aryl deletion but with terminal alkyl ethers. The molecule with the cyclohexyl ring (**3.55**) was much more potent and selective than the cyclopentyl (**3.56**) with a K_i value at 0.11 at SphK1 and 470 fold selective. At the time, this was our most selective and potent inhibitor.

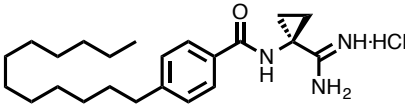
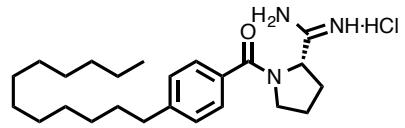
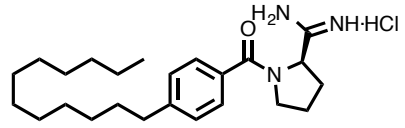
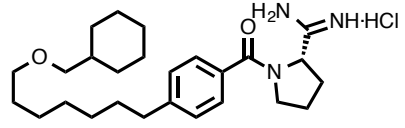
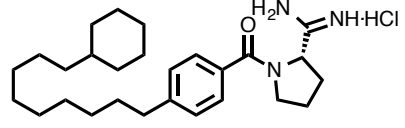
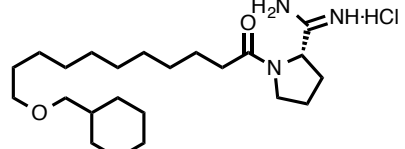
3.5.2 Head Group Analysis of Second-Generation Inhibitors

During the first-generation SAR of the amidine-based inhibitors, L-proline and an α,α -cyclopropyl head were found to increase the potency of our inhibitors. It was necessary to test this further using the new information obtained from the

second-generation analysis of the tail region. D-proline was used to synthesize the enantiomer of **(S)-3.38** to test for steric preference. L-proline was used to synthesize molecules with bulky alkyl rings at the terminal position. Analogues of **3.52** and **3.55** were synthesized along with a compound similar to **3.52** without the ether moiety (Table 3.5).

When using D-proline as a head group, **(R)-3.40**, potency at both SphK1 and SphK2 was lost, however, there was slight selectivity for SphK2. Continuing to use the more potent L-proline as a head group, it was interesting to see there was only a slight gain in potency with the ether containing aryl analogue, **3.57**, at SphK1 as compared to **(S)-3.40**. This led us to believe the addition of the cyclohexyl ring contributes to the SphK1-selectivity. To test the limits of solubility on potency, the ether was deleted and this inhibitor, **3.58**, only slightly lost activity at SphK1 but was more selective. When deleting the aryl ring in **3.59**, the molecule remained SphK1-selective with a slight loss of potency when compared to **3.57**. When rationalizing this loss in potency, **3.57** exhibits A^{1,3} strain which prevents rotation about the carbonyl carbon – aryl bond. This rigidifies two bonds in **3.57** as opposed to just one in **3.59**, prepaying the cost of freezing those bonds before entering the active site of the enzyme. Once again we observe a parabolic relationship between potency and solubility with the ideal ClogP near 4.2.¹³

Table 3.5: K_I values for head group modifications using alkyl rings at the terminus.

	Structure	K_I (μM) ^a		SphK1 Selectivity ^b
		SphK1	SphK2	
3.42		0.2	0.5	5
(S)-3.38		0.13	1.5	24
(R)-3.38		16	5	0.6
3.57		0.075	3	80
3.58		0.099	5.3	110
3.59		0.13	8	130

^a $K_I = [I] / (K'_M / K_M - 1)$. K'_M of sphingosine at SphK1 is 10 μM . K_M of sphingosine at SphK2 is 5 μM .

^b Selectivity = $(K_I / K_M)^{\text{SphK2}} / (K_I / K_M)^{\text{SphK1}}$.

3.5.3 A Rational Approach to Drug Design

At this time in the design of SphK inhibitors, we were making methodical changes to our lead structures without having full knowledge of how these molecules were binding in the pocket. Neither SphK1 nor SphK2 crystal structures were published but there were kinases with solved crystal structures that have close sequence homology to the ATP binding site. Among the available structures was that of diacylglycerol kinase β (DGKB) that has the largest

sequence homology to SphK1 at 20%. We decided to use this crystal structure (Figure 3.7A) to develop a homology model of the SphKs even though the homology is very low using Molecular Operating Environment (MOE). We thought we would sufficiently be able to train the homology model using known SphK inhibitors to closely predict the proper binding of the amidine inhibitors and K_i values of proposed structures. This homology model would be useful to rationally design inhibitors with larger structural changes saving us time and money while achieving our goal of potent dual and subtype-selective inhibitors.

Once the homology model was generated from DGKB (Figure 3.7B), our library of amidine inhibitors was docked into the SphK1 model and displayed an interesting mode of binding for our inhibitors. It appears that the amidine of our inhibitors chelates, in a bidentate fashion, the γ phosphate of ATP (Figure 3.7C and D). This supports the mechanism where SphK binds ATP and the inhibitor and the inhibitor then stabilizes the [SphK • ATP • I] complex.¹³

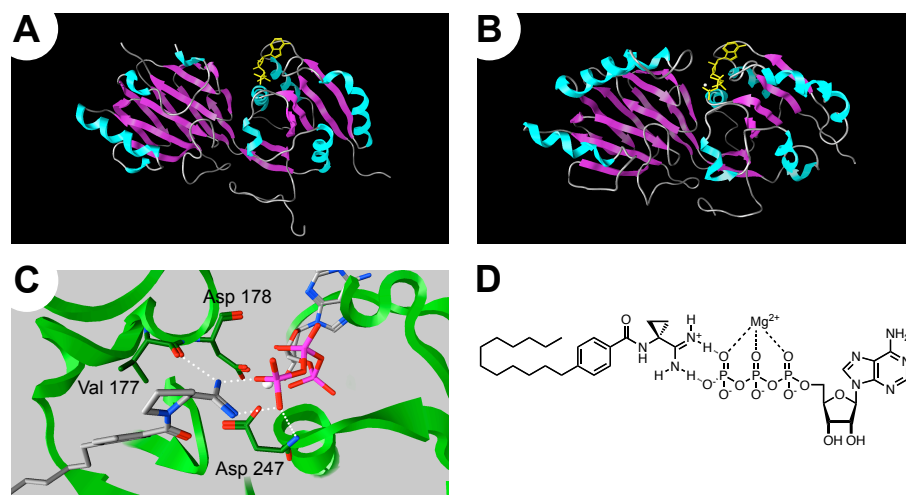


Figure 3.7: SphK homology model: (A) crystal structure of DGKB (α -helices = teal, β -sheets = lavender, ATP = yellow stick model, and Mg^{+2} = white sphere); (B) SphK1 homologue; (C) theoretical binding orientation of compound **3.57** with ATP and protein backbone; (D) 2D representation of the amidine in compound **3.57** chelating to ATP.

Using this SphK1 homology model and the information gained from previous experimental data, we were hoping the model could predict potent structures containing alkyl, aryl, and heterocyclic rings in the tail region of **3.57** (Figure 3.8A). These rings would prepay the cost of freezing bonds before the inhibitors enter the active site of the kinase. To accomplish this goal, we assumed that the amidine head group and the cyclohexyl moiety in the tail are bound accurately (Figure 3.8B). These elements were frozen and the model was allowed to insert tail fragments between the benzene of **3.57** and the terminal cyclohexane ring using benzenes, heteroaromatics, saturated rings, fused rings, and alkyl spacers in varying orders (Figure 3.8C). From the results the general scaffold in Figure 3.9 was found to have potent K_i values and the presence of the heterocycle would allow for tuning of solubility since there appears to be a relationship between potency and solubility of our inhibitors.¹³

Using this new scaffold, an oxazole, imidazole, and thiazole were synthesized and their biological activity tested (Table 3.6). Each of these heterocycles would offer differing solubilities and thus the ideal solubility may be found as well as verify the homology model and its ability to accurately predict the activity of an amidine-based inhibitor.¹³

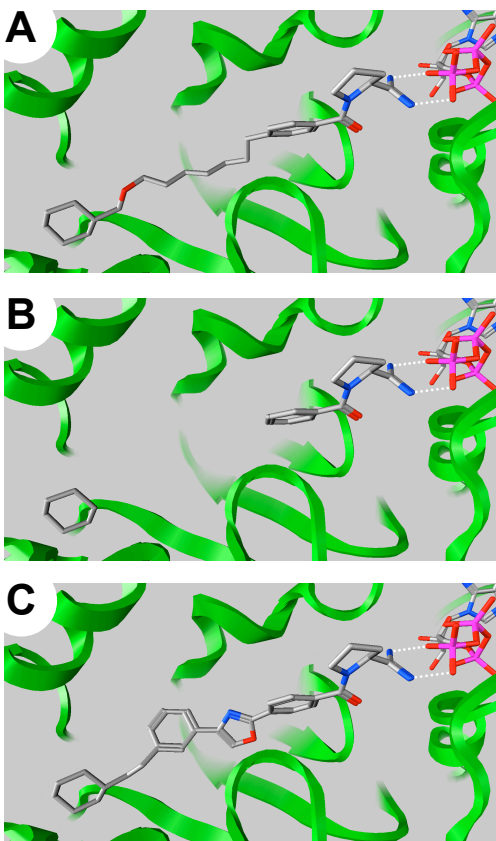


Figure 3.8: Progression of linker design: (A) theoretical binding orientation of compound **3.57** chelating to ATP; (B) deletion of aliphatic linker between the aryl amide and cyclohexyl group in **3.57**; (C) generation of a new linker (**3.61**) with a reduced number of rotatable bonds.

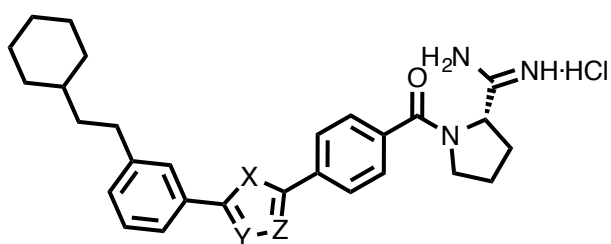


Figure 3.9: Generic scaffold for the linker designed in the homology model.

Table 3.6: K_i values for the predicted inhibitors.

Compound	Structure	K_i (μM) ^a					SphK1 Selectivity ^b
		Predicted SphK1	Lower Limit	Upper Limit	SphK1	SphK2	
3.57		-	-	-	0.075	3.0	80
3.60		0.065	0.01	0.45	2.0	20	20
3.61		0.031	0.005	0.21	0.047	4.2	180
3.62		0.035	0.006	0.24	0.11	6.0	110

^a $K_i = [I] / (K'_M / K_M - 1)$. K_M of sphingosine at SphK1 is 10 μM . K_M of sphingosine at SphK2 is 5 μM .

^b Selectivity = $(K_i / K_M)^{\text{SphK2}} / (K_i / K_M)^{\text{SphK1}}$.

As previously observed, there was a dependency on solubility for potency. The model was able to accurately predict, within 95% confidence, the K_i values for **3.61** and **3.62** at SphK1. However, the experimental K_i value for **3.60** fell outside this limit due to the model's inability to accurately predict the charge present on the imidazole ring at biological pH. This would make **3.60** too water-soluble and thus the model predicted its activity to be greater than observed. From this, we were able to obtain a highly potent and selective SphK1-selective inhibitor. Since this model proves to be useful in predicting potent SphK1 inhibitors, it will be used to design future scaffolds of the amidine-based inhibitors.

3.6 Conclusion

Upon the discovery of the first amidine-based inhibitor, the Macdonald Laboratory has been successful at synthesizing inhibitors of the SphKs using classical SARs. The first-generation of amidine-based SphK inhibitors resembled substrates of the SphKs, such as sphingosine and **FTY720**. Using this scaffold, we were able to elucidate some of the pharmacophore of our inhibitors, most notably, the necessity of our amidine warhead. With the goals of designing a dual as well as subtype-selective SphK inhibitors, we were able to achieve one of our goals with the synthesis of **3.35** as a mid-nanomolar dual inhibitor.

During the development of our second-generation amidine-based SphK inhibitors, we used the previous data to further test the limits of the substrate-binding domain. We determined that the tail-binding region of SphK1 is much larger than SphK2, which was necessary for inhibitors with the inverse-amide configuration (Table 3.3) leading to SphK1-selective inhibitors. This was surprising since during previous research, it was difficult to design selective-SphK1 substrates. Also, we discovered a parabolic relationship between solubility and potency, which was clearly demonstrated in the model-predicted heterocyclic inhibitor series (Table 3.6). During the second-generation inhibitor design, we were able to synthesize the most potent low-nanomolar SphK1-selective inhibitors available in the literature at the time. Using the new SphK1 homology model, we will be able to predict future structures of inhibitors in order to more rationally design future molecules that will be potent inhibitors.

3.7 References

- (1) Brinkmann, V. *Pharmacol. Ther.* **2007**, *115* (1), 84-105.
- (2) Mandala, S.; Hajdu, R.; Bergstrom, J.; Quackenbush, E.; Xie, J.; Milligan, J.; Thornton, R.; Shei, G.-J.; Card, D.; Keohane, C.; Rosenbach, M.; Hale, J.; Lynch, C. L.; Rupprecht, K.; Parsons, W.; Rosen, H. *Science* **2002**, *296* (5566), 346-349.
- (3) Zhu, R.; Snyder, A. H.; Kharel, Y.; Schaffter, L.; Sun, Q.; Kennedy, P. C.; Lynch, K. R.; Macdonald, T. L. *J Med Chem* **2007**, *50* (25), 6428-6435.
- (4) Clemens, J. J.; Davis, M. D.; Lynch, K. R.; Macdonald, T. L. *Bioorg Med Chem Lett* **2003**, *13* (20), 3401-3404.
- (5) Davis, M. D.; Clemens, J. J.; Macdonald, T. L.; Lynch, K. R. *J Biol Chem* **2005**, *280* (11), 9833-9841.
- (6) Clemens, J. J.; Davis, M. D.; Lynch, K. R.; Macdonald, T. L. *Bioorg Med Chem Lett* **2005**, *15* (15), 3568-3572.
- (7) Foss, F. W., Jr.; Mathews, T. P.; Kharel, Y.; Kennedy, P. C.; Snyder, A. H.; Davis, M. D.; Lynch, K. R.; Macdonald, T. L. *Bioorg Med Chem* **2009**, *17* (16), 6123-6136.
- (8) Mathews, T. P.; Kennedy, A. J.; Kharel, Y.; Kennedy, P. C.; Nicoara, O.; Sunkara, M.; Morris, A. J.; Wamhoff, B. R.; Lynch, K. R.; Macdonald, T. L. *J Med Chem* **2010**, *53* (7), 2766-2778.
- (9) Lynch, K. R.; Macdonald, T. L. *Biochim. Biophys. Acta* **2008**, *1781* (9), 508-512.
- (10) Kharel, Y.; Mathews, T. P.; Kennedy, A. J.; Houck, J. D.; Macdonald, T. L.; Lynch, K. R. *Analytical biochemistry* **2011**, *411* (2), 230-235.
- (11) Roesner, S.; Casatejada, J. M.; Elford, T. G.; Sonawane, R. P.; Aggarwal, V. K. *Organic Letters* **2011**, *13* (21), 5740-5743.
- (12) Brinkmann, V.; Davis, M. D.; Heise, C. E.; Albert, R.; Cottens, S.; Hof, R.; Bruns, C.; Prieschl, E.; Baumruker, T.; Hiestand, P.; Foster, C. A.; Zollinger, M.; Lynch, K. R. *J Biol Chem* **2002**, *277* (24), 21453-21457.
- (13) Kennedy, A. J.; Mathews, T. P.; Kharel, Y.; Field, S. D.; Moyer, M. L.; East, J. E.; Houck, J. D.; Lynch, K. R.; Macdonald, T. L. *J Med Chem* **2011**, *54* (10), 3524-3548.

4

Design of Amidine-based SphK2-selective Inhibitors

A stereochemical preference of the amidine-based SphK inhibitors was observed during the first generation SAR of these molecules. This was further investigated through the synthesis of enantiomeric pairs with longer, more potent tails. Among this earlier trend was also observed that bulkier groups showed preference for SphK2 over SphK1. This was investigated by synthesizing inhibitors containing bulkier groups at the position alpha to the amidine. Since this position appeared to be the key to SphK2-selectivity, the carbon at this position was replaced with a nitrogen. This would alter the geometry and the electronics of this region of the molecule possibly leading to SphK2-selectivity.

Since the homology model for SphK1 was very successful in suggesting SphK1-selective structures, a SphK2 homology model was designed in a similar manner. A thiazole inhibitor was suggested using this model and synthesized. Also, it appeared that the substrate-binding pocket of SphK2 is larger than SphK1 and so this was tested using naphthalene derivatives. None of the molecules synthesized in these series led to SphK2-selectivity. The inhibitors were either dual inhibitors or SphK1-selective. Each of these molecules had low-mid micromolar K_i values giving a very flat SAR in which little information can be gained.

4.1 Introduction

Of the two Sphingosine kinases, SphK2 has been studied much less; however, in the past few years, new cellular locations and roles have been uncovered. As described in Chapter 2, when either kinase is individually knocked-out of mice, the other isoform will step up and produce S1P to perform all necessary roles. However, when both kinases are knocked-out, it is embryonically lethal at day 13. Along with the differences in cellular location, this led researchers to believe that SphK1 and SphK2 produce S1P to perform different but complementary cellular functions. Since SphK1 has been recognized as a target of interest in many different diseases, it has been studied more extensively. Still, much is unknown about these kinases, especially SphK2.

Recently the Lynch and Santos laboratories have shown that inhibiting SphK2 will actually increase the amount of cellular S1P. Normally inhibiting the function of a kinase would reduce the amount of phosphorylated product, thus, reducing the signaling effects of this molecule.¹ However, the rise in S1P levels from these studies is complementary to S1P levels observed in SphK2-null mice. Olivera *et al* saw an increase in S1P levels in SphK2-null mice relative to wild-type mice.² This is not yet completely understood but may be due to SphK1 being deregulated by the lack of SphK2.¹ Also, S1P produced within the nucleus has been shown to bind to HDAC 1/2 which ultimately leads to cell cycle arrest, which opposes all other known survival roles of S1P.³ Prior to these findings, we set out to synthesize sub-type selective inhibitors to use them as tools to better understand the cellular roles of each of these kinases. With these new results, it

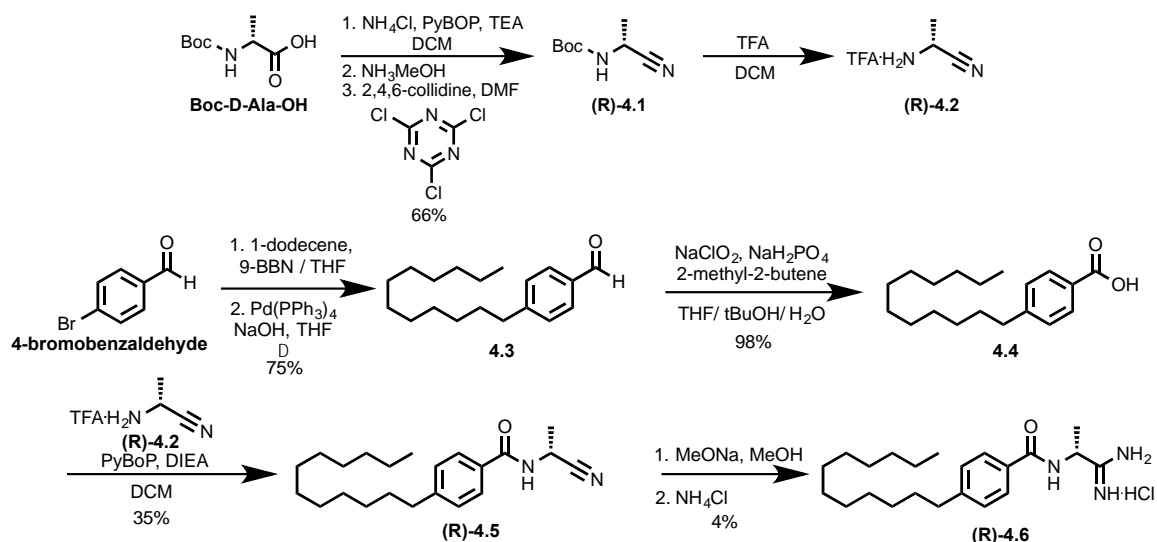
is even more important to develop a potent SphK2-selective inhibitor to further study its function in normal and diseased cells.

4.2 Stereochemical Preference by Sphingosine Kinase 2

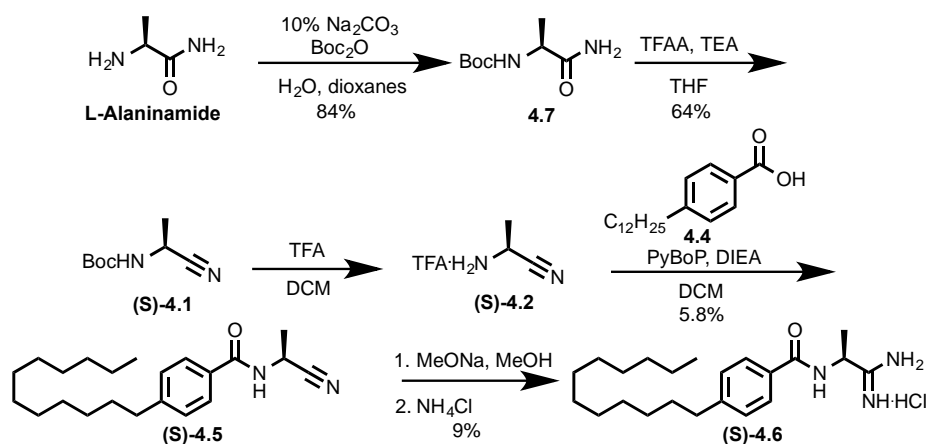
During the first-generation SAR of amidine-based SphK inhibitors, there appeared to be a stereochemical preference for inhibition of the SphKs. (Table 3.1). We further investigated this by synthesizing enantiomeric pairs of inhibitors with varying functionality at the position alpha to the amidine.

4.2.1 Synthesis of Inhibitors Containing Bulky Groups at the Alpha Position

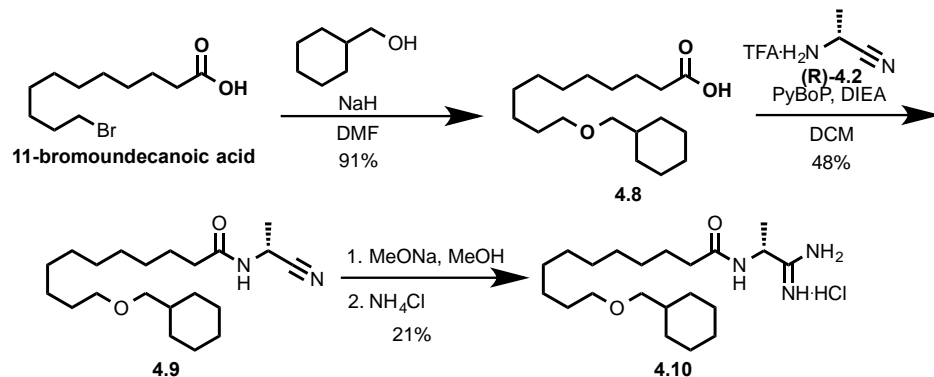
The series began with the synthesis of derivatives of (*R*)- and (*S*)-**3.8** with a 12-carbon tail to see if the trend held true. The synthesis of (*R*)-**4.6** started with the conversion of Boc-D-Ala-OH to a primary amide using PyBOP and without purification dehydrated using Gold's Reagent to afford nitrile (*R*)-**4.1** (Scheme 4.1). The Boc-group was removed using trifluoroacetic acid to yield amine (*R*)-**4.2** as a hydrochloride salt. The synthesis of the tail started with a Suzuki coupling of 4-bromobenzaldehyde and 1-dodecene to yield **4.3**. Using a Pinnick oxidation, the aldehyde was oxidized to the corresponding carboxylic acid **4.4**.⁴ Carboxylic acid **4.4** was coupled to (*R*)-**4.2** to afford nitrile (*R*)-**4.5** using PyBOP. Modified Pinner conditions were used to convert the nitrile to the primary amidine hydrochloride salt (*R*)-**4.6**.



The synthesis of (*S*)-4.6 began with the Boc-protection of L-alaninamide to yield amide **4.7**, which was subsequently dehydrated using trifluoroacetic acid to yield nitrile (*S*)-4.1 (Scheme 4.2). The Boc-group of (*S*)-4.1 was removed using TFA and then coupled to **4.4** using PyBOP to afford nitrile (*S*)-4.5. Using modified Pinner conditions, the nitrile was converted to the primary amidine (*S*)-4.6 as a hydrochloride salt.

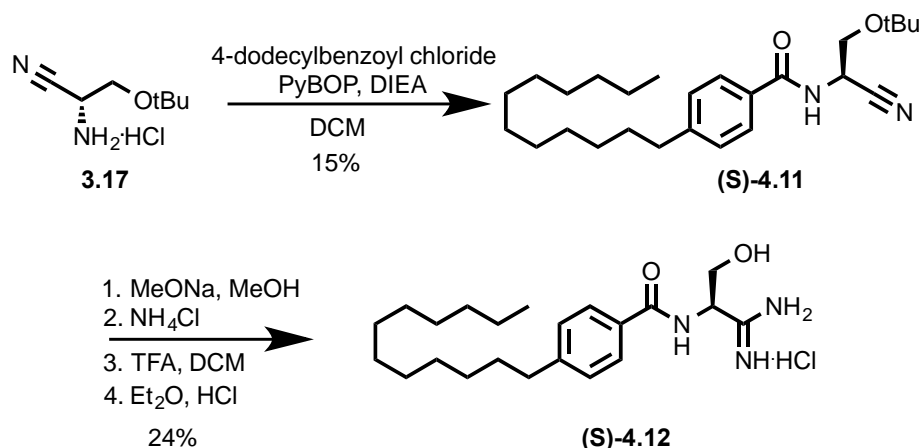


A similar molecule was synthesized with the cyclohexyl ether tail that was originally shown to be selective for SphK1. This was done to test if the stereochemistry of the alpha-position and this potent tail would lend itself to increase potency and selectivity for SphK2 (Scheme 4.3). The synthesis of the tail began with a Williamson ether synthesis of 11-bromoundecanoic acid and cyclohexane methanol to afford carboxylic acid **4.8**. This was then coupled to amine (*R*)-**4.2** using PyBOP to yield nitrile **4.9**. Using the modified Pinner conditions, the nitrile was converted to the primary amidine hydrochloride salt **4.10**.



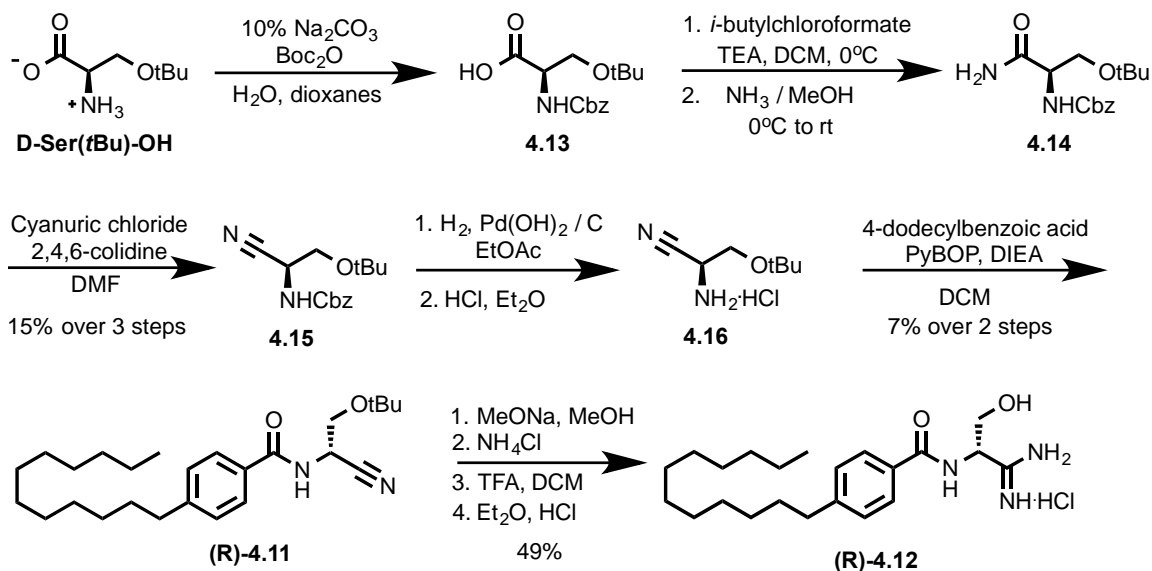
Scheme 4.3: Synthesis of **4.10** beginning with 11-bromoundecanoic acid.

As a comparison to the C-8 L-serine derivative, **3.22**, (*R*)- and (*S*)-derivatives were synthesized with C-12 tails. The synthesis of the (*S*)-derivative began with the coupling of 4-dodecylbenzoyl chloride and amine **3.17** to yield nitrile (*S*)-**4.11** (Scheme 4.4). Using modified Pinner conditions, the nitrile was converted to the primary amidine and subsequently deprotected using TFA. The hydrochloride salt was obtained by reaction with HCl in Et₂O to yield (*S*)-**4.12**.



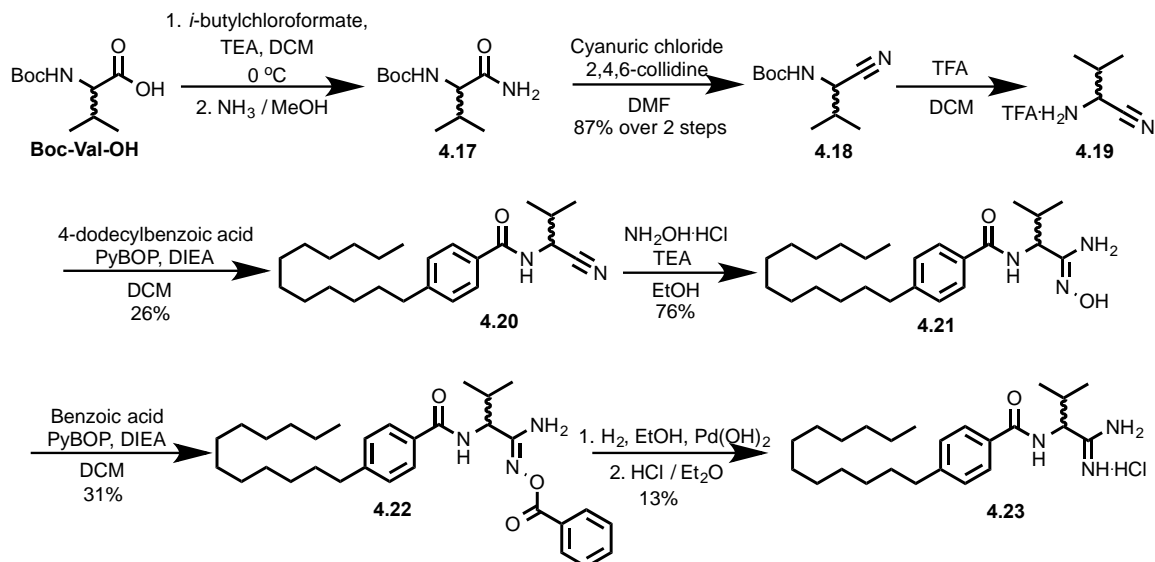
Scheme 4.4: Synthesis of L-serine derivative (**(S)-4.12**).

Synthesis of the (*R*)-serine derivative began with the Cbz-protection of D-Ser(*t*Bu)-OH to yield **4.13** (Scheme 4.5). The carboxylic acid of **4.13** was converted to the primary amide using *i*-butylchloroformate and ammonia in methanol followed by dehydration to the nitrile using Gold's Reagent to yield nitrile **4.15**. Using a Pd-catalyzed hydrogenation to remove the Cbz-group resulted in the hydrochloride amine salt **4.16**, which was then coupled to carboxylic acid **4.4** using PyBOP to afford (**R**)-**4.11**. The nitrile was converted to the primary amidine under basic Pinner conditions and subsequently deprotected using TFA. The hydrochloride salt was obtained by reaction with HCl in Et₂O to afford (**R**)-**4.12**.



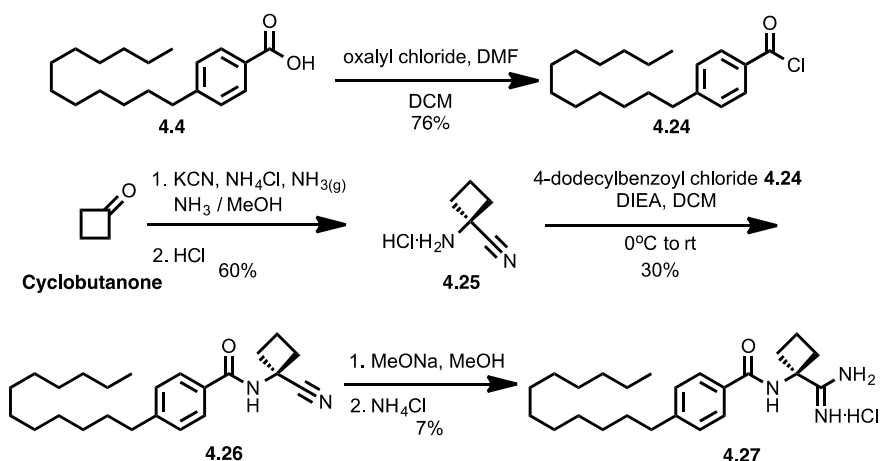
Scheme 4.5: Synthesis of D-serine analogue ((*R*)-4.12).

The effect of sterics at the position alpha to the amidine was investigated using bulkier groups, such as *i*-propyl, cyclobutyl, and cyclopentyl. The *R*- and *S*-*i*-propyl analogues were synthesized starting with the conversion of the carboxylic acid of the corresponding Boc-Val-OH to the amide using *i*-butylchloroformate and ammonia in methanol to afford amide **4.17** (Scheme 4.6). The crude amide was dehydrated using Gold's Reagent to nitrile **4.18**. Upon cleavage of the Boc-group using TFA, **4.19** was coupled to **4.4** using PyBOP to yield nitrile **4.20**. The nitrile was converted to amideoxime **4.21**, which was then protected using benzoic acid through a PyBOP coupling to give **4.22**. The N-O bond was cleaved using a Pd-catalyzed hydrogenation to afford the primary amidine **4.23** as a hydrochloride salt.



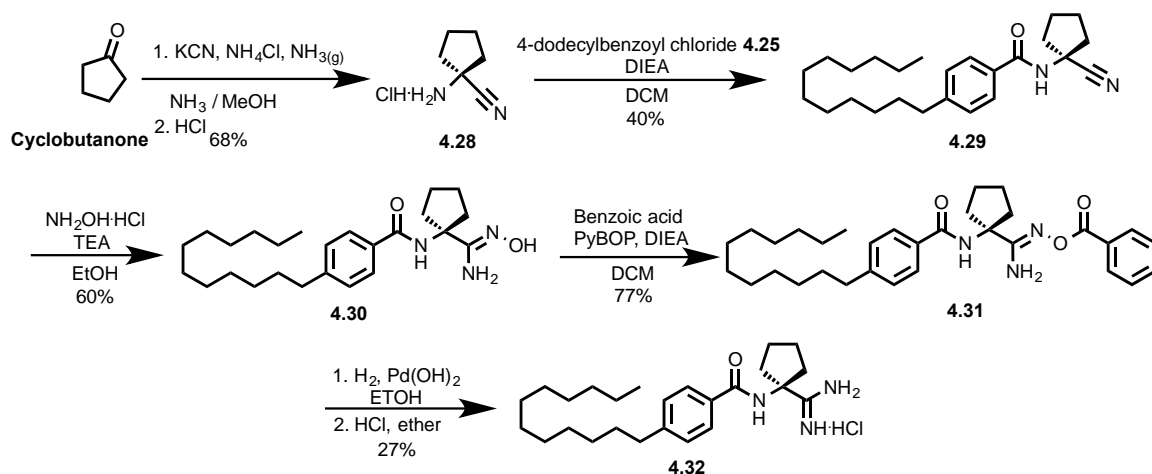
Scheme 4.6: Synthesis of (*R*)- and (*S*)-**4.23** starting from the corresponding Boc-Val-OH.

The tail of the cyclobutyl and cyclopentyl analogues were synthesized by converting the carboxylic acid of **4.4** to the acid chloride **4.24** using oxalyl chloride (Scheme 4.7). Strecker conditions were used to convert cyclobutanone to the aminonitrile **4.25**.⁵ The amide bond was formed by reaction with 4-dodecylbenzoyl chloride **4.24** to afford nitrile **4.26**. Using the modified Pinner conditions, the nitrile was successfully converted to the primary amidine hydrochloride salt **4.27**.⁶



Scheme 4.7: Synthesis of cyclobutyl analogue (4.27) to demonstrate the maximum amount of steric bulk accepted at the alpha position.

Synthesis of the cyclopentyl derivative was similar to 4.27 (Scheme 4.8). Using Strecker conditions, cyclopentanone was converted to aminonitrile 4.25, which was then coupled to acid chloride 4.24 to yield nitrile 4.29. Using hydroxylamine hydrochloride, the nitrile was converted to amideoxime 4.30. This was protected using benzoic acid and PyBOP to afford 4.31. Using Pd-catalyzed hydrogenation, the N-O bond was cleaved to yield primary amidine 4.32 as a hydrochloride salt.



Scheme 4.8: Synthesis of 4.32 starting from cyclopentanone.

4.2.2 Biological Evaluation of Inhibitors with Varying Alpha Substituents

When testing the different head groups in the first generation SAR studies of our inhibitors, we saw an interesting trend between the stereochemistry of the alpha substituent and selective inhibition of the SphKs (Table 3.1). Methyl-containing **(R)**-3.8 was selective for SphK2 whereas **(S)**-3.8 was a dual inhibitor. Interestingly, **3.22** from L-serine displayed selectivity for SphK2. We hypothesized that synthesizing inhibitors that have groups of different sizes and stereochemistry would lead to a potent SphK2-selective inhibitor (Table 4.1).

Since the greatest potency was seen with a 12-carbon tail (Table 3.2), we synthesized analogues of **(R)**-3.8 and **(S)**-3.8 with the longer tails. However, upon testing, the original SphK2-selectivity observed with **(R)**-3.8 was not observed with **(R)**-4.6. High-nanomolar dual inhibition was obtained using **(S)**-4.6, but **(R)**-4.6 was a mid-nanomolar 214-fold SphK1-selective inhibitor. The non-aryl ether tail in **4.10** was used in other inhibitors that led to SphK1-selectivity, so we used it to test if reversing the stereochemistry of the methyl group would lead to a potent SphK2-selectivity. Unfortunately it did not lead to SphK2-selectivity and was much less potent at both kinases. Previous SAR had shown an increase in potency when lengthening the alkyl tail to 12 carbons. The L-serine derivative **3.22** displayed mid-micromolar SphK2-selectivity; however, when the tail was lengthened to 12-carbons in **(S)**-4.12 it does not appear potency has increased or that it is SphK2-selective. The raw data (not shown) implies that it and its enantiomer, **(R)**-4.12, is a mid-micromolar dual inhibitor.

When testing the effect of bulky substituents at the alpha position, both molecules with *i*-propyl substituents, **(R)-4.23** and **(S)-4.23**, were low micromolar dual inhibitors. The cyclobutyl and cyclopentyl derivatives, **4.27** and **4.32** respectively, lost potency at both kinases compared to **(S)-4.6**. This information led us to believe the size of this area of the substrate-binding pocket has been exceeded and the cyclopropyl derivative **3.42** is the ideal substituent at this position.

Table 4.1: K_i values for inhibitors testing stereochemical preference.

Compound	R_1	R_2	K_i (μM) ^a		SphK1 Selectivity ^b
			SphK1	SphK2	
(S)-4.6	H	Me	0.5	0.9	3.6
(R)-4.6	Me	H	0.168	18	214
(S)-4.12	H	CH ₂ OH	>10	>10	N/A
(R)-4.12	CH ₂ OH	H	>10	>10	N/A
(S)-4.23	H	<i>i</i> Pr	~5	>10	N/A
(R)-4.23	<i>i</i> Pr	H	~5	~10	4
4.27			1.6	5	6.3
4.32			~1	~8	16

^a $K_i = [I] / (K'_M / K_M - 1)$. K_M of sphingosine at SphK1 is 10 μM . K_M of sphingosine at SphK2 is 5 μM .

^b Selectivity = $(K_i / K_M)^{\text{SphK2}} / (K_i / K_M)^{\text{SphK1}}$.

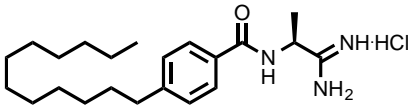
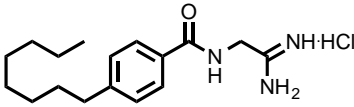
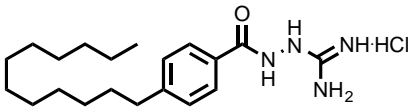
4.3 Hydrazine-based Inhibitors

A series of inhibitors was designed to replace the carbon alpha to the amidine with a nitrogen. The additional nitrogen would give the molecule slightly different geometry and any substituent on this nitrogen would be presented at a different angle than the carbon-containing inhibitors. It was envisioned that different substituents similar to those in other inhibitors could be tested using commercially available mono-substituted hydrazines. However, the only molecule able to be synthesized was the inhibitor made with hydrazine. An effort to synthesis a methyl hydrazine inhibitor was made, unfortunately, all attempts to couple the benzohydrazide to *N,N'*-di-boc-1*H*-pyrazole-1-carboxamidine failed. This is probably due to the methyl group on the nucleophilic nitrogen creating too much steric hindrance to form the bond with the Boc-protected amidine.

The hydrazine-based molecule was synthesized to compare to the glycine-based inhibitor **3.32** (Scheme 4.9). The synthesis began with the esterification of carboxylic acid **4.4** to the methyl ester **4.33**. This was then coupled to hydrazine in anhydrous ethanol under refluxing conditions to afford benzohydrazide **4.34**. The hydrazine was coupled to *N,N'*-di-boc-1*H*-pyrazole-1-carboxamidine to yield the Boc-protected amidine **4.35**.^{7,8} Using TFA, the Boc-groups were removed to afford the amidine hydrochloride salt **4.36**.

The biological results were not surprising since **4.36** is not a very potent inhibitor. The glycine-based molecule **3.32** was SphK2-selective and not very potent, but if **3.22** were re-tested with the longer 12-carbon tail, it would most likely be more potent at both kinases, as was observed with **4.36**. The hypothesis of replacing the carbon with nitrogen did not help us reach our goal of synthesizing a potent SphK2-selective inhibitor since **4.36** is a micromolar dual inhibitor. To gain more information about the usefulness of these hydrazine-based inhibitors, it is necessary to synthesize molecules with substituents on the nitrogen alpha to the amidine, such as a methyl group as in **(S)-4.6**. Unfortunately, synthesis of this molecule could not be accomplished and thus, this series of inhibitors was no longer attempted.

Table 4.2: K_i values for the hydrazine-based and related inhibitors.

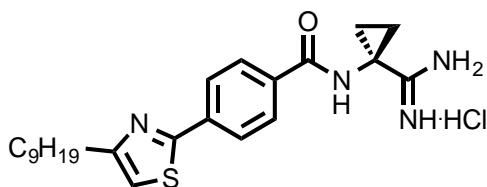
Compound	Structure	K_i (mM) ^a		SphK1 Selectivity ^b
		SphK1	SphK2	
(S)-4.6		0.5	0.9	3.6
3.32		100	60	1.2
4.36		~15	~15	2

^a $K_i = [I] / (K'_M / K_M - 1)$. K_M of sphingosine at SphK1 is 10 μ M. K_M of sphingosine at SphK2 is 5 μ M.

^b Selectivity = $(K_i / K_M)^{\text{SphK2}} / (K_i / K_M)^{\text{SphK1}}$.

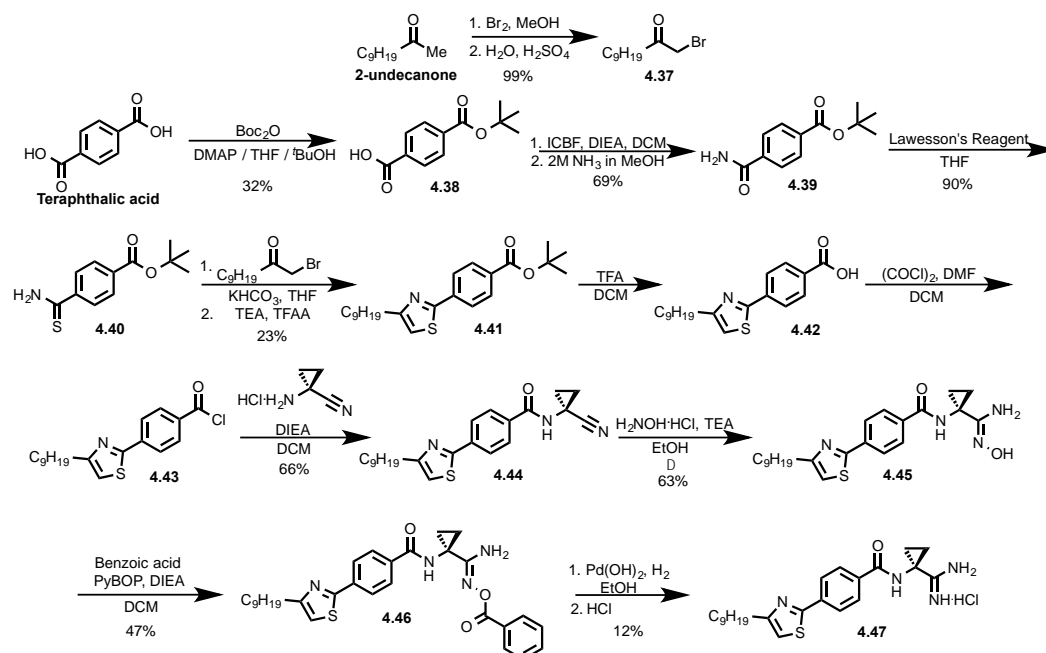
4.4 Rationally Designed SphK2-selective Inhibitors

The homology model of SphK1 was very successful in determining the binding mode of our amidine-based inhibitors and suggesting potent SphK1-selective molecules. The success was due to the numerous SphK1-selective inhibitors available in the literature and our lab that were used to train the homology model. Even though there are not very many SphK2-selective inhibitors available, a SphK2 homology model was created. Just as the SphK1-selective inhibitors **3.60** – **3.62** were predicted, a SphK2-selective inhibitor was suggested (Figure 4.1).

**Figure 4.1:** Inhibitor suggested by the SphK2 homology model to be a SphK2-selective inhibitor.

4.4.1 Synthesis of Rationally Designed SphK2-selective Inhibitors

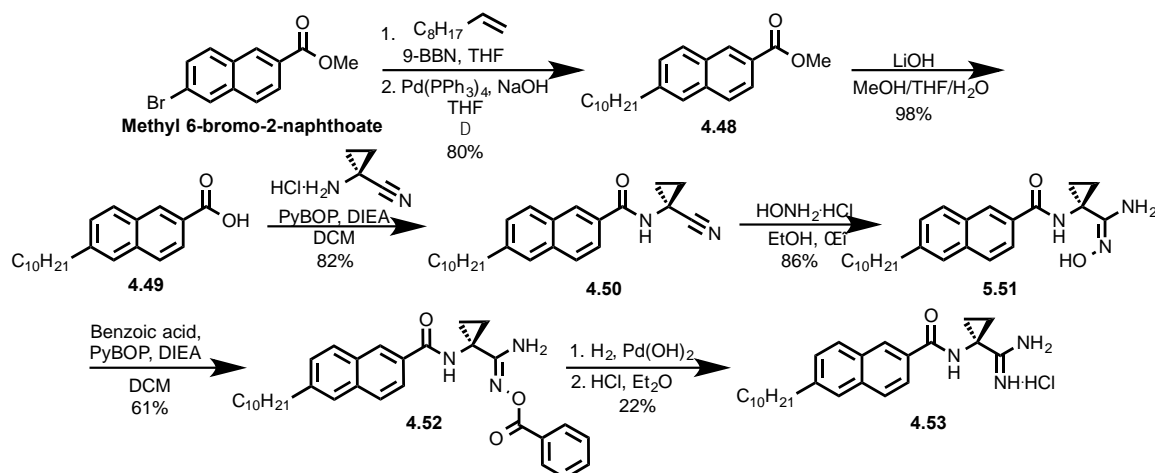
The suggested SphK2-selective inhibitor was synthesized starting with the bromination of 2-undecanone using bromine to afford **4.37** (Scheme 4.10).⁹ Next, terephthalic acid was mono-protected using Boc-anhydride yielding **4.38**.¹⁰ The carboxylic acid of **4.38** was converted to an amide to afford **4.39**. Using Lawesson's Reagent, this amide was transformed to the thioamide **4.40**,¹¹ which was then reacted with α -bromoketone **4.37** to form the thiazole ring in **4.41**.⁶ Hydrolysis of the ester yielded carboxylic acid **4.42**, which was subsequently converted to the acid chloride **4.43** via the Vilsmeier reagent. This was coupled to 1-amino-1-cyclopropanecarbonitrile hydrochloride to yield nitrile **4.44**. Using hydroxylamine hydrochloride, the nitrile was converted to amideoxime **4.45** followed by protection using benzoic acid and PyBOP to afford **4.46**. Using a Pd-catalyzed hydrogenation, the N-O bond was cleaved resulting in the primary amidine **4.47** as a hydrochloride salt.



Scheme 4.10: Synthesis of **4.47** starting from 2-undecanone and Terephthalic acid.

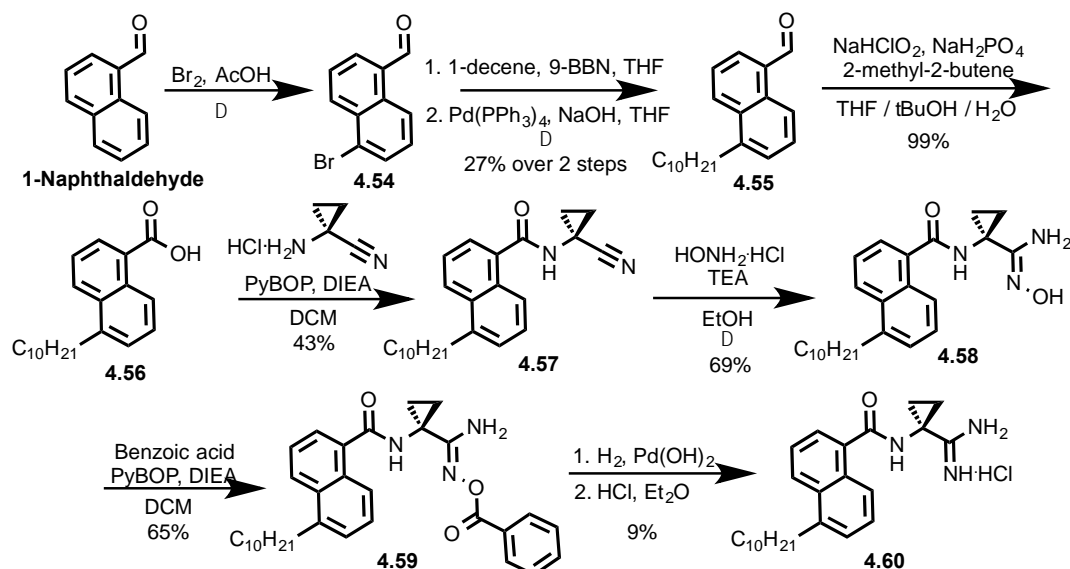
According to the homology model, the area where the benzene ring in our inhibitors resides within the pocket of the enzymes appears to be larger in SphK2 as compared to SphK1. A series of naphthalene-based inhibitors was designed to test this observation. To begin, a 2,6-substituted naphthalene molecule was synthesized as the more linear derivative (Scheme 4.11). The synthesis started with a Suzuki coupling to append the 10-carbon alkyl tail to methyl 6-bromo-2-naphthoate to yield **4.48**. The ester was saponified to carboxylic acid **4.49** followed by coupling to 1-amino-1-cyclopropanecarbonitrile hydrochloride using PyBOP to afford nitrile **4.50**. This nitrile was reacted with hydroxylamine hydrochloride to yield amideoxime **4.51**, which was then protected using benzoic acid and PyBOP resulting in protected amideoxime **4.52**. The N-O bond was

cleaved using a Pd-catalyzed hydrogenation to yield the primary amidine **4.53** as a hydrochloride salt.



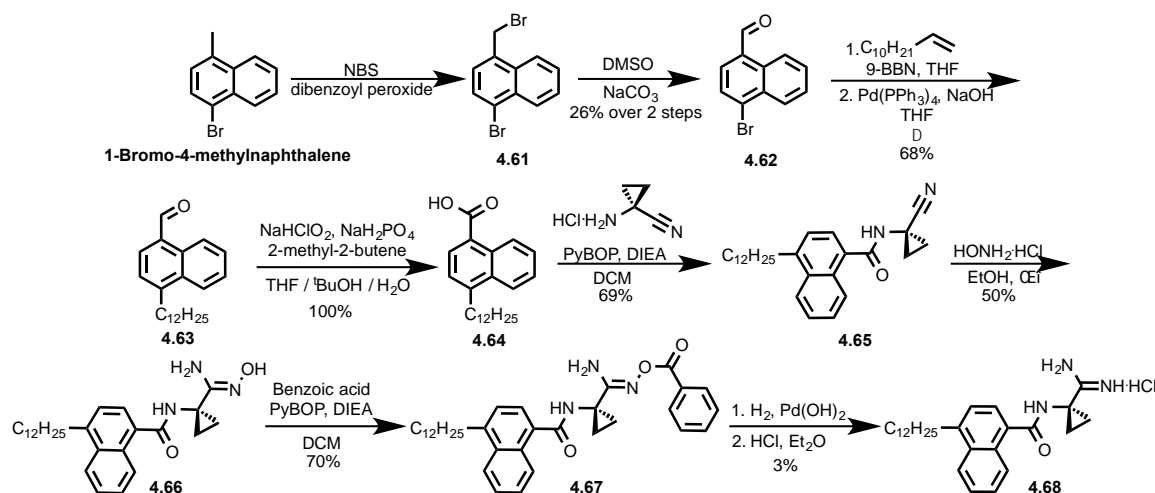
Scheme 4.11: Synthesis of 2,6-naphthalene substituted inhibitor **4.53**.

Two other naphthalene-based inhibitors were synthesized to fully test the size of this region of the pocket. Next, a 1,5-substituted derivative was synthesized (Scheme 4.12). Starting with the bromination of 1-naphthaldehyde using bromine and acetic acid to **4.54**.^{12,13} A Suzuki coupling of **4.54** and 1-decene appended the 10-carbon tail to afford **4.55**. Using a Pinnick oxidation, the aldehyde was converted to a carboxylic acid in **4.56**.⁴ 1-Amino-1-cyclopropanecarbonitrile hydrochloride was coupled to **4.56** using PyBOP to yield nitrile **4.57**. Hydroxylamine hydrochloride was used to convert the nitrile to amideoxime **4.58**, which was then protected using benzoic acid and PyBOP to afford **4.59**. Using a Pd-catalyzed hydrogenation, the N-O bond was cleaved to yield primary amidine **4.60** as a hydrochloride salt.



Scheme 4.12: Synthesis of the 1,5-naphthalene based inhibitor **4.60**.

The final derivative synthesized was a 1,4-naphthalene substituted molecule (Scheme 4.13). Synthesis of this derivative began with bromination of the benzylic position of 1-bromo-4-methylnaphthalene using NBS to yield **4.61**.¹⁴ The primary bromide was converted to aldehyde **4.62** using DMSO and sodium carbonate.¹⁴ A Suzuki coupling appended the 12-carbon tail to yield aldehyde **4.63**. Oxidation of the aldehyde to carboxylic acid using a Pinnick oxidation yielded **4.64**.⁴ PyBOP was used to couple the carboxylic acid and 1-amino-1-cyclopropanecarbonitrile hydrochloride to afford **4.65**. Conversion of the nitrile to amideoxime **4.66** was accomplished using hydroxylamine hydrochloride followed by protection using benzoic acid and PyBOP to afford **4.67**. Using a Pd-catalyzed hydrogenation, the N-O bond was cleaved to yield primary amidine **4.68** as a hydrochloride salt.



Scheme 4.13: Synthesis of the 1,4-substituted naphthalene derivative **4.68**.

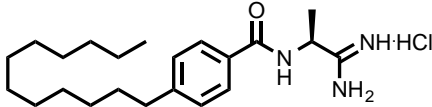
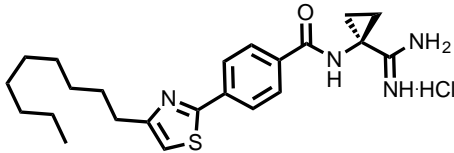
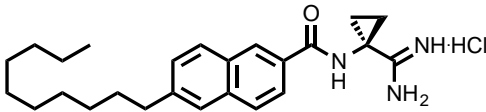
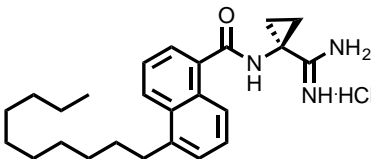
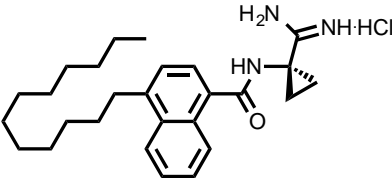
4.4.2 Evaluation of Rationally Designed SphK2-selective Inhibitors

Using the SphK2 homology model, a potential SphK2-selective inhibitor was suggested. Once synthesized, this molecule was tested and unfortunately was not found to be SphK2-selective (Table 4.3). This thiazole-containing inhibitor is slightly more potent at SphK1 and its potency at SphK2 is at a level similar to previous inhibitors.

The naphthalene-derived inhibitors, **4.53** – **4.68**, gave interesting results (Table 4.3). The more linear 2,6-substituted derivative **4.53** is a low micromolar dual inhibitor. This molecule was the only naphthalene derivative that showed inhibition of SphK2. All SphK inhibition was lost with the 1,4-substituted derivative **4.68**, which was not surprising since it is very wide and bulky with the extra benzene ring protruding from the molecule in comparison to the 12-carbon cyclopropyl derivative **3.35**. Since **4.60** is much more potent at SphK1 than SphK2, we believe the substrate pocket in SphK1 is much larger than SphK2,

even though our SphK2 homology model showed the opposite. From this data, we can conclude that our SphK2 homology model is not a proper representation of the actual enzyme and cannot be used to suggest potential SphK2-selective inhibitors. Once more potent SphK2-selective inhibitors are reported in the literature, the model can be redesigned and used to suggest inhibitors.

Table 4.3: K_i values of rationally designed SphK2-selective inhibitors.

Compound	Structure	K_i (mM) ^a		SphK1 Selectivity ^b
		SphK1	SphK2	
(S)-4.6		0.5	0.9	3.6
4.47		~5	~10	4
4.53		~5	~3	1.2
4.60		~5	>10	N/A
4.68		>10	>10	N/A

^a $K_i = [I] / (K'_M / K_M - 1)$. K_M of sphingosine at SphK1 is 10 μ M. K_M of sphingosine at SphK2 is 5 μ M.

^b Selectivity = $(K_i / K_M)^{\text{SphK2}} / (K_i / K_M)^{\text{SphK1}}$.

4.5 Conclusion

During the first generation SAR of our amidine-based inhibitors, there appeared to be a stereochemical preference for SphK2 over SphK1. Using this information, we thought we would be able to design potent SphK2-selective inhibitors and thus achieve all of our goals. Unfortunately, when investigated, these enantiomers did not display a differential preference for SphK2 over SphK1 (Table 4.1). All of these inhibitors are selective for SphK1, but are not as potent and selective as molecules synthesized with the purpose of being SphK1-selective (Table 3.6). It does appear as though these molecules are more selective for SphK2 at shorter tail lengths; however, potency is lost with these shorter molecules. The hydrazine-based inhibitor gave similar results, as it is a dual inhibitor (Table 4.2). Substituted hydrazine-based molecules need to be synthesized in order to gain more useful information from this core structure.

Using a SphK2 homology model, a potential SphK2-selective inhibitor was suggested and once tested, it was slightly SphK1-selective (Table 4.3). From the model, it appeared as though the pocket of SphK2 was wider and to test this, we synthesized naphthalene-based inhibitors. Unfortunately, none of these molecules were selective for SphK2 either. From this series, though, we determined the pocket of SphK1 is wider than SphK2 since **4.60** was more selective for SphK1.

All of these molecules, and others synthesized in different series, inhibit SphK2 to a similar degree displaying a flat SAR. Most have K_i values between 5 – 50 μ M, which leads us to believe SphK2 is a promiscuous protein since it binds

molecules of varying functionality to a similar extent. This supports the fact that SphK2, and not SphK1, was found to phosphorylate most substrates designed to be agonists/antagonists of the S1P receptors. This will make it difficult to design a potent SphK2-selective inhibitor, as we have experienced. In order to accomplish the goal of a potent SphK2-selective inhibitor, the core structure of our inhibitors will most likely need to be drastically altered.

4.6 References

- (1) Kharel, Y.; Raje, M.; Gao, M.; Gellett, A. M.; Tomsig, J. L.; Lynch, K. R.; Santos, W. L. *Biochem J* **2012**, *447* (1), 149-157.
- (2) Olivera, A.; Mizugishi, K.; Tikhonova, A.; Ciaccia, L.; Odom, S.; Proia, R. L.; Rivera, J. *Immunity* **2007**, *26* (3), 287-297.
- (3) Hait, N. C.; Allegood, J.; Maceyka, M.; Strub, G. M.; Harikumar, K. B.; Singh, S. K.; Luo, C.; Marmorstein, R.; Kordula, T.; Milstien, S.; Spiegel, S. *Science* **2009**, *325* (5945), 1254-1257.
- (4) Roesner, S.; Casatejada, J. M.; Elford, T. G.; Sonawane, R. P.; Aggarwal, V. K. *Organic Letters* **2011**, *13* (21), 5740-5743.
- (5) Asha, D.; Malviya, M.; Chandrappa, S.; Sadashiva, C. T.; Vinaya, K.; Prasanna, D. S.; Rangappa, K. S. *Lett Drug Des Discov* **2009**, *6* (8), 637-643.
- (6) Kennedy, A. J.; Mathews, T. P.; Kharel, Y.; Field, S. D.; Moyer, M. L.; East, J. E.; Houck, J. D.; Lynch, K. R.; Macdonald, T. L. *J Med Chem* **2011**, *54* (10), 3524-3548.
- (7) Balakrishnan, S.; Zhao, C.; Zondlo, N. J. *Journal of Organic Chemistry* **2007**, *72* (25), 9834-9837.
- (8) Zahariev, S.; Guarnaccia, C.; Lamba, D.; Cemazar, M.; Pongor, S. *Tetrahedron Lett* **2004**, *45* (51), 9423-9426.
- (9) Shao, H.; Shi, S. H.; Huang, S. L.; Hole, A. J.; Abbas, A. Y.; Baumli, S.; Liu, X. R.; Lam, F.; Foley, D. W.; Fischer, P. M.; Noble, M.; Endicott, J. A.; Pepper, C.; Wang, S. D. *Journal of Medicinal Chemistry* **2013**, *56* (3), 640-659.
- (10) Mineno, T.; Ueno, T.; Urano, Y.; Kojima, H.; Nagano, T. *Organic Letters* **2006**, *8* (26), 5963-5966.
- (11) Mayhoub, A. S.; Marler, L.; Kondratyuk, T. P.; Park, E. J.; Pezzuto, J. M.; Cushman, M. *Bioorgan Med Chem* **2012**, *20* (1), 510-520.
- (12) Repine, J. T.; Johnson, D. S.; White, A. D.; Favor, D. A.; Stier, M. A.; Yip, J.; Rankin, T.; Ding, Q. Z.; Maiti, S. N. *Tetrahedron Lett* **2007**, *48* (31), 5539-5541.
- (13) Repine, J. T.; Johnson, D. S.; Stuk, T.; White, A. D.; Stier, M. A.; Li, T.; Yang, Z.; Maiti, S. N. *Tetrahedron Lett* **2007**, *48* (46), 8189-8191.
- (14) Chen, H. X.; Luzy, J. P.; Gresh, N.; Garbay, C. *European Journal of Organic Chemistry* **2006** (10), 2329-2335.

5

Optimization of the Metabolism of Sphingosine Kinase Inhibitors

Previous SphK inhibitors were tested *in vivo* and were effective at lowering S1P levels for a short time. Levels of the drug were measured using LC-MS indicating the half-life of these amide-containing inhibitors to be approximately 90 min. To increase the half-life of the amidine-based SphK inhibitors, the amide bond was replaced with 5-membered heterocyclic rings to mimic the planarity and electronics of the amide while increasing the metabolic stability. The half-life of these heterocyclic inhibitors did increase, but the blood concentrations were much lower than their amide counterparts. One method to increase blood concentration is to increase the solubility of the triazole-containing inhibitor. Solubility of these inhibitors was adjusted using a pyridine ring instead of a phenyl ring.

5.1 *In vivo* Evaluation of Amide-containing SphK Inhibitors

In order to use small molecules as tools to elucidate the roles of the SphKs, it was necessary to determine their efficacy at lowering cellular S1P levels in whole animals. Using a mouse model, **3.57** was administered by intraperitoneal (IP) injection at a dose of 10 mg/kg and blood was drawn at ASAP, 20 min, 1 h, 2 h, and 4h. This experiment showed whole blood S1P levels

dropped rapidly to nearly half the initial levels within 1 h after injection proving this compound is effective at inhibiting the production of S1P (Figure 5.1A). However, S1P levels began to rise after 1 h implying the molecule may be metabolized quickly. To test this, levels of **3.57** were measured using LC-MS and it was confirmed that levels of this molecule decreased dramatically to less than half of the initial amount at 2 h (Figure 5.1B).¹ Since this molecule and other SphK inhibitors in our library are cleared from whole blood quickly, they are not useful tools in determining the roles of the SphKs.^{1,2}

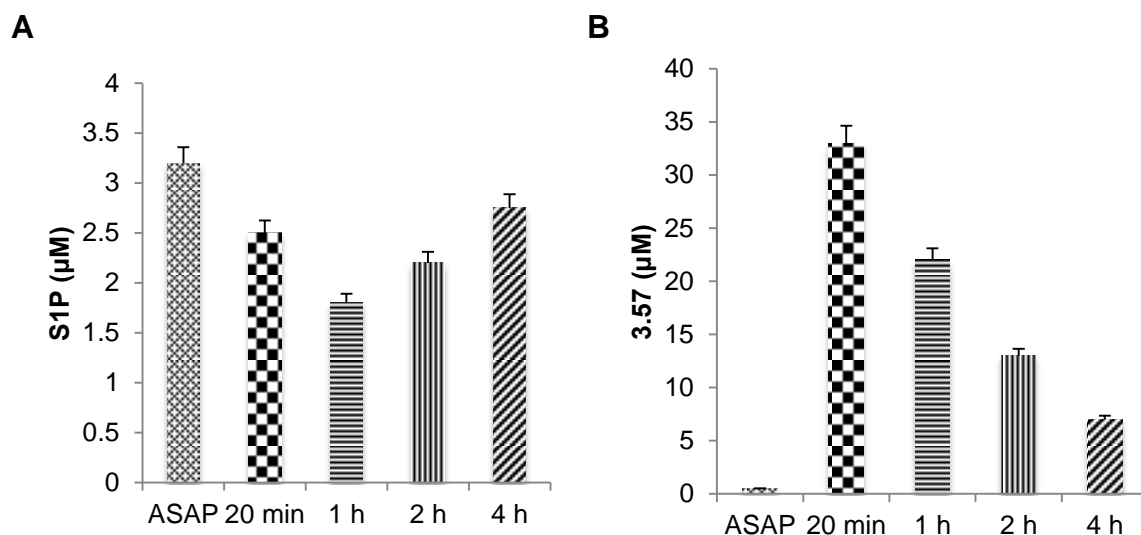


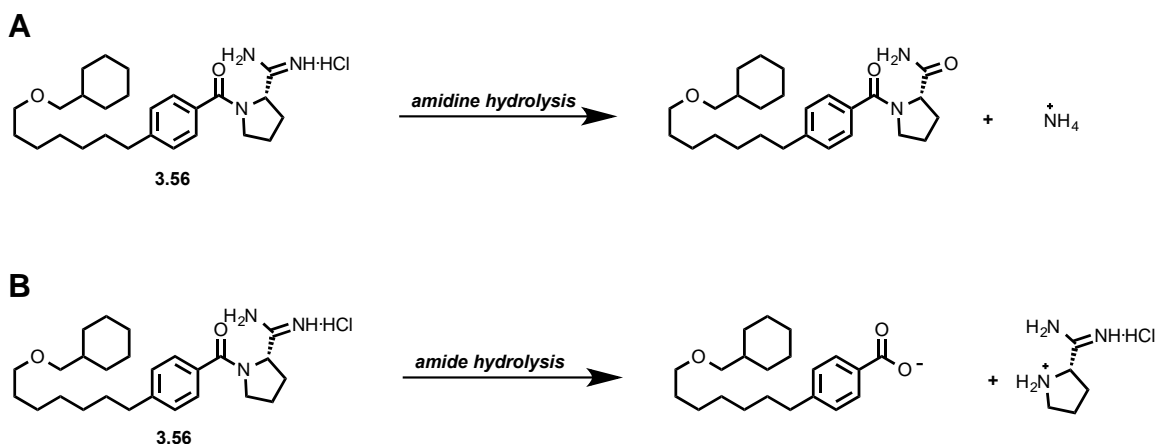
Figure 5.1: Wild-type mice dosed with 10 mg/kg of **3.57** via IP injection. Blood samples were taken after injection at times indicated. Levels of S1P and **3.57** were measured using LC-MS. (A) S1P and (B) Compound **3.57**.

5.2 Investigating Possible Modes of Metabolism

There are two conventional sites of metabolism of the amidine-based sphingosine kinase inhibitors: oxidation of the aromatic ring by cytochrome

P450s in the liver and hydrolysis of the amidine or amide bond. The most likely mode of metabolism of these molecules is through hydrolysis since it is faster than oxidation.¹

Amidines are rare moieties in natural and pharmaceutical molecules. Primary amidines are protonated at physiological pH, making absorption through the gastrointestinal tract unlikely, allowing them to be easily hydrolyzed (Scheme 5.1A). Hydrolysis of amides is a common form of metabolism of molecules making amides useful as pro-drugs. Since hydrolysis by amidase is facile, it may be the culprit for the fast removal of these inhibitors from the blood stream (Scheme 5.1B). If the amidine and/or the amide is being hydrolyzed, it will render these inhibitors inactive toward the SphKs.¹



Scheme 5.1: Modes of metabolism of **3.57**. (A) Amidine hydrolysis and (B) amide hydrolysis.

5.2.1 Amidine Prodrugs

To determine if the metabolism of the amidine is decreasing the half-life of these compounds, prodrugs were synthesized and tested *in vivo*. Prodrugs are

inactive compounds that are converted into active molecules by means of phosphorylation or hydrolysis. This is a common practice in the design of pharmaceuticals to improve various pharmacokinetic properties.¹

Various amidine prodrugs were synthesized and tested *in vivo*: an amideoxime of compound **3.57** (**5.1**), substituted oxadiazoles of compound (**S**)-**3.40** (**5.2a-c**), and substituted oxadiazoles of compound **3.35** (**5.3a-c**) (Figure 5.2). The substituent on the oxadiazole ranged from methyl (**a**), phenyl (**b**), and p-nitrophenyl (**c**) to tune the reduction potential of the N-O bond. These compounds were tested in the recombinant enzyme assay *in vitro* to determine if they inhibit the SphKs (data not shown). Not surprisingly, none of these compounds were active inhibitors of the SphKs. These molecules were tested against U937 leukemia cells and in whole animal, but none lowered S1P levels. LC-MS was used to determine if these pro-drugs were being metabolized to the active amidine inhibitor, however, none was observed (data not shown). From these data, it is conclusive that these amideoxime and oxadiazoles are poor prodrugs for amidines possibly due to poor bioavailability, sequestration, or are highly protein bound.¹

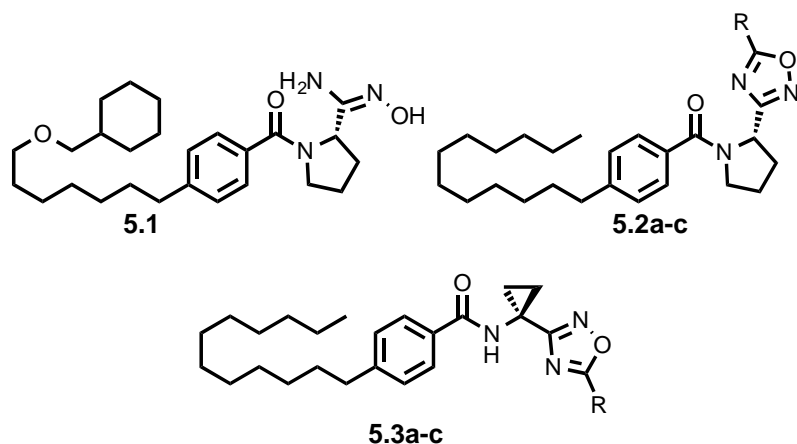


Figure 5.2: Structures of amidine prodrugs used to determine if metabolism at the amidine reduces the half-life of our inhibitors.

5.2.2 Amide Isosteres

The other mode of metabolism of the SphK inhibitors is hydrolysis of the amide bond. To circumvent this, isosteres of the amide were synthesized and tested for efficacy *in vitro* and *in vivo*. An isostere is a functional group that is similar chemically and physically to another. There are various functional groups that would serve as amide mimics, for instance, double bonds and ketones would mimic the planarity, whereas, an amine would mimic the hydrogen bond donor ability.¹ Groups that contain both, such as a urea, thioamide, and nitrogen-containing heterocycles, are ideal candidates.^{1,3} Heterocycles offer an additional advantage by reducing the degrees of freedom, which in the past has led to an increase in potency. Since the original SphK inhibitors were designed from heterocycle-containing substrates, it was decided they would be the ideal isostere to determine if hydrolysis of the amide bond is shortening the half-life (Figure 5.3).¹

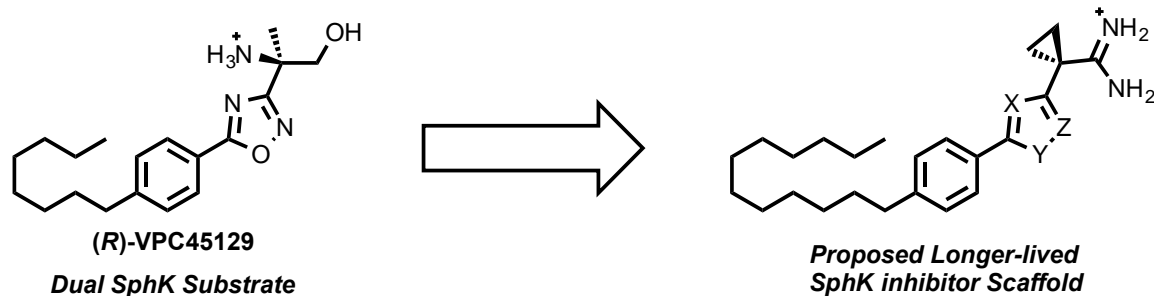
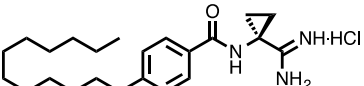
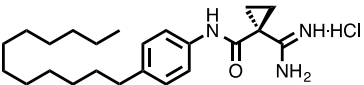
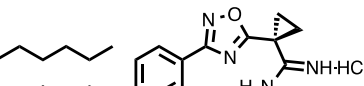
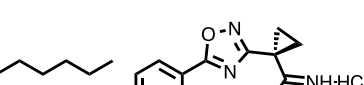
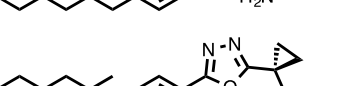
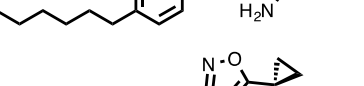
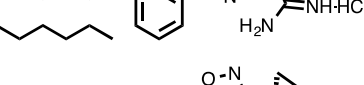
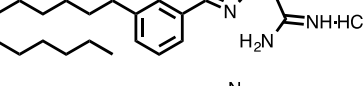


Figure 5.3: Design of heterocyclic isosteres based on **(R)-VPC45129**.

The substrate from which these inhibitors were designed contains an oxadiazole. The most successful substitutions of the amide bond of these substrates were oxadiazoles; therefore, the first heterocycles synthesized in the inhibitors were the three different isomers of the oxadiazoles (Table 5.1).¹ The inhibitory efficacy of these molecules was measured by calculating a K_i value via a $[\gamma\text{-}^{32}\text{P}]\text{ATP}$ *in vitro* assay.⁴ The overall shape of these new inhibitors presents the amidine at a slightly different angle to the γ -phosphate of ATP, which may lower the K_i value and cause the molecule to not fit as well in the active-site of the enzymes. This was corrected by synthesizing *meta*-substituted analogs of these molecules (Table 5.1).¹

Table 5.1: K_I and IC_{50} values of *para*- and *meta*-oxadiazole inhibitors compared to amides **3.35** and **3.42**.¹

Compound	Structure	K_I (μM) ^a		SphK1 Selectivity ^b	IC_{50} (μM)
		SphK1	SphK2		
3.35		0.2	0.5	5	–
3.42		0.3	6	40	–
5.4		0.32	8	50	1
5.5		3	3.4	2.3	28
5.6		1.6	1.2	1.5	0.2
5.7		0.04	14.1	705	4
5.8		0.40	10.2	51	1.2
5.9		0.2	8.1	81	0.2

^a $K_I = [I] / (K'_M / K_M - 1)$. K_M of sphingosine at SphK1 is 10 μM . K_M of sphingosine at SphK2 is 5 μM .

^b Selectivity = $(K_I / K_M)^{SphK2} / (K_I / K_M)^{SphK1}$.

From these *in vitro* data, it was concluded that the most potent oxadiazole isomer is the 1,2,4-oxadiazole (**5.4** and **5.7**). When comparing all of these oxadiazole inhibitors to amides **3.35** and **3.42**, it appears as though these molecules mimic the amide configuration of **3.42** leading to SphK1-selectivity. The *meta*-substitution increased potency for all isomers with the most potent and selective of all six molecules being the *meta*-substituted 1,2,4-oxadiazole **5.7**

being 705-fold selective for SphK1. Also, these inhibitors were tested in U937 cells to measure the effectiveness in lowering S1P levels. IC_{50} values were calculated in order to compare these values between molecules and to the K_i values (Table 5.1). The IC_{50} is the concentration of inhibitor required to reduce S1P levels by 50% and similarly to K_i values, a smaller value indicates a more potent inhibitor. Since in whole cells, endogenous sphingosine is present at the K_M , it is expected that the K_i and IC_{50} values should be equivalent. Unfortunately, this is not the case for most of these inhibitors. The 1,3,4-oxadiazole inhibitors **5.4** and **5.7** are the only molecules whose IC_{50} values were equal to or below the K_i value. This demonstrates the discrepancy between *in vitro* and *ex vivo* data.¹

To determine if these molecules increase the half-life of the amidine-based SphK inhibitors *in vivo*, they were injected into mice and tested for longevity of the compound and their ability to lower S1P levels. With each of these molecules displaying similar data, it was determined that the half-life of these oxadiazoles is longer than their amide counterparts (Figure 5.4A). The half-life has increased from 1.5 h to longer than 4 h; however, these molecules do not significantly lower S1P levels (Figure 5.4B). If levels of the inhibitor are low in the blood, it seems to reason that the molecule will not be able to reach its target to lower S1P levels thus giving the profile observed.¹ The initial increase in S1P levels can be explained by this molecule inhibiting SphK2, which when inhibited, has been shown to increase S1P levels.⁵

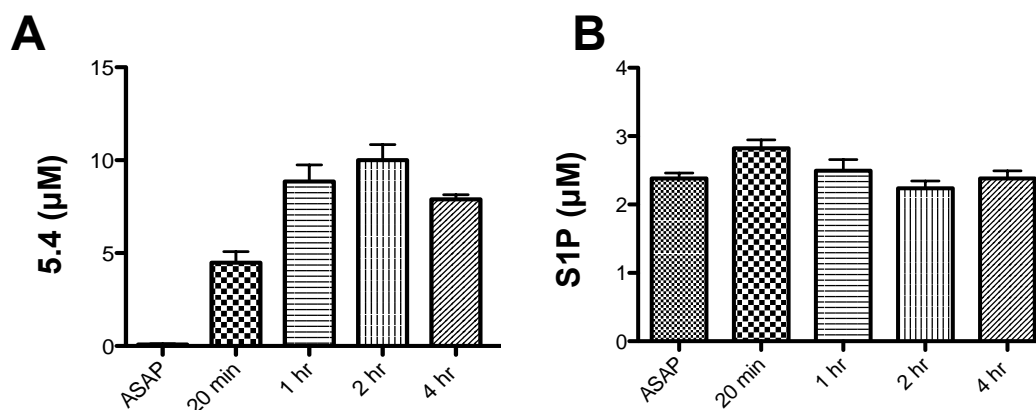


Figure 5.4: Wild-type C57BL/6 mice were dosed with 10 mg/kg of compound **5.4** via IP injection. Blood samples were taken after injection at times indicated. Levels of compound **5.4** (A) and S1P (B) were measured using LC-MS.

Interesting results were observed with the isomers of the oxadiazoles. It has been reported in the literature that the two 1,2,4-oxadiazole regioisomers and the 1,3,4-oxadiazole isomer have different physical and pharmacological properties. The three isomers have different water solubility, plasma protein binding, and metabolic stability.^{1,3,6} The most potent of the three isomers was the first 1,2,4-oxadiazole listed (**5.4** and **5.7**), which corresponds to the least water-soluble of the three isomers, linking the effect of solubility to potency.⁶ When the oxadiazole-containing inhibitors were tested in U937 cells, only the K_i value of the 1,3,4-oxadiazole matched the IC_{50} value.¹ The 1,2,4-oxadiazole IC_{50} values are greater than the K_i values indicating that these molecules are not as effective *in vivo*. Since the IC_{50} value of the 1,3,4-oxadiazole is equal to its K_i value, it may indicate that the metabolism of the 1,2,4-oxadiazole is faster than the 1,3,4-oxadiazole in whole cells and whole animals. The *in vitro* testing does not have the enzymes necessary for metabolism and thus the molecules can adequately reach their target enzyme. Metabolism of the 1,2,4-oxadiazole most likely occurs

with the cleavage of the N-O bond and since the 1,3,4-oxadiazole does not contain this, it is not as easily metabolized.^{3,7}

Even though the *in vitro* data does not align with the *in vivo* data, an increase in half-life was observed and further SAR must be completed in order to fully investigate 5-membered heterocycles as amide isosteres. It could be the oxadiazoles are not the ideal heterocycle to replace the amide and other heterocycles may increase potency, selectivity, and have longer half-lives while able to enter cells and lower S1P levels *in vivo*.

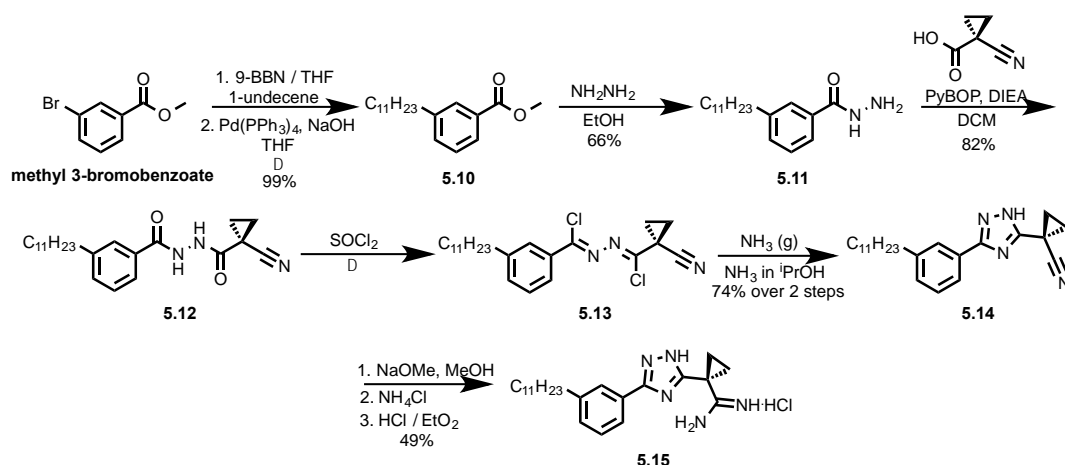
5.3 Nitrogen-based 5-Membered Heterocyclic Amide Bioisostere Inhibitors

When considering other heterocycles in place of the oxadiazoles, nitrogen-based heterocycles should be tested to investigate their effectiveness in increasing the half-life. Previous SAR indicated that solubility plays a large factor in the potency of these amidine-based inhibitors. An imidazole analog was synthesized and was found to be a weak inhibitor of the SphKs [K_i = 10.2 (SphK1) and 12.2 (SphK2)]. The pK_a of imidazole is near biological pH causing this heterocycle to be too water-soluble.¹ When analyzing the literature for the metabolism of 5-membered heteroaromatic compounds, adding nitrogen to rings increases the metabolic stability. The addition of nitrogen raises the ionization potential and the particular placement in the ring will have an effect on pK_a , cLogP, as well as the ionization potential. All of these factors influence the metabolic stability of heterocycles and thus a full range of heterocycles must be tested. Syntheses of a pyrrole, pyrazole, and 1,2,4-triazole were designed and all

but the pyrrole were completed. Synthesis of the pyrrole inhibitor has been difficult due to volatility and water solubility of early intermediates.

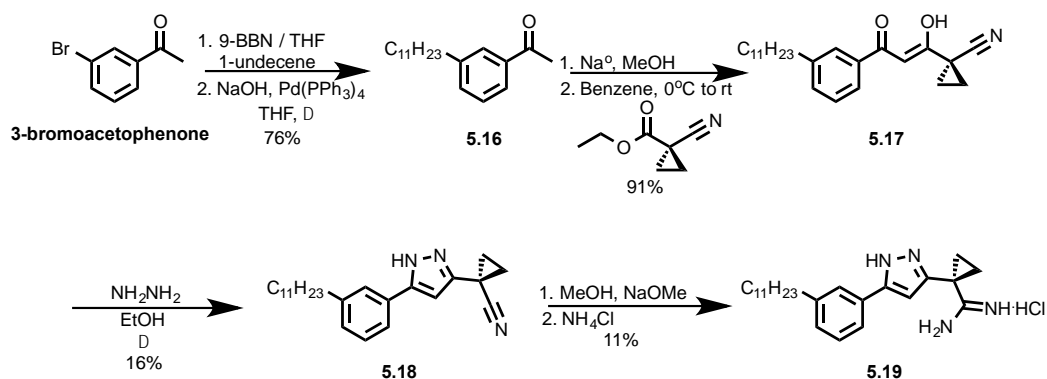
5.3.1 Synthesis of N-based Heterocycles

The first heterocycle synthesized was the 1,2,4-triazole since more heteroatoms in the ring allows for bonds to be formed more easily (Scheme 5.2). The synthesis began with a Suzuki coupling to append the C-11 tail on methyl 3-bromobenzoate to yield ester **5.10**. The ester was converted to benzohydrazide **5.11** by reaction with pure hydrazine in ethanol.⁸ Using a PyBOP coupling, 1-cyanocyclopropane-1-carboxylic acid was coupled to **5.11** to form dihydrazide **5.12**. Conversion of the oxygens of **5.12** to chlorides was accomplished using thionyl chloride in refluxing conditions followed by cyclization to the 1,2,4-triazole using ammonia to afford **5.14**.⁹⁻¹¹ Basic Pinner conditions were used to convert the nitrile to the primary amidine hydrochloride salt **5.15**.



Scheme 5.2: Synthesis of 1,2,4-triazole analogue **5.15**.

Synthesis of the pyrazole began with a Suzuki coupling to append the C-11 tail onto 3-bromoacetophenone to yield **5.16** (Scheme 5.3). Combining this with ethyl 1-cyanocyclopropane-1-carboxylate in a mixed Claisen condensation, afforded 1,3-diketone **5.17**.¹² Cyclization to the pyrazole **5.18** was accomplished using pure hydrazine in ethanol under refluxing conditions.¹² Conversion of the nitrile to primary amidine hydrochloride salt **5.19** was achieved using basic Pinner conditions.

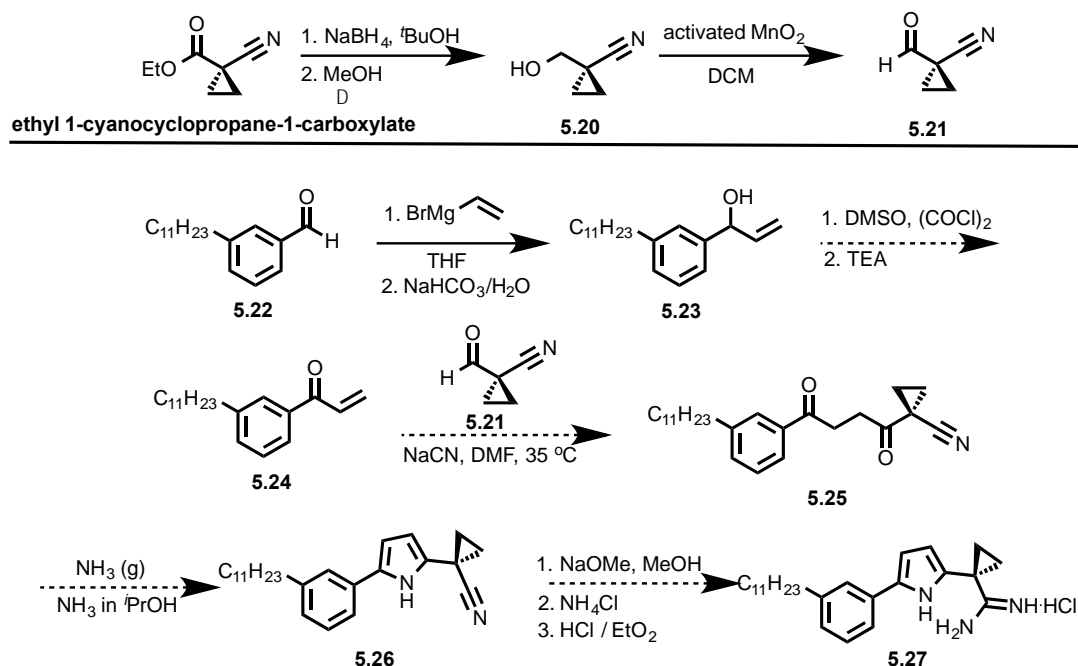


Scheme 5.3: Synthesis of pyrazole analogue **5.19**.

The most challenging heterocycle to synthesize, thus far, has been the pyrrole (Scheme 5.4). All routes of synthesis have attempted to synthesize a 1,4-diketone **5.25**, which will be reacted with ammonia to cyclize to the pyrrole ring. Synthesis of the 1,4-diketone can be accomplished by reaction of two ketones or an aldehyde and an α,β -unsaturated ketone. Unfortunately the head group can only be purchased as a carboxylic acid or ethyl ester. Conversion of these to the ketone was attempted but all routes failed. The more realistic conversion is to the aldehyde. Even though this route should easily be accomplished, the low

molecular weight of the intermediates and the aldehyde cause it to be water-soluble and volatile making purification and isolation difficult. Also, reagents to oxidize the primary alcohol **5.20** to the aldehyde **5.21** have been difficult to find. Swern oxidation, Dess-Martin, PCC, and activated MnO_2 have all been attempted with the most successful reaction being the continual addition of activated MnO_2 throughout the length of the reaction. Even through this route, the yield has been low. With the water solubility and high volatility of the product, the reaction should not require high boiling or aqueous solvents. Also, other means of oxidation run the risk of over oxidation to the carboxylic acid.

Synthesis of the remainder of the molecule is accomplished by reaction of vinyl magnesium bromide with 3-undecylbenzaldehyde to afford **5.23**. The vinyl alcohol was oxidized α,β -unsaturated ketone **5.24** using a Swern oxidation. This will then be reacted with aldehyde **5.21** to form the 1,4-diketone **5.25**. Cyclization the pyrrole **5.26** using ammonia followed by conversion of the nitrile to the primary amidine hydrochloride salt **5.27** will be accomplished using basic Pinner conditions.

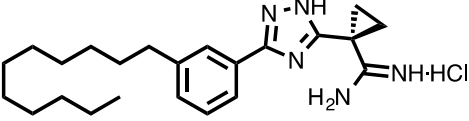
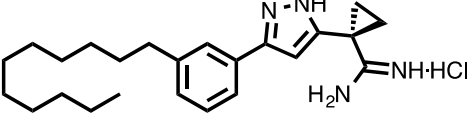
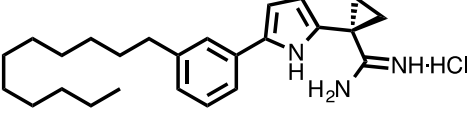


Scheme 5.4: Proposed synthesis of pyrrole analogue **5.27**.

5.3.2 Biological Evaluation of N-based Heterocyclic Analogues

The K_i values of these inhibitors was determined via a [γ - 32 P]ATP *in vitro* assay of SphK enzymatic activity (Table 5.2). The most potent of the completed molecules is the 1,2,4-triazole compound **5.15**, which is equipotent to the 1,3,4-oxadiazole inhibitor **5.9**. Since the 1,2,4-triazole inhibitor is SphK1-selective, it mimics the amide orientation of **3.42** as was observed with all of the oxadiazole molecules. Interestingly, the pyrazole inhibitor **5.19** completely lost activity at each kinase indicating there must be a negative interaction between this molecule and the substrate binding pocket.

Table 5.2: K_i values of N-based heterocyclic inhibitors.

Compound	Structure	K_i (μM) ^a			
		SphK1	SphK2	SphK1 Selectivity ^b	Predicted
5.15		0.373	6.9	37	0.330
5.19		>10	>10	N/A	0.140
5.27		--	--	N/A	0.270

^a $K_i = [I] / (K'_M / K_M - 1)$. K'_M of sphingosine at SphK1 is 10 μM . K_M of sphingosine at SphK2 is 5 μM .

^b Selectivity = $(K_i / K_M)^{\text{SphK2}} / (K_i / K_M)^{\text{SphK1}}$.

Since **5.15** is the only molecule that inhibits the kinases, it was tested *ex vivo* in U937 leukemia cells to determine if this molecule would inhibit the production of S1P in whole cells. Indeed, **5.15** displayed low concentration of S1P after 2 hours similar to the oxadiazole inhibitors with an IC_{50} value of approximately 0.2 μM (data not shown). This is similar to the 1,3,4-oxadiazoles with the IC_{50} value being the same or less than the K_i value. Since the goal of these molecules is to increase the half-life of our inhibitors, this molecule was tested in mice. Once again, at greater than 4 h, the half-life of this heterocycle is much longer than its amide counterpart (Figure 5.5A). The blood concentration of this molecule is low, thus, not greatly reducing S1P levels (Figure 5.5B). If metabolism at the heterocycle ring is causing these molecules to not reach their

target, then the addition of the nitrogen atom did not increase the metabolic stability of these inhibitors.

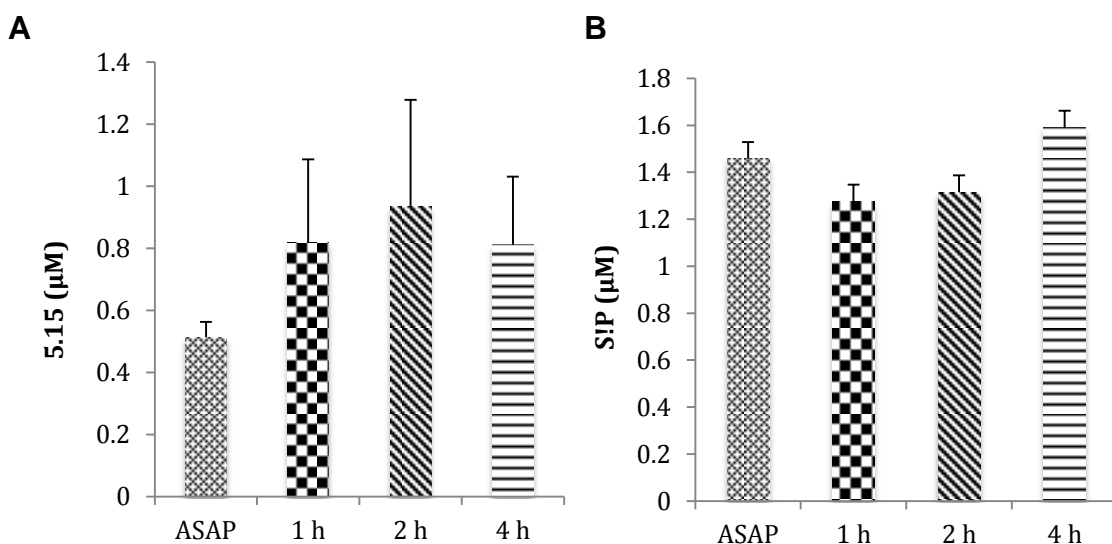


Figure 5.5: Wild-type C57BL/6 mice were dosed with 10 mg/kg of compound **5.15** via IP injection. Blood samples were obtained after injection at the times indicated. Levels of compound **5.15** (A) and S1P (B) were measured by LC-MS.

According to the literature, one of the most metabolically stable heterocycles is the pyrazole. Unfortunately, the molecule containing the pyrazole ring completely lost activity. The three nitrogen-based heterocyclic inhibitors were docked in the SphK1 homology model to predict the K_i values and to rationalize the experimental results (Figure 5.6 and Table 5.2). The predicted K_i values for the triazole **5.15** matched very closely to the experimental K_i value. Surprisingly, the pyrazole **5.19** was predicted to be the most potent. From the model, the N-H group on the pyrazole ring hydrogen bonds to the nearby Asp81 that participates in the chelation of the Mg^{2+} ion with ATP. It is reasonable to assume that this

hydrogen bonding interaction removes enough of the chelation to destabilize the Enzyme • Inhibitor • ATP complex resulting in poor inhibition by **5.19**. The pyrrole inhibitor is predicted to be a more potent inhibitor than **5.15**, so it will be interesting if this holds true once synthesis of this molecule is completed.

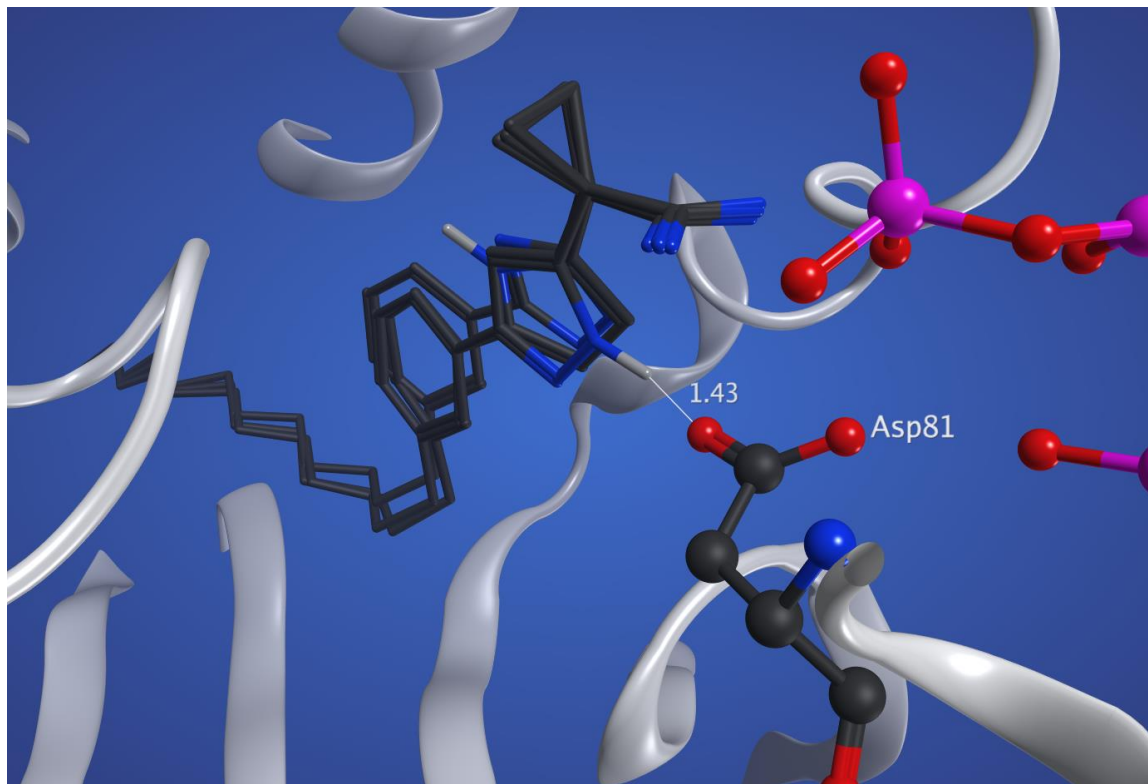


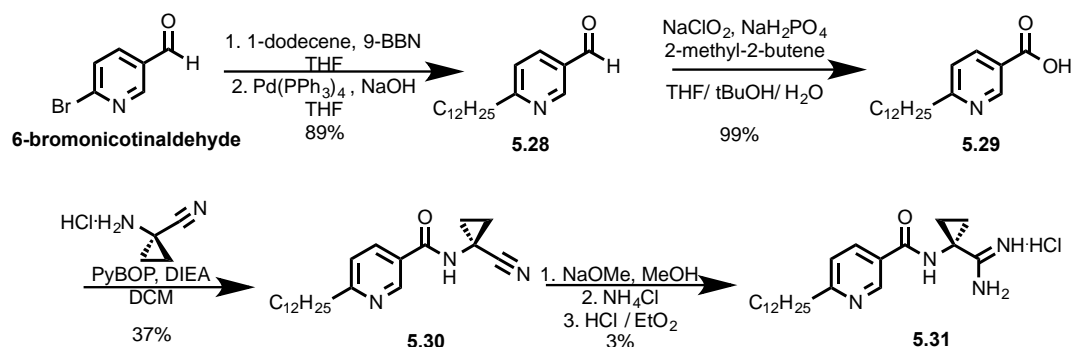
Figure 5.6: **5.15**, **5.19**, and **5.27** docked in the SphK1 homology model. Hydrogen bonding interaction between the pyrazole N-H and Asp81 predicted to increase potency of this inhibitor, but experimental data shows it must be a negative interaction. The tautomer of the triazole ring can place the N-H group on the opposite side of the ring as in pyrrole.

5.4 Pyridine Inhibitors

Over the past generations of amidine-based SphK inhibitors, not much SAR has been completed at the benzene ring besides deleting and replacing it with a double bond. It is known, however, that deletion of the ring removes SphK2 inhibition but does not have much of an effect on SphK1 inhibition.

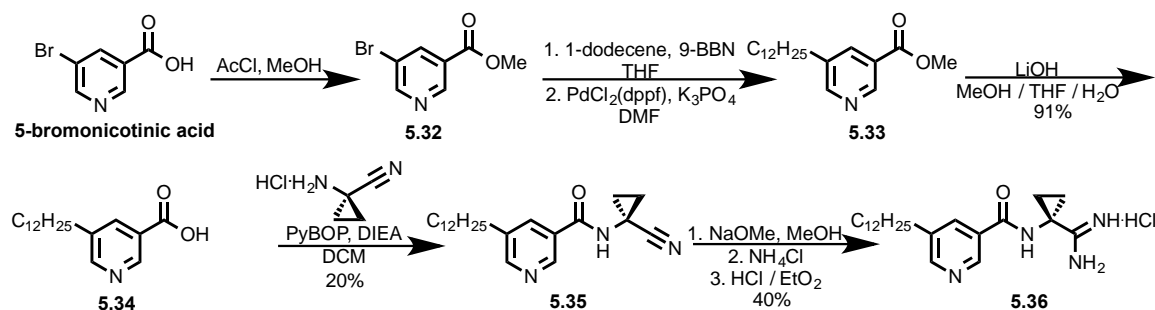
Through the previous data collected from ether-containing inhibitors and the three oxadiazole isomers, it is clear that solubility can play a large part in potency of these inhibitors. Replacing the benzene ring with a pyridine should make the inhibitors more water-soluble, which may be desirable to combine with more lipophilic moieties of previous molecules. Also, the nitrogen can be located at different positions around the ring allowing for possible interactions with the substrate-binding pocket. If metabolism of these inhibitors is occurring due to oxidation of the aromatic ring by P450 enzymes, then the nitrogen atom may block this from occurring.

Pyridine-based inhibitors were designed from commercially available bromopyridines containing aldehydes or carboxylic acids. The first pyridine-based inhibitor synthesized was a *para*-substituted inhibitor to compare to the original benzene molecules (Scheme 5.5). It began with a Suzuki coupling to append the C-12 tail on 6-bromonicotinaldehyde to afford aldehyde **5.28**. A Pinnick oxidation converted the aldehyde to carboxylic acid **5.29**. Using PyBOP, 1-aminocyclopropane-1-carbonitrile hydrochloride was coupled to **5.29** to form the amide bond of **5.30**. Standard Pinner conditions were used to convert the nitrile to the primary amidine hydrochloride salt of **5.31**.



Scheme 5.5: Synthesis of **5.31** starting from 6-bromonicotinaldehyde.

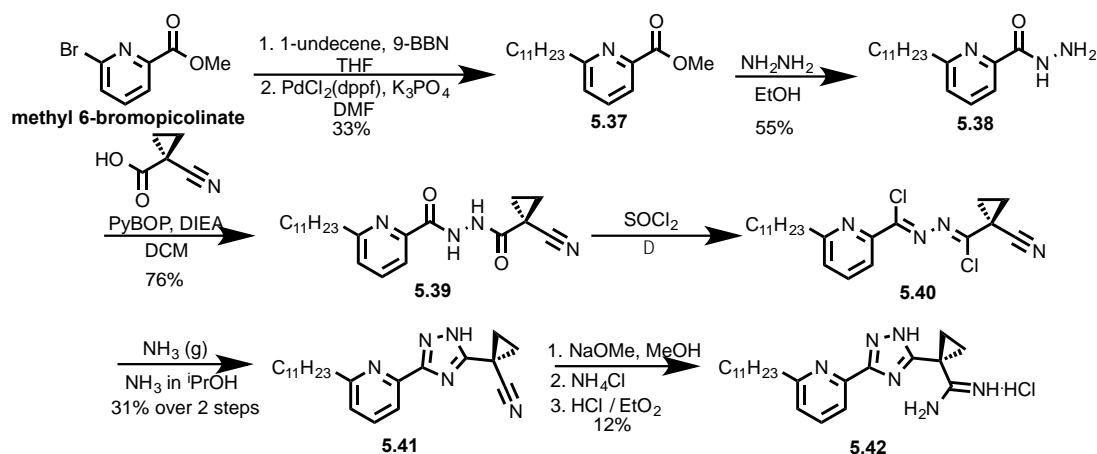
The same molecule, but with *meta*-substitution was synthesized starting with an esterification of 5-bromonicotinic acid to yield methyl ester **5.32** (Scheme 5.6). A Suzuki coupling was used to append the C-12 tail to afford ester **5.33**. Saponification to the carboxylic acid followed by a PyBOP-mediated coupling with 1-aminocyclopropane-1-carbonitrile hydrochloride gave nitrile **5.35**. Standard Pinner conditions were used to convert the nitrile to the primary amidine hydrochloride salt **5.36**.



Scheme 5.6: Synthesis of **5.36** starting from 5-bromonicotinic acid.

From previous SAR, it was known that *meta*-substituted molecules are more potent with heterocycles in place of the amide. Two inhibitors containing both pyridine and a triazole ring were synthesized. Synthesis of these molecules was accomplished under similar means; therefore, a representative synthesis is shown (Scheme 5.7). The syntheses began with a Suzuki coupling to append the C-11 tail.¹³ The ester was then reacted with pure hydrazine in ethanol to form the hydrazide **5.38**. A PyBOP coupling with 1-cyanocyclopropane-1-carboxylic acid yielded the dihydrazide **5.39**. Conversion of the oxygens to chlorides to increase electrophilicity was accomplished using thionyl chloride **5.40**.^{9,10} This was then reacted with ammonia to cyclize to the triazole ring **5.41**.¹¹ Standard Pinner

conditions were used to convert the nitrile to the primary amidine hydrochloride salt **5.42**.



Scheme 5.7: Synthesis of **5.42** starting from methyl 6-bromopicolinate. Representative synthesis of inhibitors containing both pyridine and a triazole.

The inhibitory efficacy of these molecules was determined from a [γ - ^{32}P]ATP *in vitro* assay of SphK enzymatic activity (Table 5.3). None of these inhibitors were as potent against SphK1 as **5.15**, most oxadiazole inhibitors, and amides **3.35** and **3.42**. Since these pyridine molecules are not very potent in the *in vitro* assay, they were not tested *ex vivo* or *in vivo*. It is possible these molecules could be more metabolically stable than **5.15**, but these biological tests would need to be conducted to be conclusive. The K_i value for **5.31** is lower than 1 μM which is much more potent than **5.36**. In order to properly compare it to its phenyl counterpart **3.35**, it will need to be retested at concentrations below 1 μM to observe its true K_i value. From the one-point assay data (not shown), it appears that **5.31** is slightly less potent than **3.35** at SphK1 but much less potent

at SphK2 making it a SphK1-selective inhibitor. From this, it can be concluded that the increase in water-solubility from the addition of the pyridine ring has not greatly affected potency at SphK1. With the loss in potency at SphK2, perhaps the electrons on the nitrogen negatively interact with a nearby residue in the pocket. To determine if the presence of the nitrogen has lengthened the half-life, it will need to be subjected to the *in vivo* testing.

Table 5.3: K_i values of pyridine-based inhibitors.

Compound	Structure	K_i (mM) ^a	
		SphK1	SphK2
5.31		<1	~8
5.36		>1	7.4
5.42		~7	>10
5.43		~7	~10

^a $K_i = [I] / (K'_M / K_M - 1)$. K_M of sphingosine at SphK1 is 10 μ M. K_M of sphingosine at SphK2 is 5 μ M.

5.5 Conclusion

One goal of the SphK inhibition project is to develop potent and selective inhibitors of the SphKs to further elucidate the cellular roles of each of these enzymes. In order to accomplish this, the molecules need to be long lived in whole animals. Unfortunately, our most potent SphK1-selective inhibitors have a

half-life in whole animals of approximately 90 min. The main site of metabolism is most likely hydrolysis of the amide bond. To circumvent this, bioisosteres of the amide were synthesized. Isomers of oxadiazole rings were first synthesized and tested. The most potent *in vitro* inhibitor was 1,2,4-oxadiazole **5.7** but the most potent *ex vivo* inhibitor was 1,3,4-oxadiazole **5.9**.¹ This discrepancy may be due to metabolism of the heterocyclic ring or difficulty in transporting these molecules into cells.

The addition of nitrogen atoms usually increases the metabolic stability of heterocyclic rings. Nitrogen-based heterocyclic inhibitors were synthesized and the 1,2,4-triazole inhibitor was as potent as the **5.9**. The IC₅₀ value of **5.15** was similar to **5.9** possibly indicating these heterocycles are being metabolized more slowly than the 1,2,4-oxadiazoles or the 1,3,4-oxadiazoles can be transported into cells more easily. Unfortunately, in whole animals the concentration of these heterocyclic inhibitors is low, thus not allowing them to effectively lower S1P levels.

To investigate the effect of increasing the water-solubility and metabolic effects of replacing the benzene ring, pyridine-containing inhibitors were synthesized and tested *in vitro*. Unfortunately, most of these molecules were not very potent *in vitro* and were not tested *ex vivo* or *in vivo*. Since **5.31** has a K_i value below 1 μ M, it should be tested *in vivo* to determine if it lengthens the half-life. The addition of the nitrogen in the aromatic ring may block sites of oxidation by P450 enzymes.

While accomplishing the goal of increasing the half-life of these amidine-based SphK inhibitors, a new problem has arisen. The cause of the low blood concentration needs to be determined, so new molecules circumventing this may be designed and tested. These molecules may be metabolized or are highly protein bound, leading to low blood concentrations and the inhibitors not reaching their target enzymes.

5.6 References

- (1) Houck, J. D., The University of Virginia, 2013.
- (2) Kharel, Y.; Mathews, T. P.; Gellett, A. M.; Tomsig, J. L.; Kennedy, P. C.; Moyer, M. L.; Macdonald, T. L.; Lynch, K. R. *Biochem J* **2011**, *440* (3), 345-353.
- (3) Jean, D. J. S.; Fotsch, C. *Journal of Medicinal Chemistry* **2012**, *55* (22), 10315-10315.
- (4) Kharel, Y.; Mathews, T. P.; Kennedy, A. J.; Houck, J. D.; Macdonald, T. L.; Lynch, K. R. *Analytical biochemistry* **2011**, *411* (2), 230-235.
- (5) Kharel, Y.; Raje, M.; Gao, M.; Gellett, A. M.; Tomsig, J. L.; Lynch, K. R.; Santos, W. L. *Biochem J* **2012**, *447* (1), 149-157.
- (6) Goldberg, K.; Groombridge, S.; Hudson, J.; Leach, A. G.; MacFaul, P. A.; Pickup, A.; Poultney, R.; Scott, J. S.; Svensson, P. H.; Sweeney, J. *Medchemcomm* **2012**, *3* (5), 600-604.
- (7) Dalvie, D. K.; Kalgutkar, A. S.; Khojasteh-Bakht, S. C.; Obach, R. S.; O'Donnell, J. P. *Chemical Research in Toxicology* **2002**, *15* (3), 269-299.
- (8) Li, L. Y.; Zhu, L.; Chen, D. G.; Hu, X. L.; Wang, R. H. *European Journal of Organic Chemistry* **2011** (14), 2692-2696.
- (9) Kotlyarov, V. G.; Burdukovskii, V. F.; Mogonov, D. M. *Russ Chem B+* **2011**, *60* (1), 194-195.
- (10) Clodt, J. I.; Wigbers, C.; Reiermann, R.; Frohlich, R.; Wurthwein, E. U. *European Journal of Organic Chemistry* **2011** (17), 3197-3209.
- (11) Gautun, O. R.; Carlsen, P. H. J. *Molecules* **2001**, *6* (12), 969-978.
- (12) Hengst, J. A.; Wang, X. J.; Sk, U. H.; Sharma, A. K.; Amin, S.; Yun, J. K. *Bioorganic & Medicinal Chemistry Letters* **2010**, *20* (24), 7498-7502.
- (13) Meier, P.; Legrauerant, S.; Muller, S.; Schaub, J. *Synthesis-Stuttgart* **2003** (4), 551-554.

6

Experimental Section

6.1 Biological Methods

Sphingosine Kinase Assay. Human SphK1 and mouse SphK2 cDNAs were used to generate mutant baculoviruses that encoded these proteins. Infection of Sf9 insect cells with the viruses for 72 h resulted in >1000-fold increase in SphK activity in 10000g supernatant fluid from homogenized cell pellets. The enzyme assay conditions were exactly as described,¹ except infected Sf9 cell extract containing 2-3 µg protein was used as a source of enzyme.

Pharmacokinetic Analysis. Groups of 8-12-week-old mice (strain C57BL/6J) were injected (intraperitoneally) with either compounds (at a dose of 10 mg/kg) or an equal volume of vehicle [2% solution of hydropropyl-β-cyclodextrin (Cargill Cavitron 82004)]. After injection, animals were bled at the specified time points [ASAP (as soon as possible) time points were 1-2 min after dosing]. whole blood was processed immediately for LC-MS analysis as described below.

U937 Cell Culture Assay. U937 cells were grown in RPMI 1640 medium supplemented with L-glutamate, 10% FBS (fetal bovine serum) and 1%

penicillin/streptomycin at 37 °C in an atmosphere containing 5% CO₂ at 24 h before adding inhibitors, the growth medium was replaced with medium containing 0.5% FBS. After 2 hrs of drug treatment, cells were collected and lipids were extracted according to the protocol mentioned below.

Sample Preparation. Cell pellets (approximately 4 million cells) or whole blood (20 µL) was mixed with 2 mL of a methanol/chloroform solution (3:1) and transferred into a capped glass vial. Suspensions were supplemented with 10 µL of internal standard solution containing 10 pmoles each of C17-S1P or deuterated (d7) S1P, C17-Sph or deuterated (d7) Sph. The mixture was placed in a bath sonicator for 10 min and incubated at 48 °C for 16 h. The mixture was then cooled to ambient temperature (22 °C) and mixed with 200 µL of 1M potassium hydroxide in methanol. The samples were sonicated again and incubated a further 2 h at 37 °C. Samples were then neutralized by the addition of 20 µL of glacial acetic acid and transferred into 2mL microcentrifuge tubes. Samples were then centrifuged at 12000 g for 12 min at 4 °C. The supernatant fluid was collected in a separate glass vial and evaporated under a stream of nitrogen gas. Immediately prior to LC (liquid chromatography)-MS analysis, the dried material was dissolved in 0.3 mL of methanol and centrifuged at 12000 g for 12 min at 4 °C. The, 50 µL of the resulting supernatant fluid was analyzed.

LC-MS Protocol. Analyses were performed by LC-MS using a triple quadrupole mass spectrometer (AB-Sciex 4000 Q-Trap) coupled to a Shimadzu LC-20AD

LC-system. A binary solvent gradient with a flow rate of 1 mL/min was used to separate shingolipids and drugs by reverse-phase chromatography using a Supelco Discovery C18 column (50 mm x 2.1 mm, 5 μ m bead size). Mobile phase A consisted of water/methanol/formic acid (79:20:1, by vol.), whereas mobile phase B was methanol/formic acid [99:1 (v/v)]. The run started with 100% A for 0.5 min. solvent B was then increase linearly to 100% B in 5.1 min and held at 100% for 4.3 min. The column was dinally re-equilibrated to 100% A for 1 min. Natural sphingolipids were detected using MRM (multiple reaction monitoring) protocols described as follows: C17-S1P (366.4, 250.4), S1P (380.4, 264.4), dihydroS1P (382.4, 266.4); deuterated (d7) C18-S1P (387.4, 271.3), C17-Sph (286.4, 250.3), Sph (300.5, 264.4), dhSph (sphinganine) (302.5, 260.0) and deuterated (d7) Sph (307.5, 271.3). Quantification was carried out by measuring peak areas using commercially available solftware (Analyst 1.5.1).

6.2 Chemical Syntheses

General Synthetic Materials and Methods. All non-aqueous reactions were carried out in flame-dried glassware under nitrogen or argon atmosphere using dry solvents and magnetic stirring. The argon and nitrogen gasses were dried by passing through a tube of Drierite. Anhydrous diethyl ether (Et_2O), dichloromethane (DCM), dimethylformamide (DMF), and tetrahydrofuran (THF) were purchased from Fisher or VWR Chemicals and used as received. Anhydrous methanol was purchased from Acros chemicals. THF, DMF, and

DCM were dried over activated molecular sieves (4 Å) prior to use. All other reagents were purchased from VWR and Aldrich Chemicals. Triethylamine (TEA) was distilled from calcium hydride and stored over potassium hydroxide prior to use.

Unless otherwise stated, reactions were monitored by TLC using 0.25 mm Whatman precoated silica gel plates. Flash chromatography was performed using Sorbent Technologies silica gel (particle size 40 - 63 µm).

Proton (^1H) and carbon (^{13}C) NMR spectra were recorded on a Varian Unity Nova 500 or Varian Unity Nova 300 at 298 K. Chemical shifts are reported in ppm (δ) values relative to the solvent as follows: CDCl_3 (δ 7.26 for proton and δ 77.16 for carbon NMR), CD_3OD (δ 3.31 for proton and δ 49.00 for carbon NMR), and DMSO-d_6 (δ 2.50 for proton and δ 39.52 for carbon NMR).

Other abbreviations: tetrahydrofuran (THF), water (H_2O), chloroform (CHCl_3), ether (Et_2O), ethyl acetate (EtOAc), methanol (MeOH), *tert*-butanol (*t*-BuOH), dimethyl formamide (DMF), hydrochloric acid (HCl), dichloromethane (DCM), triethylamine (TEA), minute (min), hour (h), room temperature (r.t.), singlet (s), doublet (d), triplet (t), quintet (quin.), doublet of doublets (dd), multiplet (m), broad singlet (bs), broad doublet (bd).

Liquid Chromatography and Mass Spectrometry for Evaluation of Chemical Purity. All compounds submitted for biological evaluation were determined to be >95% pure by LCMS evaluation performed by the Mass Spectrometry Laboratory in the School of Chemical Sciences at the University of Illinois Urbana-

Champagne (Urbana, IL). High performance liquid chromatography mass spectrometry (LCMS) was carried out using an Agilent 2.1 mm x 50 mm C-18 column and a Micromass Q-tof Ultima mass spectrometer. Mobile phase A consisted of HPLC grade H₂O and 0.01% TFA. Mobile phase B consisted of MeCN and 0.01% TFA. LCMS identification and purity utilized a binary gradient starting with 90% A and 10% B and linearly increasing to 100% B over the course of 6 min, followed by an isocratic flow of 100% B for an additional 3 min. A flow rate of 0.5 mL/min was maintained throughout the HPLC method. The purity of all products was determined by integration of the total ion count (TIC) spectra and integration of the ultraviolet (UV) spectra at 214 nm. Retention times are abbreviated as t_R ; mass to charge ratios are abbreviated as m/z .

General Procedure A: Conversion of Nitriles to Amidines.

To a solution of a nitrile (1.0 equiv) in MeOH (0.10 M) was added a 0.5 M solution of sodium methoxide in MeOH (0.50 equiv) at room temperature. The mixture was then heated to 40 °C for 24 h. The intermediate imidate was detectable by TLC; however, since it is in equilibrium with the nitrile, full conversion does not occur. Ammonium chloride (2.0 equiv) was then added in one portion at that temperature and allowed to react until the imidate was completely consumed by TLC analysis. The mixture was then cooled to room temperature and evacuated to dryness to yield a crude solid. The solid was reconstituted with CHCl₃ and filtered through a fine glass fritted funnel in order to remove excess ammonium chloride, and the filtrate was again evacuated to

dryness. The material was then triturated in Et₂O to yield the pure amidine hydrochloride salt except in a few cases where the product was purified via flash column chromatography. The yields varied greatly depending upon substrate because amidine formation is dependent upon the equilibrium ratio between nitrile and imidate established under the sodium methoxide conditions.

General Procedure B: PyBOP Mediated Couplings of Amines and Anilines

to Carboxylic Acids. To a suspension of an amine (1.0 eq.), carboxylic acid (1.0 eq.), and PyBOP (1.1 eq.) in DCM (0.05 – 0.1 M) at room temperature was added DIPEA (10.0 eq.). The mixture was allowed to stir for 12 h unless otherwise stated. The mixture was then evaporated to dryness and immediately purified by flash chromatography.

General Procedure C: Suzuki Coupling. To a solution of alkene (1.5 eq.) in THF (0.2 M) at room temperature was added a 0.5 M solution of 9-BBN in THF (1.5 eq.) and left to stir overnight. The mixture was then treated with 3 M NaOH(aq) or 3 M K₃PO₄(aq) (3 M) and diluted with either THF or DMF (2 M relative to the starting bromide) as indicated. The aryl bromide (1 eq.) and Pd catalyst were then sequentially added, and the mixture was allowed to reflux for 4 h unless otherwise stated. The mixture was evaporated to a dark oil and immediately purified by flash chromatography.

General Procedure D: Pinnick Oxidation. To a solution of an aldehyde (1.0 eq.) and 2-methyl-2-butene (8 eq.) in THF (0.08 M) and tBuOH (0.08 M) at room temperature was added NaH_2PO_4 (3 eq.) and NaHClO_2 (3 eq.) dissolved in water (0.24 M), and the mixture was allowed to stir overnight. The mixture was diluted with EtOAc (150 mL) and washed 3 times with 1 N HCl (30 mL). The organic layer was washed with brine (30 mL) then dried with Na_2SO_4 and evaporated to a white solid. No further purification was necessary.

General Procedure E: Acid Chloride Formation. To a solution of a carboxylic acid (1 eq.) and DMF (cat.) in CH_2Cl_2 (0.3 M) at 0 °C was added oxalyl chloride (3 eq.) dropwise, and the mixture was allowed to warm to room temperature. After 3 h the mixture was evaporated to dryness and then immediately purified by flash chromatography.

General Procedure F: Acid Chloride and Amine Coupling.

To a solution of an acid chloride (1.3 eq.) in DCM (0.1 M) at room temperature was added DIPEA (6 eq.) followed by an amine HCl salt (1 eq.), and the mixture was stirred for 12 h. The mixture was then evaporated to dryness then dissolved in EtOAc (75 mL). The solution was washed three times with 1N HCl (20 mL), once with brine (20 mL), dried with Na_2SO_4 , and then evaporated to dryness. The mixture was purified by flash chromatography.

General Procedure G: Ether Synthesis. To a stirring solution of 4-hydroxybenzaldehyde (1 eq.) in DMF (0.6 M), the alkyl bromide (1.5 eq.) and cesium carbonate (2 eq.) were added and the reaction mixture was heated to 65 °C. Once complete by TLC analysis, the reaction was cooled and the salt removed *via* filtration through a coarse-fritted funnel. The supernatant was diluted with EtOAc (150 mL) and extracted several times with deionized H₂O (30 mL) alternating with brine (30 mL). The organic layer was dried over magnesium sulfate and the solvent removed under reduced pressure to afford a tan oil. The crude product was purified *via* flash column chromatography (silica gel, 10% ethyl acetate in hexanes) to yield a white crystalline solid.

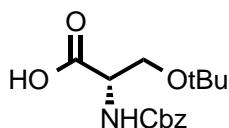
General Procedure H: Williamson Ether Synthesis. To a solution of an alcohol (2 eq.) in DMF (0.15 M) at 0 °C was added 60% sodium hydride dispersed in mineral oil (3 eq.) at 0 °C. Then the mixture was allowed to warm to room temperature and then allowed to react for 45 min. The alkyl bromide (1 eq.) was then added in one portion, and the mixture was stirred for 12 h. The reaction was quenched with 1N HCl and extracted into EtOAc (3 times the volume of DMF). The organic layer was washed several times with DI water (50 mL), once with brine, then dried with Na₂SO₄, evaporated to a yellow oil, and immediately purified by flash chromatography.

General Procedure I: Trifluoroacetic Acid Mediated Deprotection of N-Boc Protected Amines or O-tBu Protected Esters. To a stirring solution of the N-

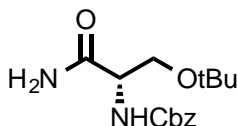
Boc protected amino-nitrile (1 eq.) in anhydrous DCM (0.1 M) was added TFA, dropwise (0.1 M) at room temperature. After 15 min, the reaction mixture was evaporated to dryness. Three different 5 mL portions of Et₂O were added and immediately evaporated to yield the trifluoroacetate salt as an off-white solid. The salts were dried under high vacuum for a minimum of 1 h before being carried forth.

General Procedure J: Primary Carboxylic Acid to Primary Amide. To a stirring solution of carboxylic acid (1 eq.), NH₄Cl (1 eq.), and PyBOP (1 eq.) in dry DCM (0.1 M), was added TEA (10 eq.). The reaction was stirred at rt overnight whence it was filtered via a fine frit and the solvent removed under reduced pressure. The crude product was dried under high vacuum for a minimum of 1 h before being carried forth.

General Procedure K: Dehydration of Primary Amide to Nitrile. To a stirring solution of cyanuric chloride (3.15 eq.) in DMF (0.21 M) at 0 °C was added 2,4,6-colidine (8.8 eq.). The rust-colored mixture was allowed to stir at 0 °C for 10 min before adding the amide (1 eq.) in DMF (0.52 M). The reaction became very viscous and dark orange-red and was stirred at room temperature overnight. The reaction was slowly quenched with sat. NaHCO₃ and then extracted into EtOAc. The organic layer was washed three times with 1N HCl, once with brine, dried with MgSO₄, and the solvent removed under reduced pressure. The crude product was purified via flash chromatography.

***N*-((benzyloxy)carbonyl)-*O*-(*tert*-butyl)-*L*-serine (3.14):****3.14**

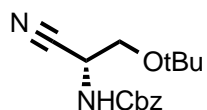
To a solution of Na₂CO₃ (2.50 g, 23.59 mmol) in DI H₂O (25 mL) was added H-Ser(tBu)-OH (1.50 g, 9.30 mmol), N-(benzyloxycarbonyloxy) succinimide (4.60 g, 18.60 mmol), and 1,4-dioxane (18.6 mL). The reaction was stirred at rt for 15 h. Once complete, the reaction was washed with EtOAc (30 mL) and then acidified with 3M HCl to a pH = 1. The mixture was then extracted with EtOAc (3 x 30 mL), washed with brine (20 mL), dried with MgSO₄, and the solvent removed under reduced pressure. The material was carried on crude.

Benzyl (S)-(1-amino-3-(*tert*-butoxy)-1-oxopropan-2-yl)carbamate (3.15):**3.15**

Crude **3.14** (2.74 g, 9.30 mmol) and TEA (3.76 g, 37.20 mmol, 5.2 mL) were dissolved in DCM (0.5 M) and cooled to -25 °C. *i*-Butylchloroformate (2.54 g, 18.60 mmol, 1.7 mL) was added to the cooled reaction. Once consumed, ammonium hydroxide (0.981 g, 28.0 mmol, 3.5 mL) was added and the reaction warmed to rt. After stirring at rt for 17 h the solvent was removed under reduced pressure. The crude material was dissolved in EtOAc (50 mL), washed with DI

H₂O (3 x15 mL), brine (15 mL), and dried with MgSO₄. The solvent was removed under reduced pressure and carried on crude.

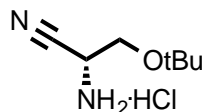
Benzyl (*R*)-(2-(*tert*-butoxy)-1-cyanoethyl)carbamate (3.16):



3.16

To a solution of **3.15** (2.74 g, 9.30 mmol) in THF (0.1 M) was added TEA (1.90 g, 18.90 mmol, 2.7 mL) and the reaction cooled to 0 °C. To the cooled mixture was added TFAA (2.34 g, 11.16 mmol, 1.6 mL) and stirred for 25 min. Once complete the solvent was removed under reduced pressure and the crude material was dissolved in EtOAc (50 mL), washed with 1 N HCl (3 x 20 mL), brine (20 mL), dried with MgSO₄, and then the solvent removed under reduced pressure. The crude material was purified via flash chromatography to afford **3.16** (1.14 g, 4.11 mmol, 65%): *R_f* = 0.62 (25% EtOAc in Hex); ¹H NMR (500 MHz, CDCl₃) δ 7.38 (s, 5H), 5.16 (s, 2H), 4.76 (s, 1H), 3.74 – 3.49 (m, 2H), 1.22 (s, 9H); ¹³C NMR (126 MHz, CDCl₃) δ 155.49, 135.53, 128.75, 128.65, 128.47, 117.61, 74.66, 67.96, 61.58, 60.86, 43.72, 27.32.

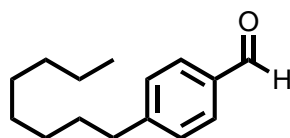
(*R*)-2-amino-3-(*tert*-butoxy)propanenitrile hydrochloride (3.17):



3.17

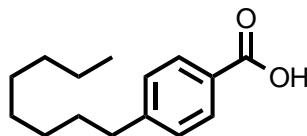
To a solution of **3.16** (1.14 g, 4.11 mmol) in EtOH (0.1 M) was added 20% by wt Pd(OH)₂ (cat.). The reaction was run under H₂ (1 atm) and stirred overnight. Once complete, the reaction was filtered through Celite with MeOH and the solvent removed under reduced pressure. The crude material was dissolved in MeOH (100 mL) and 2 M HCl (2.05 mL) was added and the mixture stirred for 10 min. Once complete, the solvent was removed under reduced pressure and co-evaporated with Et₂O (20 mL) to yield a foamy brown solid (0.077 g, 0.43 mmol, 31%); ¹H NMR (500 MHz, CD₃OD) δ 4.90 (s, 3H), 4.66 (t, *J* = 4.3 Hz, 1H), 3.81 (dd, *J* = 4.2, 2.9 Hz, 2H), 1.28 (s, 9H); ¹³C NMR (126 MHz, CD₃OD) δ 115.80, 76.22, 60.80, 43.28, 27.48.

4-octylbenzaldehyde (3.18):

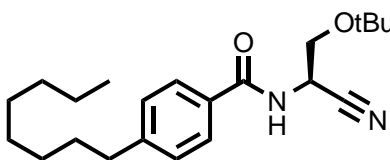


3.18

General procedure C was used to couple 1-octene (0.681 g, 8.10 mmol) and *p*-bromobenzaldehyde (1.00 g, 5.40 mmol) to yield crude **3.18**. The crude material was purified via flash chromatography to yield the title compound (0.95 g, 4.35 mmol, 81%). *R*_f = 0.65 (10% EtOAc in Hex); ¹H NMR (300 MHz, CDCl₃) δ 9.97 (s, 1H), 7.80 (d, *J* = 8.2 Hz, 2H), 7.34 (d, *J* = 8.1 Hz, 2H), 2.68 (t, *J* = 7.5 Hz, 2H), 1.62 (dd, *J* = 15.0, 7.4 Hz, 2H), 1.31 - 1.26 (m, 10H), 0.88 (t, *J* = 6.8 Hz, 3H).

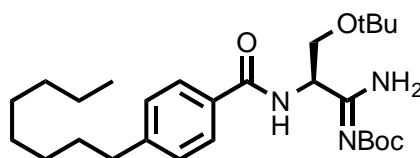
4-octylbenzoic acid (3.19):**3.19**

General procedure D was used to oxidize **3.18** (0.95 g, 4.35 mmol) to aldehyde **3.19** (1.01 g, 4.31 mmol, 99%). ^1H NMR (300 MHz, CDCl_3) δ 9.97 (s, 1H), 7.80 (d, J = 8.2 Hz, 2H), 7.34 (d, J = 8.1 Hz, 2H), 2.68 (t, J = 7.5 Hz, 2H), 1.62 (dd, J = 15.0, 7.4 Hz, 2H), 1.29 (dd, J = 10.4, 4.8 Hz, 10H), 0.88 (t, J = 6.8 Hz, 3H).

(*R*)-*N*-(2-(*tert*-butoxy)-1-cyanoethyl)-4-octylbenzamide (3.20):**3.20**

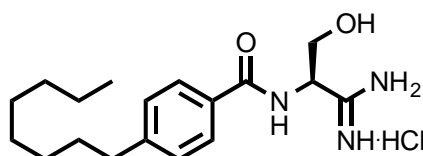
General procedure B was used to couple **3.17** (0.077 g, 0.43 mmol) and **3.19** (0.100 g, 0.43 mmol) to yield nitrile **3.20** (0.082 g, 0.23 mmol, 53%): R_f = 0.56 (25% EtOAc in Hex); ^1H NMR (500 MHz, CDCl_3) δ 7.71 (d, J = 8.0 Hz, 2H), 7.27 (d, J = 8.0 Hz, 2H), 5.24 (dt, J = 8.5, 3.5 Hz, 1H), 3.69 (ddd, J = 13.4, 9.4, 3.5 Hz, 2H), 2.65 (t, J = 7.5 Hz, 2H), 1.66 – 1.57 (m, 2H), 1.36 – 1.22 (m, 10H), 0.88 (t, J = 6.9 Hz, 3H); ^{13}C NMR (126 MHz, CDCl_3) δ 166.67, 148.10, 130.19, 128.93, 127.36, 117.88, 74.67, 61.79, 41.76, 35.99, 31.97, 31.29, 29.53, 29.34, 27.48, 22.77, 14.23.

***tert*-Butyl (*R,Z*)-(1-amino-3-(*tert*-butoxy)-2-(4-octylbenzamido)propylidene) carbamate (3.21):**

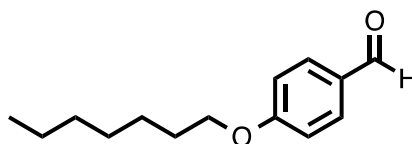


3.21

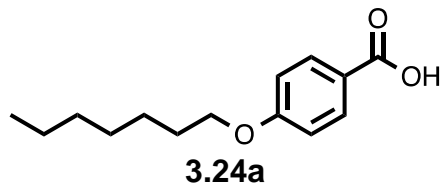
To a solution of a nitrile (1.0 equiv) in MeOH (0.35 M) was added a 0.5 M solution of sodium methoxide in MeOH (0.50 equiv) at rt. The mixture was stirred for 24 h. Ammonium bromide (3.0 equiv) was then added in one portion at rt and allowed to react until the imidate was completely consumed by TLC analysis. The mixture was evacuated to dryness to yield a crude solid that was dissolved in THF (0.1 M). To the mixture was added Boc₂O (6 equiv) and K₂CO₃ (6 equiv) and the reaction stirred at rt for 13 h. Once complete, the solvent was removed under reduced pressure and purified via flash chromatography to yield the title compound (0.052 g, 0.110 mmol, 48%): *R*_f = 0.36 (25% EtOAc in Hex); ¹H NMR (500 MHz, CDCl₃) δ 7.73 (d, *J* = 8.2 Hz, 2H), 7.25 (d, *J* = 9.5 Hz, 2H), 4.00 (dd, *J* = 8.8, 4.2 Hz, 1H), 3.44 (t, *J* = 8.8 Hz, 1H), 2.68 – 2.61 (t, *J* = 7.5 Hz, 2H), 1.64 – 1.58 (m, 2H), 1.51 (s, 9H), 1.34 – 1.21 (m, 19H), 0.87 (t, *J* = 7.0 Hz, 3H); ¹³C NMR (126 MHz, CDCl₃) δ 169.79, 167.38, 149.10, 147.61, 130.97, 128.82, 128.74, 127.27, 82.69, 75.06, 62.62, 61.05, 53.80, 35.99, 31.99, 31.33, 29.55, 29.36, 28.27, 28.10, 27.61, 27.46, 22.79, 14.25.

(*R*)-*N*-(1-amino-3-hydroxy-1-iminopropan-2-yl)-4-octylbenzamide**hydrochloride (3.22):****3.22**

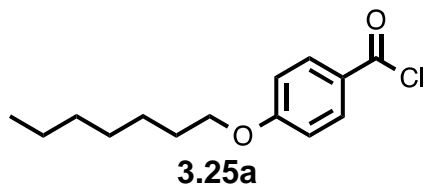
General procedure I was used to deprotect the hydroxyl and amidine groups to yield the desired compound (0.007 g, 0.02 mmol, 20%); ^1H NMR (500 MHz, CD_3OD) δ 8.99 (s, 2H), 8.71 (s, 2H), 8.47 (s, 1H), 7.86 (d, $J = 8.0$ Hz, 2H), 7.33 (d, $J = 8.1$ Hz, 2H), 4.73 – 4.69 (m, 1H), 4.03 – 3.88 (m, 2H), 2.72 – 2.66 (t, $J = 7.5$ Hz, 2H), 1.71 – 1.59 (m, 2H), 1.39 – 1.24 (m, 10H), 0.89 (t, $J = 7.0$ Hz, 3H); ^{13}C NMR (126 MHz, CD_3OD) δ 171.67, 149.27, 131.41, 129.72, 128.87, 62.69, 55.65, 36.77, 33.02, 32.35, 30.55, 30.41, 30.29, 23.73, 14.43.

4-(heptyloxy)benzaldehyde (3.23a):**3.23a**

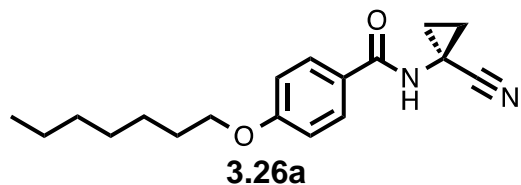
General procedure **G** was used to convert 4-hydroxybenzaldehyde (1.0 g, 8.2 mmol) to **3.23a** (1.5 g, 6.6 mmol, 80%): $R_f = 0.46$ (10% EtOAc in hexanes); ^1H NMR (300 MHz, CDCl_3) δ 9.87 (s, 1H), 7.82 (d, $J = 8.8$ Hz, 2H), 6.99 (d, $J = 8.7$ Hz, 2H), 4.03 (t, $J = 6.5$ Hz, 2H), 1.81 (quin., $J = 6$ Hz, 1H), 1.24 – 1.53 (m, 8H), 0.89 (t, $J = 6.8$ Hz, 3H); ^{13}C NMR (75 MHz, CDCl_3) δ 191.0, 164.4, 132.13, 129.8, 114.9, 68.6, 31.9, 29.18, 29.1, 26.1, 22.7, 14.2.

4-(heptyloxy)benzoic acid (3.24a):

General procedure **D** was used to convert **3.23a** (1.5 g, 6.6 mmol) to **3.24a** (1.6 g, 6.6 mmol, 100%): $R_f = 0.0$ (40% EtOAc in hexanes); ^1H NMR (300 MHz, DMSO- d_6) δ 7.87 (d, $J = 8.7$ Hz, 2H), 6.99 (d, $J = 8.8$ Hz, 2H), 4.01 (t, $J = 6.4$ Hz, 2H), 1.71 (quin., $J = 6.5$ Hz, 2H), 1.47 – 1.19 (m, 4H), 0.86 (t, $J = 6.5$ Hz, 3H); ^{13}C NMR (75 MHz, DMSO- d_6) δ 167.0, 162.3, 131.3, 122.8, 114.17, 67.8, 31.2, 28.5, 28.4, 25.4, 22.0, 13.9.

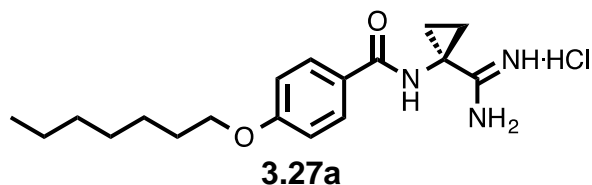
4-(heptyloxy)benzoyl chloride (3.25a):

General procedure **E** was used to convert **3.24a** (0.26 g, 1.1 mmol) to **3.25a**: $R_f = 0.39$ (40% EtOAc in hexanes).

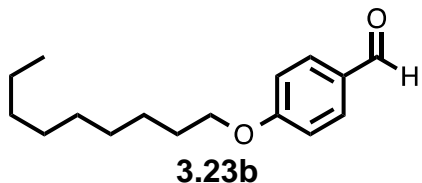
***N*-(1-cyanocyclopropyl)-4-(heptyloxy)benzamide (3.26a):**

General procedure **F** was used to couple 1-amino-1-cyclopropanecarbonitrile hydrochloride (0.10 g, 0.84 mmol) to crude **3.26a** (0.28 g, 1.1 mmol) to obtain **3.26a** (0.06 g, 0.20 mmol) in 18% yield over two steps: R_f = 0.47 (40% EtOAc in hexanes); ^1H NMR (300 MHz, CDCl_3) δ 7.77 (d, J = 8.8 Hz, 2H), 6.85 (d, J = 8.8 Hz, 2H), 3.94 (t, J = 6.5 Hz, 2H), 1.76 (quin., J = 5 Hz, 2H), 1.53 (t, J = 5.7 Hz, 2H), 1.25 - 1.45 (m, 8H), 0.88 (t, J = 6.7 Hz, 3H); ^{13}C NMR (75 MHz, CDCl_3) δ 168.2, 162.6, 129.4, 124.6, 120.7, 114.4, 68.3, 31.8, 29.8, 29.2, 29.1, 26.0, 22.7, 21.0, 16.88, 14.2.

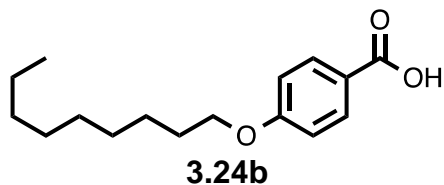
***N*-(1-carbamimidoylcyclopropyl)-4-(heptyloxy)benzamide hydrochloride (3.27a):**



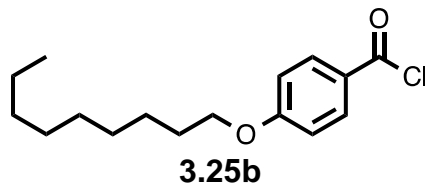
General procedure **A** was used to convert **3.26a** (0.06 g, 0.20 mmol) to **3.27a** (0.045 g, 0.13 mmol, 64%): R_f = 0.08 (40% EtOAc in hexanes); ^1H NMR (500 MHz, CD_3OD) δ 7.87 (d, J = 8.6 Hz, 2H), 6.98 (d, J = 8.7 Hz, 2H), 4.04 (t, J = 6.4 Hz, 2H), 1.84 – 1.71 (m, 4H), 1.56 (bs, 2H), 1.52 – 1.43 (quin., J = 7.5 Hz, 2H), 1.41 – 1.32 (m, 6H), 0.92 (t, J = 6.8 Hz, 3H); ^{13}C NMR (125 MHz, CD_3OD) δ 174.0, 170.9, 164.0, 130.8, 126.1, 115.20, 69.3, 34.0, 33.0, 30.3, 30.2, 27.1, 23.7, 19.6, 14.4.

4-(nonyloxy)benzaldehyde (3.23b):

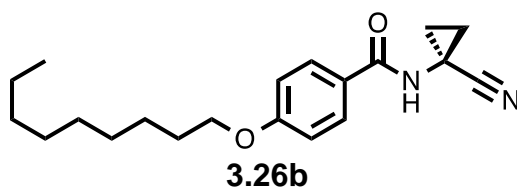
General procedure **G** was used to convert 4-hydroxybenzaldehyde (1.0 g, 8.2 mmol) to **3.23b** (1.6 g, 6.5 mmol, 79%): $R_f = 0.42$ (10% EtOAc in hexanes); ^1H NMR (300 MHz, CDCl_3) δ 9.88 (s, 1H), 7.83 (d, $J = 8.9$ Hz, 2H), 6.99 (d, $J = 8.7$ Hz, 2H), 4.04 (t, $J = 6.6$ Hz, 2H), 1.76 – 1.85 (m, 2H), 1.14 – 1.53 (m, 12H), 0.88 (t, $J = 6.6$ Hz, 3H); ^{13}C NMR (75 MHz, CDCl_3) δ 164.40, 132.11, 114.86, 68.55, 31.98, 29.47, 29.37, 29.18, 28.90, 28.31, 26.08, 22.79, 14.23.

4-(nonyloxy)benzoic acid (3.24b):

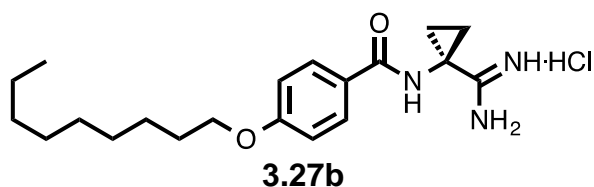
General procedure **D** was used to convert **3.23b** (1.6 g, 6.5 mmol) to **3.24b** (1.7 g, 6.5 mmol, 100%): $R_f = 0.0$ (40% EtOAc in hexanes); ^1H NMR (300 MHz, DMSO-d_6) δ 7.87 (d, $J = 8.8$ Hz, 2H), 6.99 (d, $J = 8.8$ Hz, 2H), 4.02 (t, $J = 6.5$ Hz, 2H), 1.71 (quin., $J = 6.8$ Hz, 2H), 1.48 – 1.35 (m, 2H), 1.25 (bs, 12H), 0.85 (t, $J = 6.6$ Hz, 3H); ^{13}C NMR (75 MHz, CDCl_3) δ 167.0, 162.3, 131.3, 122.8, 114.2, 67.7, 31.3, 29.0, 28.7, 28.6, 28.5, 25.4, 22.1, 13.9.

4-(nonyloxy)benzoyl chloride (3.25b):

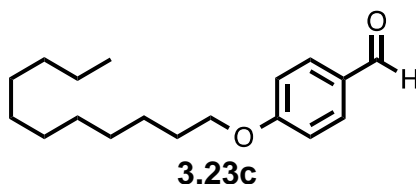
General procedure **E** was used to convert **3.24b** (0.29 g, 1.1 mmol) to **3.25b**: $R_f = 0.41$ (40% EtOAc in hexanes).

***N*-(1-cyanocyclopropyl)-4-(nonyloxy)benzamide (3.26b):**

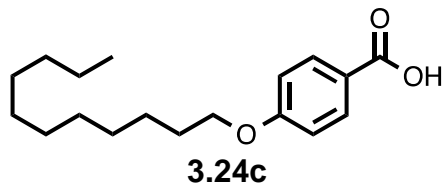
General procedure **F** was used to couple 1-amino-1-cyclopropanecarbonitrile hydrochloride (0.10 g, 0.84 mmol) to **3.25b** (0.31 g, 1.10 mmol) to obtain **3.26b** (0.19 g, 0.59 mmol) 54% yield over two steps: $R_f = 0.45$ (40% EtOAc in hexanes); ^1H NMR (300 MHz, CDCl_3) δ 7.71 (d, $J = 8.9$ Hz, 2H), 6.90 (d, $J = 8.9$ Hz, 2H), 3.99 (t, $J = 6.6$ Hz, 2H), 1.79 (quin., $J = 6$ Hz, 1H), 1.61 – 1.65 (m, 2H), 1.19 – 1.50 (m, 14H), 0.88 (t, $J = 6.8$ Hz, 1H); ^{13}C NMR (75 MHz, CDCl_3) δ 129.4, 114.7, 95.6, 68.6, 38.0, 32.2, 29.9, 29.6, 29.4, 26.3, 23.0, 17.3, 14.5.

N*-(1-carbamimidoylcyclopropyl)-4-(nonyloxy)benzamide hydrochloride*(3.27b):**

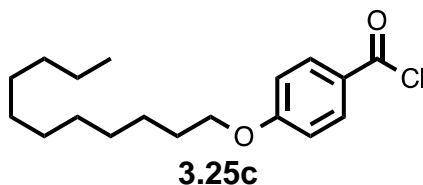
General procedure **A** was used to convert **3.26b** (0.19 g, 0.59 mmol) to **3.27b** (0.003 g, 0.008 mmol, 1.3%): $R_f = 0.09$ (40% EtOAc in hexanes); ^1H NMR (500 MHz, CD_3OD) δ 7.88 (d, $J = 8.6$ Hz, 2H), 6.97 (d, $J = 8.6$ Hz, 2H), 4.03 (t, $J = 6.3$ Hz, 2H), 1.78 (m, 4H), 1.56 (bs, 2H), 1.47 (bd, 2H), 1.29 (bs, 8H), 0.90 (t, $J = 6.7$ Hz, 1H); ^{13}C NMR (125 MHz, CD_3OD) δ 164.1, 130.8, 130.5, 126.1, 115.3, 115.2, 69.3, 33.1, 30.7, 30.5, 30.4, 30.3, 27.1, 23.8, 19.6, 17.0, 14.5; $t_R = 10.60$ min, $(m/z) = 347.19$.

4-(undecyloxy)benzaldehyde (3.23c):

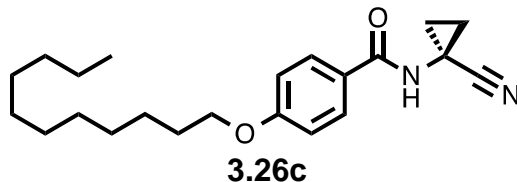
General procedure **G** was used to convert 4-hydroxybenzaldehyde (1.0 g, 8.2 mmol) to **3.23c** (1.7 g, 6.5 mmol, 74%): $R_f = 0.70$ (10% EtOAc in hexanes); ^1H NMR (300 MHz, CDCl_3) δ 9.87 (s, 1H), 7.82 (d, $J = 8.8$ Hz, 2H), 6.99 (d, $J = 8.8$ Hz, 2H), 4.03 (t, $J = 6.5$ Hz, 3H), 1.76 – 1.87 (m, 2H), 1.26 – 1.48 (m, 16H), 0.88 (t, $J = 6.7$ Hz, 3H); ^{13}C NMR (75 MHz, CDCl_3) δ 191.0, 164.4, 132.1, 129.8, 114.9, 68.6, 34.3, 33.0, 32.1, 29.7, 29.6, 29.5, 29.2, 29.0, 28.3, 26.1, 22.8, 14.3.

4-(undecyloxy)benzoic acid (3.24c):

General procedure **D** was used to convert **3.23c** (1.7 g, 6.5 mmol) to **3.24c** (1.8 g, 6.5 mmol, 100%): $R_f = 0.0$ (40% EtOAc in hexanes); ^1H NMR (500 MHz, CDCl_3) δ 8.05 (d, $J = 8.8$ Hz, 2H), 6.93 (d, $J = 8.8$ Hz, 2H), 4.02 (t, $J = 6.6$ Hz, 3H), 1.76 – 1.84 (m, 2H), 1.39 – 1.50 (m, 2H), 1.19 – 1.39 (m, 14H), 0.88 (t, $J = 6.8$ Hz, 3H); ^{13}C NMR (75 MHz, DMSO-d_6) δ 167.0, 162.3, 131.3, 122.8, 114.2, 67.7, 31.3, 29.0, 28.7, 28.5, 25.4, 22.1, 13.9.

4-(undecyloxy)benzoyl chloride (3.25c):

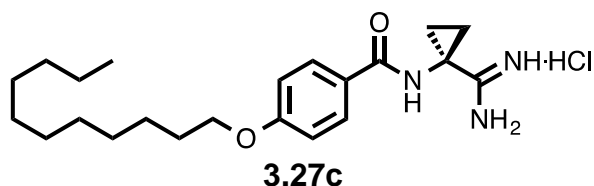
General procedure **E** was used to convert **3.24c** (0.32 g, 1.10 mmol) to **3.25c**: $R_f = 0.44$ (40% EtOAc in hexanes).

***N*-(1-cyanocyclopropyl)-4-(undecyloxy)benzamide (3.26c):**

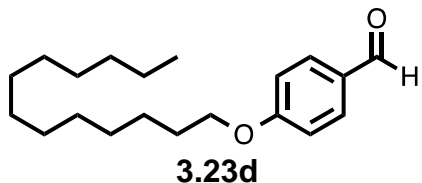
General procedure **F** was used to couple 1-amino-1-cyclopropanecarbonitrile hydrochloride (0.10 g, 0.84 mmol) to **3.25c** (0.34 g, 1.10

mmol) to obtain **3.26c** (0.10 g, 0.27 mmol) in 24% yield over two steps: $R_f = 0.46$ (40% EtOAc in hexanes); ^1H NMR (500 MHz, CDCl_3) δ 7.71 (d, $J = 8.6$ Hz, 2H), 6.90 (d, $J = 8.6$ Hz, 2H), 3.98 (t, $J = 6.6$ Hz, 2H), 1.79 (quin., $J = 5$ Hz, 2H), 1.62 (dd, $J = 9.1, 6.3$ Hz, 2H), 1.45 (quin., $J = 5$ Hz, 2H), 1.35 (dd, $J = 9.0$ Hz, 6.1 Hz, 2H), 1.20 – 1.32 (m, 14H), 0.88 (t, $J = 6.9$ Hz, 3H); ^{13}C NMR (125 MHz, CDCl_3) δ 168.2, 162.8, 129.6, 124.8, 120.8, 114.6, 68.5, 32.2, 29.90, 29.87, 29.68, 29.65, 29.4, 26.3, 23.0, 21.2, 17.2, 14.4.

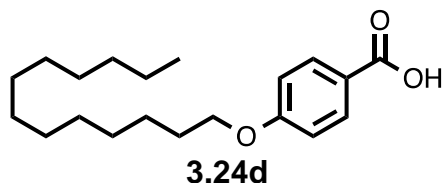
***N*-(1-carbamimidoylcyclopropyl)-4-(undecyloxy)benzamide hydrochloride (3.27c).**



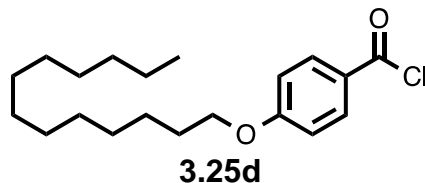
General procedure **A** was used to convert **3.26c** (0.10 g, 0.27 mmol) to **3.27c** (0.048 g, 0.12 mmol, 44%): $R_f = 0.10$ (40% EtOAc in hexanes); ^1H NMR (500 MHz, CD_3OD) δ 7.88 (d, $J = 8.6$ Hz, 2H), 6.97 (d, $J = 8.6$ Hz, 2H), 4.03 (t, $J = 6.3$ Hz, 2H), 1.81 – 1.74 (m, 4H), 1.56 (t, $J = 6.9$ Hz, 2H), 1.47 (quin., $J = 6.3$ Hz, 2H), 1.41 – 1.21 (m, 14H), 0.90 (t, $J = 6.7$ Hz, 3H); ^{13}C NMR (125 MHz, CD_3OD) δ 174.8, 171.7, 164.9, 131.68, 131.4, 126.9, 116.0, 70.1, 34.9, 33.9, 31.6, 31.4, 31.1, 28.0, 24.6, 20.4, 17.9, 15.3; $t_R = 10.69$ min, $(m/z) = 374.16$.

4-(tridecyloxy)benzaldehyde (3.23d).

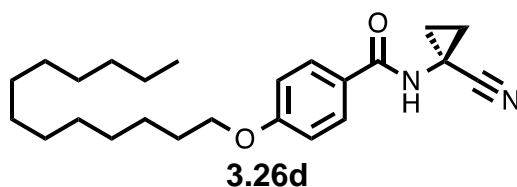
General procedure **G** was used to convert 4-hydroxybenzaldehyde (1.0 g, 8.2 mmol) to **3.23d** (2.1 g, 7.3 mmol, 89%): $R_f = 0.62$ (10% EtOAc in hexanes); ^1H NMR (300 MHz, CDCl_3) δ 9.88 (s, 1H), 7.83 (d, $J = 8.8$ Hz, 2H), 6.99 (d, $J = 8.7$ Hz, 2H), 4.04 (t, $J = 6.5$ Hz, 2H), 1.76 – 1.88 (m, 2H), 1.52 – 1.08 (m, 20H), 0.88 (t, $J = 6.7$ Hz, 3H).

4-(tridecyloxy)benzoic acid (3.24d).

General procedure **D** was used to convert **3.23d** (2.1 g, 7.3 mmol) to **3.24d** (2.2 g, 7.3 mmol, 100%): $R_f = 0.0$ (40% EtOAc in hexanes); ^1H NMR (300 MHz, CDCl_3) δ 7.87 (d, $J = 8.9$ Hz, 2H), 6.98 (d, $J = 8.9$ Hz, 2H), 4.01 (t, $J = 6.5$ Hz, 2H), 1.80 – 1.71 (m, 2H), 1.49 – 1.13 (m, 20H), 0.85 (t, $J = 6.5$ Hz, 3H); ^{13}C NMR (75 MHz, CDCl_3) δ 166.9, 162.2, 131.3, 122.8, 114.1, 67.7, 35.1, 32.2, 31.3, 29.0, 28.9, 28.7, 28.5, 28.1, 27.5, 25.4, 22.1, 13.9.

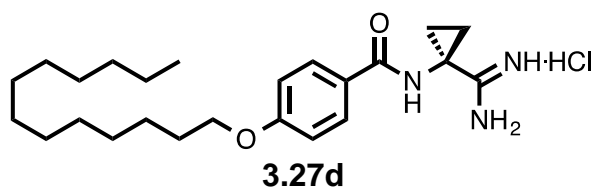
4-(tridecyloxy)benzoyl chloride (3.25d)

General procedure **E** was used to convert **3.24d** (0.33 g, 1.10 mmol) to **3.25d**: $R_f = 0.45$ (40% EtOAc in hexanes).

***N*-(1-cyanocyclopropyl)-4-(tridecyloxy)benzamide (3.26d).**

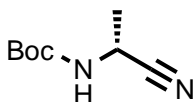
General procedure **F** was used to couple 1-amino-1-cyclopropanecarbonitrile hydrochloride (0.10 g, 0.84 mmol) to **3.35d** (0.35 g, 1.10 mmol) to obtain **3.26d** (0.10 g, 0.28 mmol) in 25% yield over two steps: $R_f = 0.5$ (40% EtOAc in hexanes); ^1H NMR (300 MHz, CDCl_3) δ 7.72 (d, $J = 8.9$ Hz, 2H), 6.90 (d, $J = 8.9$ Hz, 2H), 3.98 (t, $J = 6.6$ Hz, 2H), 1.86 – 1.69 (m, 2H), 1.61 (dd, $J = 10.0, 7.3$ Hz, 2H), 1.51 – 1.01 (m, 22H), 0.87 (t, $J = 6.0$ Hz, 3H); ^{13}C NMR (75 MHz, CDCl_3) δ 129.4, 129.3, 114.7, 68.6, 68.5, 51.6, 32.3, 30.0, 29.7, 29.4, 26.3, 17.3.

***N*-(1-carbamimidoylcyclopropyl)-4-(tridecyloxy)benzamide hydrochloride (3.27d).**



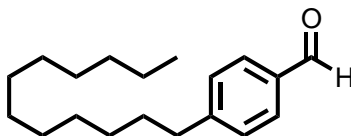
General procedure **A** was used to convert **3.26d** (0.10 g, 0.28 mmol) to **3.27d** (0.044 g, 0.10 mmol, 39%): R_f = 0.12 (40% EtOAc in hexanes); ^1H NMR (500 MHz, DMSO- d_6) δ 9.16 (s, 1H), 7.80 (d, J = 8.1 Hz, 2H), 6.99 (d, J = 8.1 Hz, 2H), 4.01 (t, J = 6.3 Hz, 2H), 1.70 (quin., J = 5 Hz, 2H), 1.53 (t, J = 6.5 Hz, 2H), 1.38 (quin., J = 6.5 Hz, 2H), 1.27 (bs, 18H), 0.85 (t, J = 6.5 Hz, 3H); ^{13}C NMR (125 MHz, CD_3OD) δ 167.7, 162.6, 130.3, 125.8, 122.1, 115.0, 68.7, 32.3, 30.0, 29.9, 29.7, 29.5, 26.4, 23.1, 21.3, 16.7, 14.9; t_R = 11.57 min, (m/z) = 402.22.

(*R*)-*tert*-butyl (1-cyanoethyl)carbamate ((*R*)-4.1).

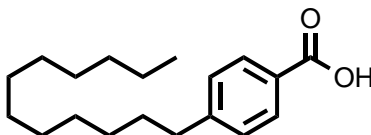


(*R*)-4.1

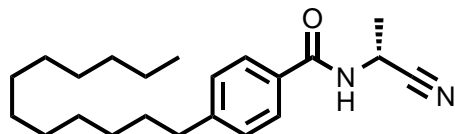
General procedure **J** was used to convert Boc-D-Ala-OH (2.00 g, 10.57 mmol) to corresponding amide. Then general procedure **K** was used to convert the amide (1.99 g, 10.57 mmol) to **(*R*)-4.1** (1.185 g, 6.96 mmol, 66% over two steps); R_f = 0.39 (25% EtOAc in Hex); ^1H NMR (500 MHz, CDCl_3) δ 4.82 (bs, 1H), 4.62 (bs, 1H), 1.54 (d, J = 7.2, 3H), 1.46 (s, 8H); ^{13}C NMR (126 MHz, CDCl_3) δ 154.10, 119.53, 37.57, 28.21, 19.62.

4-dodecylbenzaldehyde (4.3).**4.3**

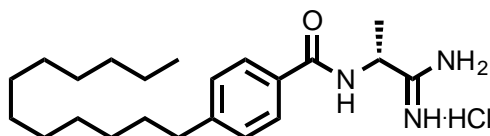
General procedure C was used to couple *p*-bromobenzaldehyde (4.5 g, 24.32 mmol) and 1-dodecene (6.14 g, 8.1 mL, 36.50 mmol) using PdPPh₄ (cat.) to afford the product **4.3** (5.00 g, 18.22 mmol, 75%); *R*_f = 0.52 (5% EtOAc in Hex); ¹H NMR (300 MHz, CDCl₃) δ 9.97 (s, 1H), 7.80 (d, *J* = 8.1 Hz, 1H), 7.33 (d, *J* = 8.0 Hz, 1H), 2.81 – 2.48 (m, 2H), 1.74 – 1.57 (m, 2H), 1.39 – 1.19 (m, 17H), 0.88 (t, *J* = 6.7 Hz, 3H); ¹³C NMR (75 MHz, CDCl₃) δ 192.15, 150.63, 134.48, 130.00, 129.19, 42.06, 36.34, 32.04, 31.22, 29.76, 29.67, 29.57, 29.48, 29.38, 27.27, 25.78, 22.82, 14.25.

4-dodecylbenzoic acid (4.4).**4.4**

General procedure D was used to oxidize **4.3** (5.00 g, 18.22 mmol) to **4.4** (5.20 g, 17.92 mmol, 98%); ¹H NMR (300 MHz, DMSO) δ 7.84 (d, *J* = 7.9 Hz, 2H), 7.29 (d, *J* = 8.0 Hz, 2H), 2.62 (t, *J* = 7.6 Hz, 2H), 1.65 – 1.48 (m, 2H), 1.22 (s, 17H), 0.84 (t, *J* = 6.5 Hz, 3H).

(R)-N-(1-cyanoethyl)-4-dodecylbenzamide ((R)-4.5).**(R)-4.5**

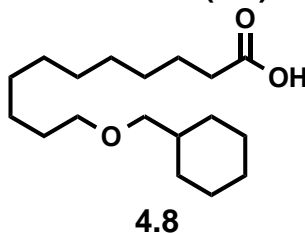
General procedure I was used to deprotect **(R)-4.1** (0.50 g, 2.94 mmol) to its corresponding trifluoroacetate salt. Then general procedure B was used to couple the amine salt (0.541 g, 2.94 mmol) to **4.4** (0.853 g, 2.94 mmol) to afford the corresponding nitrile (0.350 g, 1.021 mmol, 35%); $R_f = 0.46$ (25% EtOAc in Hex); ^1H NMR (300 MHz, CDCl_3) δ 7.71 (d, $J = 8.1$ Hz, 2H), 7.21 (d, $J = 8.1$ Hz, 2H), 5.12 (p, $J = 7.3$ Hz, 1H), 2.62 (d, $J = 7.5$ Hz, 2H), 1.64 – 1.56 (m, 5H), 1.27 (m, 17H), 0.87 (t, $J = 6.5$ Hz, 3H); ^{13}C NMR (75 MHz, CDCl_3) δ 167.11, 148.06, 130.00, 128.81, 127.42, 119.68, 51.35, 36.42, 35.94, 31.99, 31.25, 29.73, 29.66, 29.54, 29.44, 29.35, 22.76, 19.36, 14.21.

(R)-N-(1-amino-1-iminopropan-2-yl)-4-dodecylbenzamide hydrochloride ((R)-4.6).**(R)-4.6**

General procedure A was used to convert nitrile **(R)-4.5** (0.350 g, 1.021 mmol) to the amidine salt **(R)-4.6** (0.017 g, 0.042 mmol, 4%). The product was purified via trituration using EtOAc; ^1H NMR (500 MHz, DMSO) δ 8.91 (s, 2H), 8.79 (d, $J = 5.2$ Hz, 2H), 7.89 (d, $J = 8.0$ Hz, 2H), 7.30 (d, $J = 7.9$ Hz, 2H), 4.64 (dd, $J = 13.0$,

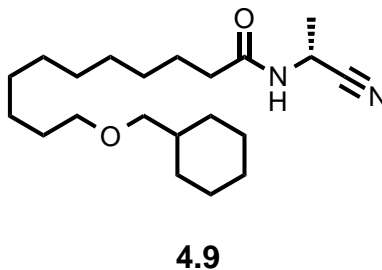
6.1 Hz, 1H), 2.62 (t, $J = 7.4$ Hz, 2H), 1.56 (m, 2H), 1.49 (d, $J = 7.2$ Hz, 3H), 1.25 (m, 17H), 0.85 (t, $J = 6.2$ Hz, 3H); ^{13}C NMR (126 MHz, DMSO) δ 172.42, 166.71, 146.61, 130.53, 128.10, 127.90, 47.36, 34.97, 31.30, 30.76, 30.71, 29.01, 28.83, 28.72, 28.59, 22.11, 18.28, 13.98.

11-(cyclohexylmethoxy)undecanoic acid (4.8).



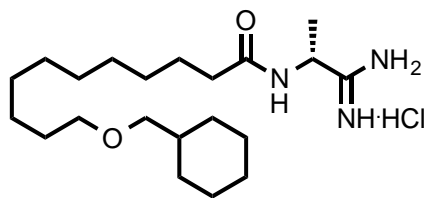
General procedure H was used to couple 11-bromoundecanoic acid (5.00 g, 18.85 mmol) and cyclohexanemethanol (4.31 g, 4.6 mL, 37.71 mmol) using 60% NaH in mineral oil (1.36 g, 56.56 mmol) to yield the title compound (5.14 g, 17.22 mmol, 91%); $R_f = 0.29$ (50% EtOAc in Hex); ^1H NMR (500 MHz, CDCl_3) δ 6.46 (s, 1H), 3.30 (d, $J = 6.6$ Hz, 2H), 2.21 (t, $J = 7.5$ Hz, 2H), 1.72-0.95 (m, 27H), 0.93-0.65 (m, 2H). ^{13}C NMR (126 MHz, CDCl_3) δ 177.87, 76.69, 71.00, 40.15, 34.00, 30.03, 29.52, 29.45, 29.36, 29.32, 29.18, 29.02, 26.52, 25.78, 24.73.

(*R*)-*N*-(1-cyanoethyl)-11-(cyclohexylmethoxy)undecanamide (4.9).



General procedure I was used to deprotect **(R)**-**4.1** (0.293 g, 1.72 mmol) to its corresponding trifluoroacetate salt **(R)**-**4.2**. Then general procedure **B** was used to convert **(R)**-**4.2** (0.541 g, 2.94 mmol) and **4.8** (0.877 g, 2.94 mmol) to **4.9** (0.429 g, 1.22 mmol, 48%): $R_f = 0.23$ (25% EtOAc in Hex); ^1H NMR (300 MHz, CDCl_3) δ 4.93 – 4.80 (m, 1H), 3.38 (dd, $J = 12.5, 6.7$ Hz, 2H), 3.19 (d, $J = 6.6$ Hz, 2H), 2.24 (d, $J = 7.6$ Hz, 2H), 1.92 – 1.58 (m, 4H), 1.54 (d, $J = 7.2$ Hz, 3H), 1.27 (s, 20H), 0.89 (m, 2H); ^{13}C NMR (75 MHz, CDCl_3) δ 173.15, 119.45, 76.68, 70.97, 51.23, 37.86, 35.85, 35.65, 32.68, 30.04, 29.20, 29.08, 28.95, 28.76, 28.61, 28.01, 26.54, 26.03, 25.76, 25.35, 18.88.

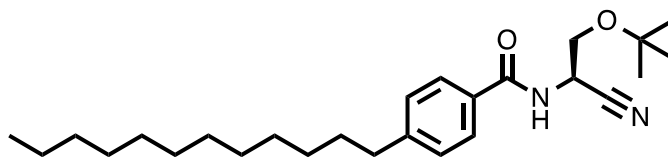
(R)-1-amino-2-(11-(cyclohexylmethoxy)undecanamido)propan-1-iminium chloride (**4.10**).



4.10

General procedure **A** was used to convert **4.9** (0.429 g, 1.22 mmol) to **4.10** (0.1046 g, 0.259 mmol, 21%). The product was purified via trituration; ^1H NMR (300 MHz, CD_3OD) δ 4.41 (q, $J = 7.3$ Hz, 1H), 3.56 – 3.35 (m, 2H), 3.21 (d, $J = 6.5$ Hz, 2H), 2.29 (t, $J = 7.6$ Hz, 2H), 1.97 – 1.53 (m, 4H), 1.50 (d, $J = 7.3$ Hz, 3H), 1.33 (s, 20H), 0.94 (m, 2H); ^{13}C NMR (75 MHz, CD_3OD) δ 176.88, 174.44, 77.82, 72.08, 48.87, 39.29, 36.25, 34.86, 34.48, 31.18, 30.68, 30.52, 30.47, 30.42, 30.33, 30.15, 29.81, 27.74, 27.26, 26.98, 26.38.

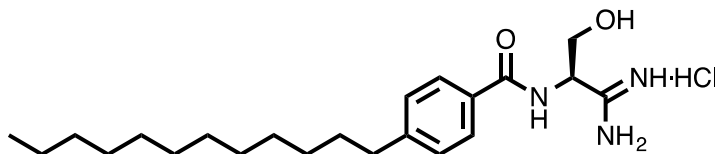
(*R*)-*N*-(2-(*tert*-butoxy)-1-cyanoethyl)-4-dodecylbenzamide ((*S*)-4.11).



((*S*)-4.11

General procedure F was used to couple 4-dodecylbenzoyl chloride (0.110 g, 0.355 mmol) and amine **3.17** (0.070 g, 0.391 mmol) to yield the title compound (0.0191 g, 0.062 mmol, 15%). $R_f = 0.46$ (25% EtOAc in Hexanes); ^1H NMR (300 MHz, CDCl_3) δ 7.67 (d, $J = 8.2$ Hz, 2H), 7.22 (d, $J = 8.2$ Hz, 2H), 3.87 (dd, $J = 10.8, 3.5$ Hz, 2H), 3.72 (dd, $J = 11.8, 6.0$ Hz, 1H), 2.72 – 2.56 (m, 2H), 1.66 – 1.51 (m, 2H), 1.35 – 1.14 (m, 18H), 0.92 (d, $J = 6.7$ Hz, 9H), 0.87 (t, $J = 6.7$ Hz, 3H); ^{13}C NMR (75 MHz, CDCl_3) δ 167.42, 147.07, 131.85, 128.71, 127.05, 118.00, 71.07, 35.95, 35.38, 34.07, 32.06, 31.37, 29.78, 29.71, 29.60, 29.49, 29.37, 27.80, 22.83, 19.20, 14.27.

(*R*)-*N*-(1-amino-3-hydroxy-1-iminopropan-2-yl)-4-dodecylbenzamide hydrochloride ((*S*)-4.12).

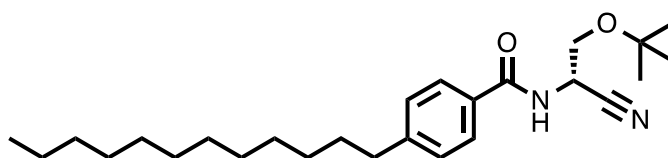


((*S*)-4.12

General procedure A was used to convert nitrile **(S)-4.11** to the amidine. Once complete, the crude material was dissolved in anhydrous DCM (0.1 M) followed by TFA (0.1 M). The reaction was stirred at rt for 15 min. Once

complete, the solvent was removed under reduced pressure and then co-evaporated twice with Et₂O. The mixture was purified via flash chromatography to afford the primary amidine. The pure material was dissolved in Et₂O and a few drops of 12.1 M HCl added. The mixture was swirled, the solvent removed under reduced pressure, and then co-evaporated twice with Et₂O to yield the title compound (0.0052 g, 0.0126 mmol, 24%). *R*_f = 0.33 (10% MeOH in CHCl₃); ¹H NMR (300 MHz, DMSO) δ 8.45 (t, *J* = 5.4 Hz, 1H), 7.74 (d, *J* = 8.1 Hz, 2H), 7.25 (d, *J* = 8.1 Hz, 2H), 3.44 (dd, *J* = 12.7, 7.1 Hz, 4H), 2.74 – 2.52 (m, 2H), 1.67 – 1.49 (m, 2H), 1.23 (s, 18H), 0.85 (t, *J* = 6.6 Hz, 3H); ¹³C NMR (75 MHz, DMSO) δ 172.87, 166.07, 145.78, 145.71, 131.85, 128.12, 127.19, 127.11, 126.63, 37.94, 37.69, 36.86, 35.51, 34.92, 34.70, 33.83, 31.30, 30.71, 29.01, 28.82, 28.71, 28.60, 22.10, 13.97.

(*S*)-*N*-(2-(*tert*-butoxy)-1-cyanoethyl)-4-dodecylbenzamide ((*R*)-4.11).

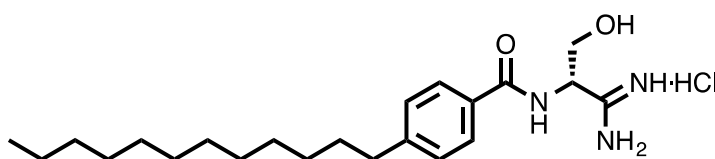


(*R*)-4.11

General procedure B was used to couple amine **4.16** (0.085 g, 0.473 mmol) to benzoic acid **4.4** (0.137 g, 0.473 mmol) to afford the title compound (0.0124 g, 0.0346 mmol, 7%). *R*_f = 0.33 (25% EtOAc in Hexanes); ¹H NMR (300 MHz, CDCl₃) δ 7.67 (d, *J* = 8.3 Hz, 2H), 7.22 (d, *J* = 8.3 Hz, 2H), 3.89 (d, *J* = 6.7 Hz, 1H), 3.72 (dd, *J* = 11.8, 6.0 Hz, 2H), 2.65 (dd, *J* = 9.7, 4.0 Hz, 2H), 1.66 – 1.55 (m, 2H), 1.36 – 1.19 (m, 18H), 0.92 (d, *J* = 6.7 Hz, 9H), 0.86 (d, *J* = 6.9 Hz,

3H); ^{13}C NMR (125 MHz, CDCl_3) δ 168.27, 147.06, 128.71, 127.05, 117.96, 77.42, 77.16, 76.91, 71.07, 49.89, 49.87, 49.85, 44.90, 44.89, 35.96, 35.42, 34.10, 32.06, 31.36, 29.81, 29.71, 29.61, 29.49, 29.38, 27.82, 22.83, 19.21, 14.26, 1.78, 1.76.

(S)-N-(1-amino-3-hydroxy-1-iminopropan-2-yl)-4-dodecylbenzamide hydrochloride ((R)-4.12).

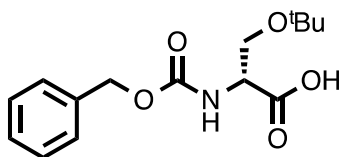


(R)-4.12

General procedure A was used to convert nitrile **(R)-4.11** (0.0124 g, 0.035 mmol) to the amidine. Once complete, the crude material was dissolved in anhydrous DCM (0.1 M) followed by TFA (0.1 M). The reaction was stirred at rt for 15 min. Once complete, the solvent was removed under reduced pressure and then co-evaporated twice with Et_2O . The mixture was purified via flash chromatography to afford the primary amidine. The pure material was dissolved in Et_2O and a few drops of 12.1 M HCl added. The mixture was swirled, the solvent removed under reduced pressure, and then co-evaporated twice with Et_2O to yield the title compound (0.007 g, 0.017 mmol, 49%). R_f = 0.24 (10% MeOH in CHCl_3); ^1H NMR (600 MHz, DMSO) δ 8.43 (d, J = 3.9 Hz, 1H), 7.74 (d, J = 8.1 Hz, 2H), 7.25 (d, J = 8.0 Hz, 2H), 3.57 – 3.56 (m, 1H), 3.46 – 3.42 (m, 2H), 2.60 (t, J = 7.3 Hz, 2H), 1.56 (bs, 2H), 1.24 (bs, 18H), 0.85 (t, J = 6.8 Hz, 3H); ^{13}C NMR (151 MHz, DMSO) δ 172.92, 166.11, 145.75, 131.84, 128.09,

127.16, 35.51, 34.91, 33.86, 31.28, 30.69, 29.01, 28.99, 28.96, 28.80, 28.69, 28.57, 22.09, 13.95.

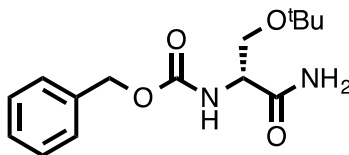
***N*-((benzyloxy)carbonyl)-*O*-(*tert*-butyl)-*D*-serine (4.13).**



4.13

H-D-Ser(OtBu)-OH (0.500 g, 3.10 mmol) was dissolved in 10% Na₂CO₃ solution (0.37 M) and N-(Benzyloxycarbonyloxy)succinimide (1.55 g, 6.20 mmol) followed by 1,4-dioxane (0.5 M) was added. The reaction was stirred overnight. Once complete, the reaction was washed with EtOAc (3 x 30 mL), acidified to pH = 2, extracted into EtOAc (3 x 30 mL), dried with Na₂SO₄, and the solvent removed under reduced pressure. The material was carried on crude.

benzyl (*R*)-(1-amino-3-(*tert*-butoxy)-1-oxopropan-2-yl)carbamate (4.14).

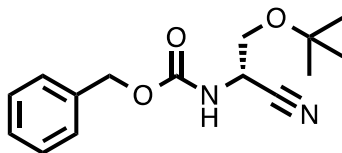


4.14

Carboxylic acid **4.13** (0.916 g, 3.10 mmol) was dissolved in dry DCM (0.5 M). TEA (0.942 g, 1.3 mL, 9.31 mmol) was added to the reaction and cooled to 0 °C. *iso*-Butylchloroformate (0.466 g, 0.52 mL, 3.41 mmol) was added to the reaction dropwise and then the reaction allowed to warm to rt and stirred at rt for

1 h. 7 M NH_3 in MeOH (3 M) was added to the reaction and allowed to stir at rt overnight. Once complete, the solvent was removed under reduced pressure and dried under high vacuum for 1 h. The material was carried on crude.

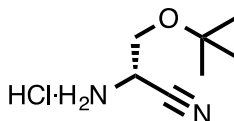
benzyl (S)-(2-(*tert*-butoxy)-1-cyanoethyl)carbamate (4.15).



4.15

General procedure K was used to convert amide **4.14** (0.913 g, 3.10 mmol) to nitrile **4.15** (0.130 g, 0.473 mmol, 15%). $R_f = 0.44$ (25% EtOAc in Hexanes); ^1H NMR (300 MHz, CDCl_3) δ 7.56 – 7.29 (m, 5H), 5.15 (t, $J = 6.8$ Hz, 1H), 5.09 (s, 2H), 3.87 (d, $J = 6.7$ Hz, 2H), 1.21 (s, 9H); ^{13}C NMR (75 MHz, CDCl_3) δ 140.58, 128.79, 128.66, 119.75, 51.40, 36.71, 34.51, 27.77, 27.55, 27.40, 27.25, 27.15, 19.19.

(S)-2-amino-3-(*tert*-butoxy)propanenitrile hydrochloride (4.16).

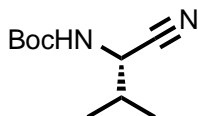


4.16

Amine **4.15** (0.131 g, 0.473 mmol) was dissolved in anhydrous EtOH (0.1 M) and 20% $\text{Pd}(\text{OH})_2 / \text{C}$ was added. The reaction was equipped with 1 atm. of H_2 and stirred over night. Once complete, the reaction was filtered through Celite and the solvent removed under reduced pressure. The crude material was

dissolved in Et₂O and a few drops of 12.1 M HCl was added. The reaction was swirled, the solvent removed under reduced pressure, then co-evaporated twice with Et₂O to afford the title compound. The material was carried on crude.

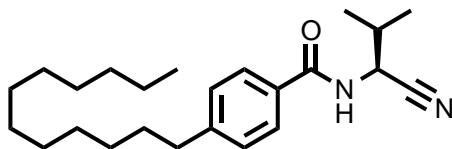
(S)-tert-butyl (1-cyano-2-methylpropyl)carbamate ((S)-4.18).



(S)-4.18

General procedure J was used to convert Boc-Val-OH (2.00 g, 9.206 mmol) to the primary amide. General procedure K was used to dehydrate the primary amide (1.991 g, 9.206 mmol) to the nitrile **(S)-4.18** (1.578 g, 7.959 mmol, 87%). *R*_f = 0.63 (25% EtOAc in Hex); ¹H NMR (300 MHz, CDCl₃) δ 4.46 – 4.24 (m, 1H), 1.95 (dd, *J* = 13.4, 6.7 Hz, 1H), 1.37 (bs, 9H), 0.84 (dd, *J* = 18.5, 6.9 Hz, 6H); ¹³C NMR (75 MHz, CDCl₃) δ 154.61, 118.07, 80.75, 48.40, 31.69, 28.14, 18.49, 17.96.

(S)-N-(1-cyano-2-methylpropyl)-4-dodecylbenzamide ((S)-4.20).

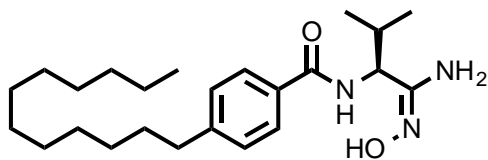


(S)-4.20

General procedure I was used to deprotect **(S)-4.18** (1.578 g, 7.959 mmol) to afford the trifluoroacetate amine salt. General procedure B was used to couple the trifluoroacetate amine salt (1.689 g, 7.96 mmol) to carboxylic acid **4.4** (2.312 g,

7.96 mmol) to afford the title compound (0.756 g, 2.04 mmol, 26%). $R_f = 0.72$ (25% EtOAc in Hex); ^1H NMR (300 MHz, CDCl_3) δ 7.72 (d, $J = 8.1$ Hz, 2H), 7.19 (d, $J = 8.1$ Hz, 2H), 5.07 – 4.88 (m, 1H), 2.61 (t, $J = 6.0$ Hz, 2H), 2.14 (dd, $J = 13.5, 6.8$ Hz, 1H), 1.57 (d, $J = 6.5$ Hz, 2H), 1.25 (s, 18H), 1.09 (dd, $J = 15.1, 6.7$ Hz, 6H), 0.87 (t, $J = 6.5$ Hz, 3H); ^{13}C NMR (75 MHz, CDCl_3) δ 167.16, 147.85, 130.17, 128.69, 127.44, 118.23, 47.10, 35.90, 31.95, 31.86, 31.23, 29.70, 29.52, 29.40, 29.31, 22.73, 18.77, 18.30, 14.17.

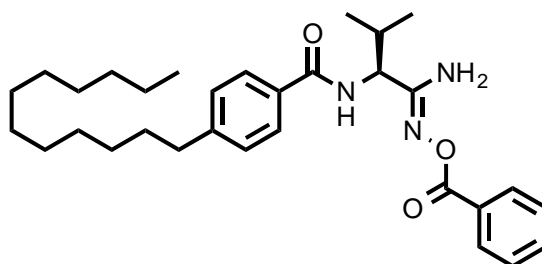
(*S,Z*)-*N*-(1-amino-1-(hydroxyimino)-3-methylbutan-2-yl)-4-dodecylbenzamide ((*S*)-4.21).



(*S*)-4.21

To a stirring solution of **(*S*)-4.20** (0.756 g, 2.04 mmol, 1 eq.) and hydroxylamine (0.709 g, 10.20 mmol, 5 eq.) in EtOH (0.02 M) was added TEA (2.064 g, 2.8 mL, 20.20 mmol, 10 eq.). The reaction was heated to 60 °C overnight. Solvent was removed under reduced pressure and immediately purified via flash chromatography to afford the title compound (0.623 g, 1.544 mmol, 76%). $R_f = 0.25$ (50% EtOAc in Hex, Seebach's Dip); ^1H NMR (300 MHz, CDCl_3) δ 7.74 (d, $J = 8.2$ Hz, 1H), 7.20 (d, $J = 8.2$ Hz, 1H), 4.32 (t, $J = 8.6$ Hz, 1H), 2.69 – 2.54 (t, $J = 7.5$ Hz, 2H), 1.69 – 1.49 (m, 1H), 1.27 (d, $J = 12.1$ Hz, 18H), 1.00 (dd, $J = 6.6, 3.3$ Hz, 6H), 0.87 (t, $J = 6.7$ Hz, 3H).

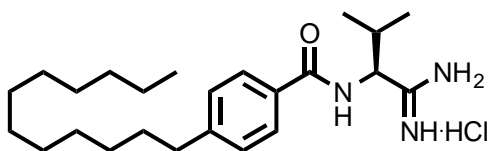
(S,Z)-N-(1-amino-1-((benzoyloxy)imino)-3-methylbutan-2-yl)-4-dodecylbenzamide ((S)-4.22).



(S)-4.22

To a stirring solution of amideoxime **(S)-4.22** (0.623 g, 1.54 mmol, 1 eq.), benzoic acid (0.189 g, 1.54 mmol, 1 eq.), and PyBOP (0.804 g, 1.54 mmol, 1 eq.) in DCM (0.05 M) was added DIPEA (0.998 g, 1.3 mL, 7.72 mmol, 5 eq.). The reaction was stirred overnight whence the solvent was removed under reduced pressure. The crude product was dissolved in EtOAc (100 mL), washed three times with sat. NH_4Cl (30 mL), once with brine (30 mL), dried with Na_2SO_4 , and evaporated under reduced pressure. The product was purified via flash chromatography to afford the title compound (0.242 g, 0.477 mmol, 31%). R_f = 0.73 (50% EtOAc in Hex); ^1H NMR (300 MHz, CDCl_3) δ 8.04 (d, J = 7.6 Hz, 2H), 7.75 (d, J = 8.0 Hz, 2H), 7.56 (t, J = 7.4 Hz, 1H), 7.43 (t, J = 7.7 Hz, 2H), 7.21 (d, J = 8.0 Hz, 2H), 4.29 (t, J = 8.5 Hz, 1H), 2.63 (t, J = 7.5 Hz, 2H), 1.84 (bs, 2H), 1.66 – 1.53 (m, 1H), 1.37 – 1.17 (m, 18H), 1.08 (dd, J = 12.6, 6.6 Hz, 6H), 0.87 (t, J = 6.6 Hz, 3H); ^{13}C NMR (75 MHz, CDCl_3) δ 187.59, 178.78, 166.95, 163.97, 158.98, 133.26, 129.65, 128.96, 128.81, 128.65, 127.42, 58.57, 51.44, 36.00, 32.06, 31.36, 31.14, 29.81, 29.63, 29.50, 29.38, 22.84, 21.63, 19.88, 19.40, 14.27.

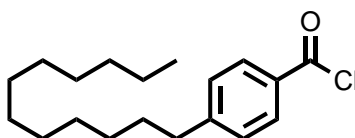
(S)-N-(1-amino-1-imino-3-methylbutan-2-yl)-4-dodecylbenzamide hydrochloride ((S)-4.23).



(S)-4.23

To a stirring solution of protected amideoxime (0.242 g, 0.477 mmol) in EtOH (0.1 M) was added 20% by wt Pd(OH)₂ (0.1 eq.). The reaction was run under H₂ (1 atm). Once complete, the reaction was filtered through Celite and washed with EtOH. The solvent was removed under reduced pressure and immediately purified via flash chromatography. The product was dissolved in Et₂O and a drop of 12.1 N HCl to afford the HCl salt (0.027 g, 0.0636 mmol, 13%). R_f = 0.025 (10% MeOH in CHCl₃); ¹H NMR (500 MHz, DMSO) δ 9.28 (s, 2H), 8.79 (d, *J* = 29.3 Hz, 2H), 7.89 (dd, *J* = 27.1, 10.0 Hz, 2H), 7.28 (t, *J* = 17.7 Hz, 2H), 4.57 – 4.43 (m, 1H), 2.62 (t, *J* = 7.4 Hz, 2H), 2.27 (dd, *J* = 22.9, 16.0 Hz, 1H), 1.52 (bs, 2H), 1.33 – 1.17 (m, 18H), 0.97 (dd, *J* = 14.6, 6.4 Hz, 6H), 0.84 (t, *J* = 6.5 Hz, 3H); ¹³C NMR (126 MHz, DMSO) δ 170.61, 167.05, 147.11, 131.01, 128.69, 128.22, 57.50, 35.39, 31.74, 31.18, 30.70, 29.45, 29.27, 29.16, 29.03, 22.55, 19.65, 19.22, 14.43.

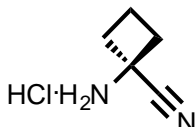
4-dodecylbenzoyl chloride (4.24).



4.24

General procedure E was used to convert carboxylic acid **4.4** (0.500 g, 1.72 mmol) to the acyl chloride **4.24**. The crude material was purified via flash chromatography (0.402 g, 1.30 mmol). $R_f = 0.9$ (10% EtOAc in Hex).

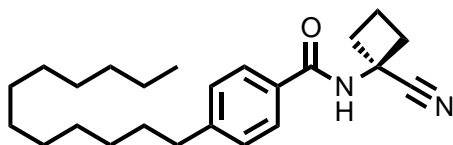
1-aminocyclobutanecarbonitrile hydrochloride (4.25).



4.25

To a solution of cyclobutanone (0.930 g, 1.0 mL, 13.269 mmol, 1.0 eq.) in 2 N NH_3/MeOH (0.2 M) were added potassium cyanide (2.0 eq.) and ammonium chloride (2.0 eq.). The reaction was run under ammonia gas (1 atm) at room temperature for 17 h. The mixture was then evaporated and the inorganic salts precipitated in CHCl_3 and removed via filtration through a fine frit. The solution was diluted in MeOH (100 mL), cooled to 0 °C, and treated with 12.1 N HCl (2.0 eq.). The mixture was allowed to stir for 5 min and then evaporated to dryness to yield the title compound (1.051 g, 7.930 mmol, 60%). White solid. ^1H NMR (300 MHz, CD_3OD) δ 2.73-2.47 (m, 2H), 2.29 (dt, $J = 12.7, 8.8$ Hz, 2H), 2.19-1.93 (m, 2H); ^{13}C NMR (75 MHz, CD_3OD) δ 123.66, 37.44, 35.80, 15.47.

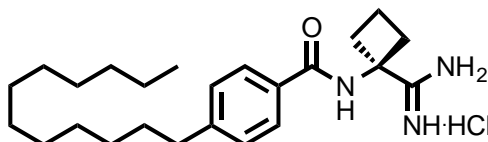
N-(1-Cyanocyclobutyl)-4-dodecylbenzamide (4.26).



4.26

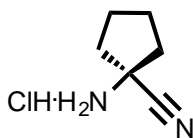
General procedure F was used to couple **4.25** (0.638 g, 6.635 mmol) and **4.26** (2.664 g, 8.63 mmol) to yield the title compound (1.477 g, 1.357 mmol, 30%). Clear and colorless oil. $R_f = 0.48$ (25% EtOAc in hexanes, Seebach's dip). ^1H NMR (300 MHz, CDCl_3) δ 8.44 (d, $J = 8.2$ Hz, 2H), 7.99 (d, $J = 8.7$ Hz, 2H), 7.26 (s, 1H), 3.71-3.52 (m, 2H), 3.44-3.33 (m, 2H), 3.21 (dd, $J = 21.0, 9.6$ Hz, 2H), 3.11-2.78 (m, 2H), 2.35 (m, 2H), 2.16-1.91 (m, 18H), 1.62 (t, $J = 6.6$ Hz, 3H). ^{13}C NMR (126 MHz, CDCl_3) δ 166.71, 147.92, 130.05, 128.73, 127.21, 120.88, 48.00, 35.86, 34.14, 31.90, 31.16, 29.63, 29.56, 29.45, 29.34, 29.22, 22.68, 16.17, 14.13.

N-(1-Carbamimidoylcyclobutyl)-4-dodecylbenzamide (4.27).

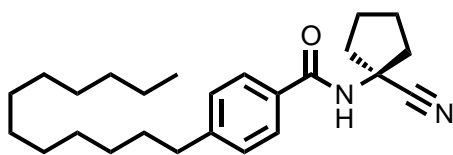


4.27

General procedure A was used to convert **4.26** (0.500 g, 1.357 mmol) to the title compound (0.371 g, 0.879 mmol, 7%). White solid. ^1H NMR (500 MHz, DMSO) δ 9.15 (s, 1H), 8.82 (s, 4H), 7.88 (d, $J = 8.2$ Hz, 2H), 7.30 (d, $J = 8.2$ Hz, 2H), 2.68-2.56 (m, 4H), 2.42 (dd, $J = 17.6, 11.1$ Hz, 2H), 2.10-1.96 (m, 1H), 1.96-1.82 (m, 1H), 1.55 (pent, $J = 6.8$ Hz, 2H), 1.25 (m, 18H), 0.85 (t, $J = 6.8$ Hz, 3H). ^{13}C NMR (126 MHz, DMSO) δ 172.70, 166.46, 146.63, 130.64, 128.08, 127.95, 57.31, 34.98, 31.32, 31.01, 30.80, 29.03, 28.85, 28.73, 28.58, 22.12, 15.05, 13.99. LCMS: $t_R = 5.29$; $m/z = 386.3$. HRMS m/z calcd for $\text{C}_{24}\text{H}_{40}\text{N}_3\text{O}$ ($M + \text{H}$), 386.3171; found, 386.3178.

1-aminocyclopentane-1-carbonitrile hydrochloride (4.28).**4.28**

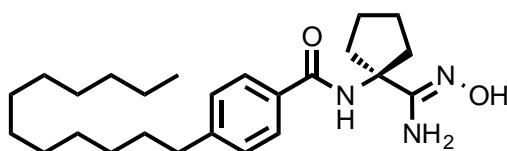
To a solution of cyclopentanone (0.950 g, 1.0 mL, 11.29 mmol, 1.0 eq.) in 7 N NH_3/MeOH (0.2 M) were added potassium cyanide (2.0 eq.) and ammonium chloride (2.0 eq.). The reaction was run under ammonia gas (1 atm) at room temperature for 24 h. The mixture was then evaporated and the inorganic salts precipitated in CHCl_3 and removed via filtration through a fine frit. The solution was diluted in MeOH (100 mL), cooled to 0 °C, and treated with 12.1 N HCl (2.0 eq.). The mixture was allowed to stir for 5 min and then evaporated to dryness to yield the title compound (1.23 g, 8.42 mmol, 75%). White solid; ^1H NMR (300 MHz, DMSO) δ 9.54 (s, 3H), 2.36 – 2.22 (m, 2H), 2.21 – 2.09 (m, 2H), 1.91 - 1.85 (m, 2H), 1.80 – 1.65 (m, 2H); ^{13}C NMR (75 MHz, DMSO) δ 119.69, 54.16, 36.97, 23.03.

***N*-(1-cyanocyclopentyl)-4-dodecylbenzamide (4.29).****4.29**

General procedure F was used to couple **4.25** (1.05 g, 3.40 mmol) and **4.28** (0.548 g, 3.74 mmol) to yield the title compound (0.501 g, 1.36 mmol, 40%). Clear and colorless oil. R_f = 0.48 (25% EtOAc in hexanes, Seebach's dip); ^1H

NMR (300 MHz, CDCl_3) δ 7.67 (d, $J = 8.2$ Hz, 2H), 7.20 (d, $J = 8.2$ Hz, 2H), 6.50 (bs, 1H), 2.66 – 2.57 (t, $J = 7.5$, 2H), 2.56 – 2.43 (m, 2H), 2.26 – 2.12 (m, 2H), 1.88 (m, 4H), 1.59 (m, 2H), 1.27 (d, $J = 10.9$ Hz, 18H), 0.87 (t, $J = 6.6$ Hz, 3H); ^{13}C NMR (75 MHz, CDCl_3) δ 167.69, 147.50, 130.49, 128.51, 127.44, 121.43, 55.54, 39.03, 35.85, 31.94, 31.22, 29.69, 29.51, 29.38, 23.17, 22.71, 14.15.

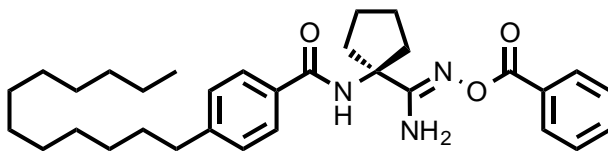
(Z)-4-dodecyl-N-(1-(N-hydroxycarbamimidoyl)cyclopentyl)benzamide (4.30).



4.30

To a stirring solution of **4.29** (0.501 g, 1.36 mmol, 1 eq.) and hydroxylamine (0.473 g, 6.80 mmol, 5 eq.) in EtOH (0.02 M) was added TEA (1.38 g, 1.9 mL, 13.60 mmol, 10 eq.). The reaction was heated to 60 °C overnight. Solvent was removed under reduced pressure and immediately purified via flash chromatography to afford the title compound (0.339 g, 0.816 mmol, 60%). R_f = 0.07 (25% EtOAc in Hex, Seebach's Dip);

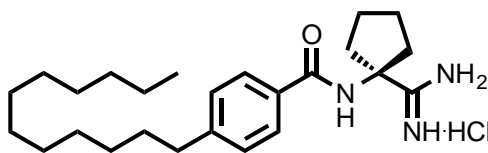
(Z)-N-(1-(N-(benzoyloxy)carbamimidoyl)cyclopentyl)-4-dodecylbenzamide (4.32).



4.32

To a stirring solution of amideoxime **4.31** (0.339 g, 0.816 mmol, 1 eq.), benzoic acid (0.099 g, 0.816 mmol, 1 eq.), and PyBOP (0.425 g, 0.816 mmol, 1 eq.) in DCM (0.05 M) was added DIEA (0.527 g, 0.71 mL, 4.08 mmol, 5 eq.). The reaction was stirred overnight whence the solvent was removed under reduced pressure. The crude product was dissolved in EtOAc (100 mL), washed three times with sat. NH_4Cl (30 mL), once with brine (30 mL), dried with Na_2SO_4 , and evaporated under reduced pressure. The product was purified via flash chromatography to afford the title compound (0.327 g, 0.628 mmol, 77%). R_f = 0.85 (50% EtOAc in Hex); ^1H NMR (300 MHz, CDCl_3) δ 7.98 (d, J = 8.1 Hz, 2H), 7.69 (d, J = 7.9 Hz, 2H), 7.49 (t, J = 7.5 Hz, 1H), 7.34 (t, J = 7.6 Hz, 2H), 7.13 (d, J = 7.9 Hz, 2H), 7.02 (s, 1H), 6.12 (s, 2H), 2.58 (t, J = 7.6 Hz, 2H), 2.43 - 2.31 (m, 4H), 1.73 - 1.73 (m, 4H), 1.63 - 1.49 (m, 2H), 1.25 (s, 18H), 0.87 (t, J = 6.4 Hz, 3H); ^{13}C NMR (75 MHz, CDCl_3) δ 168.87, 164.53, 162.25, 147.25, 132.77, 131.70, 129.82, 129.48, 128.55, 128.37, 127.35, 65.70, 51.32, 35.88, 31.97, 31.27, 29.72, 29.65, 29.53, 29.41, 29.30, 22.91, 22.74, 14.18.

***N*-(1-carbamimidoylcyclopentyl)-4-dodecylbenzamide hydrochloride (4.33).**

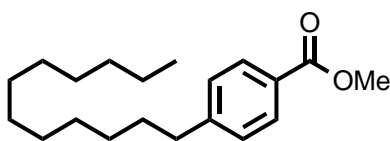


4.33

General procedure A was used to convert **4.32** (0.327 g, 0.628 mmol) to the title compound (0.012 g, 0.028 mmol, 27%). White solid. R_f = 0.12 (10% MeOH in CHCl_3); ^1H NMR (600 MHz, DMSO) δ 8.92 (s, 2H), 8.70 (s, 2H), 8.63 (s, 1H),

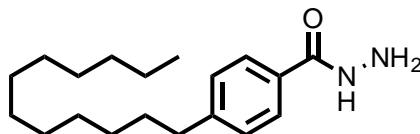
7.85 (d, $J = 8.2$ Hz, 2H), 7.27 (d, $J = 8.3$ Hz, 2H), 2.61 (t, $J = 7.6$ Hz, 2H), 2.20 (dd, $J = 11.1, 6.6$ Hz, 2H), 2.07 (dt, $J = 13.8, 6.8$ Hz, 2H), 1.82 – 1.68 (m, 4H), 1.60 – 1.52 (m, 2H), 1.33 – 1.15 (m, 18H), 0.85 (t, $J = 7.0$ Hz, 3H); ^{13}C NMR (151 MHz, DMSO) δ 173.75, 166.70, 146.39, 131.08, 128.01, 127.94, 64.51, 36.39, 34.96, 31.30, 30.80, 29.03, 29.02, 29.01, 28.83, 28.71, 28.56, 23.44, 22.10, 13.97.

Methyl 4-dodecylbenzoate (4.34).

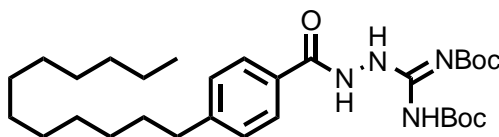


4.34

To a stirring solution of anhydrous MeOH (1 M) at 0 °C was added Acyl chloride (2M in MeOH) dropwise. The reaction was stirred for 10 min at rt followed by the carboxylic acid **4.4** (0.500 g, 1.722 mmol, 1 eq.) added in one portion. The reaction was heated to reflux and stirred overnight. Once complete, the solvent was removed under reduced pressure and purified by flash chromatography to afford the target compound (0.398 g, 1.307 mmol, 76%). $R_f = 0.66$ (10 % EtOAc in Hex); ^1H NMR (300 MHz, CDCl_3) δ 7.95 (d, 2H, $J = 8.2$ Hz), 7.24 (d, 2H, $J = 8.1$ Hz), 3.90 (s, 3H), 2.72 – 2.58 (m, 2H), 1.66 – 1.53 (m, 2H), 1.27 (m, 18H), 0.88 (t, 3H, $J = 6.7$ Hz); ^{13}C NMR (75 MHz, CDCl_3) δ 162.66, 148.67, 129.74, 128.56, 52.09, 51.44, 36.15, 32.06, 31.29, 29.78, 29.70, 29.60, 29.50, 29.40, 22.84, 14.27.

4-dodecylbenzohydrazide (4.35):**4.35**

To a stirring solution of methyl ester **4.34** (0.398 g, 1.307 mmol) in anhydrous ethanol (2.0 mL), hydrazine (0.36 mL, 3.921 mmol) was added. The mixture was heated to reflux overnight. Once complete, the reaction was cooled, upon which a solid formed. The solvent was removed under reduced pressure and the solid washed with hexanes and filtered via a fine fritted funnel yielding 0.236 g (0.77 mmol, 59%): ^1H NMR (300 MHz, DMSO) δ 9.68 (s, 1H), 7.72 (d, 2H, J = 8.3 Hz), 7.24 (d, 2H, J = 8.3 Hz), 4.51 (bs, 2H), 2.64 – 2.56 (m, 2H), 1.56 (m, 2H), 1.24 (m, 18H), 0.85 (t, 3H, J = 6.7 Hz); ^{13}C NMR (75 MHz, DMSO) δ 165.90, 145.69, 130.76, 128.18, 126.96, 94.88, 46.10, 34.96, 31.33, 30.74, 29.05, 28.86, 28.75, 28.67, 22.14, 14.01.

Tert-butyl (((tert-butoxycarbonyl)imino)(2-(4-dodecylbenzoyl)hydrazinyl) methyl)carbamate (4.36)**4.36**

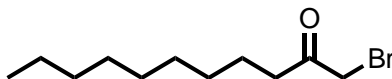
To a stirring solution of **4.35** (0.236 g, 0.774 mmol) and *N,N'*-di-boc-1*H*-pyrazole-1-carboxamidine (0.264 g, 0.852 mmol) in acetonitrile (3.9 mL) was added DIPEA (0.4 mL, 2.322 mmol). The reaction was stirred for 24 hrs at room

CCCCCCCCc1ccc(cc1)C(=O)NNC(=N)N

To a stirring solution of **4.36** (0.240 g, 0.427 mmol) in DCM (4.2 mL) was added TFA (4.2 mL). The reaction was allowed to stir for 15 min. The reaction was concentrated under reduced pressure and co-evaporated with Et₂O (2 x 10 mL). The remaining residue was dissolved and stirred in 6M HCl (1.4 mL) for 5 min. The reaction was concentrated under reduced pressure and then co-evaporated with Et₂O (2 x 10 mL) to yield 0.163 g (0.43 mmol, 100%): ¹H NMR (500 MHz, DMSO) δ 10.59 (s, 2H), 9.69 (s, 2H), 7.86 (d, 2H, *J* = 8.1 Hz), 7.55 (s, 2H), 7.32 (d, 2H, *J* = 8.1 Hz), 2.63 (t, 2H, *J* = 7.6 Hz), 1.77 – 1.45 (m, 2H), 1.25 (m, 18H),

0.85 (t, 3H, $J = 6.9$ Hz); ^{13}C NMR (126 MHz, DMSO) δ 166.47, 158.84, 147.14, 129.23, 128.27, 128.03, 35.02, 31.34, 30.77, 29.06, 28.88, 28.76, 28.63, 22.15, 14.02.

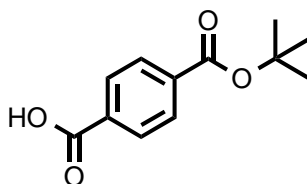
1-bromoundecan-2-one (4.38).



4.38

To a solution of 2-undecanone (0.913 g, 1.1 mL, 5.36 mmol, 1 eq.) in MeOH (0.65M) at -10°C was added Br_2 (0.856 g, 0.3 mL, 5.36 mmol, 1 eq.) dropwise. The reaction was stirred at -10°C for 1 hr then at rt for 1 hr. The reaction was then cooled to 0°C then DI water (3.25 M) was added followed by H_2SO_4 (1.85 M) and stirred at rt overnight. Once complete, the reaction was extracted with DCM (3 x 30 mL), dried with Na_2SO_4 , and the solvent removed under reduced pressure to yield the title compound (1.353 g, 5.36 mmol, 99%); ^1H NMR (300 MHz, CDCl_3) δ 3.87 (s, 2H), 2.62 (t, $J = 7.3$ Hz, 2H), 1.67 – 1.54 (m, 2H), 1.24 (s, 12H), 0.85 (t, $J = 6.4$ Hz, 3H).

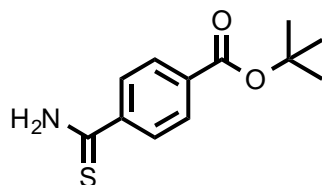
4-(*tert*-butoxycarbonyl)benzoic acid (4.39).



4.39

A stirring solution of terephthalic acid (5.00 g, 30.10 mmol, 1 eq.), Di-tert-butyl dicarbonate (6.57 g, 30.10 mmol, 1 eq.), 4-Dimethylaminopyridine (0.918 g, 7.52 mmol, 0.25 eq.) in tBuOH (0.1 M) and THF (0.3 M) was heated to reflux overnight. Once complete, the solvent was removed under reduced pressure and purified via flash chromatography to yield the title compound (1.793 g, 8.066 mmol, 27%). R_f = 0.20 (5% MeOH in DCM); ^1H NMR (300 MHz, CDCl_3) δ 8.16 (d, J = 8.6 Hz, 2H), 8.08 (d, J = 8.7 Hz, 2H), 1.62 (s, 9H); ^{13}C NMR (75 MHz, CDCl_3) δ 164.94, 163.96, 130.18, 129.63, 82.07, 28.28.

tert-butyl 4-carbamothioylbenzoate (4.41)

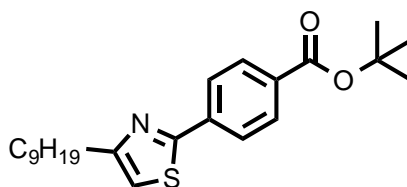


4.41

4.39 (1.793 g, 8.066 mmol) was then dissolved in DCM (0.3 M) at 0 °C and treated with TEA (3.0 eq.) and then isobutyl chloroformate (1.1 eq.). The mixture turned turbid after the addition and was allowed to warm to room temperature before slowly clearing over time. After 1 h at room temperature, the mixture was treated with 2 N NH_3 in MeOH (2.0 eq.) and allowed to stir for overnight. The mixture was evaporated to a white solid and purified by flash chromatography to yield the corresponding amide (1.265 g, 5.718 mmol, 66%). White solid. R_f = 0.39 (60% EtOAc in hexanes, UV). ^1H NMR (300 MHz, CDCl_3) δ 8.02 (d, J = 8.1 Hz, 2H), 7.84 (d, J = 8.1 Hz, 2H), 6.48 (s, 2H), 1.59 (s, 9H); ^{13}C NMR (75 MHz,

CDCl₃) δ 169.25, 165.10, 137.02, 135.22, 129.87, 127.47, 81.99, 28.35. The amide was then dissolved in THF (0.5 M) and treated with Lawesson's reagent (0.6 eq.) in one portion. The mixture was allowed to stir for 3 h before being evaporated to dryness and purified by flash chromatography to yield the title compound (1.151 g, 4.851 mmol, 92%). Yellow/ green solid. R_f = 0.93 (50% EtOAc in hexanes, Seebach's dip). ¹H NMR (500 MHz, DMSO) δ 10.06 (s, 1H), 9.65 (s, 1H), 8.12-7.55 (m, 4H), 1.53 (s, 9H); ¹³C NMR (126 MHz, DMSO) δ 199.69, 164.80, 143.60, 133.51, 129.12, 127.88, 81.62, 28.18.

***tert*-butyl 4-(4-nonylthiazol-2-yl)benzoate (4.42).**

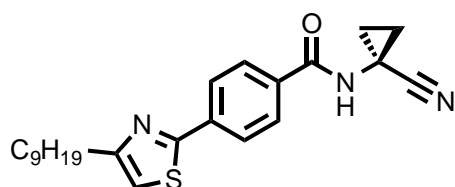


4.42

To a solution of **4.41** (1.151 g, 4.851 mmol) and KHCO₃ (1.1 eq.) in THF (0.2 M) at -5 °C was added **4.38** (1.353 g, 5.431 mmol). The mixture was allowed to warm to room temperature. The mixture was allowed to stir for 2 h and then cooled to -5 °C again and treated with TEA (2.2 eq.) and TFAA (1.1 eq.). The mixture was allowed to warm to room temperature and was stirred overnight. The mixture was concentrated under reduced pressure and then dissolved in DI H₂O (100 mL). The aqueous layer was washed three times with DCM (30 mL) then dried with Na₂SO₄, evaporated to dryness, and immediately purified by flash chromatography to yield the title compound (0.753 g, 1.942 mmol, 40%). Yellow

solid. $R_f = 0.60$ (10% EtOAc in Hex, blue under UV, Seebach's dip); ^1H NMR (300 MHz, CDCl_3) δ 8.03 (d, $J = 8.6$ Hz, 2H), 7.98 (d, $J = 8.8$ Hz, 2H), 6.93 (s, 1H), 2.83 (t, $J = 7.5$ Hz, 2H), 1.83 – 1.70 (m, 2H), 1.61 (s, 9H), 1.44 – 1.12 (m, 12H), 0.88 (t, $J = 6.7$ Hz, 3H); ^{13}C NMR (75 MHz, CDCl_3) δ 172.90, 165.08, 153.32, 135.18, 130.13, 130.01, 126.27, 113.86, 51.51, 51.44, 32.04, 32.01, 31.87, 29.70, 29.61, 29.48, 29.38, 28.34, 22.84, 14.28, 9.82.

***N*-(1-cyanocyclopropyl)-4-(4-nonylthiazol-2-yl)benzamide (4.45).**

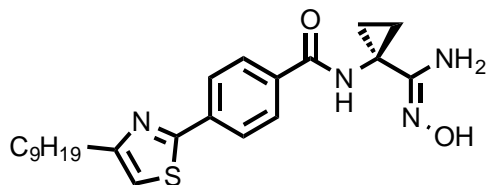


4.45

General procedure I was used to deprotect the *t*-butyl ester on compound **4.42** (0.753 g, 1.942 mmol) to yield the corresponding carboxylic acid (0.644 g, 1.942 mmol). General procedure E was used to convert the carboxylic acid to the corresponding acid chloride (0.419 g, 1.198 mmol). General procedure F was used to couple the acid chloride and 1-Amino-1-cyclopropanecarbonitrile hydrochloride (0.156 g, 1.318 mmol) to yield the title compound (0.311 g, 0.787 mmol, 66%). Yellow solid. $R_f = 0.70$ (50% EtOAc in Hex, Seebach's dip); ^1H NMR (300 MHz, CDCl_3) δ 7.98 (d, $J = 8.6$ Hz, 2H), 7.81 (d, $J = 8.6$ Hz, 2H), 7.06 (s, 1H), 2.81 (t, $J = 7.5$ Hz, 2H), 1.80 – 1.68 (m, 2H), 1.64 (dd, $J = 8.4, 5.8$ Hz, 2H), 1.39 (dd, $J = 8.5, 5.8$ Hz, 2H), 1.27 (m, 12H), 0.87 (t, $J = 6.6$ Hz, 3H); ^{13}C NMR (75 MHz, CDCl_3) δ 167.47, 165.79, 159.68, 137.50, 133.34, 128.03, 126.74,

120.16, 114.15, 32.02, 31.82, 29.68, 29.58, 29.45, 29.37, 22.81, 21.10, 17.08, 14.26.

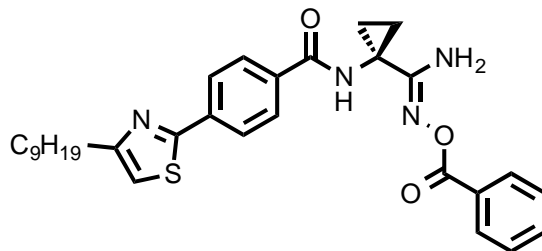
(Z)-N-(1-(N-hydroxycarbamimidoyl)cyclopropyl)-4-(4-nonylthiazol-2-yl)benzamide (4.46).



4.46

To a stirring solution of **4.45** (0.311 g, 0.787 mmol, 1 eq.) and hydroxylamine (0.273 g, 3.935 mmol, 5 eq.) in EtOH (0.02 M) was added TEA (0.796 g, 1.1 mL, 7.870 mmol, 10 eq.). The reaction was heated to 60 °C overnight. Solvent was removed under reduced pressure and immediately purified via flash chromatography. R_f = 0.12 (50% EtOAc in Hex); ^1H NMR (300 MHz, CD_3OD) δ 8.01 (d, J = 8.7 Hz, 2H), 7.92 (d, J = 8.7 Hz, 2H), 7.22 (s, 1H), 2.83 (t, J = 7.6 Hz, 2H), 1.84 – 1.68 (m, 2H), 1.46 – 1.23 (m, 14H), 1.07 (dd, J = 7.5, 5.2 Hz, 2H), 0.89 (t, J = 6.5 Hz, 3H); ^{13}C NMR (75 MHz, DMSO) δ 166.91, 166.81, 166.61, 165.19, 158.45, 152.99, 135.58, 135.03, 128.36, 125.68, 115.14, 31.85, 31.73, 31.31, 30.92, 28.97, 28.84, 28.71, 22.14, 13.99, 13.46.

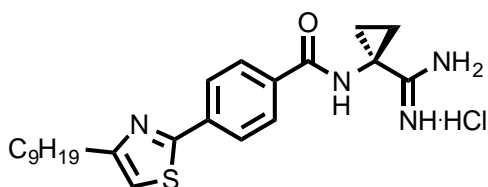
(Z)-N-(1-(N-(benzyloxy)carbamimidoyl)cyclopropyl)-4-(4-nonylthiazol-2-yl)benzamide (4.47).



4.47

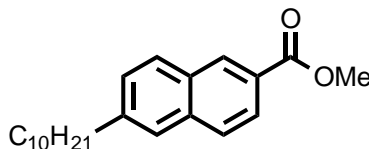
To a stirring solution of amideoxime **4.46** (0.213 g, 0.497 mmol, 1eq.), benzoic acid (0.061 g, 0.497 mmol, 1 eq.), and PyBOP (0.259 g, 0.497 mmol, 1 eq.) in DCM (0.05 M) was added DIPEA (0.321 g, 0.4 mL, 2.484 mmol, 5 eq.). The reaction was stirred overnight whence the solvent was removed under reduced pressure. The crude product was dissolved in EtOAc (100 mL), washed three times with sat. NH_4Cl (30 mL), once with brine (30 mL), dried with Na_2SO_4 , and evaporated under reduced pressure. The product was purified via flash chromatography to afford the title compound (0.123 g, 0.231 mmol, 47%). R_f = 0.59 (50% EtOAc in Hex); ^1H NMR (300 MHz, CDCl_3) δ 8.03 (d, J = 2.2 Hz, 2H), 8.00 (d, J = 1.4 Hz, 2H), 7.81 (d, J = 8.5 Hz, 2H), 7.57 (dd, J = 10.9, 3.9 Hz, 1H), 7.44 (t, J = 7.5 Hz, 2H), 7.16 (s, 1H), 6.94 (s, 1H), 2.82 (t, J = 7.5 Hz, 2H), 1.85 – 1.68 (m, 1H), 1.31 (m, 18H), 1.22 (dd, J = 7.7, 5.8 Hz, 6H), 0.87 (t, J = 6.7 Hz, 3H); ^{13}C NMR (75 MHz, CDCl_3) δ 169.48, 161.86, 159.69, 155.12, 153.99, 149.91, 149.33, 133.18, 129.55, 128.63, 127.93, 126.73, 114.01, 42.10, 37.45, 32.03, 31.84, 29.68, 29.59, 29.46, 29.38, 22.83, 14.27, 14.20, 13.85.

***N*-(1-carbamimidoylcyclopropyl)-4-(4-nonylthiazol-2-yl)benzamide hydrochloride (4.48).**

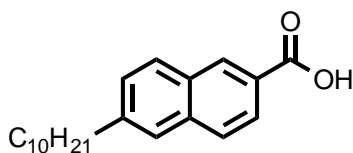


4.48

To a stirring solution of **XX** (0.123 g, 0.231 mmol, 1 eq.) in EtOH (0.1 M) was added 20% by wt. Pd(OH)₂ (0.13 eq.). The reaction was stirred under H₂ (1 atm) for 24 hrs. Once complete the reaction was filtered through a plug of Celite and washed with anhydrous EtOH. The solvent was removed under reduced pressure and immediately purified via flash chromatography. The product was dissolved in Et₂O and a drop of 12.1 M HCl was added. The material was co-evaporated three times with Et₂O to afford the title compound as a HCl salt (0.0012 g, 0.0027 mmol, 12%); R_f = 0.0 (10% MeOH in CHCl₃); ¹H NMR (300 MHz, DMSO) δ 9.36 (s, 1H), 8.92 (s, 2H), 8.64 (s, 2H), 8.02 (q, *J* = 8.5 Hz, 4H), 7.43 (s, 1H), 2.76 (t, *J* = 7.5 Hz, 2H), 1.70 (bs, 2H), 1.43 (t, *J* = 7.0 Hz, 2H), 1.40 – 1.16 (m, 14H), 0.84 (t, *J* = 6.5 Hz, 3H); ¹³C NMR (126 MHz, DMSO) δ 171.81, 167.03, 158.51, 135.86, 134.27, 128.83, 125.55, 115.30, 31.30, 30.91, 28.96, 28.83, 28.74, 28.69, 22.13, 18.08, 14.00. LCMS: t_R = 4.44; *m/z* = 413.2. HRMS *m/z* calcd for C₂₃H₃₃N₄OS (M + H), 413.2375; found, 413.2366.

methyl 6-decyl-2-naphthoate (4.49).**4.49**

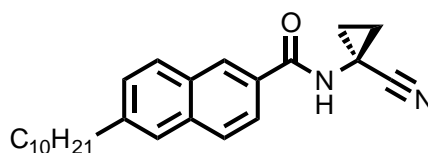
General procedure C was used to couple methyl 6-bromo-2-naphthoate (1.00 g, 3.77 mmol) and 1-decene (0.794 g, 5.66 mmol) to afford the title compound (0.979 g, 3.00 mmol, 80%). $R_f = 0.57$ (5% EtOAc in Hex); ^1H NMR (300 MHz, CDCl_3) δ 8.58 (s, 1H), 8.05 (dd, $J = 8.6, 1.7$ Hz, 1H), 7.87 (d, $J = 8.4$ Hz, 1H), 7.80 (d, $J = 8.6$ Hz, 1H), 7.64 (s, 1H), 7.39 (dd, $J = 8.4, 1.6$ Hz, 1H), 3.98 (s, 3H), 2.79 (t, $J = 7.5$ Hz, 2H), 1.84 – 1.63 (m, 2H), 1.32 (m, 14H), 0.90 (t, $J = 6.7$ Hz, 3H); ^{13}C NMR (75 MHz, CDCl_3) δ 167.45, 143.43, 135.91, 131.06, 130.92, 129.27, 128.37, 127.68, 126.66, 126.28, 125.36, 52.20, 51.40, 51.36, 36.36, 32.02, 31.31, 29.71, 29.63, 29.46, 22.81, 14.23.

6-decyl-2-naphthoic acid (4.50).**4.50**

To a stirring solution of ester **4.49** (0.979 g, 3.00 mmol, 1 eq.) in MeOH (1 M) and THF (1 M) was added lithium hydroxide (0.216 g, 9.00 mmol, 3 eq.) in H_2O (1 M). The reaction was stirred at rt overnight. Once complete, the reaction was diluted with EtOAc, washed once with 1 M HCl, and back extracted with EtOAc. The

combined organic layers were dried with Na_2SO_4 then the solvent removed under reduced pressure to afford the target compound (0.918 g, 2.94 mmol, 98%); ^1H NMR (300 MHz, CDCl_3) δ 8.68 (s, 1H), 8.10 (dd, J = 8.6, 1.6 Hz, 1H), 7.91 (d, J = 8.5 Hz, 1H), 7.85 (d, J = 8.7 Hz, 1H), 7.67 (s, 1H), 7.42 (dd, J = 8.4, 1.4 Hz, 1H), 2.80 (t, J = 7.5 Hz, 2H), 1.81 – 1.64 (m, 2H), 1.31 (m, 14H), 0.88 (t, J = 6.7 Hz, 3H); ^{13}C NMR (75 MHz, CDCl_3) δ 172.30, 136.39, 132.07, 129.52, 128.58, 127.91, 126.40, 125.51, 77.82, 54.80, 51.43, 36.45, 32.06, 31.35, 29.77, 29.67, 29.50, 22.84.

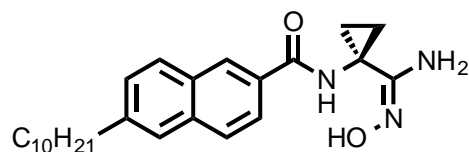
***N*-(1-cyanocyclopropyl)-6-decyl-2-naphthamide (4.51).**



4.51

General procedure B was used to couple 1-amino-1-cyclopropanecarbonitrile hydrochloride (0.100 g, 0.844 mmol) and carboxylic acid **4.50** (0.264 g, 0.844 mmol) to afford the title compound (0.262 g, 0.696 mmol, 82%). R_f = 0.18 (25% EtOAc in Hex); ^1H NMR (300 MHz, CDCl_3) δ 8.23 (s, 1H), 7.77 (m, 2H), 7.60 (s, 1H), 7.36 (dd, J = 8.4, 1.5 Hz, 1H), 7.10 (s, 1H), 2.76 (t, J = 7.7 Hz, 2H), 1.77 – 1.58 (m, 4H), 1.41 (dd, J = 8.4, 5.8 Hz, 2H), 1.29 (m, 14H), 0.87 (t, J = 6.1 Hz, 3H); ^{13}C NMR (75 MHz, CDCl_3) δ 168.35, 164.19, 143.44, 135.50, 130.99, 128.99, 128.77, 128.29, 127.99, 126.31, 123.49, 120.34, 36.35, 32.03, 31.33, 29.71, 29.64, 29.46, 22.81, 21.14, 17.13, 14.25.

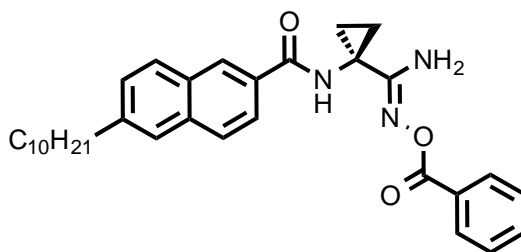
(Z)-6-decyl-N-(1-(*N*-hydroxycarbamimidoyl)cyclopropyl)-2-naphthamide (4.52).



4.52

To a stirring solution of nitrile **4.51** (0.262 g, 0.696 mmol, 1 eq.), hydroxylamine (0.242 g, 3.50 mmol, 5 eq.) in EtOH (0.02 M) was added TEA (0.666 g, 0.9 mL, 6.96 mmol, 10 eq.). The reaction was heated to 60 °C and stirred overnight. Once complete, the solvent was removed under reduced pressure and the crude material purified via flash chromatography to afford the title compound (0.246 g, 0.601 mmol, 86%). R_f = 0.07 (25% EtOAc in Hex); ^1H NMR (300 MHz, DMSO) δ 9.05 (s, 1H), 8.42 (s, 1H), 7.92 (s, 1H), 7.89 (s, 2H), 7.73 (s, 1H), 7.45 (d, J = 8.4 Hz, 1H), 5.42 (bs, 1H), 2.75 (t, J = 7.6 Hz, 2H), 1.71 – 1.57 (m, 2H), 1.40 – 1.16 (m, 23H), 0.97 (t, J = 6.2 Hz, 2H), 0.84 (t, J = 6.2 Hz, 3H).

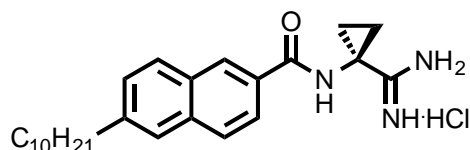
(Z)-N-(1-(*N*-(benzoyloxy)carbamimidoyl)cyclopropyl)-6-decyl-2-naphthamide (4.53).



4.53

To a stirring solution of amideoxime **4.52** (0.246 g, 0.601 mmol, 1 eq.), benzoic acid (0.0734 g, 0.601 mmol, 1 eq.), and PyBOP (0.313 g, 0.601 mmol, 1 eq.) in DCM (0.05 M) was added DIPEA (0.388 g, 0.5 mL, 3.00 mmol, 5 eq.). The reaction was stirred overnight whence the solvent was removed under reduced pressure. The crude product was dissolved in EtOAc (100 mL), washed three times with 1 M HCl (30 mL), once with brine (30 mL), dried with Na₂SO₄, and evaporated under reduced pressure. The product was purified via flash chromatography to afford the title compound (0.187 g, 0.364 mmol, 61%). R_f = 0.65 (50% EtOAc in Hex);

***N*-(1-carbamimidoylcyclopropyl)-6-decyl-2-naphthamide hydrochloride (4.54).**

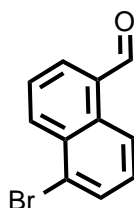


4.54

To a stirring solution of **4.53** (0.188 g, 0.364 mmol, 1 eq.) in EtOH (0.1 M) was added 20% by wt. Pd(OH)₂ (0.10 eq.). The reaction was stirred under H₂ (1 atm) for 24 hrs. Once complete the reaction was filtered through a plug of Celite and washed with anhydrous EtOH. The solvent was removed under reduced pressure and immediately purified via flash chromatography. The material was then dissolved in Et₂O and a drop of 12.1 M HCl was added. The material was co-evaporated three times with Et₂O to afford the title compound as a HCl salt (0.034 g, 0.078 mmol, 22%). R_f = 0.0 (10% MeOH in CHCl₃); ¹H NMR (600 MHz,

DMSO) δ 9.33 (s, 1H), 8.91 (s, 2H), 8.62 (s, 2H), 8.50 (s, 1H), 7.95 (dd, J = 8.6, 1.7 Hz, 1H), 7.92 (d, J = 8.6 Hz, 1H), 7.90 (d, J = 8.7 Hz, 1H), 7.75 (s, 1H), 7.46 (dd, J = 8.4, 1.6 Hz, 1H), 2.78 – 2.73 (t, J = 9.0 Hz, 2H), 1.72 (q, J = 5.7 Hz, 2H), 1.69 – 1.63 (m, 1H), 1.45 (q, J = 5.7 Hz, 2H), 1.31 (d, J = 3.8 Hz, 2H), 1.27 – 1.15 (m, 6H), 0.84 (t, J = 7.0 Hz, 3H); ^{13}C NMR (151 MHz, DMSO) δ 171.86, 167.83, 142.23, 134.57, 130.41, 129.87, 129.21, 128.75, 128.26, 128.08, 127.09, 125.91, 124.52, 35.35, 32.76, 31.28, 30.63, 28.97, 28.85, 28.72, 28.68, 22.08, 17.97, 13.95.

5-bromo-1-naphthaldehyde (4.55).

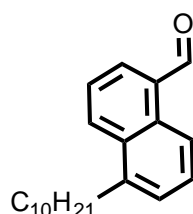


4.55

To a stirring solution of 1-Naphthaldehyde (1.00 g, 6.40 mmol, 1 eq.) in acetic acid (1.2 M) was added Bromine (1.11 g, 0.4 mL, 6.92 mmol, 1.08 eq.) and heated to reflux. The reaction was stirred for 72 hours whence the reaction was cooled and filtered through a fine frit. The solvent was removed under reduced pressure and immediately purified via flash chromatography to afford the title compound (0.590 g, 2.51 mmol, 39%). R_f = 0.30 (5% EtOAc in Hex, orange in DNP); ^1H NMR (300 MHz, CDCl_3) δ 10.19 (s, 1H), 9.07 (d, J = 8.6 Hz, 1H), 8.28 (d, J = 8.5 Hz, 1H), 7.89 (d, J = 8.2 Hz, 1H), 7.68 (d, J = 7.5 Hz, 1H), 7.57 (t, J =

7.7 Hz, 1H), 7.30 (t, $J = 8.0$ Hz, 1H); ^{13}C NMR (75 MHz, CDCl_3) δ 193.22, 136.83, 134.95, 133.60, 130.83, 128.91, 128.25, 126.68, 125.88, 124.61, 124.35.

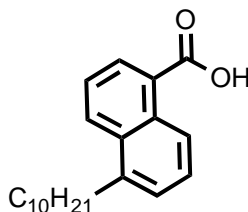
5-decyl-1-naphthaldehyde (4.56).



4.56

General procedure C was used to couple aldehyde **4.55** (0.590 g, 2.51 mmol) to 1-decene (0.880 g, 1.2 mL, 6.27 mmol) to afford the title compound (0.199 g, 0.670 mmol, 27%). $R_f = 0.65$ (5% EtOAc in Hex, DNP); ^1H NMR (300 MHz, CDCl_3) δ 10.40 (s, 1H), 9.15 (d, $J = 8.6$ Hz, 1H), 8.33 (d, $J = 8.5$ Hz, 1H), 7.94 (d, $J = 7.0$ Hz, 1H), 7.61 (dd, $J = 15.4, 8.2$ Hz, 2H), 7.42 (d, $J = 7.0$ Hz, 1H), 3.08 (t, $J = 9.0$ Hz, 2H), 1.83 – 1.66 (m, 2H), 1.53 – 1.19 (m, 14H), 0.91 (t, $J = 6.6$ Hz, 3H); ^{13}C NMR (75 MHz, CDCl_3) δ 193.49, 139.58, 135.96, 132.24, 131.91, 131.23, 131.00, 128.75, 127.08, 124.57, 122.90, 33.58, 31.98, 31.24, 29.84, 29.70, 29.60, 29.42, 22.77, 14.21.

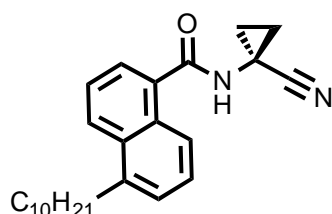
5-decyl-1-naphthoic acid (4.57).



4.57

General procedure D was used to convert aldehyde **4.56** (0.199 g, 0.670 mmol) to the carboxylic product (0.209 g, 0.670 mmol, 100%);

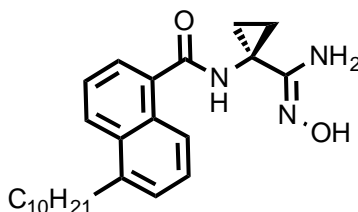
***N*-(1-cyanocyclopropyl)-5-decyl-1-naphthamide (4.58).**



4.58

General procedure C was used to couple carboxylic acid **4.57** (0.209 g, 0.670 mmol) and 1-Amino-1-cyclopropanecarbonitrile hydrochloride (0.079 g, 0.670 mmol) to afford the desired compound (0.108 g, 0.288 mmol, 43%). $R_f = 0.26$ (25% EtOAc in Hex); ^1H NMR (300 MHz, CDCl_3) δ 8.11 (d, $J = 8.4$ Hz, 1H), 8.05 (d, $J = 8.4$ Hz, 1H), 7.50 – 7.30 (m, 4H), 6.78 (s, 1H), 3.04 (t, $J = 7.5$ Hz, 2H), 1.70 (m, 2H), 1.61 (dd, $J = 8.3, 5.9$ Hz, 2H), 1.49 – 1.18 (m, 16H), 0.88 (t, $J = 6.6$ Hz, 3H); ^{13}C NMR (75 MHz, CDCl_3) δ 170.51, 139.58, 133.07, 132.21, 127.34, 127.27, 126.84, 124.94, 124.34, 123.29, 120.11, 33.44, 32.02, 31.08, 29.89, 29.75, 29.65, 29.46, 22.81, 20.99, 17.08, 14.25.

(*Z*)-5-decyl-*N*-(1-(*N*-hydroxycarbamimidoyl)cyclopropyl)-1-naphthamide (4.59).

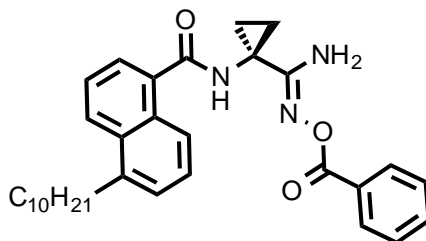


4.59

To a stirring solution of nitrile **4.58** (0.109 g, 0.288 mmol, 1 eq.), hydroxylamine (0.100 g, 1.44 mmol, 5 eq.) in EtOH (0.02 M) was added TEA (0.292 g, 0.4 mL, 2.88 mmol, 10 eq.). The reaction was heated to 60 °C and stirred overnight.

Once complete, the solvent was removed under reduced pressure and the crude material purified via flash chromatography to afford the title compound (0.081 g, 0.199 mmol, 69%). $R_f = 0.0$ (25% EtOAc in Hex); ^1H NMR (300 MHz, DMSO) δ 9.04 (s, 1H), 8.14 (d, $J = 6.8$ Hz, 1H), 8.01 (d, $J = 8.7$ Hz, 1H), 7.55 (d, $J = 7.3$ Hz, 2H), 7.50 – 7.42 (m, 1H), 7.38 (d, $J = 6.6$ Hz, 1H), 3.04 (t, $J = 7.5$ Hz, 2H), 1.75 – 1.55 (m, 2H), 1.23 (bs, 16H), 0.99 (bs, 2H), 0.85 (t, $J = 5.8$ Hz, 3H).

(Z)-N-(1-(N-(benzoyloxy)carbamimidoyl)cyclopropyl)-5-decyl-1-naphthamide (4.60).

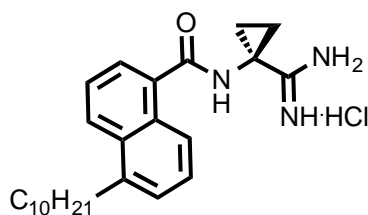


4.60

General procedure B was used to couple amideoxime **4.59** (0.081 g, 0.199 mmol) to benzoic acid (0.024 g, 0.199 mmol) to afford the title compound (0.066 g, 0.128 mmol, 65%). $R_f = 0.61$ (50% EtOAc in Hex); ^1H NMR (300 MHz, CDCl_3) δ 8.03 (d, $J = 8.0$ Hz, 1H), 7.97 (d, $J = 8.1$ Hz, 1H), 7.55 (t, $J = 7.0$ Hz, 1H), 7.49 – 7.34 (m, 2H), 7.34 – 7.23 (m, 1H), 6.19 (bs, 1H), 3.03 – 2.93 (t, $J = 7.5$ Hz, 2H), 1.80 – 1.64 (m, 2H), 1.61 (t, $J = 6.6$ Hz, 2H), 1.48 – 1.14 (m, 16H), 0.88 (t, $J = 6.4$

Hz, 3H); ^{13}C NMR (75 MHz, CDCl_3) δ 173.06, 164.31, 159.91, 139.48, 133.79, 133.04, 132.16, 130.38, 129.54, 128.51, 126.99, 126.93, 126.60, 124.79, 124.37, 123.22, 33.43, 32.78, 32.00, 31.02, 29.89, 29.74, 29.64, 29.44, 22.79, 14.23, 13.88.

***N*-(1-carbamimidoylcyclopropyl)-5-decyl-1-naphthamide hydrochloride (4.61).**

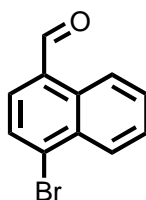


4.61

To a stirring solution of **4.60** (0.066 g, 0.128 mmol, 1 eq.) in EtOH (0.1 M) was added 20% by wt. $\text{Pd}(\text{OH})_2$ (0.10 eq.). The reaction was stirred under H_2 (1 atm) for 24 hrs. Once complete the reaction was filtered through a plug of Celite and washed with anhydrous EtOH. The solvent was removed under reduced pressure and immediately purified via flash chromatography. The material was then dissolved in Et_2O and a drop of 12.1 M HCl was added. The material was co-evaporated three times with Et_2O to afford the title compound as a HCl salt (0.0049 g, 0.0114 mmol, 9%). R_f = 0.14 (10% MeOH in CHCl_3); ^1H NMR (600 MHz, DMSO) δ 9.20 (s, 1H), 8.94 (s, 2H), 8.67 (s, 2H), 8.20 (d, J = 8.6 Hz, 1H), 8.07 (d, J = 8.5 Hz, 1H), 7.87 (d, J = 7.0 Hz, 1H), 7.58 (dd, J = 8.5, 7.1 Hz, 1H), 7.47 (dd, J = 8.5, 7.0 Hz, 1H), 7.40 (d, J = 6.2 Hz, 1H), 3.06 (t, J = 7.3 Hz, 2H), 1.74 (dd, J = 8.0, 5.6 Hz, 1H), 1.64 (dt, J = 15.2, 7.6 Hz, 1H), 1.46 (q, J = 5.8 Hz,

1H), 1.40 – 1.33 (m, 2H), 1.32 – 1.22 (m, 12H), 0.85 (t, $J = 7.0$ Hz, 3H); ^{13}C NMR (151 MHz, DMSO) δ 171.58, 170.48, 138.82, 133.47, 131.40, 130.26, 126.39, 126.33, 126.29, 125.91, 124.52, 123.89, 123.06, 40.06, 32.83, 32.47, 31.28, 30.72, 29.05, 28.99, 28.98, 28.89, 28.69, 22.09, 17.98, 17.57, 16.70, 15.17, 13.97, 8.45.

4-bromo-1-naphthaldehyde (4.63).

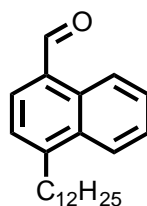


4.63

A stirring solution of 1-Bromo-4-methylnaphthalene (1.00 g, 4.52 mmol, 1 eq.), N-Bromosuccinimide (0.878 g, 4.93 mmol, 1.09 eq.), and benzoyl peroxide (0.044 g, 0.181 mmol, 0.04 eq.) in CCl_4 (0.28 M) was heated to reflux overnight. Once complete, the reaction was cooled, filtered, the solvent removed via flash chromatography, and immediately purified via flash chromatography to afford the brominated product. $R_f = 0.68$ (10% EtOAc in Hex). To a stirring solution of 1-bromo-4-(bromomethyl)naphthalene (1.23 g, 4.11 mmol) in DMSO (0.25 M) was added NaHCO_3 and heated to 95°C for 3 hrs. The reaction was cooled, diluted three times the amount of DMSO with DI H_2O , extracted three times into EtOAc (20 mL), dried with Na_2SO_4 , and the solvent removed under reduced pressure. The crude material was purified via flash chromatography to afford the title compound (0.275 g, 1.17 mmol, 29%). $R_f = 0.72$ (20% EtOAc in Hex); ^1H NMR

(300 MHz, CDCl_3) δ 10.29 (s, 1H), 9.20 (d, $J = 8.3$ Hz, 1H), 8.27 (d, $J = 9.4$ Hz, 1H), 7.86 (d, $J = 7.7$ Hz, 1H), 7.74 – 7.57 (m, 3H); ^{13}C NMR (75 MHz, CDCl_3) δ 192.58, 136.07, 132.04, 131.33, 131.28, 130.82, 129.76, 129.32, 128.26, 127.68, 125.11.

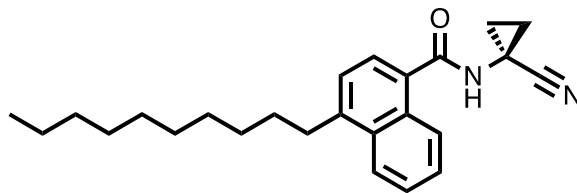
4-dodecyl-1-naphthaldehyde (4.64).



4.64

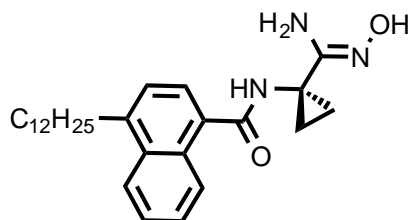
General procedure B was used to couple aldehyde **4.63** (0.275 g, 1.17 mmol) and 1-dodecene (0.296 g, 1.76 mmol) to afford the title compound (0.258 g, 0.795 mmol, 68%). $R_f = 0.41$ (5% EtOAc in Hex); ^1H NMR (300 MHz, CDCl_3) δ 10.32 (s, 1H), 9.36 (d, $J = 8.9$ Hz, 1H), 8.12 (d, $J = 9.0$ Hz, 1H), 7.86 (d, $J = 7.3$ Hz, 1H), 7.64 (dddd, $J = 21.0, 8.2, 6.9, 1.3$ Hz, 2H), 7.46 (d, $J = 7.3$ Hz, 1H), 3.10 (dd, $J = 17.1, 9.2$ Hz, 2H), 1.90 – 1.65 (m, 2H), 1.59 – 1.13 (m, 18H), 1.04 – 0.74 (t, $J = 6.0$ Hz, 3H); ^{13}C NMR (75 MHz, CDCl_3) δ 193.32, 147.55, 136.94, 132.12, 131.06, 129.97, 128.55, 126.78, 125.66, 125.16, 124.25, 33.94, 32.02, 30.74, 29.92, 29.76, 29.59, 29.46, 22.80, 14.24.

***N*-(1-cyanocyclopropyl)-4-dodecyl-1-naphthamide (4.66).**

**4.66**

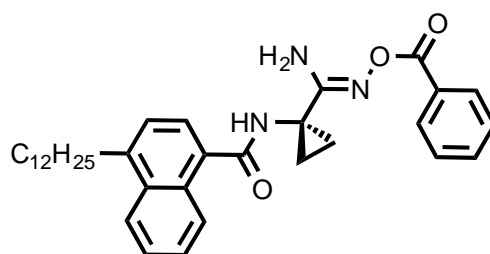
General procedure D was used to convert aldehyde **4.64** (0.258 g, 0.795 mmol) to the carboxylic acid. General procedure B was used to couple the carboxylic acid (0.271 g, 0.794 mmol) and 1-Amino-1-cyclopropanecarbonitrile hydrochloride (0.094 g, 0.794 mmol) to afford the desired compound (0.223 g, 0.551 mmol, 69%). $R_f = 0.28$ (25% EtOAc in Hex). ^1H NMR (300 MHz, CDCl_3) δ 8.30 – 8.22 (m, 1H), 8.06 – 7.97 (m, 1H), 7.54 – 7.43 (m, 2H), 7.36 (d, $J = 7.3$ Hz, 1H), 7.12 (d, $J = 7.3$ Hz, 1H), 7.05 (s, 1H), 3.00 (t, $J = 7.5$ Hz, 2H), 1.68 (dt, $J = 15.2, 7.6$ Hz, 2H), 1.54 (dd, $J = 8.0, 5.9$ Hz, 2H), 1.47 – 1.16 (m, 13H), 0.89 (t, $J = 6.6$ Hz, 2H); ^{13}C NMR (75 MHz, CDCl_3) δ 170.54, 143.13, 132.09, 130.47, 130.30, 126.96, 126.41, 125.86, 125.40, 124.49, 124.20, 120.22, 33.45, 32.03, 30.77, 29.92, 29.78, 29.62, 29.46, 22.80, 20.94, 16.97, 14.24.

(Z)-4-dodecyl-N-(1-(N-hydroxycarbamimidoyl)cyclopropyl)-1-naphthamide (4.67).

**4.67**

To a stirring solution of nitrile **4.66** (0.223 g, 0.551 mmol, 1 eq.) and hydroxylamine (0.191 g, 2.76 mmol, 5 eq.) in EtOH (0.02 M) was added TEA (0.558 g, 0.8 mL, 5.51 mmol, 10 eq.). The reaction was heated to 60 °C overnight whence it was cooled and the solvent removed under reduced pressure. The crude product was purified via flash chromatography to afford the title compound (0.120 g, 0.225 mmol, 50%). R_f = 0.0 (25% EtOAc in Hex); ^1H NMR (300 MHz, DMSO) δ 9.33 (bs, 1H), 8.96 (s, 1H), 8.25 (dd, J = 6.5, 3.2 Hz, 1H), 8.14 – 8.03 (m, 2H), 7.63 – 7.51 (m, 4H), 7.36 (d, J = 7.3 Hz, 1H), 5.97 (bs, 1H), 3.05 (t, J = 7.5 Hz, 2H), 1.65 (dt, J = 14.9, 7.6 Hz, 2H), 1.45 – 0.95 (m, 22H), 0.85 (t, J = 6.4 Hz, 3H); ^{13}C NMR (75 MHz, DMSO) δ 170.46, 157.36, 140.98, 126.18, 126.08, 126.02, 125.31, 125.16, 124.76, 124.66, 123.98, 32.42, 31.69, 31.32, 30.53, 29.34, 29.06, 28.92, 28.73, 22.12, 13.98.

(Z)-N-(1-(N-(benzoyloxy)carbamidoyl)cyclopropyl)-4-dodecyl-1-naphthamide (4.68).

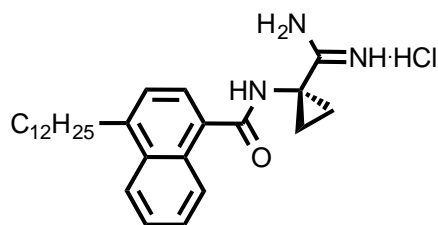


4.68

General procedure B was used to couple amideoxime (0.099 g, 0.225 mmol) and benzoic acid (0.028 g, 0.225 mmol) to afford the title compound (0.085 g, 0.157 mmol, 70%). R_f = 0.70 (50% EtOAc in Hex); ^1H NMR (300 MHz, CDCl_3) δ 8.26 (dd, J = 6.8, 3.0 Hz, 1H), 8.02 – 7.92 (m, 3H), 7.59 – 7.31 (m, 6H), 7.13 (d, J =

7.3 Hz, 1H), 6.17 (bs, 2H), 2.98 (t, $J = 7.5$ Hz, 2H), 1.74 – 1.55 (m, 2H), 1.25 (m, 22H), 0.87 (t, $J = 6.7$ Hz, 3H); ^{13}C NMR (75 MHz, CDCl_3) δ 172.92, 164.26, 159.95, 142.80, 133.02, 132.13, 131.23, 130.44, 129.51, 128.51, 126.81, 126.29, 125.78, 125.22, 124.61, 124.28, 60.49, 51.38, 33.42, 32.76, 32.02, 30.74, 29.90, 29.77, 29.74, 29.62, 29.45, 22.79, 21.14, 14.29, 14.23, 13.92.

***N*-(1-carbamimidoylcyclopropyl)-4-dodecyl-1-naphthamide hydrochloride (4.69).**

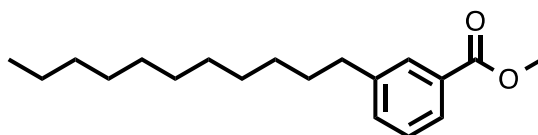


4.69

To a stirring solution of **4.68** (0.085 g, 0.157 mmol, 1 eq.) in EtOH (0.1 M) was added 20% by wt. $\text{Pd}(\text{OH})_2$ (0.10 eq.). The reaction was stirred under H_2 (1 atm) for 24 hrs. Once complete the reaction was filtered through a plug of Celite and washed with anhydrous EtOH. The solvent was removed under reduced pressure and immediately purified via flash chromatography. The material was then dissolved in Et_2O and a drop of 12.1 M HCl was added. The material was co-evaporated three times with Et_2O to afford the title compound as a HCl salt (0.002 g, 0.005 mmol, 3%). $R_f = 0.11$ (10% MeOH in CHCl_3); ^1H NMR (497 MHz, DMSO) δ 9.15 (s, 1H), 8.93 (s, 2H), 8.66 (s, 2H), 8.32 (d, $J = 8.2$ Hz, 1H), 8.12 (d, $J = 7.7$ Hz, 1H), 7.80 (d, $J = 7.3$ Hz, 1H), 7.62 – 7.53 (m, 2H), 7.39 (d, $J = 7.2$ Hz, 1H), 3.07 (t, $J = 7.4$ Hz, 2H), 1.73 (bs, 2H), 1.69 – 1.59 (m, 2H), 1.46 (bs, 2H),

1.40 – 1.16 (m, 18H), 0.85 (t, J = 6.4 Hz, 3H); ^{13}C NMR (151 MHz, DMSO) δ 171.66, 170.30, 141.79, 131.36, 130.87, 130.33, 126.32, 32.82, 32.43, 31.28, 30.72, 30.68, 30.52, 29.07, 29.04, 29.02, 28.99, 28.69, 22.09, 13.96.

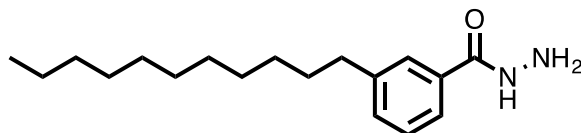
methyl 3-undecylbenzoate (5.10).



5.10

General procedure C was used to couple methyl 3-undecylbenzoate (0.880 g, 4.09 mmol) and 1-undecene (0.947 g, 6.14 mmol) to afford the desired compound (0.818 g, 2.82 mmol, 69%). R_f = 0.44 (5% EtOAc in Hex); ^1H NMR (300 MHz, CDCl_3) δ 7.90 – 7.81 (m, 2H), 7.35 (dd, J = 5.7, 4.0 Hz, 2H), 3.91 (t, J = 7.5 Hz, 3H), 2.69 – 2.61 (m, 2H), 1.62 (dt, J = 13.7, 6.7 Hz, 2H), 1.40 – 1.15 (m, 16H), 0.88 (t, J = 6.7 Hz, 3H); ^{13}C NMR (75 MHz, CDCl_3) δ 167.53, 143.38, 133.23, 129.64, 128.38, 127.05, 52.20, 51.42, 35.90, 32.06, 31.55, 29.78, 29.71, 29.62, 29.49, 29.39, 22.84, 14.28.

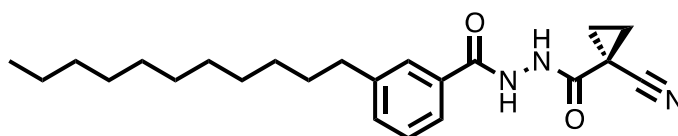
3-undecylbenzohydrazide (5.11).



5.11

To a stirring solution of **5.10** (0.560 g, 1.93 mmol, 1 eq.) in anhydrous EtOH (0.6 M) was added NH_2NH_2 (0.185 g, 0.2 mL, 5.78 mmol, 3 eq.). The solution was heated to reflux overnight whence the solvent was removed under reduced pressure and immediately purified via flash chromatography to afford the desired compound (0.369 g, 1.27 mmol, 66%). $R_f = 0.32$ (75% EtOAc in Hex);

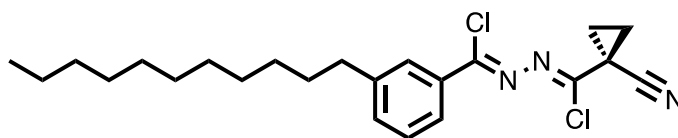
***N'*-(1-cyanocyclopropanecarbonyl)-3-undecylbenzohydrazide (5.12).**



5.12

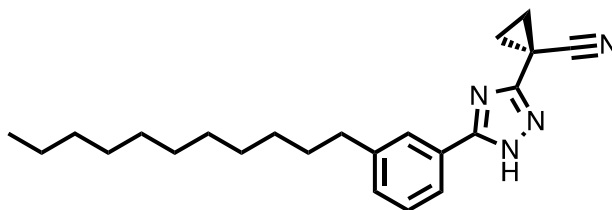
General procedure B was used to couple **5.11** (0.369 g, 1.27 mmol) and 1-cyanocyclopropanecarboxylic acid (0.141 g, 1.27 mmol) to afford the title compound (0.298 g, 1.04 mmol, 82%). $R_f = 0.62$ (50% EtOAc in Hex); ^1H NMR (300 MHz, CDCl_3) δ 9.27 (s, 1H), 9.00 (s, 1H), 7.65 (s, $J = 5.3$ Hz, 1H), 7.64 – 7.59 (m, 1H), 7.64 – 7.59 (m, 1H), 7.32 (d, $J = 7.2$ Hz, 2H), 2.67 – 2.52 (m, 2H), 1.71 (dd, $J = 8.3, 4.6$ Hz, 2H), 1.56 (dd, $J = 8.2, 4.6$ Hz, 4H), 1.24 (bs, 16H), 0.87 (t, $J = 6.7$ Hz, 3H); ^{13}C NMR (75 MHz, CDCl_3) δ 165.77, 164.48, 143.89, 132.89, 131.02, 128.73, 127.63, 124.68, 118.89, 51.38, 35.89, 32.03, 31.46, 29.78, 29.75, 29.70, 29.59, 29.46, 29.42, 22.80, 18.62, 14.26, 12.64.

(1*Z*,*N'Z*)-*N'*-(chloro(1-cyanocyclopropyl)methylene)-3-undecylbenzohydrazonoyl chloride (5.13).**

**5.13**

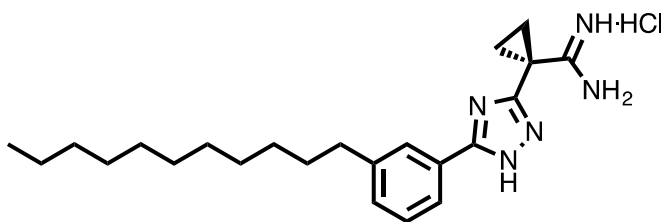
A solution of **5.12** (0.398 g, 1.04 mmol, 1 eq.) in thionyl chloride (2.47 g, 1.64 mL, 20.78 mmol, 20 eq.) was heated to reflux for 24 hrs. The solvent was removed under reduced pressure and co-evaporated twice with Et₂O. The product was carried on crude.

1-(5-(3-undecylphenyl)-1*H*-1,2,4-triazol-3-yl)cyclopropanecarbonitrile (5.14).

**5.14**

A solution of **5.13** (0.437 g, 1.04 mmol) in *i*-propanol saturated with NH₃ (0.02 M) was stirred under NH₃ (1 atm) overnight whence it was refluxed for 30 h. The reaction was cooled, the solvent removed under reduced pressure, and immediately purified via flash chromatography to afford the desired compound (0.280 g, 0.766 mmol, 74%). *R*_f = 0.40 (25% EtOAc in Hex); ¹H NMR (300 MHz, Acetone) δ 7.87 (s, 1H), 7.85 – 7.80 (m, 1H), 7.50 (t, *J* = 5.7 Hz, 1H), 7.47 (d, *J* = 2.1 Hz, 1H), 2.77 – 2.63 (m, 1H), 2.03 (qd, *J* = 3.5, 2.2 Hz, 2H), 1.73 – 1.59 (m, 1H), 1.40 – 1.22 (m, 6H), 0.86 (t, *J* = 6.7 Hz, 1H); ¹³C NMR (75 MHz, Acetone) δ 165.93, 163.61, 145.16, 133.08, 130.18, 127.46, 125.09, 124.57, 118.97, 47.08, 36.33, 32.74, 32.32, 30.48, 30.28, 30.03, 23.44, 19.26, 14.48, -2.97, -6.84.

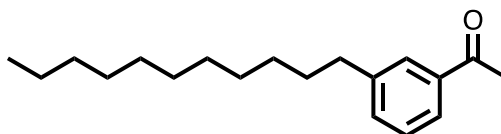
1-(5-(3-undecylphenyl)-1*H*-1,2,4-triazol-3-yl)cyclopropanecarboximidamide hydrochloride (5.15).



5.15

General procedure A was used to convert nitrile **5.14** (0.280 g, 0.766 mmol) to afford the title compound (0.156 g, 0.373 mmol, 49%). $R_f = 0.24$ (10% MeOH in CHCl_3); ^1H NMR (600 MHz, DMSO) δ 9.44 (d, $J = 33.7$ Hz, 2H), 7.80 (d, $J = 6.0$ Hz, 1H), 7.47 (dd, $J = 24.6, 7.3$ Hz, 1H), 2.65 (d, $J = 6.9$ Hz, 2H), 1.95 (d, $J = 4.6$ Hz, 2H), 1.85 (d, $J = 4.5$ Hz, 2H) 1.58 (s, 2H), 1.25 (d, $J = 32.4$ Hz, 16H), 0.83 (d, $J = 7.0$ Hz, 3H); ^{13}C NMR (151 MHz, DMSO) δ 166.90, 164.22, 163.87, 143.71, 132.04, 129.29, 126.19, 124.06, 123.12, 34.81, 31.25, 30.84, 28.99, 28.95, 28.80, 28.66, 28.57, 22.05, 20.27, 16.93, 13.89.

1-(3-undecylphenyl)ethanone (5.16).

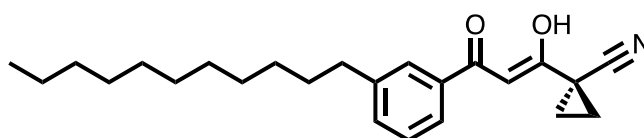


5.16

General procedure C was used to couple acetophenone (1.00 g, 5.02 mmol) to 1-undecene (1.16 g, 7.54 mmol) using 3 M NaOH and $\text{Pd}(\text{PPh}_3)_4$ to afford the title compound (1.04 g, 3.79 mmol, 76%). $R_f = 0.34$ (25% EtOAc in Hex); ^1H NMR (300 MHz, CDCl_3) δ 7.77 (dd, $J = 5.2, 2.2$ Hz, 2H), 7.37 (dd, $J = 5.9, 1.0$ Hz, 2H),

2.71 – 2.62 (t, $J = 7.5$ Hz, 2H), 2.60 (s, 3H), 1.62 (dd, $J = 8.7, 5.0$ Hz, 2H), 1.30 – 1.25 (m, 16H), 0.88 (t, $J = 6.6$ Hz, 3H); ^{13}C NMR (75 MHz, CDCl_3) δ 182.90, 133.44, 128.57, 128.26, 126.00, 35.98, 32.06, 31.60, 29.77, 29.72, 29.63, 29.49, 29.41, 26.88, 22.84, 14.29.

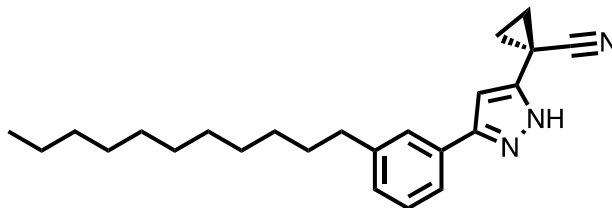
(Z)-1-(1-hydroxy-3-oxo-3-(3-undecylphenyl)prop-1-en-1-yl)cyclopropanecarbonitrile (5.17).



5.17

To stirring a stirring solution of **5.16** (0.541 g, 1.97 mmol) and ethyl 1-cyanocyclopropanecarboxylate in benzene (0.22 M) at 0 °C was added sodium metal (0.054 g, 2.37 mmol) dissolved in anhydrous MeOH (3.33 M) dropwise. The reaction was warmed to rt and stirred overnight. Once complete, the reaction was quenched with 1 N HCl and the solvent removed under reduced pressure. The material was dissolved in DCM and the salts removed via vacuum filtration. The solvent was removed under reduced pressure and the material was carried on crude. ^1H NMR (300 MHz, CDCl_3) δ 10.51 (bs, 1H), 7.83 – 7.66 (m, 2H), 7.45 – 7.27 (m, 2H), 6.81 (s, 1H), 2.71 – 2.61 (t, $J = 7.5$ Hz, 5H), 1.78 – 1.70 (m, 2H), 1.70 – 1.50 (m, 4H), 1.29 – 1.25 (m, 16H), 0.87 (t, $J = 6.4$ Hz, 3H).

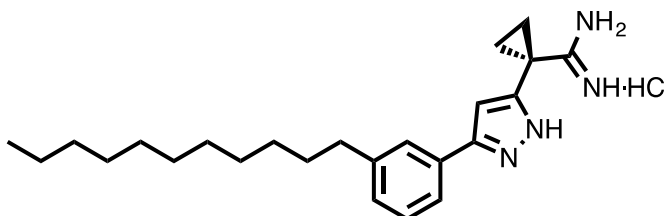
1-(3-(3-undecylphenyl)-1*H*-pyrazol-5-yl)cyclopropanecarbonitrile (5.18).



5.18

To a stirring solution of **5.17** (0.660 g, 1.80 mmol, 1 eq.) in anhydrous EtOH (0.16 M) was added NH_2NH_2 (0.461 g, 0.45 mL, 14.37 mmol, 8 eq.). The reaction was heated to reflux overnight. Once complete, the solvent was removed under reduced pressure and immediately purified via preparative thin layer chromatography to afford the desired compound (0.106 g, 0.292 mmol, 15 % over 2 steps). $R_f = 0.43$ (25% EtOAc in Hex, UV); ^1H NMR (600 MHz, Acetone) δ 7.57 (s, 1H), 7.17 (t, $J = 7.6$ Hz, 1H), 7.13 (t, $J = 7.7$ Hz, 1H), 7.07 (d, $J = 7.5$ Hz, 1H), 6.50 (s, 1 H), 2.49 – 2.45 (t, $J = \text{Hz}$ 2H), 1.51 – 1.42 (m, 2H), 1.23 – 1.02 (m, 20H), 0.70 (t, $J = 6.9$ Hz, 3H); ^{13}C NMR (151 MHz, Acetone) δ 157.99, 143.61, 139.75, 130.35, 129.03, 127.38, 124.86, 100.95, 36.64, 32.74, 32.47, 30.49, 30.45, 30.45, 30.34, 30.31, 30.18, 30.10, 18.13, 15.12, 14.56, 14.48.

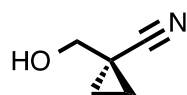
1-(3-(3-undecylphenyl)-1*H*-pyrazol-5-yl)cyclopropanecarboximidamide hydrochloride (5.19).



5.19

General procedure A was used to convert nitrile **5.18** (0.106 g, 0.292 mmol) to the desired compound (0.013 g, 0.032 mmol, 11%). ^1H NMR (600 MHz, DMSO) δ : two tautomers = 13.28 (bs, 1H), 9.01 (bs, 1H), 8.92 (bs, 1H), 7.98 (dd, J = 7.9, 1.0 Hz, 1H), 7.70 (dd, J = 7.7, 1.7 Hz, 1H), 7.48 (td, J = 7.6, 1.2 Hz, 1H), 7.27 – 7.19 (m, 1H), 6.65 (s, 1H), 2.61 – 2.57 (t, J = 6.0 Hz, 2H), 1.62 – 1.53 (m, 4H), 1.42 (bs, 2H), 1.28 – 1.23 (m, 16H), 1.14 (dd, J = 7.1, 4.7 Hz, 2H), 0.93 (dd, J = 7.1, 4.7 Hz, 2H), 0.84 (t, J = 7.0 Hz, 3H); ^{13}C NMR (151 MHz, DMSO) δ : two tautomers = 180.23, 180.08, 180.01, 179.95, 140.48, 132.41, 130.02, 128.15, 99.53, 94.12, 63.89, 31.30, 29.97, 29.05, 29.01, 29.00, 28.89, 28.72, 28.70, 22.11, 13.98, 12.42, 11.21. LCMS: t_R = 4.94; m/z = 381.3. HRMS m/z calcd for $\text{C}_{24}\text{H}_{37}\text{N}_4$ ($M + H$), 381.3018; found, 381.3003.

1-(hydroxymethyl)cyclopropane-1-carbonitrile (**5.20**).

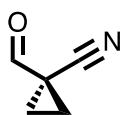


5.20

To a stirring solution of ethyl 1-cyanocyclopropane-1-carboxylate (1.077 g, 7.74 mmol) in anhydrous *t*-butanol (0.25 M) was added sodium borohydride (0.732 g, 19.35 mmol). The solution was heated to reflux whence anhydrous MeOH (1.26 M) was added dropwise to the reaction and refluxed for 1 h. Once complete, the reaction was cooled and the solvent removed under reduced pressure. The mixture was quenched with saturated NH_4Cl (0.59 M), extracted into DCM (3 x 15 mL), the organic layers dried with Na_2SO_4 , and the solvent

removed under reduced pressure. The crude material was purified via flash chromatography to yield the desired compound (0.133 g, 0.700 mmol, 19%). $R_f = 34$ (50% EtOAc in Hexanes, KMnO_4); ^1H NMR (300 MHz, CDCl_3) δ 3.61 (s, 2H), 1.28 (dd, $J = 7.4, 4.9$ Hz, 2H), 0.98 (dd, $J = 7.3, 4.9$ Hz, 2H); ^{13}C NMR (75 MHz, CDCl_3) δ 122.63, 65.72, 51.36, 12.78, 12.09.

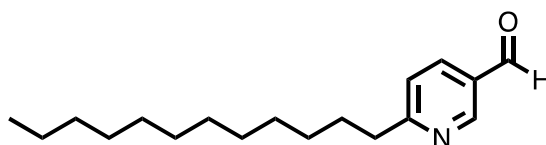
1-formylcyclopropane-1-carbonitrile (5.21).



5.21

To a stirring solution of **XX** (0.547 g, 5.64 mmol) in anhydrous DCM (0.03 M) was added activated MnO_2 (9.80 g, 112.71 mmol) continuously over the course of the reaction for 24 h. Once complete, the reaction was filtered through Celite and washed with DCM. The DCM was removed at atmospheric pressure and not put under vacuum due to volatility. The desired compound was carried on crude. ^1H NMR (300 MHz, CDCl_3) δ 8.53 (s, 1H), 1.93 (dd, $J = 7.9, 4.2$ Hz, 2H), 1.45 (dd, $J = 7.8, 4.1$ Hz, 2H); ^{13}C NMR (75 MHz, CDCl_3) δ 198.39, 127.34, 51.43, 17.29.

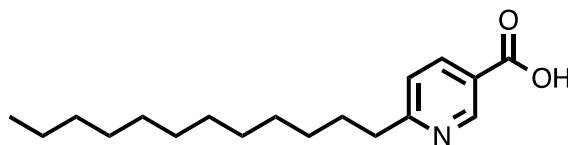
6-dodecylnicotinaldehyde (5.28).



5.28

General procedure C was used to couple 6-bromonicotinaldehyde (1.00 g, 5.38 mmol) and 1-dodecene (1.36 g, 1.8 mL, 8.06 mmol) to afford the title compound (1.32 g, 4.81 mmol, 89%). $R_f = 0.32$ (5% EtOAc in Hex); ^1H NMR (300 MHz, CDCl_3) δ 10.06 (s, 1H), 8.97 (d, $J = 1.9$ Hz, 1H), 8.08 (dd, $J = 8.1, 2.2$ Hz, 1H), 7.31 (d, $J = 8.0$ Hz, 1H), 2.87 (t, $J = 7.5$ Hz, 2H), 1.91 – 1.58 (m, 6H), 1.57 – 1.39 (m, 4H), 1.39 – 1.30 (m, 10H), 1.24 (s, 1H), 0.87 (t, $J = 6.6$ Hz, 3H); ^{13}C NMR (75 MHz, CDCl_3) δ 190.78, 169.25, 152.30, 136.01, 129.49, 123.37, 39.00, 32.37, 32.17, 32.05, 29.76, 29.65, 29.57, 29.49, 26.61, 26.34, 22.91, 22.12, 14.28.

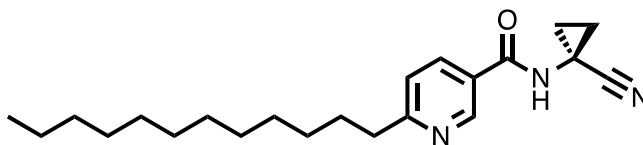
6-dodecylnicotinic acid (5.29).



5.29

General procedure D was used to oxidize **5.28** (1.32 g, 4.81 mmol) to afford the title compound. The product was carried on crude. ^1H NMR (300 MHz, DMSO) δ 8.98 – 8.91 (m, 1H), 8.14 (dd, $J = 8.1, 2.2$ Hz, 1H), 7.36 (d, $J = 8.1$ Hz, 1H), 2.77 (t, $J = 7.5$ Hz, 2H), 1.68 (dt, $J = 13.8, 6.5$ Hz, 2H), 1.24 (d, $J = 13.8$ Hz, 18H), 0.84 (t, $J = 6.2$ Hz, 3H).

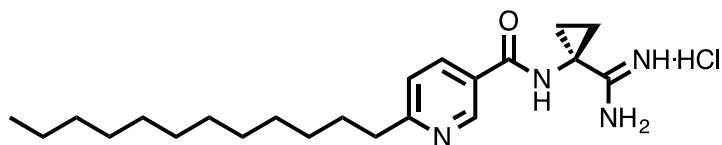
***N*-(1-cyanocyclopropyl)-6-dodecylnicotinamide (5.30).**



5.30

General procedure B was used to couple crude **5.29** (1.40 g, 4.81 mmol) and 1-Amino-1-cyclopropanecarbonitrile hydrochloride (0.570 g, 4.81 mmol) to afford the desired compound (0.632 g, 1.78 mmol, 37% over 2 steps). $R_f = 0.21$ (50% EtOAc in Hex); ^1H NMR (300 MHz, CDCl_3) δ 8.87 (d, $J = 2.2$ Hz, 1H), 8.06 (dd, $J = 8.1, 2.3$ Hz, 1H), 7.79 (s, 1H), 7.21 (d, $J = 8.1$ Hz, 1H), 2.78 (t, $J = 7.5$ Hz, 2H), 1.73 – 1.62 (m, 2H), 1.59 (dd, $J = 8.3, 5.8$ Hz, 2H), 1.37 (dd, $J = 8.4, 5.9$ Hz, 2H), 1.30 – 1.20 (m, 4H), 0.85 (t, $J = 6.6$ Hz, 3H); ^{13}C NMR (75 MHz, CDCl_3) δ 166.90, 166.84, 147.74, 136.04, 126.05, 122.85, 120.31, 38.51, 32.00, 29.80, 29.73, 29.64, 29.54, 29.45, 22.78, 20.95, 16.90, 14.23.

N-(1-carbamimidoylcyclopropyl)-6-dodecylnicotinamide hydrochloride (5.31).

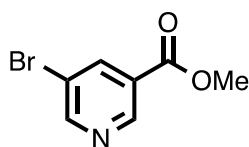


5.31

General procedure A was used to convert **5.30** (0.632 g, 1.78 mmol) to amidine **XX** (0.018 g, mmol, 3%). $R_f = 0.08$ (10% MeOH in CHCl_3); ^1H NMR (600 MHz, DMSO) δ 9.98 (s, 1H), 9.26 (s, 1H), 9.07 (s, 1H), 8.78 (d, $J = 7.9$ Hz, 1H), 8.75 (s, 1H), 7.96 (d, $J = 8.1$ Hz, 1H), 3.06 (t, $J = 7.5$ Hz, 2H), 1.74 (t, $J = 6.2$ Hz, 4H), 1.48 (q, $J = 5.4$ Hz, 2H), 1.31 – 1.16 (m, 18H), 0.84 (t, $J = 6.9$ Hz, 3H); ^{13}C NMR (151 MHz, DMSO) δ 171.54, 163.94, 160.24, 143.22, 142.05, 129.60, 125.88, 32.58, 31.30, 29.04, 29.03, 29.02, 29.01, 28.90, 28.84, 28.72, 28.63, 28.37,

22.10, 18.17, 13.97. LCMS: t_R = 5.15; m/z = 373.3. HRMS m/z calcd for $C_{22}H_{37}N_4O$ ($M + H$), 373.2956; found, 373.2967.

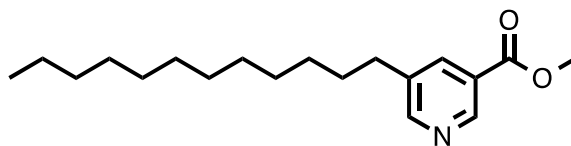
methyl 5-bromonicotinate (5.32).



5.32

To a stirring solution of MeOH (1 M) at 0 °C was added acetic chloride (2 M in MeOH) and stirred for 10 min. 5-Bromonicotinic acid (1.00 g, 3.44 mmol) was added in one portion and the mixture refluxed overnight. Once complete, the reaction was cooled, the solvent removed under reduced pressure, and immediately purified via flash chromatography to yield the title compound **5.32**. R_f = 0.50 (20% EtOAc in Hex); 1H NMR (300 MHz, $CDCl_3$) δ 9.13 (d, J = 1.8 Hz, 1H), 8.84 (d, J = 2.3 Hz, 1H), 8.46 – 8.40 (m, 1H), 3.97 (s, 3H); ^{13}C NMR (75 MHz, $CDCl_3$) δ 164.26, 154.16, 148.45, 139.54, 127.27, 120.52, 49.94.

methyl 5-dodecylnicotinate (5.33).

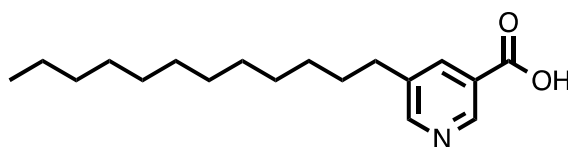


5.33

General procedure C was used to couple ester **5.32** (0.470 g, 2.18 mmol) and 1-dodecene (0.333 g, 1.98 mmol) using a 3 M solution of K_3PO_4 (3 eq.) and

$\text{PdCl}_2(\text{dppf}) \cdot \text{CH}_2\text{Cl}_2$ (5 mol%) to afford the title compound (0.408 g, 1.34 mmol, 62%). $R_f = 0.34$ (10% EtOAc in Hex); ^1H NMR (300 MHz, CDCl_3) δ 8.55 (d, $J = 1.9$ Hz, 1H), 8.05 (d, $J = 8.0$ Hz, 1H), 7.63 (dd, $J = 8.0, 2.2$ Hz, 1H), 3.99 (s, 3H), 2.67 (t, $J = 7.5$ Hz, 2H), 1.70 – 1.53 (m, 2H), 1.36 – 1.09 (m, 18H), 0.87 (t, $J = 6.6$ Hz, 3H); ^{13}C NMR (75 MHz, CDCl_3) δ 165.71, 153.37, 148.10, 137.70, 136.49, 125.48, 70.34, 52.07, 32.59, 32.03, 31.77, 30.84, 29.49, 29.39, 29.22, 28.98, 26.25, 22.54, 21.95, 13.94.

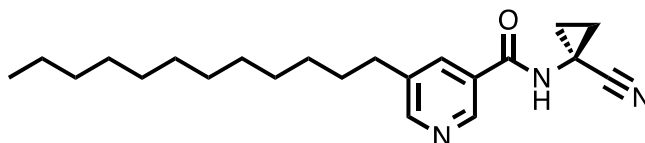
5-dodecylnicotinic acid (5.34).



5.34

To a stirring solution of ester **5.33** (0.408 g, 2.02 mmol, 1 eq.) in THF (1 M) and MeOH (1 M) was added LiOH (0.145 g, 6.07 mmol, 3 eq.) in H_2O (1 M). The reaction was stirred overnight whence it was diluted with EtOAc (60 mL), washed with 1 M HCl (15 mL), the aqueous layer was washed with EtOAc (30 mL), and dried over Na_2SO_4 . The solvent was removed under reduced pressure to afford the title compound (0.355 g, 1.22 mmol, 91%).

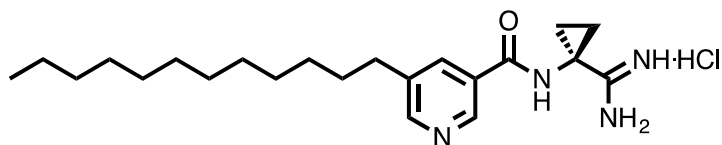
N-(1-cyanocyclopropyl)-5-dodecylnicotinamide (5.35)



5.35

General procedure B was used to couple carboxylic acid **5.34** (0.355 g, 1.22 mmol) to 1-Amino-1-cyclopropanecarbonitrile hydrochloride (0.144 g, 1.22 mmol) to afford the desired compound (0.086 g, 0.243 mmol, 20%). $R_f = 0.45$ (75% EtOAc in Hex); ^1H NMR (300 MHz, Acetone) δ 8.97 (s, 1H), 8.87 (s, 1H), 8.68 (s, 1H), 8.15 (s, 1H), 2.77 (t, $J = 7.5$ Hz, 2H), 1.73 (d, $J = 7.0$ Hz, 2H), 1.66 (dd, $J = 8.5, 5.3$ Hz, 2H), 1.49 (dd, $J = 8.2, 5.7$ Hz, 2H), 1.45 – 1.32 (m, 18H), 0.95 (t, $J = 6.6$ Hz, 3H); ^{13}C NMR (75 MHz, Acetone) δ 166.97, 153.39, 146.80, 138.74, 135.41, 129.47, 121.05, 46.85, 33.13, 32.52, 31.73, 30.57, 30.26, 30.19, 30.05, 23.23, 21.36, 16.73, 14.30.

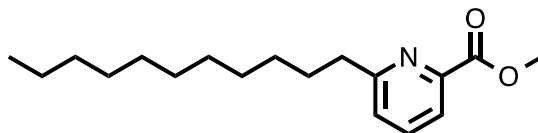
***N*-(1-carbamimidoylcyclopropyl)-5-dodecylnicotinamide hydrochloride (5.36).**

**5.36**

General procedure A was used to convert nitrile **5.35** (0.086 g, 0.243 mmol) into the desired compound (0.040 g, 0.097 mmol, 40%). $R_f = 0.10$ (10% MeOH in CHCl_3); ^1H NMR (600 MHz, DMSO) δ 10.00 (s, 1H), 9.20 (s, 1H), 9.08 (s, 1H), 8.89 (s, 1H), 8.76 (s, 1H), 2.78 (t, $J = 9.0$ Hz, 2H), 1.75 (q, $J = 5.6$ Hz, 2H), 1.70 – 1.60 (m, 2H), 1.50 (q, $J = 5.5$ Hz, 2H), 1.26 (m, 10H), 0.84 (t, $J = 7.0$ Hz, 3H); ^{13}C NMR (151 MHz, DMSO) δ 171.54, 164.26, 144.67, 142.34, 140.87, 140.66, 131.39, 127.93, 127.10, 124.34, 118.99, 109.79, 32.58, 31.63, 31.26, 30.02,

29.01, 28.98, 28.91, 28.72, 28.68, 28.47. LCMS: t_R = 4.22; m/z = 373.3. HRMS m/z calcd for $C_{22}H_{37}N_4O$ ($M + H$), 373.2967; found, 373.2954.

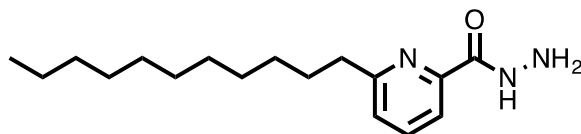
methyl 6-undecylpicolinate (5.37).



5.37

General procedure C was used to couple methyl 6-bromopicolinate (0.833 g, 3.86 mmol) and 1-undecene (0.833 g, 1.1 mL, 5.40 mmol) using 3 M NaOH (3 M) and $Pd(PPh_3)_4$ (cat.) to afford the desired compound (0.370 g, 1.27 mmol, 33%). R_f = 0.24 (10% EtOAc in Hex); 1H NMR (300 MHz, $CDCl_3$) δ 7.95 (d, J = 7.6 Hz, 1H), 7.73 (t, J = 7.8 Hz, 1H), 7.34 (d, J = 7.8 Hz, 1H), 3.99 (s, 3H), 2.88 (t, J = 7.5 Hz, 2H), 1.91 – 0.96 (m, 18H), 0.87 (t, J = 6.6 Hz, 3H); ^{13}C NMR (75 MHz, $CDCl_3$) δ 164.90, 161.43, 148.32, 137.32, 125.57, 119.33, 37.91, 31.88, 29.61, 29.54, 29.48, 29.31, 29.27, 22.65, 14.10.

6-undecylpicolinohydrazide (5.38).

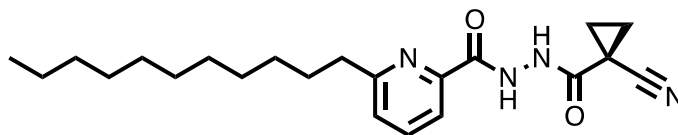


5.38

To a stirring solution of **5.37** (0.370 g, 1.27 mmol, 1 eq.) in anhydrous EtOH (0.6 M) was added NH_2NH_2 (0.122 g, 0.12 mL, 3.81 mmol, 3 eq.). The solution was

heated to reflux overnight whence the solvent was removed under reduced pressure and immediately purified via flash chromatography to afford the desired compound (0.203 g, 0.697 mmol, 55%). $R_f = 0.35$ (75% EtOAc in Hex, Ninhydrin); ^1H NMR (300 MHz, CDCl_3) δ 9.13 (s, 1H), 7.89 (d, $J = 7.7$ Hz, 1H), 7.65 (t, $J = 7.7$ Hz, 1H), 7.19 (d, $J = 7.8$ Hz, 1H), 4.11 (s, 2H), 2.69 (t, $J =$ Hz, 2H), 1.62 (dd, $J = 14.7, 7.1$ Hz, 2H), 1.36 – 1.08 (m, 16H), 0.80 (t, $J = 6.6$ Hz, 3H); ^{13}C NMR (75 MHz, CDCl_3) δ 164.90, 161.43, 148.32, 137.32, 125.57, 119.33, 37.91, 31.88, 29.61, 29.54, 29.48, 29.31, 29.27, 22.65, 14.10.

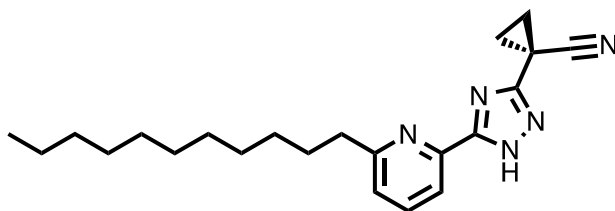
***N*-(1-cyanocyclopropanecarbonyl)-6-undecylpicolinohydrazide (5.39).**



5.39

General procedure B was used to couple **5.38** (0.203 g, 0.697 mmol) and 1-cyanocyclopropanecarboxylic acid (0.077 g, 0.697 mmol) to afford the title compound (0.204 g, 0.531 mmol, 76%). $R_f = 0.26$ (50% EtOAc in Hex); ^1H NMR (300 MHz, CDCl_3) δ 10.02 (s, 1H), 9.35 (s, 1H), 7.90 (d, $J = 7.7$ Hz, 1H), 7.64 (t, $J = 7.7$ Hz, 1H), 7.22 (d, $J = 7.8$ Hz, 1H), 2.69 (t, $J = 7.5$ Hz, 2H), 1.70 (dd, $J = 8.1, 4.4$ Hz, 2H), 1.61 (dd, $J = 13.9, 6.2$ Hz, 2H), 1.52 (dd, $J = 8.1, 4.3$ Hz, 2H), 1.40 – 0.99 (m, 16H), 0.82 (t, $J = 6.4$ Hz, 3H); ^{13}C NMR (75 MHz, CDCl_3) δ 164.30, 162.38, 161.62, 147.31, 137.35, 126.10, 119.88, 118.95, 51.19, 37.75, 31.80, 29.53, 29.51, 29.47, 29.35, 29.24, 22.58, 18.36, 14.04, 12.43.

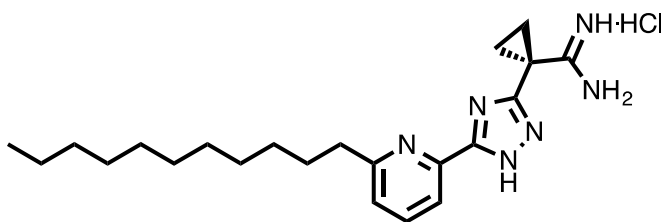
1-(3-(6-undecylpyridin-2-yl)-1*H*-1,2,4-triazol-5-yl)cyclopropanecarbonitrile
(5.41).



5.41

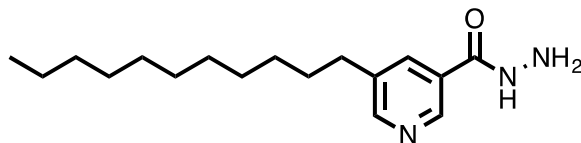
A solution of **5.39** (0.204 g, 0.532 mmol, 1 eq.) in thionyl chloride (1.26 g, 1.8 mL, 10.62 mmol, 20 eq.) was heated to reflux for 24 hrs. The solvent was removed under reduced pressure and co-evaporated twice with Et₂O. The product was carried on crude. The crude material (0.224 g, 0.532 mmol) was dissolved in *i*-propanol saturated with NH₃ (0.02 M) was stirred under NH₃ (1 atm) overnight whence it was refluxed for 30 h. The reaction was cooled, the solvent removed under reduced pressure, and immediately purified via flash chromatography to afford the desired compound (0.061 g, 0.166 mmol, 31%). *R*_f = 0.22 (25% EtOAc in Hex); ¹H NMR (300 MHz, CDCl₃) δ 7.99 (dd, *J* = 10.7, 4.1 Hz, 1H), 7.80 – 7.70 (m, 1H), 7.35 – 7.27 (m, 1H), 2.82 – 2.74 (t, *J* = 7.5 Hz, 2H), 2.00 (dd, *J* = 3.7, 2.0 Hz, 2H), 1.96 (dd, *J* = 3.7, 2.0 Hz, 2H), 1.73 (dq, *J* = 15.1, 7.6 Hz, 2H), 1.43 – 1.18 (m, 16H), 0.86 (t, *J* = 6.7 Hz, 3H); ¹³C NMR (75 MHz, CDCl₃) δ 164.06, 161.56, 148.96, 137.48, 137.39, 125.76, 125.43, 120.75, 119.66, 38.42, 38.06, 32.01, 29.94, 29.72, 29.67, 29.58, 29.51, 29.45, 29.39, 22.79, 19.32, 14.24.

1-(3-(6-undecylpyridin-2-yl)-1*H*-1,2,4-triazol-5-yl)cyclopropanecarboximidamide hydrochloride (5.42).

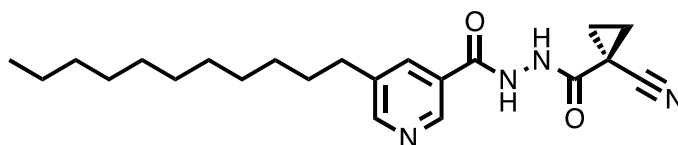


5.42

General procedure A was used to convert nitrile **5.41** (0.061 g, 0.166 mmol) into the title compound (0.008 g, 0.019 mmol, 12%). $R_f = 0.28$ (15% MeOH in CHCl_3); ^1H NMR (600 MHz, DMSO) δ : major tautomer = 9.61 (s, 1H), 9.44 – 9.24 (m, 1H), 7.99 – 7.93 (m, 2H), 7.51 (d, $J = 7.7$ Hz, 1H), 2.84 – 2.79 (m, 2H), 1.94 (dd, $J = 8.2, 5.3$ Hz, 2H), 1.84 (dd, $J = 8.2, 5.5$ Hz, 2H), 1.68 (bs, 2H), 1.30 – 1.28 (m, 2H), 1.23 (s, 14H), 0.84 (t, $J = 7.0$ Hz, 3H); and minor tautomer = 9.61 (s, 1H), 9.44 – 9.24 (m, 1H), 8.04 – 7.96 (m, 2H), 7.53 (d, $J = 7.9$ Hz, 1H), 2.84 – 2.79 (m, 2H), 1.68 (bs, 2H), 1.30 – 1.28 (m, 4H), 1.29 – 1.26 (m, 2H), 1.23 (s, 14H), 0.84 (t, $J = 7.0$ Hz, 3H); ^{13}C NMR (151 MHz, DMSO) δ : two tautomers = 166.60, 166.01, 164.61, 164.45, 163.82, 163.02, 162.96, 162.78, 142.00, 141.88, 138.13, 138.07, 125.64, 125.47, 120.72, 120.54, 53.26, 46.06, 41.63, 40.05, 38.28, 37.32, 37.31, 32.04, 31.28, 29.21, 29.19, 29.02, 29.02, 28.98, 28.97, 28.86, 28.71, 22.09, 20.34, 18.65, 17.96, 16.88, 16.70, 13.96, 12.18.

5-undecylnicotinohydrazide (5.43a).**5.43a**

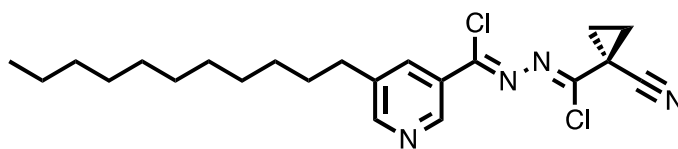
To a stirring solution of **5.33** (1.443 g, 4.95 mmol, 1 eq.) in anhydrous EtOH (0.6 M) was added NH_2NH_2 (0.476 g, 0.47 mL, 14.85 mmol, 3 eq.). The solution was heated to reflux overnight whence the solvent was removed under reduced pressure and immediately purified via flash chromatography to afford the desired compound (0.585 g, 2.01 mmol, 41%). $R_f = 0.26$ (75% EtOAc in Hex, Ninhydrin); ^1H NMR (300 MHz, CDCl_3) δ 9.35 (s, 1H), 8.22 (s, 1H), 7.93 (d, $J = 8.0$ Hz, 1H), 7.46 (d, $J = 8.0$ Hz, 1H), 4.21 (s, 2H), 2.48 (t, $J = 7.4$ Hz, 2H), 1.46 (s, 2H), 1.13 (m, 16H), 0.73 (t, $J = 5.5$ Hz, 3H); ^{13}C NMR (75 MHz, CDCl_3) δ 164.63, 148.30, 146.81, 140.96, 136.57, 121.82, 32.78, 31.69, 30.74, 29.41, 29.33, 29.19, 29.13, 28.96, 22.47, 13.91.

***N*-(1-cyanocyclopropanecarbonyl)-5-undecylnicotinohydrazide (XXb).****5.43b**

General procedure B was used to couple **5.43a** (0.585 g, 2.01 mmol) and 1-cyanocyclopropanecarboxylic acid (0.223 g, 2.01 mmol) to afford the title compound (0.567 g, 1.48 mmol, 73%). $R_f = 0.27$ (50% EtOAc in Hex); ^1H NMR

(300 MHz, CDCl₃) δ 8.28 (s, 1H), 7.99 (d, J = 7.9 Hz, 1H), 7.55 (d, J = 8.0 Hz, 1H), 2.57 (t, J = 7.6 Hz, 2H), 1.69 (dd, J = 7.7, 4.1 Hz, 2H), 1.52 (dt, J = 8.3, 5.6 Hz, 4H), 1.22 (d, J = 12.5 Hz, 16H), 0.81 (t, J = 6.2 Hz, 3H); ¹³C NMR (75 MHz, CDCl₃) δ 164.47, 162.65, 148.51, 145.81, 141.99, 136.82, 122.46, 119.01, 32.93, 31.79, 30.81, 29.51, 29.42, 29.27, 29.23, 29.03, 22.58, 18.38, 14.04, 12.43.

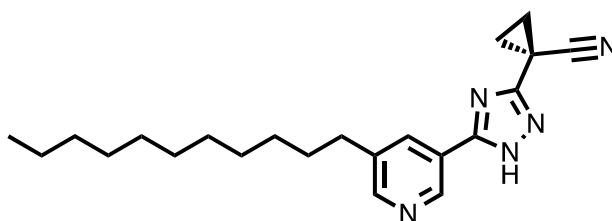
(3*Z*,*N'Z*)-*N'*-(chloro(1-cyanocyclopropyl)methylene)-5-undecylnicotinohydrazonoyl chloride (5.43c).**



5.43c

A solution of **5.34b** (0.567 g, 1.48 mmol, 1 eq.) in thionyl chloride (3.51 g, 2.1 mL, 29.49 mmol, 20 eq.) was heated to reflux for 24 hrs. The solvent was removed under reduced pressure and co-evaporated twice with Et₂O. The product was carried on crude.

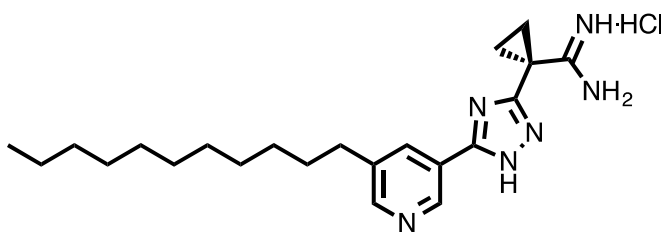
1-(5-(5-undecylpyridin-3-yl)-1*H*-1,2,4-triazol-3-yl)cyclopropanecarbonitrile (5.43d).



5.43d

A solution of **5.43c** (0.621 g, 1.48 mmol) in *i*-propanol saturated with NH₃ (0.02 M) was stirred under NH₃ (1 atm) overnight whence it was refluxed for 30 h. The reaction was cooled, the solvent removed under reduced pressure, and immediately purified via flash chromatography to afford the desired compound (0.150 g, 0.410 mmol, 28%). *R*_f = 0.13 (25% EtOAc in Hex); ¹H NMR (300 MHz, Acetone) δ 8.62 (d, *J* = 1.8 Hz, 1H), 8.10 (d, *J* = 8.1 Hz, 1H), 7.87 (dd, *J* = 8.1, 2.2 Hz, 1H), 2.75 (t, *J* = 7.5 Hz, 2H), 2.12 – 2.06 (m, 2H), 2.01 (dd, *J* = 8.6, 5.1 Hz, 2H), 1.68 (dt, *J* = 14.9, 7.2 Hz, 2H), 1.30 (m, 16H), 0.87 (t, *J* = 6.6 Hz, 3H); ¹³C NMR (75 MHz, Acetone) δ 165.38, 164.32, 151.34, 149.42, 142.23, 141.76, 137.93, 123.53, 122.55, 118.86, 47.04, 33.48, 32.71, 31.81, 30.43, 30.20, 29.69, 23.40, 19.42, 14.46, 8.05.

1-(5-(5-undecylpyridin-3-yl)-1*H*-1,2,4-triazol-3-yl)cyclopropanecarboximidamide hydrochloride (5.43).

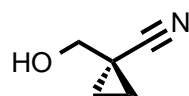


5.43

General procedure A was used to convert nitrile **5.43d** (0.150 g, 0.410 mmol) to afford the title compound (0.021 g, 0.051 mmol, 12%). *R*_f = 0.22 (15% MeOH in CHCl₃); ¹H NMR (600 MHz, DMSO) δ 10.52 (s, 1H), 10.27 (s, 1H), 9.73 (s, 1H), 9.51 – 9.42 (m, 3H), 9.20 (d, *J* = 16.3 Hz, 1H), 8.63 (d, *J* = 7.3 Hz, 1H), 8.11 (dd, *J* = 20.8, 8.0 Hz, 1H), 7.93 – 7.87 (m, 1H), 2.71 – 2.65 (m, 2H), 1.96 (dd, *J* = 8.1,

5.4 Hz, 2H), 1.81 (dd, $J = 8.1, 5.5$ Hz, 2H), 1.59 (s, 2H), 1.32 – 1.12 (m, 16H), 0.83 (t, $J = 6.9$ Hz, 3H); ^{13}C NMR (151 MHz, DMSO) δ 168.12, 166.73, 166.64, 166.16, 164.68, 164.39, 163.72, 162.69, 150.31, 141.28, 141.10, 140.22, 140.11, 137.44, 137.40, 122.85, 62.83, 41.66, 40.06, 38.24, 32.07, 32.06, 32.03, 31.32, 30.38, 29.05, 29.03, 29.01, 28.98, 28.80, 28.79, 28.73, 28.54, 22.12, 13.98.

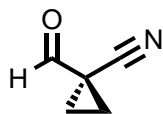
1-(hydroxymethyl)cyclopropane-1-carbonitrile (5.20).



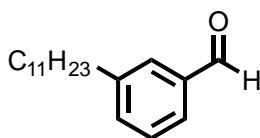
5.20

A solution of ethyl 1-cyanocyclopropane-1-carboxylate (1.08 g, 7.74 mmol) and NaBH_4 (0.732 g, 19.35 mmol) in $t\text{BuOH}$ (0.25 M) was heated to reflux. Once at refluxing temperature, anhydrous MeOH (1.26 M) was added dropwise. The reaction was heated at refluxing temperature for 1 h. Once the reaction was complete, the reaction was cooled and quenched with saturated NH_4Cl (0.59 M). The mixture was extracted into DCM (3 x 15 mL), washed with DI H_2O (15 mL), dried with Na_2SO_4 , and the solvent removed by blowing air over due to the product being highly volatile. The crude product was purified via flash chromatography to afford the title compound (0.539 g, 5.55 mmol, 72%). $R_f = 0.34$ (50% EtOAc in Hexanes, KMnO_4); ^1H NMR (300 MHz, CDCl_3) δ 3.61 (s, 2H), 2.50 (bs, 1H), 1.28 (dd, $J = 7.3, 5.1$ Hz, 2H), 0.98 (dd, $J = 7.3, 5.1$ Hz, 2H); ^{13}C NMR (75 MHz, CDCl_3) δ 122.63, 65.72, 51.36, 12.78, 12.09.

1-formylcyclopropane-1-carbonitrile (5.21).

**5.21**

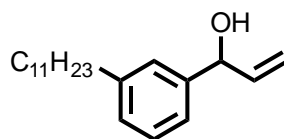
To a solution of **5.20** (1.40 g, 14.37 mmol) in DCM (0.03 M) was added activated MnO_2 (24.99 g, 287.5 mmol) continually over the course of the reaction. The reaction was stirred at rt for 24 h. Once complete, the reaction was filtered through Celite and washed with DCM to remove solids. The solvent was removed by blowing air over due to the product being volatile. The crude material was purified via flash chromatography to afford the title compound (0.010 g, 0.105 mmol, 0.7%). $R_f = 0.21$ (50% EtOAc in Hexanes, DNP); ^1H NMR (300 MHz, CDCl_3) δ 8.53 (s, 1H), 1.93 (dd, $J = 7.9, 4.2$ Hz, 2H), 1.45 (dd, $J = 7.8, 4.1$ Hz, 2H); ^{13}C NMR (75 MHz, CDCl_3) δ 198.39, 127.34, 51.43, 17.29.

3-undecylbenzaldehyde (5.22).**5.22**

General procedure C was used to convert 3-bromobenzaldehyde (0.500 g, 2.70 mmol) to **5.22** (0.470 g, 1.81 mmol, 67%). $R_f = 0.93$ (5% EtOAc in Hexanes, Seebach's Dip and DNP); ^1H NMR (300 MHz, CDCl_3) δ 10.00 (s, 1H), 7.81 – 7.57 (m, 2H), 7.54 – 7.36 (m, 2H), 2.68 (t, $J = 7.5$ Hz, 2H), 1.64 (dt, $J = 14.8, 7.2$ Hz, 2H), 1.36 – 1.21 (m, 16H), 0.88 (t, $J = 6.7$ Hz, 3H); ^{13}C NMR (75 MHz, CDCl_3)

δ 192.84, 144.15, 136.65, 134.88, 129.49, 129.03, 127.65, 35.79, 32.06, 31.27, 29.77, 29.70, 29.61, 29.48, 29.37, 22.84, 14.28.

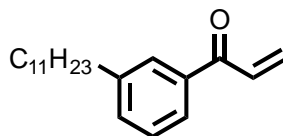
1-(3-undecylphenyl)prop-2-en-1-ol (5.23).



5.23

To a solution of **5.22** (0.470 g, 1.81 mmol) in anhydrous THF (0.2 M) at 0 °C was added vinylmagnesium bromide (0.237 g, 1.81 mmol) dropwise. The reaction was stirred for 10 min at 0 °C then warmed to rt and stirred for 4 h. Once complete, the reaction was quenched with saturated aqueous NH_4Cl . The mixture was extracted into Et_2O (3 x 15 mL), the organic layers dried with brine, dried over Na_2SO_4 and the solvent removed under reduced pressure. The product was carried on crude. ^1H NMR (300 MHz, CDCl_3) δ 7.37 – 7.03 (m, 4H), 6.06 (ddd, J = 16.6, 10.4, 6.4 Hz, 1H), 5.36 (dt, J = 1.9, 1.3 Hz, 1H), 5.21 (dd, J = 3.7, 2.7 Hz, 1H), 5.18 (s, 1H), 3.80 – 3.68 (m, 1H), 2.60 (t, J = 7.5 Hz, 2H), 1.92 – 1.80 (m, 2H), 1.28 (d, J = 12.0 Hz, 16H), 0.88 (t, J = 6.7 Hz, 3H).

1-(3-undecylphenyl)prop-2-en-1-one (5.24).



5.24

To a solution of oxalyl chloride (0.231 g, 1.82 mmol, 0.16 mL) in anhydrous DCM (0.2M) at -78 °C was added DMSO (0.284 g, 3.64 mmol, 0.26 mL) dropwise and the mixture stirred for 10 min. In anhydrous DCM, **5.23** (0.437 g, 1.52 mmol) was added to the reaction mixture dropwise at -78 °C and the reaction stirred for 15 min. Then TEA (0.767 g, 7.58 mmol, 1.1 mL) was added to the reaction mixture and then it was warmed to rt and stirred for an additional 1.5 hr. Once complete the mixture was poured into 3M HCl (0.27 M) at 0 °C. The aqueous layer was saturated with NaCl then extracted with DCM (3 x 15 mL), dried with NaSO₄, and the solvent removed under reduced pressure.

Reference:

(1) Kharel, Y.; Mathews, T. P.; Kennedy, A. J.; Houck, J. D.; Macdonald, T. L.; Lynch, K. R. *Analytical biochemistry* **2011**, 411 (2), 230-235.